

UNCLASS

SECURITY CLASSIFICATION OF THIS PAGE (When Data Entered)

AFIT

REPORT DOCUMENTATION PAGE

READ INSTRUCTIONS BEFORE COMPLETING FORM

1. REPORT NUMBER
19 CT-79-215D

2. GOVT ACCESSION NO.
ADA107256

3. RECIPIENT'S CATALOG NUMBER

4. TITLE (and Subtitle)
An Investigation of Flame Stability in a Coaxial Lump Combustor

5. TYPE OF REPORT & PERIOD COVERED
THESIS/DISSERTATION

7. AUTHOR(s)
Edward T. Curran

1

6. PERFORMING ORG. REPORT NUMBER

8. CONTRACT OR GRANT NUMBER(s)

9 Doctoral thesis

9. PERFORMING ORGANIZATION NAME AND ADDRESS
AFIT STUDENT AT: School of Engineering, AFIT

10. PROGRAM ELEMENT, PROJECT, TASK AREA & WORK UNIT NUMBERS

11. CONTROLLING OFFICE NAME AND ADDRESS
AFIT/NR
WPAFB OH 45433

12. REPORT DATE
18 May 1979

13. NUMBER OF PAGES
243

14. MONITORING AGENCY NAME & ADDRESS (if different from Controlling Office)
LEVEL

15. SECURITY CLASS. (of this report)
UNCLASS
15a. DECLASSIFICATION/DOWNGRADING SCHEDULE

16. DISTRIBUTION STATEMENT (of this Report)
APPROVED FOR PUBLIC RELEASE; DISTRIBUTION UNLIMITED
14 AFIT/AE/DS79-1

SDTC ELECTED NOV 6 1981 H

17. DISTRIBUTION STATEMENT (of the abstract entered in Block 20, if different from Report)
20 OCT 1981 Archie C. Lynch

18. SUPPLEMENTARY NOTES
APPROVED FOR PUBLIC RELEASE: IAW AFR 190-17

ARCHIE C. LYNCH, Major, USAF
Director of Public Affairs
Air Force Institute of Technology (AFIT)
Wright-Patterson AFB, OH 45433

19. KEY WORDS (Continue on reverse side if necessary and identify by block number)

20. ABSTRACT (Continue on reverse side if necessary and identify by block number)
ATTACHED
81 10 26 162
012225

ADA107256

COPY

AN INVESTIGATION OF FLAME STABILITY
IN A COAXIAL DUMP COMBUSTOR

by

Edward T. Curran, Ph.D.

Dr. Harold E. Wright, Advisor

An experimental investigation of the flame stability characteristics of a coaxial dump combustion chamber was made. A ⁶~~six~~-inch diameter combustor was studied, and the dump plane inlet diameter was varied from 2.5th to 5.0th inches. Tests were carried out using pre-mixed ethylene/air and JP-4/air. To avoid vitiation effects, a clean-air heater was used to vary the temperature of the inlet air. The temperature levels were generally in the range 1000-1250^oR; the corresponding inlet pressure was varied between approximately 10 and 40 psia. Inlet Mach numbers were typically in the range 0.2 to 0.9.

The flame stability data were not collapsed by a conventional dump combustor correlation. However, a correlating parameter was derived by modelling the annular recirculation zone as an adiabatic stirred reactor using a one-step chemical reaction. This derived correlating parameter was used to obtain successful correlations. The dominant variable in flame stability was the inlet temperature; the subsidiary variables were the step height, inlet pressure, and velocity. The effect of velocity on the lean extinction limit was very small. With JP-4 fuel the existence of complete stability loops was demonstrated by operating at very low combustor pressures.

→ Some tests were performed with additional fuel injection directly into the recirculation zone. Lean extinction limits were determined

cont.
↓

with varying fractions of the total fuel flow being injected into the recirculation zone. These tests yielded an estimate of the air mass flow fraction entrained into the recirculation zone.

- Finally, tests were performed using a transparent quartz combustor; it was observed that the combustion process was an oscillatory phenomenon
 - with the reaction zone moving rapidly to and fro along the combustor.
- A comprehensive review of the literature concerning the flame stability and aerodynamics of coaxial dump combustors was presented.

↖

Accession For	
NTIS GRA&I	<input checked="" type="checkbox"/>
DTIC TAB	<input type="checkbox"/>
Unannounced	<input type="checkbox"/>
Justification	
By _____	
Distribution/	
Availability Codes	
Dist	Special
A	

AN INVESTIGATION OF FLAME STABILITY
IN A COAXIAL DUMP COMBUSTOR

DISSERTATION

Presented to the Faculty of the School of Engineering
of the Air Force Institute of Technology
Air Training Command
in Partial Fulfillment of the
Requirements for the Degree of
Doctor of Philosophy

by

Edward T. Curran, B.Sc. (Eng), M.Sc.

Approved for public release; distribution unlimited.

81 10 26 162

AN INVESTIGATION OF FLAME STABILITY
IN A COAXIAL DUMP COMBUSTOR

by

Edward T. Curran, B.Sc. (Eng), M.Sc.

Approved:

Harold E. Wright 10 Jan 1979
Chairman

G. Richard Heger 10 Jan, 1979

William C. Ersk 10 Jan, 1979

Ernest A. Darks 10 Jan, 1979

Hans von Ohain 10 Jan, 1979

Accepted:

J. Przemieniecki 18 May 1979
Dean, School of Engineering

Acknowledgements

I wish to express my appreciation to Dr. Harold E. Wright, Chairman of my advisory committee, for his initial suggestion that I should enter the Doctoral program at AFIT and for his encouragement and support at all times, particularly during the preparation of this dissertation. I also wish to express my appreciation for the constructive advice and encouragement from the other members of my advisory committee who were: Dr. William C. Elrod, Dr. Ernest A. Dorko, and Dr. G. Richard Hagee. I also owe a dept of gratitude to Dr. Hans von Ohain, Chief Scientist of the Air Force Aero Propulsion Laboratory, who consented to serve as the Dean's representative on the advisory committee.

This research was conducted at the Air Force Aero Propulsion Laboratory (AFAPL), utilizing the test facilities of the Ramjet Engine Division. A special note of appreciation must go to the experimental group of the Ramjet Technology Branch of AFAPL for their active support and encouragement in carrying out the test program. Group members included: John Hojnacki, Ken Schwartzkopf, Parker Buckley, and Douglas Davis, under the able leadership of Dr. Roger R. Craig. Thanks are also due to Douglas Davis for his considerable assistance in reducing and correlating a large quantity of experimental data and to Dr. Frank D. Stull, who made the facility and the services of the test group available for this experimental investigation.

Appreciation is also expressed to the facility technicians: Robert Schelenz, Glenn Boggs, and Stevie Campbell, who assembled and maintained the numerous test rig configurations in a most professional manner.

Thanks are also expressed to the staffs of both the AFIT and the Air Force Wright Aeronautical Laboratories libraries for their services in obtaining many of the references, and to Mr. Wayne Zwart of the Foreign Technology Division for obtaining many obscure publications.

The outstanding contributions of Mrs. R. McBeth in transforming my handwritten notes into a readable, typed draft and of Miss Cynthia Lines for her expeditious and expert typing of the final version of this dissertation are most gratefully acknowledged.

Sincere appreciation is also expressed to: Col George E. Strand, Commander, AFAPL, who made possible a leave of absence to complete this dissertation; to Col Philippe O. Bouchard for his encouragement, and to my colleagues in the Ramjet Engine Division who bore an extra burden during my absence.

Finally, I must acknowledge the support and patience of my wife, who endured many lonely hours during the execution of this dissertation.

Contents

	Page
Acknowledgements	ii
List of Figures	vi
List of Tables	x
Nomenclature	xi
Abstractxviii
I. Introduction	1
II. Flame Stability and Combustor Operation	9
Stirred Reactor Characteristics	13
Application of Stirred Reactor Model to Flame Stabilization	24
Alternative Criteria for Flame Stabilization	33
Flame Stability of Dump Combustors and Similar Geometries	51
III. Theoretical Analysis	65
Aerodynamics of Coaxial Dump Configurations	65
Loading Parameter of Recirculation Zone	71
Chemical Reaction Model	76
IV. Experimental Program	81
Aims of the Experimental Program	81
Determination of Stability Limits	81
Combustor Design	85
Test Facility	87
Experimental Investigations	95
V. Results and Discussion	101
Flame Stability Tests	101
Tests with Ethylene	102
Tests with JP-4	110
Lean Extinction Tests with Split Flow Injection	118
Quartz Combustor Tests	122
Discussion of Flame Stability Data	125
Discussion of Split Flow and Quartz Combustor Tests	137
VI. Conclusions	142

Contents

	Page
VII. Recommendations for Future Work	145
Flame Stability of Coaxial Dump Combustors	145
Combustion in Coaxial Dump Combustors.	146
Aerodynamics of Coaxial Dump Combustors.	147
Summary.	148
Bibliography.	149
Appendix A: Aerodynamics of the Coaxial Dump Combustor	161
Characteristics of the Recirculation Zone	165
Entrainment in Confined Jet Systems	179
Entrainment in the Initial Region of a Turbulent Jet.	192
Residence Time Distribution Diagnostics	195
Summary	197
Appendix B: Mass Transfer in Recirculation Zones	198
Appendix C: Chemical Reaction Model.	206
Appendix D: Inlet Flow Data.	216
Vita.	220

List of Figures

<u>Figure</u>		<u>Page</u>
1	Conventional and Integral-Rocket Ramjet Engines.	2
2	Types of Dump Combustor.	3
3	Typical Flame Stability Loop for a Bluff Body.	6
4	Idealized Reactor Concepts	11
5	Progress of Reaction	15
6	Characteristic Curves of Stirred Reactor	18
7	Spherical Combustion-Reactor Characteristics	20
8	Simple Combustor Geometries.	25
9	Bluff Body Recirculation Zone.	27
10	Flame Stability Correlation Based on Peclet Number	36
11	Characteristic Ignition Time	40
12	Characteristic Ignition and Combustion Times	42
13	Characteristic Time Correlation for Lean Blow-off of Bluff Body Stabilizer	48
14	Flame Stability Correlation: Small Coaxial Dump Combustors	53
15	Flame Stability Correlation: 12" Coaxial Dump Combustor.	54
16	Flame Stability Correlation for Dump Combustors: Pre-Mixed Fuel-Air	56
17	Flame Stability Data for a Coaxial Dump Combustor and for Steps.	57
18	Flame Stability Data for a Small Coaxial Dump Combustor.	59
19	Flow Field of a Coaxial Dump Configuration	66
20	Recirculation Zone Length Ratio as a Function of Reynolds Number.	68
21	Recirculated Mass Flow Fraction - Diameter Ratio	70

<u>Figure</u>	<u>Page</u>
22 Parabolic Recirculation Zone Shape: Variation of \bar{h}_p/D . . .	74
23 Variation of Exponents s and t as a Function of E and n (Ethylene)	78
24 Components of Test Combustor	86
25 Secondary Injection Plates	88
26 Ramjet Test Stand.	90
27 Schematic Arrangement of Test Stand Flow Systems	91
28 Schematic Arrangement of Data Acquisition System	93
29 Gas Flow Paths Through Test Rig.	94
30 Installation of Quartz Combustor	100
31 Lean Extinction Limits: 3.5" Dump Dia., 0.40 Nozzle Area Ratio; Ethylene Fuel.	104
32 Lean Extinction Limits: 3.5" Dump Dia., 0.50 Nozzle Area Ratio; Ethylene Fuel.	105
33 Lean Extinction Limits: 3.5" Dump Dia., 0.60 Nozzle Area Ratio; Ethylene Fuel.	106
34 Effect of Nozzle Area Ratio on Lean Extinction Limit; Ethylene Fuel.	108
35 Effect of Inlet Mach Number on Lean Extinction Limit; Ethylene Fuel.	109
36 Effect of Step Height on Lean Extinction Limit; Ethylene Fuel.	111
37 Flame Stability Limits: 3.5" Dump Dia., 0.40 Nozzle Area Ratio; JP-4 Fuel.	112
38 Effect of Nozzle Area Ratio on Lean Extinction Limit; JP-4 Fuel.	114
39 Effect of Step Height on Lean Extinction Limit; JP-4 Fuel.	115
40 Effect of Screech on Quality of Data; JP-4 Fuel.	116
41 Effect of Combustor Length to Diameter Ratio on Stability Limits; JP-4 Fuel.	117

<u>Figure</u>	Page
42 Effect of Vitiation on Stable Range; JP-4 Fuel	119
43 Complete Stability Loop; JP-4 Fuel	120
44 Complete Stability Loop; JP-4 Fuel	121
45 Primary and RZ Fuel Flows at Lean Extinction: 2.5" Dump	123
46 Primary and RZ Fuel Flows at Lean Extinction: 4.5" Dump	124
47 Trial Correlation by X Parameter: Effect of Step Size . .	126
48 Trial Correlation by X Parameter: Effect of Inlet Temperature.	127
49 Trial Correlation by X Parameter: Effect of Inlet Temperature.	128
50 Trial Correlation by X Parameter: Effect of Step Size . .	129
51 Lean Stability Limit Correlation: 2.5" Dump Diameter; Ethylene Fuel.	131
52 Lean Stability Limit Correlation: 3.5" Dump Diameter; Ethylene Fuel.	132
53 Lean Stability Limit Correlation: 4.5" Dump Diameter; Ethylene Fuel.	133
54 Lean Stability Limit Correlation: All Dump Sizes; Ethylene Fuel.	134
55 Lean Stability Limit Correlation: All Dump Sizes; JP-4 Fuel	135
56 Overall Stability Limit Correlation: All Dump Sizes; JP-4 Fuel.	138
57 Experimental Values of Recirculated Mass Flow Fraction . .	139
A-1 Flow in a Sudden Expansion	163
A-2 Typical Variation of Measured Recirculation Flow Fraction with Distance.	164
A-3 Flow Phenomena in a Sudden Expansion	167
A-4 Recirculation Zone Length-Ratio as a Function of Reynolds Number.	169

<u>Figure</u>	<u>Page</u>
A-5 Wall Static Pressure Distribution for a Coaxial Dump Configuration (Ref 84)	171
A-6 Illustration of Forward Flow Probability (Ref 83).	174
A-7 Shape of Recirculation Zone.	176
A-8 Parabolic Recirculation Zone: Geometric Parameters.	178
A-9 Schematic Arrangement of an Industrial Furnace	180
A-10 Geometry of Entrainment Region	183
A-11 Variation of Recirculation Mass Flow Fraction with $\sqrt{m_s}$	189
A-12 Estimates of Recirculation Mass Flow Fraction from Various Sources.	190
A-13 Effect of Density Ratio on Recirculation Mass Flow Fraction	193
A-14 Entrainment in the Initial Region of a Turbulent Jet	194
A-15 Comparison of Entrainment Fractions Given by Two Theories	196
C-1 Variation of Φ'_{\max} with ϕ and T.	209
C-2 Approximation to Φ'_{\max} Function	210
C-3 Approximation to Φ'_{\max} Function	211
C-4 Variation of s and t: Ethylene.	212
C-5 Variation of s and t: JP-4.	213
C-6 Variation of Exponents with E and n (Ethylene)	215
D-1 Flow Profile for 2.5" Inlet.	217
D-2 Flow Profile for 3.5" Inlet.	218
D-3 Flow Profile for 4.5" Inlet.	219

List of Tables

<u>Table</u>	<u>Page</u>
I Combustor Geometries Tested.	103
A-I Investigations of Axisymmetric Sudden Expansions	166
A-II Similarity Parameters of Experimental Hardware	188

Nomenclature

English letter symbols

A	Area
A_f	Projected area of flame stabilizer
A_0	Area at dump inlet plane
A_{ref}	Reference area of gas turbine combustor; see Eq(22)
B	Similarity parameter defined by Eq(A-17)
C_f	Concentration of fuel
C_m	Exchange coefficient; see Eq(B-1)
C_o	Concentration of oxygen
C_t	Craya-Curtet number
C_2	Entrainment coefficient; see Eq(A-31)
D	Combustor diameter
D_B	Molecular diffusion coefficient
D_f	Diameter of flameholder
D_{ref}	Reference diameter associated with A_{ref}
E	Apparent activation energy
$E(\tau)$	Exit age distribution function
E_v	Turbulent exchange velocity; see Eq(B-6)
H	Dimensionless group defined in Eq(B-11)
K	Karlovitz number; see Eq(28)
K_{FL}	Characteristic factor, see Eq(38)
L	Length of a recirculation zone
\bar{L}	Non-dimension RZ length (L/h)
L_c	Length of combustion chamber

M	Mach number
Mi	Mikhel'son criteria; see Eq(30)
P	Static pressure
p ^l	Pressure in atmospheres
P _{eu}	Peclet number based on flow velocity
P _{es}	Peclet number based on laminar flame speed
P _{max}	Maximum duct pressure; see Fig A-5
P _{min}	Minimum duct pressure; see Fig A-5
P _o	Pressure at dump inlet plane
P _r	Pressure in reaction zone
P _t	Total pressure
ΔP _t	Total pressure loss in combustor
R	Universal gas constant
Re	Reynolds number based on relevant diameter: d for coaxial combustor, D _f for baffle, and D _{ref} for GT combustor
S	Effective entrainment surface area; see Eq(47)
S _l	Surface area of step RZ - linear approximation
S _p	Surface area of step RZ - parabolic approximation
S _t	Strouhal number
S _T	Turbulent flame speed
S _u	Laminar flame speed
T	Initial temperature
ΔT	Adiabatic temperature rise during combustion
T ^l	Temperature (°R)/1000
T _o	Temperature at dump inlet plane
T _r	Temperature of stirred reaction zone
T _{sl}	Temperature of shear layer
T _{to}	Total temperature at dump inlet plane

U	Velocity of flow upstream of flameholder
U^+	Characteristic entrance velocity; see Eq(A-17)
U_{BO}	Measured blow-off velocity
U_d	Primary jet velocity (equivalent to inlet velocity)
U_{dyn}	Dynamic mean velocity; see Eq(A-15)
U_D	Secondary flow velocity
U_k	Kinematic mean velocity; see Eq(A-14)
U_ℓ	"Adjusted" velocity at lip of flameholder, see Eq(41)
U_m	Downstream velocity of flow past flameholder
U_o	Velocity at dump inlet plane
U_p	Upstream velocity in RZ behind flameholder
U_{ref}	Reference velocity in GT combustor
U_{rel}	Sum of U_m and U_p
U_{rz}	Mean upstream velocity along axis of RZ
U_{rzmax}	Maximum upstream velocity along axis of RZ
V	Volume of a recirculation zone
V_ℓ	Volume of RZ behind step; see Eq(55)
V_p	Volume of RZ behind step, see Eq(61)
V_z	Effective volume of RZ; see Eq(A-35)
X_f	Mole fraction of fuel
X_o	Mole fraction of oxygen
W	Width of flameholder wake
a	Thermal diffusivity
\bar{a}	Effective thermal diffusivity
b	Constant defined by Eq(9)
c	Index in Eq(21): subscript in Eq(A-17)
d	Diameter of inlet at the dump plane

d^*	Exit nozzle throat diameter
d_h	Equivalent nozzle diameter; see Eq(A-30)
e	Exponential factor
f	Index in Eq(19)
\dot{f}_o	Mainstream fuel flow rate at LBO; see Eq(64)
\dot{f}_r	Fuel flow rate into RZ at LBO
\dot{f}_t	Total fuel flow rate at LBO
f_1, f_2, f_3	Functions defined in Eq(B-11), (B-12), and (B-13)
h	Step height in inches, except in Eq(46)
\bar{h}_l	Characteristic step height; see Eq(58)
\bar{h}_p	Characteristic step height; see Eq(62)
j	Index in Eq(8) and (12)
k	Length of RZ behind step, in step heights (L/h)
k_E	Entrainment factor; see Eq(52)
k_f	Energy of freestream turbulence
k_1	Reaction rate constant, see Eq(1)
k_2, k_3, k_4, k_5	Constants in Eq(25), (69), (72), (74)
l_f	Integral length scale of freestream turbulence
m	Ratio of inerts (3.76 for air)
\dot{m}_a	Secondary air mass flow
\dot{m}_e	Mass flow entrained into jet or RZ; see Eq(A-6)
\dot{m}_o	Mass flow at dump plane inlet
\dot{m}_{of}	Mass flow through projected flameholder area
\dot{m}_r	Rate of air consumption in stirred reactor
\dot{m}_{rc}	Experimentally measured recirculating mass flow
m_s	Quantity defined in Eq(A-13)
\dot{m}_x	Mass flow rate at distance X_L downstream
n	Overall reaction order

r	Volumetric reaction rate
r_p	Radius at which probe located
s	Temperature exponent in Eq(68)
t	Equivalence ratio exponent in Eq(68)
\bar{t}	Mean residence time in RZ; see Eq(A-35)
u', v', w'	RMS turbulent velocity components
x	Index in hydrocarbon expression C_xH_y
x_L	Coordinate axis: distance from dump plane
x'_L	Distance from dump plane at which entrainment ceases
x_P, x_Q, x_R	x coordinates of points P, Q, R
y	Index of hydrocarbon expression C_xH_y
y_L	Coordinate axis shown in Fig A-7
Greek letter symbols	
Λ	Free stream turbulence parameter; see Eq(B-13)
Φ	Air loading parameter
Φ'	Φ_{\max}/k_1
Φ_{\max}	Local peak value of Φ
X	Correlating parameter defined by Eq(46)
ψ	Modified air loading parameter; see Eq(10)
Ψ	Air loading parameter defined in Eq(18)
$\Omega_1, \Omega_2, \Omega_3$	Correlating groups given in Figs 51, 54, and 55
$\alpha, \beta, \gamma, \delta$	Exponents used in stability group $U^\alpha/P^\beta D_f^\gamma T^\delta$
δ_0	Representative flame thickness ($\frac{a}{S_u}$), see Eq(28) and (35)
ϵ	Fractional oxygen consumption efficiency
ϵ_*	Lowest value of ϵ for stable reactor operation
ϵ_{opt}	Value of ϵ corresponding to Φ_{\max}
ζ	Coordinate normal to streamline

η_c	Combustion efficiency (temperature-rise basis)
θ	Thring-Newby criterion; see Eq(A-9)
θ'	Quantity defined in Eq(A-24)
θ_L	Theta parameter, see Eq(23)
θ_L^{-1}	Inverse theta parameter
2λ	Flameholder characteristic dimension, see Eq(30)
ρ	Density
$\bar{\rho}$	Density term in Eq(48)
ρ_a	Ambient density; see Eq(A-5)
ρ_h	Density for hot-flow; see Eq(A-30)
ρ_0	Density at dump inlet plane
ρ_r	Mean density of RZ; see Eq(A-35) and (B-3)
ρ_{rel}	Ratio of ρ_s to ρ_0
ρ_s	Density of secondary stream
τ	Time
τ_{as}	Characteristic reaction time
τ_c	Combustion time, see Eq(33)
$\tau_c(p)$	Combustion time at pressure P atm; see Eq(32)
$\tau_c(p=1)$	Combustion time at pressure of one atm.
τ_{ce}	Characteristic time for rate to increase by exponential factor
τ_{ci}	Characteristic ignition time, see Eq(31)
τ_{cz}	Combustion reaction time, see Eq(29)
τ_{du}	Characteristic flow time (D_f/U)
τ_{hc}	Ignition delay time of hydrocarbon fuel
τ'_{hc}	Ignition delay time defined in Eq(44)
τ_{lu}	Characteristic flow time (L/U); see Eq(31)

τ_{lu_r}	Characteristic flow time (L/U_{rel})
$\tau_{lu_{rz}}$	Characteristic flow time (L/U_{rz}); see Eq(34)
τ_{rz}	Mean particle residence time in RZ; see Eq(29)
τ_{sl}	Turbulent mixing time in shear layer
ν	Molecular kinematic viscosity
ϕ	Equivalence ratio
ϕ_{LBO}	Equivalence ratio at lean blow-out

Abbreviations

$(f/a)_s$	Stoichiometric fuel-air ratio
FFP	Forward Flow Probability
IRR	Integral Rocket Ramjet
GT	Gas Turbine
LBO	Lean Blow-Out
PFR	Plug Flow Reactor
PSR	Perfectly Stirred Reactor
RBO	Rich Blow-Out
RTD	Residence Time Distribution
RZ	Recirculation Zone
SUE	Sudden Expansion

AN INVESTIGATION OF FLAME STABILITY
IN A COAXIAL DUMP COMBUSTOR

by

Edward T. Curran, Ph.D.

Dr. Harold E. Wright, Advisor

An experimental investigation of the flame stability characteristics of a coaxial dump combustion chamber was made. A six-inch diameter combustor was studied, and the dump plane inlet diameter was varied from 2.5" to 5.0". Tests were carried out using pre-mixed ethylene/air and JP-4/air. To avoid vitiation effects, a clean-air heater was used to vary the temperature of the inlet air. The temperature levels were generally in the range 1000-1250°R; the corresponding inlet pressure was varied between approximately 10 and 40 psia. Inlet Mach numbers were typically in the range 0.2 to 0.9.

The flame stability data were not collapsed by a conventional dump combustor correlation. However, a correlating parameter was derived by modelling the annular recirculation zone as an adiabatic stirred reactor using a one-step chemical reaction. This derived correlating parameter was used to obtain successful correlations. The dominant variable in flame stability was the inlet temperature; the subsidiary variables were the step height, inlet pressure, and velocity. The effect of velocity on the lean extinction limit was very small. With JP-4 fuel the existence of complete stability loops was demonstrated by operating at very low combustor pressures.

Some tests were performed with additional fuel injection directly into the recirculation zone. Lean extinction limits were determined

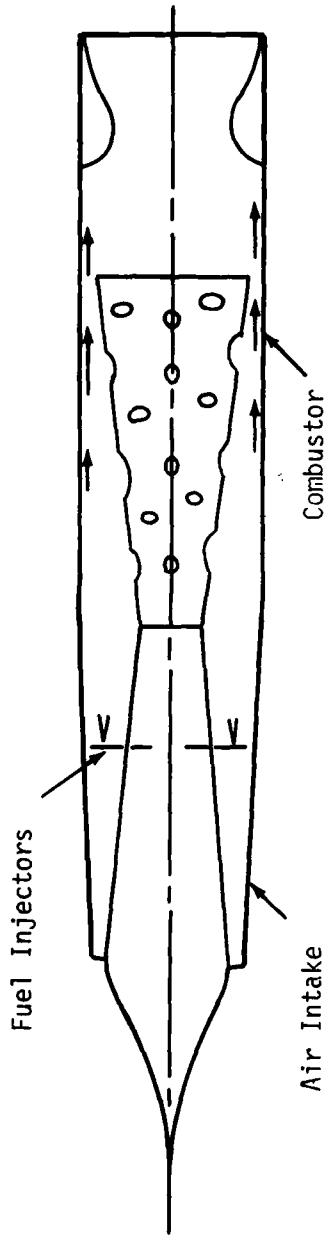
with varying fractions of the total fuel flow being injected into the recirculation zone. These tests yielded an estimate of the air mass flow fraction entrained into the recirculation zone.

Finally, tests were performed using a transparent quartz combustor; it was observed that the combustion process was an oscillatory phenomenon with the reaction zone moving rapidly to and fro along the combustor. A comprehensive review of the literature concerning the flame stability and aerodynamics of coaxial dump combustors was presented.

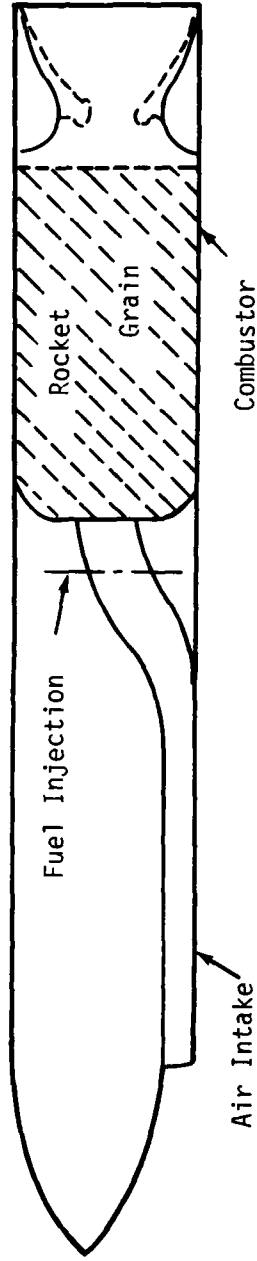
I INTRODUCTION

The subject of this study is the "sudden-expansion" combustion system which has recently been utilized in a new generation of missile propulsion engines, known as integral rocket-ramjet (IRR) engines. This engine design was conceived as a method of reducing missile volume by packaging the required rocket booster within the ramjet engine combustor. The contrast between the conventional ramjet engine and the IRR engine is shown in Fig 1. The "sudden-expansion" (SUE) combustor is the simplest version of a class of combustors generically described as "dump" combustors, examples of which are illustrated in Fig 2. It will be noted that the SUE combustor is essentially of coaxial geometry, and it is created simply by an abrupt increase in cross-sectional area. This abrupt change forces a separation of flow and a corresponding annular recirculation zone (RZ) is generated. The flow structure created provides a region in which an initial flame can be stabilized and from which flame can be propagated into the entering fuel-air mixture.

The introduction of "dump" combustors into ramjet engine systems occurred quite rapidly without the undergirding of a large data base, and the initial development test effort was largely concentrated on determination of the overall factors which influence combustion efficiency, pressure loss, and chamber integrity. Such experimental testing was essentially parametric in nature and yielded urgently needed performance data (Ref 1). Furthermore, there were little data available from related fields of research, although some data of relevance were subsequently found in industrial furnace practice.

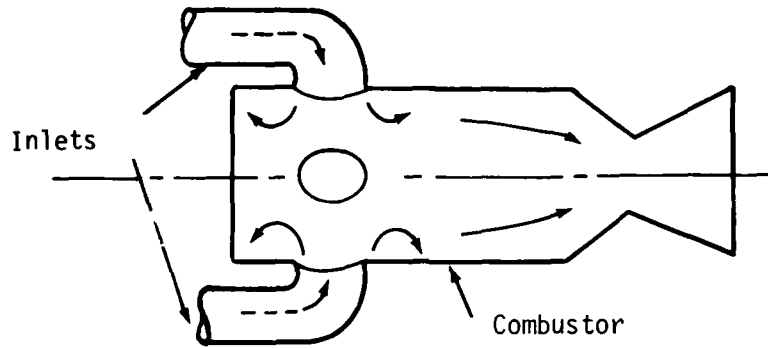


Conventional Ramjet Engine
(External Rocket Booster Required)

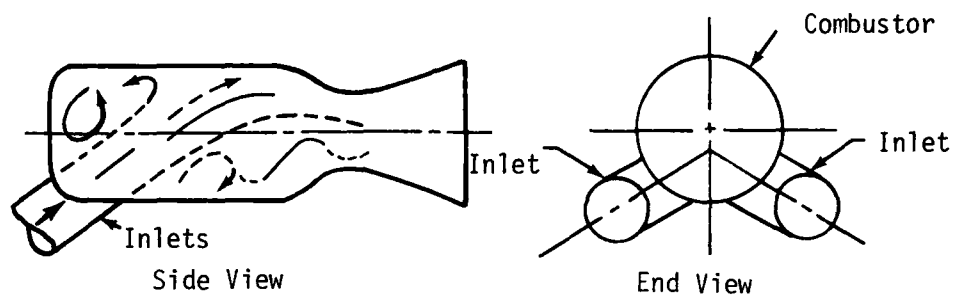


Integral-Rocket Ramjet Engine
(With Integral Rocket Booster)

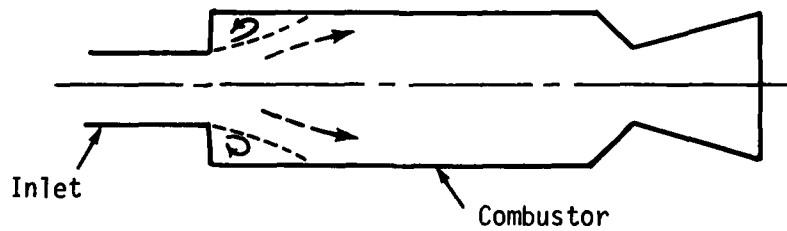
Figure 1. Conventional and Integral-Rocket Ramjet Engines



(a) 4-Port Dump Combustor



(b) 2-Port Dump Combustor



(c) Co-Axial Dump Combustor

Figure 2. Types of Dump Combustor

This situation stood in marked contrast to that existing during the intensive period of development of conventional ramjet engines (circa 1950-1960). At that time, a vast amount of very fruitful research was stimulated, which laid an adequate foundation for the parallel development of combustion systems for gas turbines, afterburners, and ramjets. A representative selection of work reported during this period may be found in the technical literature (Refs 2 through 8).

In view of the paucity of data concerning dump combustors and the general lack of understanding of these devices, a number of long term investigations has been initiated at various research organizations, and examples of recent progress have been published (Refs 9 and 10). However, an important and relatively neglected area of investigation which is vital to predicting dump combustor performance is that of flame stability.

The term "flame stability" is used to describe the retention of effective combustion within the chamber. A more precise term is thus "flame-holding," and the devices which serve to anchor the flame system within the combustor of conventional ramjet engines were often termed "flame-holders." However, current usage is to refer to such devices as "flame-stabilizers," and the process of flame retention as "flame stabilization." Generally, flame can be held within a combustor over a range of fuel/air ratios varying from a weak mixture limit to a rich mixture limit. For a given combustor geometry, the range of operation is primarily dependent on combustor entry conditions such as the velocity (U), temperature (T), and pressure (P). For a single flame-stabilizing element, such as a cone, the range of stable operation

may be displayed in terms of a parameter of the form $U^\alpha/P^\beta D_f^\gamma T^\delta$ where D_f is a representative dimension of the flame-holder. A typical flame stability loop for such a bluff body is shown in Fig 3, and in this case $\alpha = \beta = \gamma = 1$, $\delta = 1.5$. Thus, for a given size of flame-holder, the region of stable operation is enhanced by low velocity, high temperature, and high pressure. For an integral rocket-ramjet engine operating in the flight regime from Mach 2.5 to Mach 4.0, the typical range of variation for these parameters is: velocity, 900 to 1200 fps; temperature, 1100 to 1600°R; and pressure, 10 to 100 psi. In general, it will be impossible to maintain flame at extreme conditions of high velocity or at too low a temperature or pressure. In practice, the weak limit is of more importance than the rich limit because, for efficient cruising flight, it is necessary to operate the engine at very lean fuel-air ratios. The rich limit is usually achieved at fuel-air ratios greater than stoichiometric, a region in which it is not normally desired to operate the engine. Additionally, as fuel-air ratios approach the rich limit, experience shows that very unstable operating conditions are encountered which result in severe thermal and mechanical stresses on the engine.

It is thus apparent that the phenomenon of flame stabilization is, in effect, a switch which controls the "on-off" operation of the combustion system. As such, it limits the operating regime of the combustor and of the engine. Furthermore, if extinction of combustion occurs with an unmanned vehicle during flight, it is usually impractical to automatically re-establish combustion. Consequently, the vehicle flight is terminated. Thus, for all classes of ramjet engines, the maintenance of flame stability is vital.

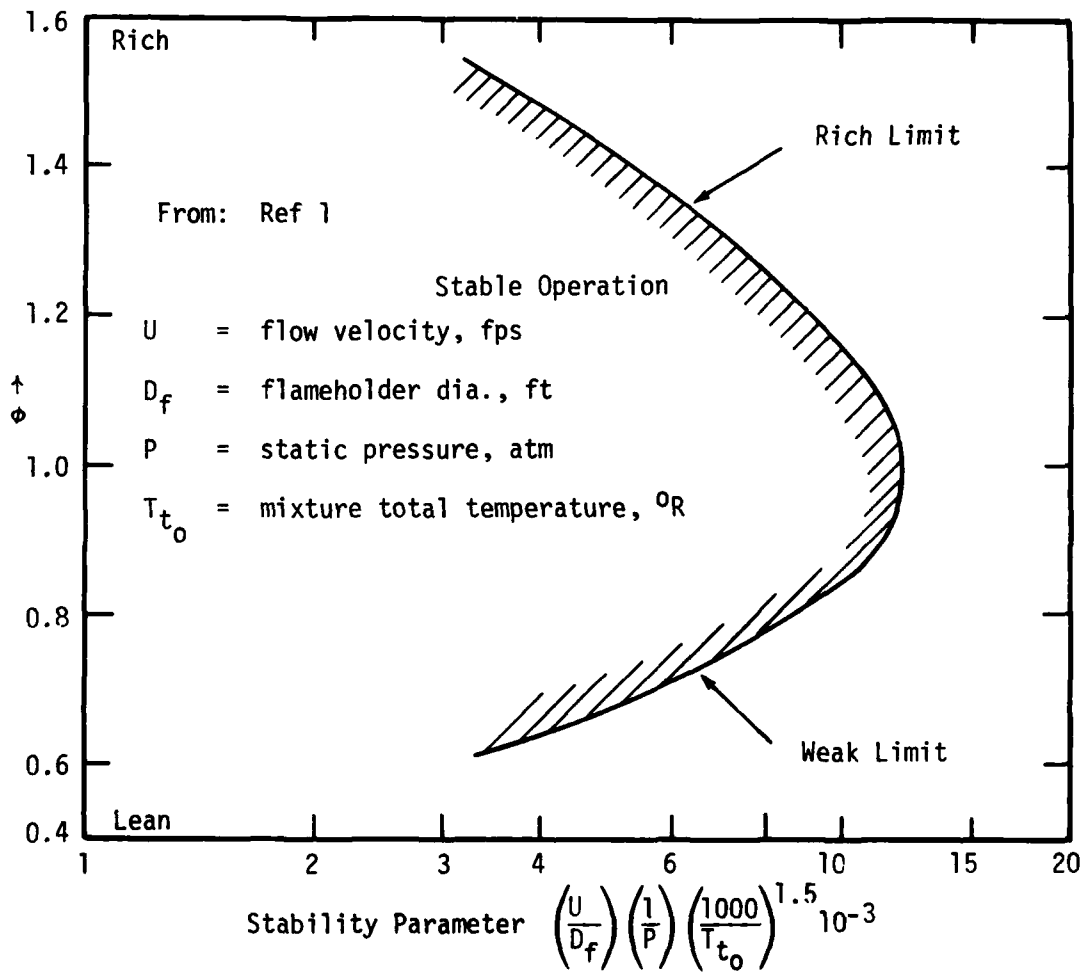


Figure 3. Typical Flame Stability Loop for a Bluff Body

In the case of the IRR combustor, the situation is more severe than for conventional ramjet combustors. The latter may employ mechanical flame-stabilizers (e.g., gutters), but in the case of the dump combustor, no stabilizers can be inserted into the combustor because of the presence of the rocket grain. Consequently, flame stability must be achieved by utilizing the flow structure created by the abrupt change in area; this primary means of stabilization may be augmented by low-blockage mechanical elements located at the dump plane. However, these latter elements are highly undesirable because of their attendant pressure losses. As noted earlier, little data are available for the flame stability of the axisymmetric step geometries associated with coaxial dump combustors, and no proven parameter exists for correlating the data that are available.

Consequently, the first goal of this exploratory investigation was to determine the flame stability characteristics of coaxial dump geometries of various diameter ratios (d/D), over a range of inlet operating conditions. A second goal was to construct a theoretical model of the flame stabilizing mechanism and to determine a suitable parameter that would correlate available experimental data.

The experimental investigation of flame stability limits was carried out in the test facilities of the Air Force Aero Propulsion Laboratory. A baseline combustor diameter of 6.0" was chosen to match the facility capability; the corresponding length was 30.0". The diameter of the inlet to the combustor was varied from 2.5" to 5.0" and thus the corresponding step heights varied from 1.75" to 0.5". Six basic combustor geometries were investigated. Furthermore, the exhaust nozzle area was also varied to provide various inlet velocity levels

to the chamber. Typically, inlet Mach numbers were in the range 0.2 to 0.9. No flameholders were employed. To avoid the vitiation effects associated with combustion pre-heaters, a clean air heater was utilized in this investigation to vary the temperature of the inlet air. The temperature levels were generally in the range 1000-1250°R; the corresponding inlet pressure was varied between 10 and 40 psia. These test conditions were selected in order to simulate relatively severe operating conditions. All tests were carried out using premixed fuel and air. Both ethylene and JP-4 were used as fuels. In addition to the primary tests to investigate flame stability, tests were carried out to investigate the effect of additional fuel injection into the recirculation zone; also a transparent quartz combustor was briefly installed to permit visual study of the internal flame pattern.

This report basically consists of four main divisions. Initially, a brief review of the flame stability characteristics of bluff bodies is given: both homogeneous reactor and characteristic time theories of flame stabilization are reviewed. This section is concluded by a survey of the relatively meager data concerning dump combustors. Secondly, an analysis of the aerodynamics and flame stability of coaxial dump combustors is presented; this is followed by a description of the experimental program. Finally, the results of this investigation are presented, and appropriate conclusions are drawn.

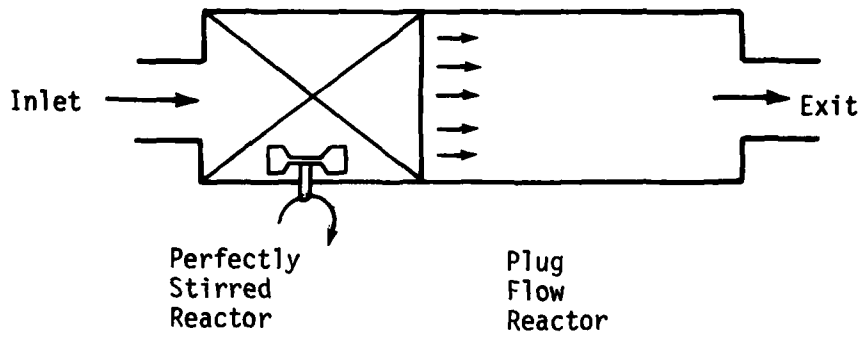
In the next chapter, a brief review will initially be given of earlier work concerning bluff-body flame stabilization, followed by a survey of both the available SUE-combustor results and data from similar geometries such as steps and recesses.

II FLAME STABILITY AND COMBUSTOR OPERATION

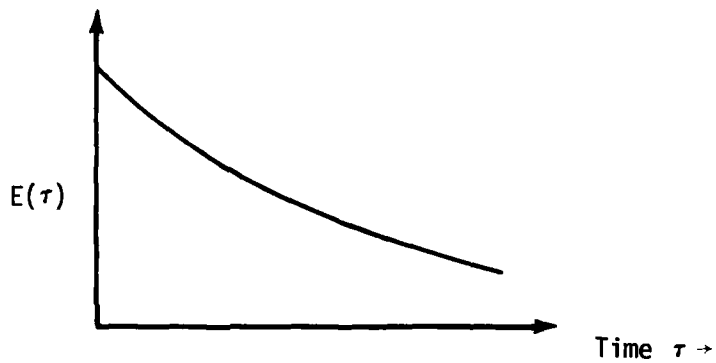
The primary function of the combustion chamber is to maximize the available energy released by the combustion process. This requires that the combustor operate at a high combustion efficiency (η_c), and with minimum pressure loss (ΔP_t). For a given level of available energy there will exist a region of trade-off between efficiency and pressure loss which permits some flexibility in the engineering design of the combustion system. The combustion process must be maintained over a given range of engine operation. Also, the process must usually be accomplished in a small volume, i.e., at high intensity, and the structural integrity of the combustor must be assured.

The combustion process itself obviously requires an intimate contact of fuel and oxidant elements at a point in their respective flow histories where rapid reaction is possible and, for effective operation, the corresponding energy release must occur before the products leave the combustor. In addition to the turbulent mixing and molecular diffusion processes in the combustor which bring about intimate contact of the reactants, it should be borne in mind that larger scale convective flow patterns exist which transfer energy from the combustion products to the entering reactants to sustain the process. These "backmixing" flows are of particular importance in dump combustors. The flow field in the combustor is obviously made much more complex by the concurrent and, in many cases, coupled processes of transport and reaction. Also for heterogeneous processes, say combustion of a liquid fuel, the processes of fuel injection, atomization, evaporation, and diffusion can be identified, without

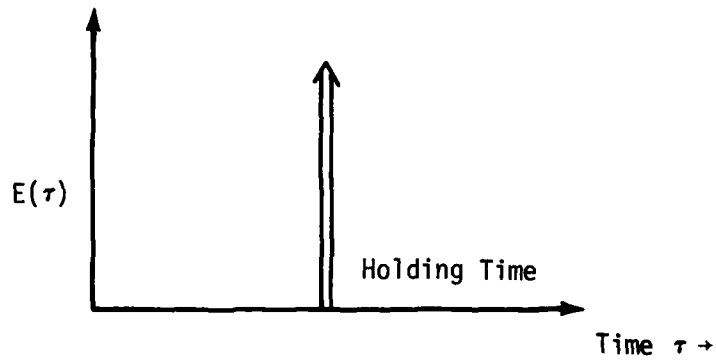
exhausting the manifold mechanisms contributing to the overall conversion of reactants into products. The introduction of simplified concepts to describe the complex combustion processes occurring in practical combustors was one of the key contributions of the work performed in the period 1950-1960. One such concept was that of the homogeneous reaction zone, later termed the Perfectly Stirred Reactor (PSR). The essential features of this concept are twofold; namely, that the reactants introduced into the reactor are instantaneously mixed throughout the reactor volume, and secondly, that reaction is immediate. It follows then that the exit products have the same composition and temperature as the gases within the reactor. Although this is indeed an idealized concept, it was found in practice that certain zones in practical combustors were so intensively mixed (or well-stirred) that they approached the ideal PSR behavior. Of course, it should be noted that the assumption of PSR operation permits relatively simple calculation of reactor behavior. Initially the stirred reactor concept was applied quite widely to the analysis of the flow regions behind bluff-body stabilizers, and this approach permitted a rational prediction of flame stability limits. The concept also permitted estimation of the upper limit of combustion intensity when mixing limitations were removed. It should be noted, however, that stable operation of a PSR is only possible when the combustion efficiency is less than 100%. This latter comment serves to introduce another significant contribution which was due to Bragg (Ref 11): he proposed that for maximum combustion intensity, the ideal combustion chamber should be one in which a PSR section was followed immediately by a Plug Flow Reactor (PFR), as illustrated in Fig 4. This latter reactor is characterized



(a) Idealized Combustor [Bragg (Ref 11)]



(b) PSR: Residence Time Distribution



(c) PFR: Residence Time Distribution

Figure 4. Idealized Reactor Concepts

as one in which all the elements move through the reactor with constant and equal velocity with no longitudinal mixing of the fluid along the flow path. The function of the PFR is to permit the unburned reactants from the PSR section to be completely consumed.

The utility of the PSR-PFR concept is that in many practical combustion systems, a stirred section is essential to provide flame stability, and such a section can be physically identified within the combustor, together with a section which enables the combustion reaction to be effectively completed. A convincing experimental demonstration of this concept is given by Beer and Lee (Ref 12). Furthermore, the basic PSR-PFR concept can be generalized so that complex combustors can be represented by an appropriate network of PSR and PFR elements. Ultimately, as increasing numbers of elemental reactors are used, one approaches a finite-difference solution of the combustor flow field. The elaboration of this reactor-module approach is dealt with in both the text due to Vulis (Ref 13) and that of Wen and Fan (Ref 14). Attention is also drawn to the contributions of Essenhigh (Refs 15, 16, and 17) and Swithenbank (Refs 18 and 19) to this literature.

At this point, it is appropriate to note that the assumption of a perfectly stirred reaction zone determines an age distribution function for particles leaving the zone. It can be shown that this "residence time distribution" (RTD) function is of an exponential decay form (Ref 20). Similarly, for a plug flow reactor, where the particles entering the reactor at a given time all subsequently exit together, the RTD function is a simple pulse, or delta function, located at the given residence time. The RTD functions are also illustrated in Fig 4. The relevance of this observation is that zones may

be identified within a combustor which approximate PSR or PFR behavior by observing the corresponding residence time distributions. However, such observations are usually carried in cold flow models, particularly in water tunnel models of combustion systems. Furthermore, if a combustor flow field is modelled by a network of PSR-PFR elements, the overall RTD of the combustor model may be experimentally determined to test the suitability of the assumed network. Unfortunately, such determinations do not necessarily confirm the uniqueness of the model configuration.

In summary, the modelling of a combustor flow by a reactor network offers a physically realistic approach which, in varying degrees, is capable of experimental verification. The network may be constructed at various levels of sophistication while maintaining a structured approach to the representation of complex reactor flows. In this current investigation, the representation of the flame stabilizing region by a stirred reactor is of immediate relevance, and this discussion will be engaged in the next section.

Stirred Reactor Characteristics

In this section, the stable operating range of a stirred reactor is discussed, and the application of this concept to the prediction of flame stability limits is introduced. Following this initial discussion, a review of experimental data is given, and a discussion of various theories of flame stabilization is presented.

The adiabatic operation of a stirred reactor is now considered. For the homogeneous combustion of fuel and oxidizer, various reaction mechanisms may be postulated. However, it will become apparent later in this discussion that a simple, one-step reaction model is quite

adequate to describe the phenomenological behavior of practical flame stabilizing systems. For purposes of illustration, an overall reaction of order two is now considered. In particular, the reaction is assumed to be of order one for both fuel and oxidizer.

The volumetric reaction rate (r) may then be written as

$$r = k_1 \left\{ \sqrt{T_r} e^{-E/RT_r} \right\} \left\{ C_o C_f \right\} \quad (1)$$

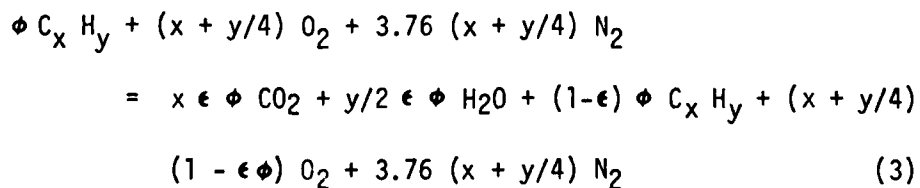
where C_o , C_f denote the concentrations of oxygen and fuel, and T_r is the reaction temperature. It is important to note in this equation that in the initial stages of the reaction, the reactants are consumed with little rise in temperature. Subsequently, the exponential temperature term soon gives rise to a rapid increase in reaction rate until depletion of the reactants causes the rate of decrease. The typical progression of this type of adiabatic reaction is shown in Fig 5. Using Eq(1), the rate of oxygen consumption by the reactor may be expressed as:

$$\frac{\dot{m}_r \phi \epsilon}{1+m} = V \left\{ k_1 \sqrt{T_r} e^{-E/RT_r} \right\} \left\{ \frac{P_r}{RT_r} \right\}^2 X_o X_f$$

or

$$\frac{\dot{m}_r}{VP_r^2} = \frac{(1+m)}{R^2} \left\{ \frac{k_1 e^{-E/RT_r}}{T_r^{3/2}} \right\} \frac{1}{\phi \epsilon} X_o X_f \quad (2)$$

Typically for a weak mixture of hydrocarbon and air, the stoichiometry of the combustion reaction may be written as follows:



Reaction Rate
Per Unit Time
And Volume

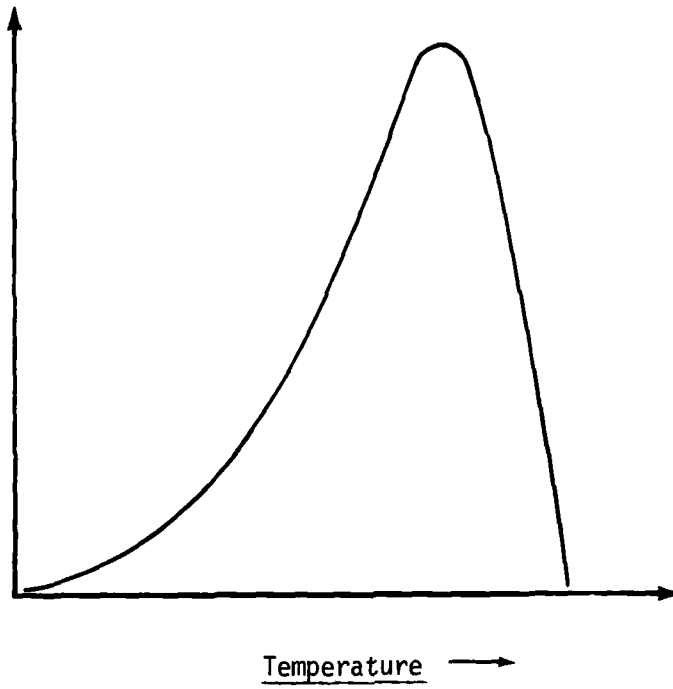


Figure 5. Progress of Reaction

where ϕ = equivalence ratio
 ϵ = fractional oxygen consumption efficiency

Utilizing Eq(3), the mole fractions of fuel and oxygen may be written

$$X_f = \frac{(1 - \epsilon) \phi}{4.76 (x + y/4) + \phi + \epsilon \phi (y/4 - 1)} \quad (4a)$$

$$X_o = \frac{(x + y/4) (1 - \epsilon \phi)}{4.76 (x + y/4) + \phi + \epsilon \phi (y/4 - 1)} \quad (4b)$$

Substitution of Eqs(4a) and (4b) into Eq(2) yields

$$\frac{\dot{m}_r}{VP_r^2} = \frac{k_1}{R^2} (m+1) \left\{ \frac{e^{-E/RT_r}}{T_r^{3/2}} \right\} \left\{ \frac{1 - \epsilon (1 - \epsilon \phi) (x + y/4)}{\epsilon (4.76(x+y/4) + \phi + \epsilon \phi (y/4 - 1))^2} \right\} \quad (5)$$

If the contributions of the smaller terms ϕ and $\epsilon \phi (y/4 - 1)$ appearing in the denominator are neglected, one may write

$$\frac{\dot{m}_r}{VP_r^2} \propto \frac{e^{-E/RT_r}}{T_r^{3/2}} \frac{(1 - \epsilon) (1 - \epsilon \phi)}{\epsilon} \quad (6)$$

For rich mixtures, a similar expression may be obtained as follows

$$\frac{\dot{m}_r}{VP_r^2} \propto \frac{e^{-E/RT_r}}{T_r^{3/2}} \frac{\phi (1 - \epsilon)^2}{\epsilon} \quad (7)$$

Thus a general expression is

$$\frac{\dot{m}_r}{VP_r^2} \propto \frac{e^{-E/RT_r}}{T_r^{3/2}} \frac{\phi (1 - \epsilon) (1 - \epsilon j)}{\epsilon j} \quad (8)$$

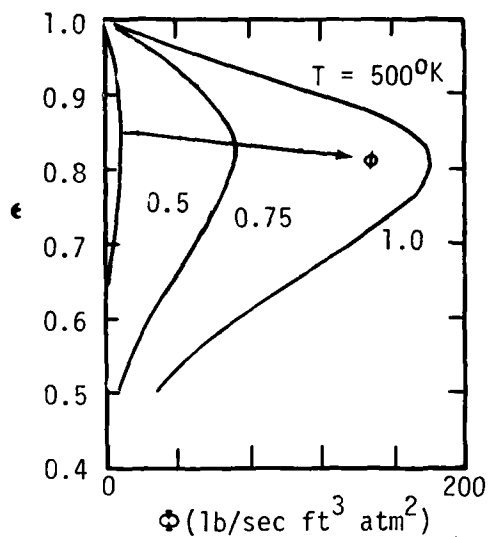
where, for $\phi \leq 1$, $j = \phi$

and for $\phi > 1$, $j = 1$

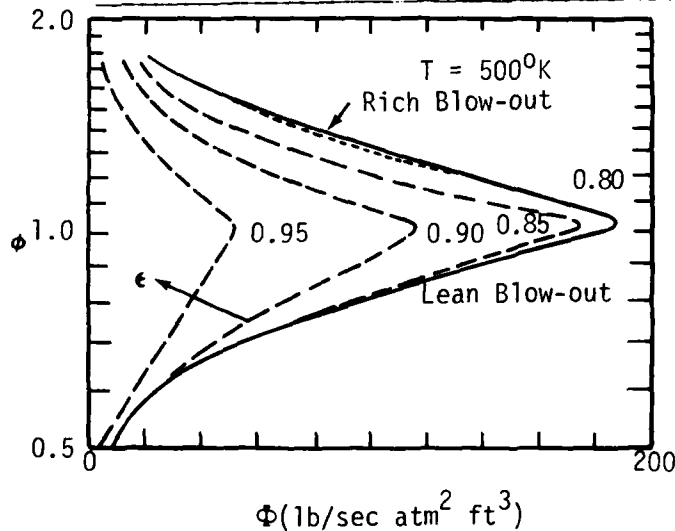
The term $\frac{\dot{m}_r}{VP_r^2}$ has come to be known as the air loading parameter ϕ of the reactor; for a given fuel, this term is a function of the variables ϕ , E , and T_r . The reaction temperature T_r , in turn,

is determined by T , ϕ , and ϵ . Herbert (Refs 21 and 22) has extensively characterized the performance of stirred reactors. In Fig 6, the various relations calculated by Herbert between $\frac{\dot{m}_r}{VP_r^2}$ and ϕ , ϵ , and T are shown schematically. Thus in Fig 6(a), it is shown that for a given ϕ and T the loading parameter ϕ rises to a local peak value ϕ_{\max} with increasing ϵ and then decreases to zero as ϵ approaches 1.0. For the condition shown, ϕ_{\max} occurs at a high value of efficiency ϵ_{opt} ($\epsilon_{\text{opt}} \geq 0.80$ approximately). Furthermore, it can be shown from heat balance considerations that stable operation of the reactor can only be obtained in the region $\epsilon_* \leq \epsilon \leq 1$, where $\epsilon_* \approx \epsilon_{\text{opt}}$.

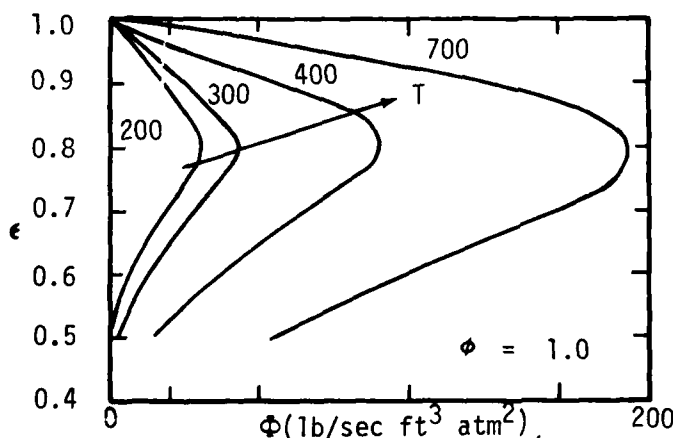
The significance of ϕ_{\max} to the phenomenon of flame stabilization is that, for a given reactor (flameholder) configuration, operating at fixed inlet conditions (T , ϕ , and P), ϕ_{\max} determines the maximum mass flow, and correspondingly, the maximum flow velocity that the reactor can sustain before extinction. It will also be noted that for a given inlet temperature, ϕ_{\max} increases with equivalence ratio in the weak mixture regime, and decreases with equivalence ratio in the rich mixture regime. The peak value of ϕ_{\max} occurs near the stoichiometric equivalence ratio. Thus, reactor operation is constrained between a weak and rich "blow-out" limit as shown in Fig 6(b). Also, it will be noted that as the reactor loading is increased, the range of equivalence ratios over which stable operation can be maintained is diminished with both rich and lean limit equivalence ratios approaching the stoichiometric value, $\phi = 1$. In Fig 6(c) it will also be observed that for a given ϕ , an increase in inlet temperature (T) causes a significant increase in the level of ϕ and correspondingly of the value of ϕ_{\max} .



(a) Relation Between Φ , ϵ , and ϕ (Constant T)



(b) Rich and Lean Blow-out Limits (Constant T)



(c) Relation Between Φ , ϵ , and T (Constant ϕ)

Figure 6. Characteristic Curves of Stirred Reactor

It is convenient at this point to introduce a modified form of air loading parameter. The blow-out air loading ϕ_{\max} is dependent on ϵ , ϕ , and T . Bragg (Ref 11) proposed that the dependence of ϕ_{\max} on T could be represented by a relation of the form $\phi_{\max} \propto e^{T/b}$, where b depends on ϕ . Subsequently, Herbert (Ref 22) proposed the following empirical equation for b , for weak mixture conditions.

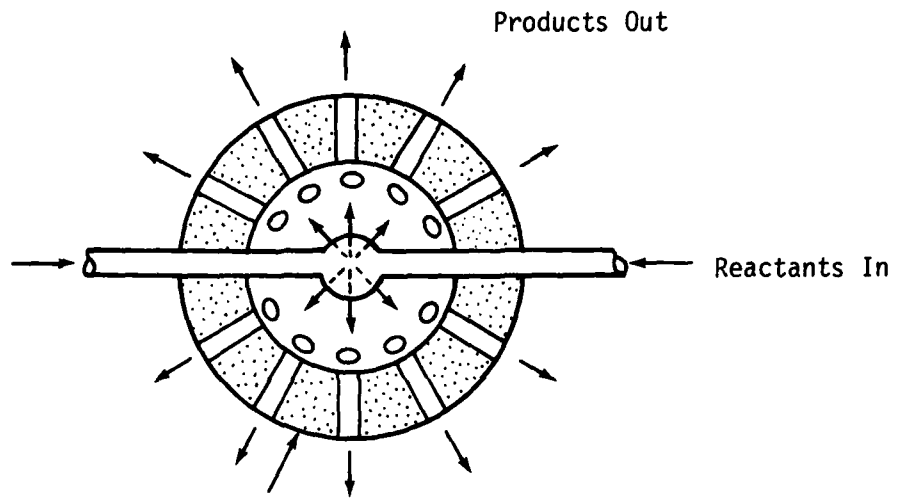
$$b = 245 (1.39 + \ln \phi/1.03), \quad \phi \leq 1.03 \quad (9)$$

This relation for b corresponds to temperature (T) expressed in degrees Kelvin.

A modified air loading parameter (ψ) is now defined as

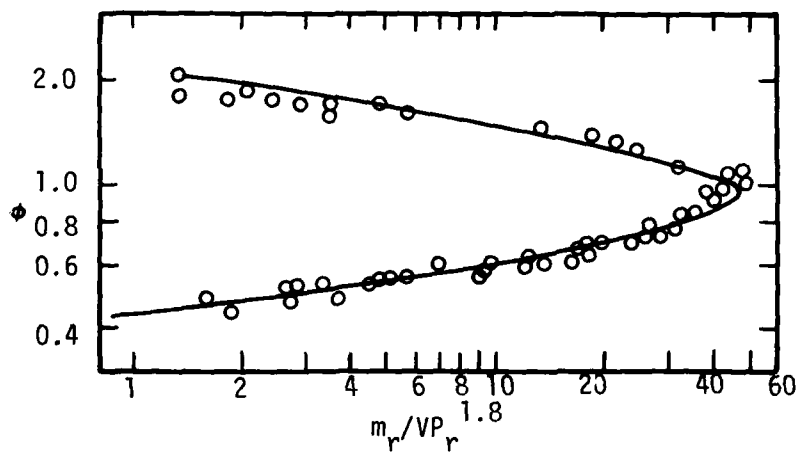
$$\psi = \frac{\phi_{\max}}{e^{T/b}} = \left(\frac{\dot{m}_r}{VP_r^2} \right)_{\max} \frac{1}{e^{T/b}} \quad (10)$$

The validity of the stirred reactor analysis was soon confirmed by the testing of idealized research reactors. Typically, these experimental reactors were of spherical design to provide minimum surface to volume ratio, of small scale, and were operated at near-adiabatic conditions. The dominant design feature, illustrated in Fig 7(a), was the use of a large number of jets to create intense mixing in the reaction zone. Obviously, a high pressure drop was required to produce these jets, and such pressure losses could not be tolerated in practical combustion systems. The principal experimental aim of these researches was to determine the "blow-out" conditions for both lean and rich mixtures at various initial conditions. By comparing experimental blow-out data with theoretical estimates based on equations simulated to Eq(5), it was possible to deduce an overall reaction order (n) for the "global"



Insulating Fire Brick

(a) Schematic Design of Spherical Reactor



(b) Typical Correlation of Data from Spherical Reactor
(Reaction Order = 1.8)

Figure 7. Spherical Combustion-Reactor Characteristics

reaction assumed, for appropriate choices of rate constant (k_1) and the apparent activation energy term (E). The classic experimental work in this area was performed by Longwell and Weiss and is reported in Ref 23: Fig 7(b) is taken from their data and confirms the excellent agreement between experimental data and theoretical prediction which can be obtained by appropriate choice of n , E , and k_1 . It is interesting to note that for the high temperature combustion of hydrocarbons in air, an overall reaction order of 1.8 with an apparent activation energy of 42 KCal/Mol was suggested.

Although much work has been done to elucidate the detailed kinetic and mixing mechanisms associated with hydrocarbon combustion in stirred reactors, the basic one-step model has continued to be of utility, and some useful extensions of this model have been made in recent years. One such refinement has been an improved estimate of the pressure exponent n occurring in the loading term $\frac{\dot{m}_r}{VP_r^n}$. From the time of the early work of Longwell and Weiss (Ref 23), n has usually been assumed to lie in the range 1.75 to 2.00. Indeed Greenhough and Lefebvre (Ref 6) utilized $n = 1.75$ for kerosene-air mixtures with very satisfactory results. However, Hottel et al. (Ref 24), in subsequent reactor studies, argued that n varied with equivalence ratio; they presented data which were compatible with n varying from 1.7 at stoichiometric conditions down to 1.0 at an equivalence ratio of 0.47. An average value of 1.3 was reported for these experiments. It should also be noted that this work was performed using a non-standard fuel, the empirical formula for which was $C_{2.04}H_{4.62}O_{0.85}$.

It is appropriate at this point to draw attention to the extended experimental efforts of Hottel et al. (Ref 25) and of Clarke and his

associates (Refs 26 and 27) in the area of stirred reactors. These investigators refined and extended the foundational work of Longwell and Weiss (Ref 23).

Subsequently, Kretschmer and Odgers (Ref 28) carried out an extensive study of data obtained from propane fueled stirred reactors; they postulated an empirical reaction rate equation based on a one-step model. In this model the value of the exponent n varied with equivalence ratio in the following manner:

$$\text{Weak mixtures} \quad n = 2\phi$$

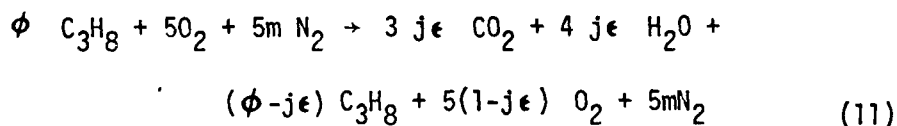
$$\text{Rich mixtures} \quad n = 2/\phi$$

and the individual reaction orders for the fuel and oxygen were assumed to be the same and thus equal to $n/2$. In a subsequent paper, Odgers and Carrier (Ref 29) modified the above-recommended exponents as follows:

<u>Range of ϕ</u>	<u>Recommended Exponent</u>
$\phi \leq 0.5$	1.0
$0.5 < \phi \leq 1.0$	2ϕ
$1.0 < \phi \leq 2.0$	$2/\phi$
$\phi > 2$	1.0

Thus in no case does the value of n become less than unity.

The basic mass balance assumed (Ref 28) was



and the corresponding loading equation becomes

$$\frac{\dot{m}_r}{VP_r^n} = \frac{k_1 (m+1) [5(1-j\epsilon)]^{n/2} [\phi - j\epsilon]^{n/2} e^{-\frac{E}{RT_r}}}{R^n j\epsilon [5(m+1) + \phi + j\epsilon]^n [T_r]^{(n-0.5)}} \quad (12)$$

where, for $\phi \leq 1$, $j = \phi$

and for $\phi > 1$, $j = 1$

However, it should be noted that the use of a semi-empirical reaction rate equation led to substantial variations in the "effective" activation energy term E/R . Despite these substantial variations in activation energy, the model proposed by Kretschmer and Odgers does harmonize a large amount of data concerning propane fueled systems. To apply a quotation from Levy and Weinberg (Ref 30:252), ". . . this may be considered rather fortunate as it tends to justify both the chemists' contempt for, and the engineers' use of the global reaction concept each within their respective fields of application."

In a related development, a recent paper by Ballal and Lefebvre (Ref 31) modelled the weak extinction limits of propane flames stabilized on hollow-cone flameholders using a simple one-step reaction approach. In formulating the analysis, the effect of equivalence ratio ϕ on the exponent n was acknowledged; however, the value of $n = 2\phi$ previously recommended (Refs 28 and 29) was not used. Instead, a value of $n = 1.25$ was assumed which, together with a fixed activation energy of 54,000 cal/g mole, yielded an excellent prediction of weak blow-out limits over equivalence ratios ranging from 0.4 to 0.8. Thus the general trend of reducing n at lower equivalence ratios has been found useful in practical flameholder testing utilizing propane as fuel. The application of basic stirred reactor theory to the prediction of weak extinction limits of flameholders will now be considered in more detail.

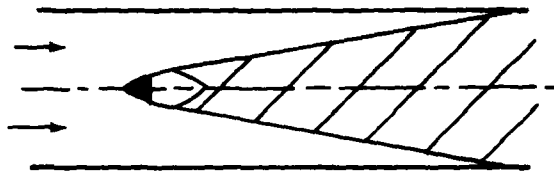
Application of Stirred Reactor Model to Flame Stabilization

Early designs of ramjet engine combustors often incorporated a single stabilizing element such as a cone. The flame pattern corresponding to this design is illustrated in Fig 8(a); for this case, it is possible to separate the combustion process into two elements: flame stabilization and flame propagation (or flame spreading). Much early research was therefore devoted to the flame stabilizing capabilities bluff bodies under various boundary conditions such as free-jet (constant pressure) operation or confined tube (constant area) operation. Examples of such early work are well documented (Refs 32 and 33). In a similar fashion, flame propagation became another area of study.

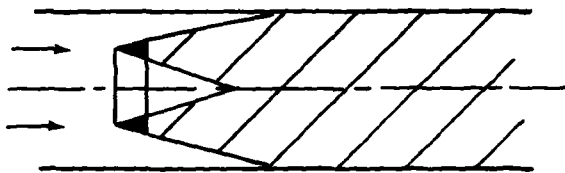
Obviously the configuration shown in Fig 8(a) represents an inefficient use of available volume. Consequently, combustor designs evolved using annular stabilizing elements and, for more controlled flow distribution, the "can" burner concept was introduced. These concepts are shown in Figs 8(b) and 8(c).

It is apparent that in contrast to the system shown in Fig 8(a), where a simple description of the flame spreading process could be given in terms of spatial coordinates and a turbulent flame propagation rate, the systems shown in Figs 8(b) and 8(c) essentially require a "volumetric" description. This volumetric description could be subdivided into a stabilizing or primary zone plus a secondary zone where combustion is effectively completed. The point to be made is that the description of the process must be related to the configuration of the combustor.

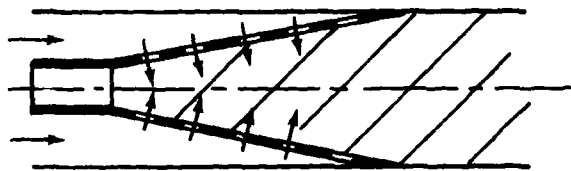
For any of the geometries shown in Figs 8(a), (b), and (c), the stabilizing zone is a region of intense mixing which may be modelled,



(a) Single Stabilizing Element



(b) Annular Gutter Stabilizer



(c) "Can" or "Colander" Burner

Figure 8. Simple Combustor Geometries

at various levels of sophistication, as a stirred reactor. Thus in Fig 9, the recirculation zone (RZ) behind a bluff body is depicted. If this RZ is considered as a stirred reactor, then Eq(10) could be applied to this zone and the corresponding blow-out limits described by a relation of the form

$$\phi_{LBO} = f(\psi) \quad (13)$$

In order to describe the RZ in these terms, two key quantities must be known; namely, the air mass flow into the RZ, and V , the volume of the RZ. For a typical bluff body immersed in a flowing homogeneous fuel-air mixture, it is generally assured that \dot{m}_r is proportional to the density of the stream (ρ), the surface area of the RZ (S), and the flow velocity at the edge of the body (U). The further assumptions are made that $S \propto D_f^2$ and that $V \propto D_f^3$. Hence

$$\frac{\dot{m}_r}{VP_r^2} \propto \frac{\rho D_f^2 U}{D_f^3 P^2} \propto \frac{U}{D_f P T} \quad (14)$$

where P_r has been put equal to P .

From Eq(10), at blow-out conditions

$$\psi = \frac{\dot{m}_r}{VP_r^2} \frac{1}{e^{T/b}} \propto \frac{U}{D_f P} \cdot \frac{1}{T e^{T/b}} \quad (15)$$

Thus for a fixed inlet temperature

$$\psi \propto \frac{U}{D_f P} \quad (16)$$

A number of assumptions have been made in order to estimate the quantities \dot{m}_r and V . The validity of these assumptions will not be discussed at this point, but will be examined later in the context of coaxial dump burners. It should be noted, however, that in a

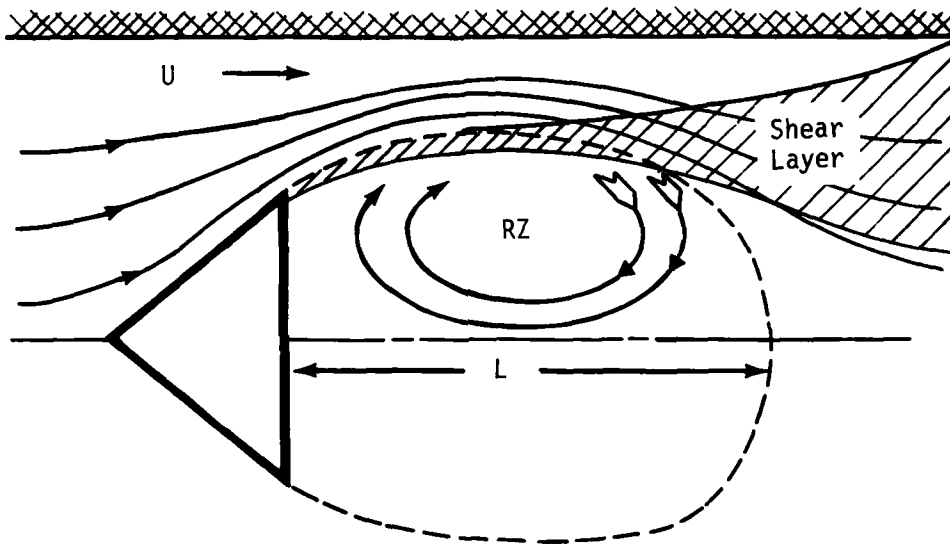


Figure 9. Bluff Body Recirculation Zone

foundational investigation of the flame stability characteristics of circular discs, published in 1955, DeZubay (Ref 32) was able to correlate the experimental data using a loading parameter of the form

$$\psi \propto \frac{U}{\rho^{0.95} D_f} D_f^{0.85} \quad (17)$$

Since that time a vast number of investigations of flame stability have successfully utilized parameters of the form $\frac{U^\alpha}{\rho^\beta D_f^\gamma}$ to correlate isolated bluff body data for constant inlet temperature conditions.

The effect of varying inlet temperature on stability has also been introduced in a direct exponent form rather than in the factor $T e^{T/b}$ of Eq(15); thus another form of loading parameter is

$$\psi_1 \propto \frac{U^\alpha}{\rho^\beta D_f^\gamma T^\delta} \quad (18)$$

The temperature exponent δ cannot be expected to be strictly constant because the appropriate temperature variation is contained in the factor $T e^{T/b}$. Thus δ can be shown to depend on both the equivalence ratio (ϕ) and the range of initial temperatures considered. However, over limited ranges of ϕ and temperature, the use of an exponent δ is acceptable for practical correlations. In a typical correlation quoted by Stull et al. (Ref 1), a value of δ equal to

* Note that U and P in this expression correspond to the values at flame blow-off: these should strictly be denoted by U_{B0} and P_{B0} . However, to avoid complex notation this distinction will not be observed when the context is clearly addressing blow-off conditions.

1.5 is given and, in general, values of δ fall in the range from 1.0 to 2.0.

Up to this point the stability of the recirculating flow region has been discussed solely in terms of homogeneous reactor chemistry. The related influence of the aerodynamics of the flow on the stabilizing process has been considered only in the determination of simple estimates of the mass flow entering the recirculation zone and the corresponding zone volume. However, it will be apparent that the fundamental processes determining flame stability are the transport phenomena occurring in the complex flow field associated with the flameholder. These phenomena are dependent on both the overall flow field generated by the flameholder and the finer details of the flow field. A key factor in determining the overall flow field is, of course, the overall Reynolds number of the flow. The states of the boundary layer/wake flows associated with the flameholder are also important. In particular, the flame stability characteristics will be affected as the state of the wake changes from laminar, through transitional, to fully turbulent. For most practical applications, the flows will be fully turbulent.

The interrelation between the chemical and aerodynamic factors has generally been acknowledged by assuming that for a given fuel/air ratio the performance of a combustion system is dependent on the loading (ψ) and the associated Reynolds number (R_e). In particular, Herbert (Ref 34) has assumed that

$$\psi \propto (R_e)^{-f} \quad (19)$$

where for fully turbulent flows f has a value in the region of 0.05 to 0.10.

One of the finer details of the flow field is the state of the approach stream turbulence; this factor can influence the flame stability to varying degrees depending on the geometry and flow conditions of the flameholder. The effect of free stream turbulence characteristics on the flow field associated with a bluff body is an emerging field of study (Ref 35), and no generalized comments can be usefully summarized at this time. However, in the recent investigation by Ballal and Lefebvre (Ref 31) of the stability of hollow cone stabilizers, it was shown that the effect of free stream turbulence intensity could be accounted for by simply modifying the local velocity term.

Another aerodynamic phenomenon of considerable significance is that of interaction of the flameholder flow field with the boundary of the surrounding flow. The blockage produced by the presence of the flameholder in a pipe results in an acceleration of the flow as it approaches the edge of the flameholder and simultaneously affects the flow field structure downstream of the flameholder. Hence, the degree of blockage is a factor of considerable importance. Thus Wright (Ref 36) found that, for a flat plate flameholder, the length of the recirculation zone (L) varied inversely as the square root of the blockage ratio (flameholder area/duct area). Interestingly, it was also found that the width of the flameholder wake (W) varied inversely as the square root of the blockage ratio. Thus the ratio L/W was found to remain approximately constant even though L and W varied markedly with blockage. It follows from the above that the blockage ratio is an important aerodynamic factor affecting the flame stability of bluff body flameholders. It should also be noted that because of the flow deflection produced by some bluff body shapes, the effective aerodynamic blockage may be significantly greater than the corresponding geometric blockage (Ref 37).

To recapitulate, it will be appreciated that the analysis of flame stability phenomena is a most complex task. The description of flameholder performance by a parameter of the form shown in Eq(18) is an attempt to account for the major controlling factors in a simplified manner. Consequently, the set of exponents $\alpha, \beta, \gamma, \delta$ will generally assume different, but nevertheless bounded values which depend on the specific flameholder configuration, fuel, and approach flow conditions.

It is convenient at this point to draw attention to a recent attempt to correlate flame stability limits by Plee and Mellor (Ref 38), utilizing a parameter denoted as the "inverse theta parameter" (θ_L^{-1}). The origin of the basic θ_L parameter may be found in the early work of Greenhough and Lefebvre (Ref 6), who were seeking a parameter to describe the efficiency of gas turbine combustors. A full derivation of this parameter was given subsequently by Lefebvre (Ref 39), and some early correlations were displayed by Lefebvre and Halls (Ref 40). In principle, the combustion process is modelled as a turbulent flame brush. An energy balance then leads to the result that combustion efficiency is proportional to the ratio of turbulent flame speed (S_T) to a reference velocity (U_{ref}) in the combustion chamber.

$$\eta_c \propto \frac{S_T}{U_{ref}} \quad (20)$$

Damköhler's relation (Ref 41) between turbulent flame speed (S_T), laminar flame speed (S_u), and Reynolds number, $S_T \propto S_u Re^c$, is then employed, yielding

$$\eta_c \propto \frac{S_u Re^c}{U_{ref}} \quad (21)$$

A second order reaction process is then assumed, which implies that S_u is independent of pressure. The effect of initial temperature is neglected at this point, leading to a semi-empirical relation which is essentially

$$\eta_c = f \left\{ \frac{p^{1.75} A_{ref} D_{ref}^{0.75}}{\dot{m}} \right\} \quad (22)$$

where the terms A_{ref} and D_{ref} are a reference combustor area and diameter, respectively.

An initial temperature correction is now introduced into the expression, yielding

$$\eta_c = f(\theta_L) \text{ where } \theta_L = \frac{p^{1.75} A_{ref} D_{ref}^{0.75} e^{T/b}}{\dot{m}} \quad (23)$$

Thus for a given combustor, the combustion efficiency is related to the pressure (P) and temperature (T) conditions at entry and the corresponding mass flow (\dot{m}). The "theta" parameter has been very successfully utilized for the correlation of combustion efficiency data and for the initial design of gas turbine combustors. The application of the theta parameter to the correlation of flame stability is an attempt to extend its utility. In this case, the reciprocal of the theta parameter, termed the "inverse theta parameter," is a more suitable form, and for a given combustor it may be expressed as

$$\theta_L^{-1} \propto \frac{U}{p^{0.75} T_e^{T/b}} \quad (24)$$

The inverse theta parameter can also be expressed as $\theta_L^{-1} \propto U^\alpha / p^\beta T^\delta$, the form conventionally used for correlating flame stability data.

However, there was little direct evidence that the θ_L^{-1} parameter would be effective in correlating flame stability data, although partial success was achieved (Ref 6). Plee and Mellor (Ref 38) subsequently found that use of the θ_L^{-1} parameter did indicate stability trends (i.e., the weak extinction limit ϕ_{LBO} increased with θ_L^{-1}), but good correlations were not generally obtained. However, it would be premature to discard the inverse theta parameter at this time pending further experimental work.

Up to this point the phenomenon of flame blow-off has been approached solely from the point of view of stirred reactor theory. However, other theories of flame stabilization have been proposed, and some are of technological interest. In the next section a brief review of such theories will be given.

Alternative Criteria for Flame Stabilization

Historically, flame stability criteria were evolved to describe the stable operating range of laboratory-type burners. These criteria were sought employing such relatively fundamental combustion concepts as the laminar and turbulent flame speeds associated with pre-mixed combustibles. A significant starting point for this discussion is the work of Putnam and Jensen (Ref 42), in which was derived a Peclet number criterion for predicting "flash back" of laboratory-type burners. These investigators used a conventional velocity gradient approach which basically assumes that stable operation occurs when flow velocity (U) and laminar flame propagation velocity (S_u) are matched: their criteria for equilibrium was that

$$P_{eu} = k_2 (P_{es})^2 \quad (25)$$

where P_{eu} is the Peclet number based on average flow velocity $(\frac{UD_f}{a})$,

P_{es} is the Peclet number based on laminar flame speed $(\frac{S_u D_f}{a})$,

D_f is a characteristic dimension of flameholder, and

a is the thermal diffusivity.

This flash-back criteria was also applied to describe blow-off data of small axial rod flameholders; a good correlation was obtained with an expression of the form given in Eq(25). An important observation made by Putnam and Jensen was that Eq(25) could be expressed as

$$\frac{D_f}{U} = \frac{a}{k_2 S_u^2} \quad (26)$$

In the above expression, the term $\frac{D_f}{U}$ may be regarded as a characteristic flow time (τ_{du}) and the term $\frac{a}{S_u^2}$ can be regarded as a characteristic reaction time (τ_{as}). Thus the Peclet number criterion can also be written as $\tau_{du} = \frac{1}{k_2} \tau_{as}$, and if τ_{du} is less than $\frac{1}{k_2} \tau_{as}$, blow-off of the flame will occur. In general, it would be anticipated that τ_{as} would be a function of fuel-type, initial temperature and pressure, and fuel-air ratio. The concept inherent in Eq(26) is a balance between a time associated with the flow (τ_{du}) and a time characteristic of the reaction (τ_{as}): this concept will appear repeatedly in this review.

The basic Peclet number criterion was placed on a more general theoretical basis by Spalding and Tall (Ref 43); for high values of Peclet number, their criterion for flame stabilization was written

$$\frac{U D_f}{a} \propto \left\{ \frac{S_u D_f}{a} \right\}^2 \quad (27)$$

which is of the same form as Eq(25). However, it must be noted that these authors introduced the laminar flame speed into their analysis as a measure of the reaction rate ($\propto S_u^2$) and not as an index of flame propagation rate. The form of correlation of data anticipated by Eq(27) is shown schematically in Fig 10. Acceptable data correlations have been published (Ref 44); however, additional data acquired since the publication of this reference have not been satisfactorily correlated as shown by Shchetinkov (Ref 45). In order to utilize the criterion of Eq(27), the Peclet number, based on the laminar flame speed, has to be evaluated. Unfortunately, neither S_u nor thermal diffusivity values are generally available for gas mixtures at conditions of technological interest; consequently, this particular criterion has not found wide application.

Another flame stability criterion which deserves brief mention is that of extinction due to "flame-stretch." This concept also arose in connection with laboratory studies of turbulent flames and was originated by Karlovitz et al. (Ref 46). It was observed that flame propagation was arrested in regions of flow where steep velocity gradients existed. The corresponding increase in flame surface area, or "flame-stretch" in the steep gradient area, was quantified using a factor termed the "Karlovitz number (K)" defined as

$$K = \frac{\delta_0}{U} \frac{dU}{d\xi} \quad (28)$$

where $U(\xi)$ is the local velocity of unburned gas, $\frac{dU}{d\xi}$ the velocity gradient, and δ_0 a representative flame thickness defined as

$$\delta_0 = a/S_u.$$

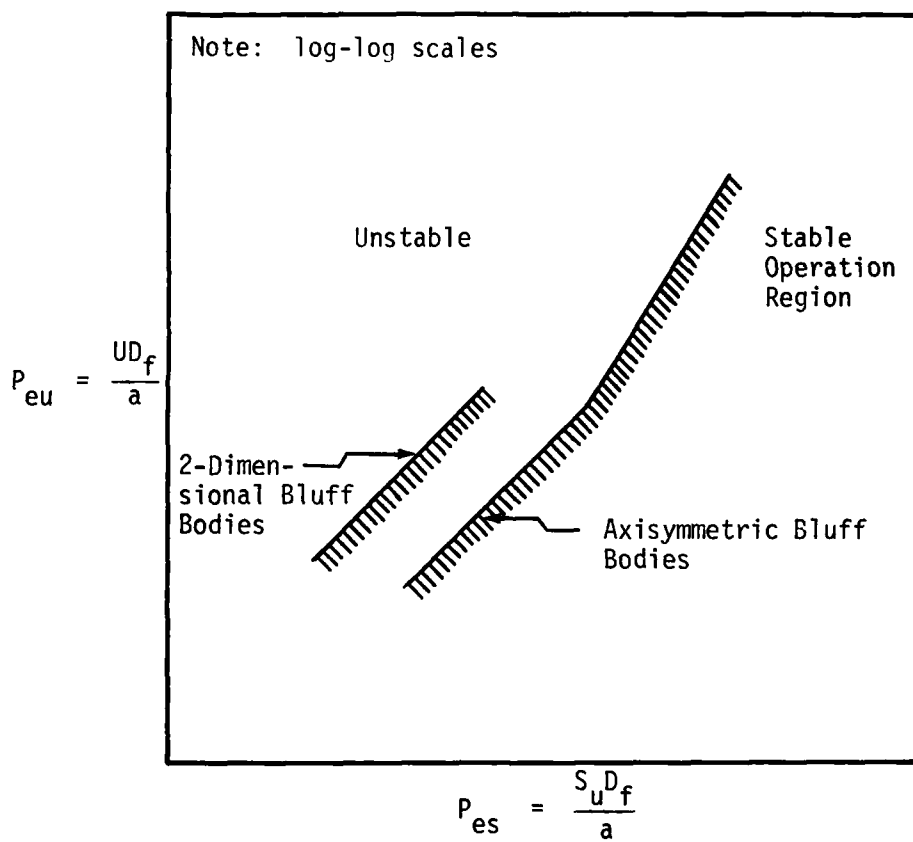


Figure 10. Flame Stability Correlation Based on Peclet Number

The utility of the Karlovitz number is that a critical value of K may be determined above which flame extinction occurs. Lewis and von Elbe (Ref 47) have applied the Karlovitz criterion to bluff-body flame stabilization with modest success. However, the validity of the flame-stretch concept is still a subject of controversy as exemplified in the discussion of Melvin and Moss (Ref 48). Also, like the Peclet number criterion, the Karlovitz number has found no general application to combustion processes of technological interest.

Meanwhile, in the early Soviet literature (Ref 49) on bluff-body flame stability, the work of Dunskey is referenced as the origin of the so-called Mikhel'son criterion (Mi), defined as

$$Mi = \frac{\tau_{rz}}{\tau_{cz}} \quad (29)$$

where τ_{rz} is the mean particle residence time in the recirculation zone (RZ) of the stabilizer and τ_{cz} is a combustion reaction time. In this case, τ_{cz} is taken as the characteristic time associated with the laminar flame speed, namely $\frac{\delta_o}{S_u}$, where δ_o is the flame thickness. Also δ_o is taken as proportional to $\frac{a}{S_u}$ so that τ_{cz} is defined as $\tau_{cz} = \frac{a}{S_u^2}$. Dunskey used a characteristic dimension 2λ so that the Mikhel'son criteria is defined as

$$Mi = \frac{\tau_{rz}}{\tau_{cz}} = \frac{2\lambda}{U} \frac{S_u^2}{a} \quad (30)$$

Shchetnikov (Ref 45) observes that Mi displays a constant value (≈ 0.45) only for limited experiments with small conical stabilizers.

A related but distinct theory put forward by Zukoski and Marble (Ref 50) in the U.S.A. has also been successful in predicting blow-off limits of certain combustor configurations and has found wide application.

A suitable configuration by which to introduce the elements of this theory is the isolated stabilizer shown in Fig 9. In this sketch the recirculation zone is seen to be enveloped by a shear layer which begins as an extension of the boundary layer and becomes progressively thicker in the downstream direction. Mass and energy exchange occurs between the outer flow and the recirculation zone flow through the shear layer. Under stable operating conditions, a flame is initiated in this mixing layer which subsequently propagates into the surrounding flow. Now, according to stirred reactor theory, this initial flame would be extinguished when the stirred reactor attained blow-out. However, Zukoski and Marble postulated that the only active combustion associated with the RZ is limited to the shear layer at the boundary, and that a portion of the burned gas from this flame zone is recirculated upstream to replenish the RZ. The criterion of flame stability is that sufficient reactant gas is ignited during its residence time in the shear layer to propagate a flame. Thus, if U is the local flow velocity and L a length representative of the RZ length, then $\tau_{lu} = L/U$ is a measure of the exposure of the fresh gas to the hot combustion products which serve as an ignition source. In particular, a critical time τ_{ci} is defined for ignition of the flow, thus

$$\tau_{ci} = \frac{L}{U_{B0}} = \tau_{lu} \quad (31)$$

where U_{B0} is the measured blow-off velocity.

The time τ_{ci} was denoted as the "characteristic ignition time." Typical experimental values of τ_{ci} derived from Zukoski and Marble (Ref 50), and from the works of Wright (Ref 36) and Broman (Ref 51) are

shown in Fig 11. The variation of τ_{ci} with ϕ and initial temperature is shown for the specific fuels utilized; the effect of pressure is not documented. Two aspects of the Zukoski-Marble model are now familiar. Firstly, the fluid dynamics of the problem are decoupled from the chemistry. τ_{lu} depends solely on the fluid dynamics and τ_{ci} on the chemistry. Secondly, the blow-off criterion, $\tau_{lu}/\tau_{ci} = 1$, can be regarded as a ratio of residence time to chemical reaction time which is in the form of Damköhler's first dimensionless group for chemical reactors (Ref 52). This residence time/reaction time approach has appeared in recent years in many forms. Thus Mironenko (Refs 53 and 54) introduces a flow time defined as $\tau_{lu_r} = \frac{L}{U_{rel}}$, where L is the length of the RZ zone and U_{rel} is the relative flow velocity. Thus $U_{rel} = U_m + U_p$ where U_m is the downstream velocity of the flow past the stabilizer and U_p is the upstream velocity in the RZ behind the flameholder. Also, a characteristic reaction time τ_{ce} is introduced related to the temperature rise required to increase the associated reaction rate by the exponential factor (e). Using these revised definitions, τ_{lu_r} and τ_{ce} , Mironenko displays good agreement with practical stabilizer configurations, both in the above references and in a more recent work co-authored with Solokhin (Ref 55).

The introduction of the recirculation zone length (L) instead of a flameholder dimension (D_f) as a characteristic length for the flow time has led to increased complexity. Typically, for turbulent flow past a flameholder, L is a rapidly fluctuating quantity and experimental determination of a time-mean value of L is difficult. Extensive investigations of the flow structure and associated L

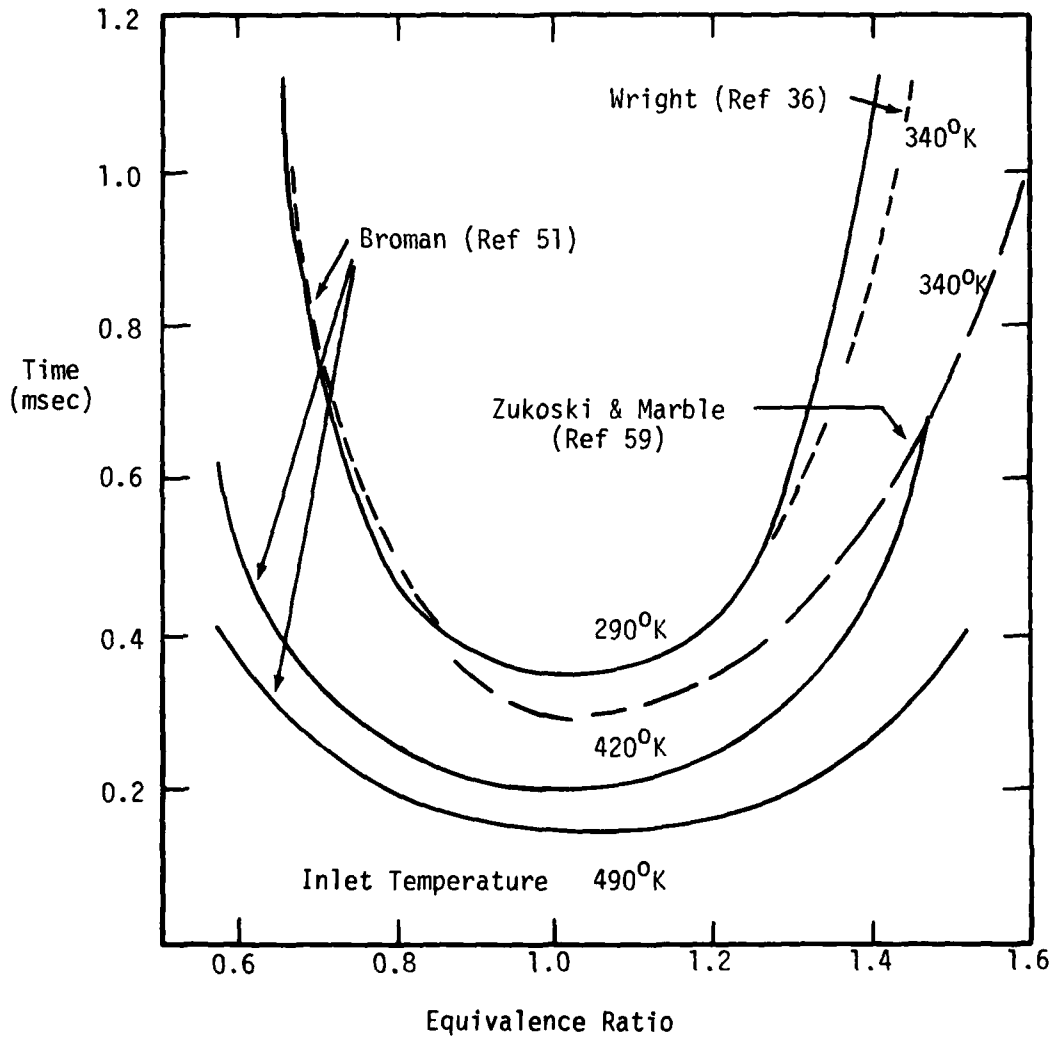


Figure 11. Characteristic Ignition Time

values behind bluff body flameholders have been carried out by Wright (Ref 36), Bovina (Ref 49), and Winterfeld (Refs 56 and 57). These investigations have shown that L is affected by flameholder shape, flow velocity and turbulence, duct blockage, and heat release. Thus the apparent decoupling of flow and chemical phenomena achieved with the τ_{du}/τ_{ci} criteria is lost when L is used as a characteristic length. Nevertheless, Baev and Tret'yakov (Ref 58) have successfully correlated data using a non-dimensional RZ length (\bar{L}), which is corrected for the influence of flameholder shape and blockage. This work is of particular interest because the chemical time utilized is a combustion time based on experimental measurements (Refs 59 and 60) and corrected for pressure variation by use of the expression

$$\tau_{c(p)} = \tau_{c(p=1)} p^{(1-n)} \quad (32)$$

where $\tau_{c(p)}$ is the combustion time corresponding to pressure P and n is the order of the reaction (quoted as 1.6 for gasoline-air mixtures and 1.2-1.3 for propane-air mixtures). The characteristic combustion times for gasoline utilized by Baev and Tret'yakov (Ref 59) are illustrated in Fig 12 and compared to the ignition times obtained experimentally by Zukoski and Marble (Ref 50). Obviously, both sources yield curves of similar shape but of differing magnitudes.

In deriving their correlation, Baev and Tret'yakov (Ref 58) utilized a quenching distance criterion where the flame thickness at blow-off was related to the transverse flameholder size. The final correlating parameter was

$$\frac{U}{D_f} \tau_c = .4624 \left(\frac{L}{D_f} \right)^2 \quad (33)$$

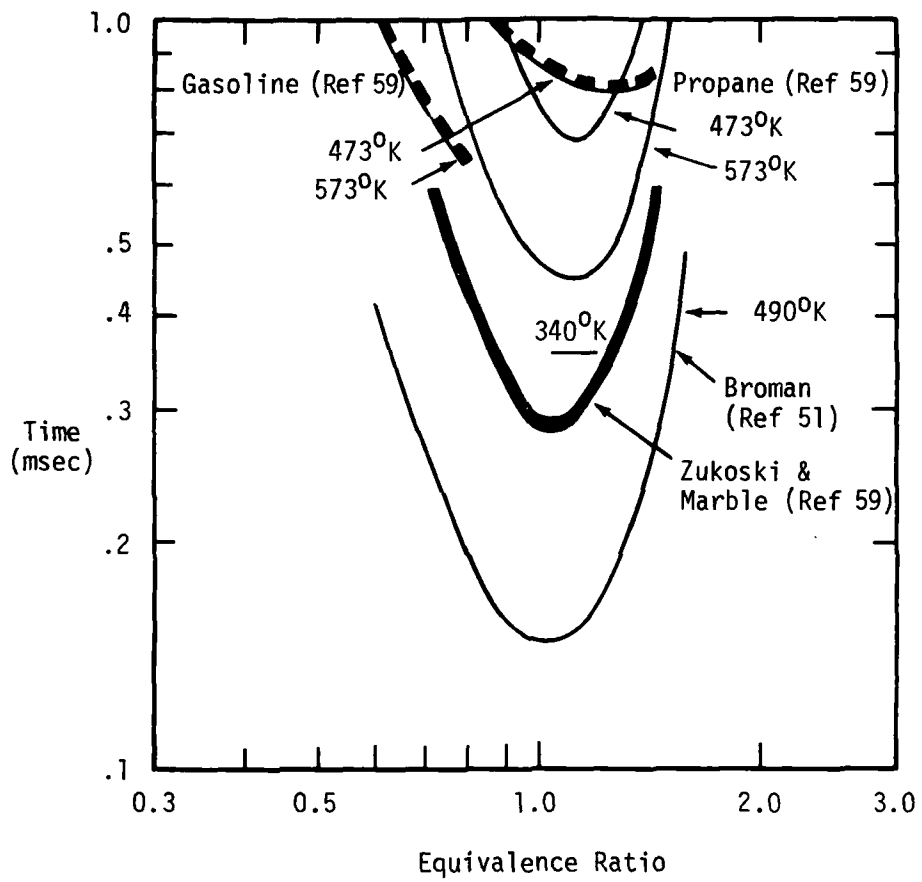


Figure 12. Characteristic Ignition and Combustion Times

As indicated earlier, Winterfeld (Ref 57) carried out a thorough study of flow phenomena associated with recirculation zones behind various shapes of bluff body. He determined both the size and shape of the recirculation zones, the associated velocity field, and the corresponding mean residence times for both cold and burning flows. He was unable to relate blow-off limits to the mean residence time in the zone and concluded that flameholding was controlled by a flow time/reaction time criterion. Winterfeld considered that flameholding would only be obtained if those flow elements which, entering the downstream end of the RZ and flowing upstream, attained ignition before they emerged at the trailing edge of the flameholder. In this case the characteristic residence time could be written $\tau_{l_{urz}}$, where U_{rz} is a mean upstream velocity along the axis of RZ. This latter velocity was assumed proportional to the maximum upstream velocity along the RZ axis, $U_{rz_{max}}$.

Finally, the appropriate residence time $\tau_{l_{urz}}$ was expressed as

$$\tau_{l_{urz}} = \left(\frac{L}{D_f} \right) \left(\frac{U}{U_{rz_{max}}} \right) \left(\frac{D_f}{U} \right) \quad (34)$$

The term $U/U_{rz_{max}}$ is of the order 0.3-0.5 for typical bluff body shapes.

In a subsequent work, however, Winterfeld (Ref 61) returned to a simpler criterion and employed the ratio of a characteristic stay time τ_{l_u} to a characteristic reaction time τ_c to describe stability. Significantly, he has pointed out that such times cannot be clearly definable when so many physio-chemical processes are occurring concurrently. However, the stay time τ_{l_u} was broadly defined as the ratio of an appropriate length and a related velocity: typically

$\tau_{L_u} = L/U$. In selecting a characteristic time for the reaction, Winterfeld effectively considered the turbulent flame as a wrinkled laminar flame with the corresponding reaction time taken as

$$\tau_{as} \propto \frac{\delta_0}{S_u} \quad (35)$$

where δ_0 is equal to a representative flame thickness. It was further assumed that $\delta_0 \propto \bar{a}/S_u$, where \bar{a} is an effective thermal diffusivity. Thus, for the characteristic reaction time τ_{as} , one has

$$\tau_{as} \propto \bar{a}/S_u^2 \quad (36)$$

and the ratio τ_{L_u}/τ_{as} can be written

$$\frac{\tau_{L_u}}{\tau_{as}} \sim \frac{L}{U} \frac{S_u^2}{\bar{a}} \quad (37)$$

Winterfeld has termed the right-hand side of Eq(37) the characteristic factor K_{FL} for flame stabilization.

$$K_{FL} = \frac{L}{U} \frac{S_u^2}{\bar{a}} \quad (38)$$

which is a useful parameter for comparing the flameholding performance of different fuels. Winterfeld further assumes that $S_u \propto p^{-0.1}$ (which implies a reaction order of 1.8) and that the thermal diffusivity is proportional to pressure; these assumptions yield an overall stability criterion given by

$$\frac{L}{Up^{0.8}} = f(\phi, T) \quad (39)$$

Yet another approach, which at first sight is similar to the Zukoski and Marble theory, is the recently introduced characteristic

time method of analysis due to Mellor (Ref 62). In principle, Mellor has divided the typical combustion process into basic phenomena such as heterogeneous processes, fluid mechanical effects, and chemical reactions. Each of these elements is characterized by an appropriate time scale, and these characteristic times are applied to those regions of the combustor where a particular phenomenon is dominant. In particular, for the case of the flameholder, the stabilization process is viewed as a competition between the ignition delay time of the fuel (τ_{hc}) and the turbulent mixing time in the shear layer (τ_{sl}) that exists between the recirculating burner gases and the surrounding free stream. The stability criterion is thus $\tau_{sl}/\tau_{hc} = 1$. The characteristic times utilized in this analysis are basically order-of-magnitude estimates of the processes which they characterize. Nevertheless, their previous utilization has led to good predictions of gaseous emissions, and more recently Plee and Mellor (Ref 63) have shown that blow-off limits of various combustor designs can be correlated by appropriate selection of τ_{sl} and τ_{hc} .

The turbulent mixing time in the shear layer is assumed to be equal to the characteristic decay time of the large scale eddies; this time is, in turn, related to the ratio of turbulence integral length scale to the turbulent rms velocity. The assumption is then made that the integral scale is proportional to the flameholder width (D_f) and that the turbulent velocity varies with an "adjusted" velocity (U_l) at the lip of the flameholder. Thus

$$\tau_{sl} \propto \frac{D_f}{U_l} \quad (40)$$

The velocity U_l is adjusted to allow for the fact that the shear layer temperature (T_{sl}) is higher than the inlet temperature (T), using the following equation

$$U_l T = U T_{sl} \quad (41)$$

The corresponding characteristic time for ignition is calculated from a simplified overall reaction rate expression as

$$\tau_{hc} \sim \frac{e^{E/RT_{sl}}}{\phi (f/a)_s} \quad (42)$$

where $(f/a)_s$ is the stoichiometric fuel-air ratio. Since this ratio is relatively constant for hydrocarbons of interest, the term $(f/a)_s$ is eliminated. Thus the criterion for blow-off becomes

$$\frac{D_f}{U} \sim \frac{e^{E/RT_{sl}}}{\phi}$$

or

$$\frac{D_f}{U} \sim \frac{T_{sl}}{T} \frac{e^{E/RT_{sl}}}{\phi} \quad (43)$$

Once again a decoupling of the fluid mechanics and the chemistry is achieved. As a concrete example of the chemical time, Plee and Mellor (Ref 63) have utilized the data of Ballal and Lefebvre (Ref 31) which related to the stabilization of pre-mixed propane-air flames to obtain

$$\tau'_{hc} = 10^{-4} \frac{T_{sl}}{T} \frac{e^{21000/RT_{sl}}}{\phi} \text{ msec} \quad (44)$$

where the prime indicates the presence of the temperature ratio in the right-hand term. Both the apparent activation energy term and the pre-exponential constant (10^{-4}) were determined empirically. By

employing τ_{sl} and τ_{hc} , a very convincing correlation of the data of Ballal and Lefebvre was obtained, described by the expression

$$\tau_{sl} = 2.11 \tau_{hc}' - 0.46 \quad (45)$$

where τ_{sl} and τ_{hc}' are in msec. This correlation is illustrated in Fig 13. Furthermore, successful stability correlations were obtained for a variety of combustion systems. However, it must be noted that no pressure dependence is included in this criterion other than the minor influence of pressure on flame temperature.

Up to this point, two simplified models of flame stability have basically been considered: the stirred reactor model and the class of models described as flow time/reaction time models. In the stirred reactor case, the stabilization process is modelled in an Eulerian manner, the homogeneous reaction zone being fixed in space. For the time-ratio models, attention is focused on the time course of the reaction.

In practice, the actual description of the RZ flow field involves both spatial and temporal viewpoints. Analysis of the processes occurring in the RZ involves a number of complex phenomena embracing several disciplines. First, the state of the approach flow needs description as a turbulent field whose structure is in general modified as the flow accelerates around the flameholder. The flow which separates from the flameholder lip entrains hot gases from the RZ. In fact, "engulfment" appears to be a better description than entrainment since recent studies of mixing interfaces have revealed large islands or parcels of ambient fluid being drawn into the jet-like flow. These islands are subsequently "rolled up" or "stretched" into

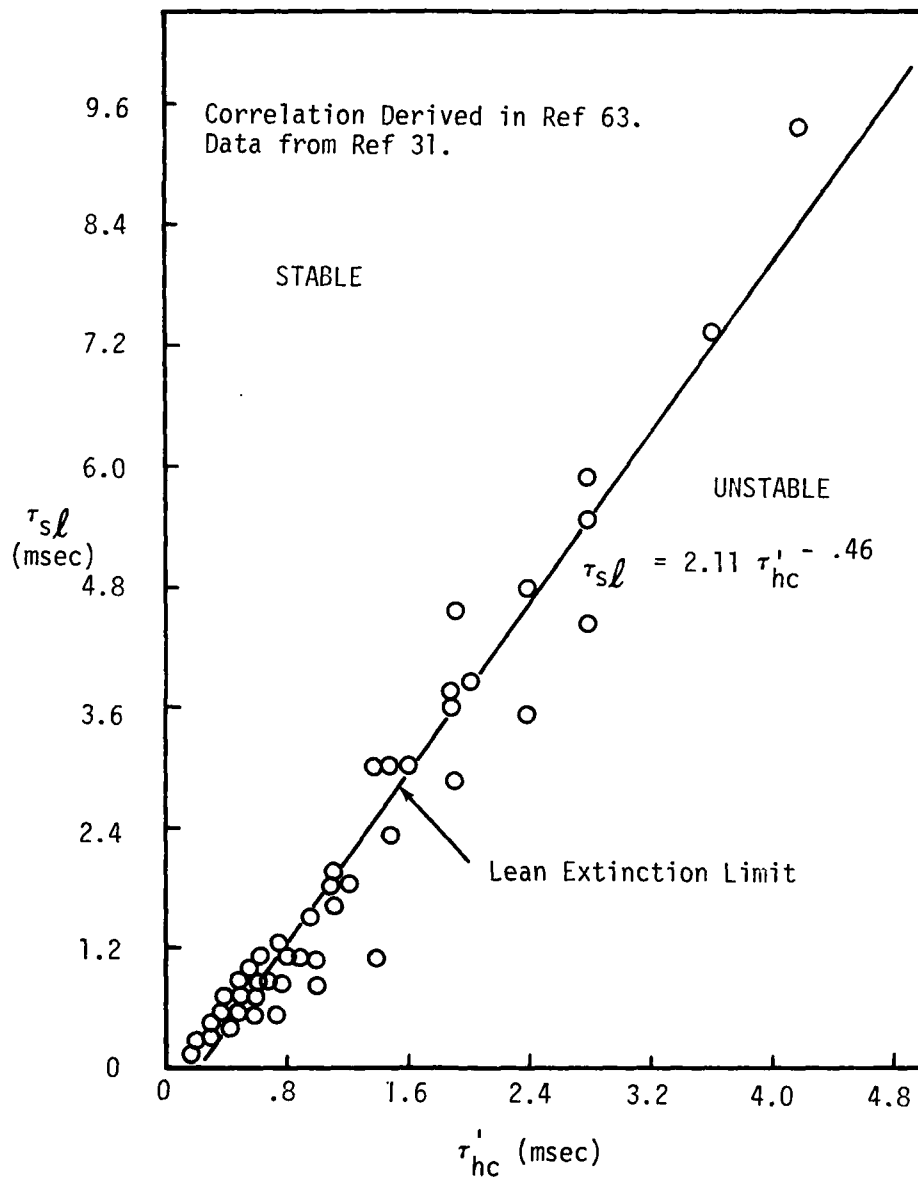


Figure 13. Characteristic Time Correlation for Lean Blow-off of Bluff Body Stabilizer

interleaving layers of fresh mixture and hot products, resulting in rapid intermixing and reaction of these gases. Meanwhile, these reacting parcels are moving downstream, and a portion of them will subsequently be captured by the recirculating flow and will emerge later from the RZ further upstream as a new parcel of hot gas which will in turn be engulfed by the surrounding flow. Thus a cycle exists of the "birth" of parcels of reacting mixture, followed by their "death" either in the RZ or the downstream flow. Successful stabilization is ultimately dependent on the statistical outcome of this "birth-death" process. There is correspondingly a complex interrelation between the fluid mechanics and the chemical aspects of this process which ultimately must be handled on a statistical basis. Obviously, treating this phenomenon either as a homogeneous adiabatic stirred reactor or as a time-ratio model is a gross simplification. Conversely, a more exact analysis is a formidable task. A start on this task has recently been made by Spalding (Ref 64), who originated the so-called "ESCIMO" theory of turbulent combustion. ESCIMO stands for the sequential events occurring in turbulent combustion described as Engulfment, Stretching, Coherence, Interdiffusion, together with a reminder that the process of interdiffusion is analyzed in the reference frame of a Moving Observer travelling with a parcel of fluid. The term coherence is used to denote that the parcels of intermixed fluids cannot be unmixed, but maintain their "coherence" as they flow downstream. The successful evolution of the ESCIMO theory should provide a powerful tool to elucidate the mechanism of flame stabilization.

In retrospect, it is surprising that both the stirred reactor approach and the time-ratio models both yield good correlations for

specific flameholders. This is probably due to the fact that the parameters involved appear in the form of ratios rather than absolute values. Thus in the case of the stirred reactor, the air-loading term $\frac{\dot{m}_r}{VP_r^2}$ involves two quantities, \dot{m}_r and V , whose absolute magnitudes are difficult to assess. However, the ratio $\frac{\dot{m}_r}{V}$ may be a meaningful statistic describing the overall entrained flow to volume ratio of a collection of parcels of reacting gas associated with the stabilizer. Similarly, in time-ratio theories the ratio of residence-to-reaction time rather than the individual absolute values will probably be more meaningful. The question as to whether the stirred reactor or the time-ratio model better represents physical reality has been previously argued (Refs 65 and 66) on the basis of limited experimental data. As noted earlier, both approaches are gross simplifications, and this discussion will not be enlarged; however, it is appropriate to point out that the Zukoski-Marble approach could be embraced by reactor theory by considering the shear layer as a "zone-reactor" and modelling the flow behind a bluff body as a reactor network rather than a single stirred reactor. In this way, a reactor-module approach to combustion modelling could be preserved as a rational framework of analysis. Furthermore, the reactor-module approach remains pertinent for those combustor configurations where a spatial description is not readily applicable (see Fig 8(c)) and in which controlling shear layer(s) cannot clearly be identified, e.g., in the multi-inlet dump combustors shown in Fig 2.

In the next section the discussion of flame stabilization will be narrowed to consider prior work which is relevant to dump combustor configurations.

Flame Stability of Dump Combustors and of Similar Geometries

As noted in Chapter I, one of the primary incentives for this investigation was the paucity of data concerning the flame stability of coaxial dump combustors. In this section, the meager data available for coaxial combustors will be discussed first, and subsequently a review of investigations concerning the flame stability of similar geometries such as steps and wall recesses will be given.

It should be noted that coaxial dump combustors have been utilized in the following applications: industrial furnaces (including "tunnel" burners); supersonic combustion ramjet engines (scramjets); and subsonic combustion IRR engines. Relevant data from industrial furnace studies will be discussed later. The coaxial dump combustor has found application in scramjet engines (Refs 67, 68, and 79), and it is interesting to note that the coaxial configuration is one that can be used with both subsonic and supersonic flows at the dump plane. However, the flow and combustion phenomena occurring with established supersonic flows differ markedly from those associated with subsonic flows. This current discussion will be restricted to subsonic flows.

Many investigations of the flame stability of basic coaxial combustors, i.e., without flameholders at the entry, have been reported. Initial parametric investigations by Barclay (Ref 70) of a number of coaxial combustor geometries with liquid fuel (JP-4) injection yielded stability data with no clearly discernable correlating parameter. Further parametric investigations by Stull et al. (Ref 1) using liquid fuel (JP-4) injected through flush wall injectors located a short distance upstream from the dump plane showed that the fuel-air ratios at blow-off could be correlated on the basis of a modified loading parameter given by

$$\chi = \frac{U}{h} \left(\frac{1}{P^1} \right) \left(\frac{1}{T^1} \right)^{1.5} 1000 \quad (46)$$

where P^1 = pressure in atmospheres,

T^1 = temperature ($^{\circ}R$)/1000,

h = step height = $(D-d)/2$,

D = combustor diameter (ft), and

d = inlet diameter at the dump plane (ft).

This data is shown in Fig 14. It is significant that the χ parameter apparently collapses data from geometrically similar combustors ranging in diameter from 2 to 5 inches. Obviously, this χ parameter is similar to the form of correlating parameter $U^{\alpha}/P^{\beta}D_f^{\gamma}T^{\delta}$ used to describe the stability of bluff body flameholders; however, the characteristic dimension of the flameholder has been replaced by the step height. It should be noted, however, that such correlations are usually applied when homogeneous fuel-air mixtures are used. In this case, however, the correlation appears successful even with wall injectors close to the dump plane.

The investigation by Stull et al. (Ref 1) indicated the potential of applying bluff body correlating parameters to coaxial combustors. However, a basic investigation where each variable was independently varied was not performed in this series, and thus the functional form of the correlation could not be confirmed. Furthermore, it will be observed (Fig 14) that a few data points were not in accord with the correlation.

Results of further investigations performed by Craig et al. (Ref 71) on large-scale dump combustors (12" diameter) are shown in Fig 15. Once again fuel was injected from the wall a short distance upstream

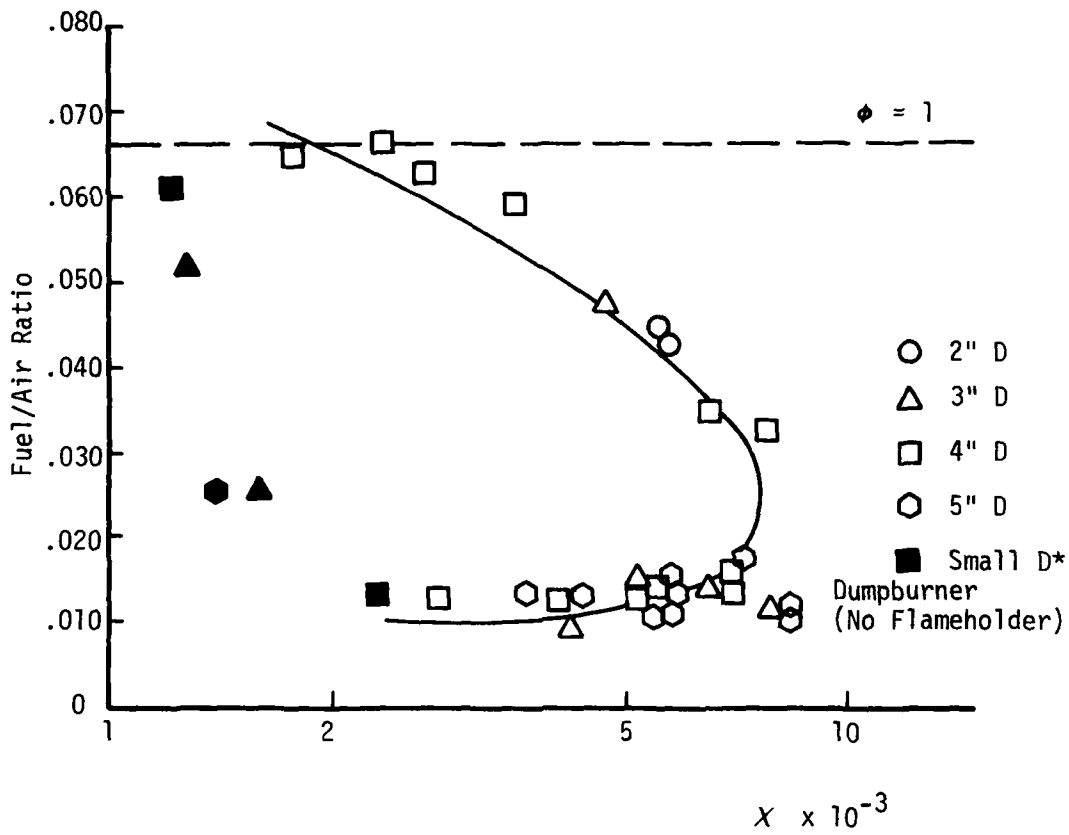


Figure 14. Flame Stability Correlation: Small Coaxial Dump Combustors

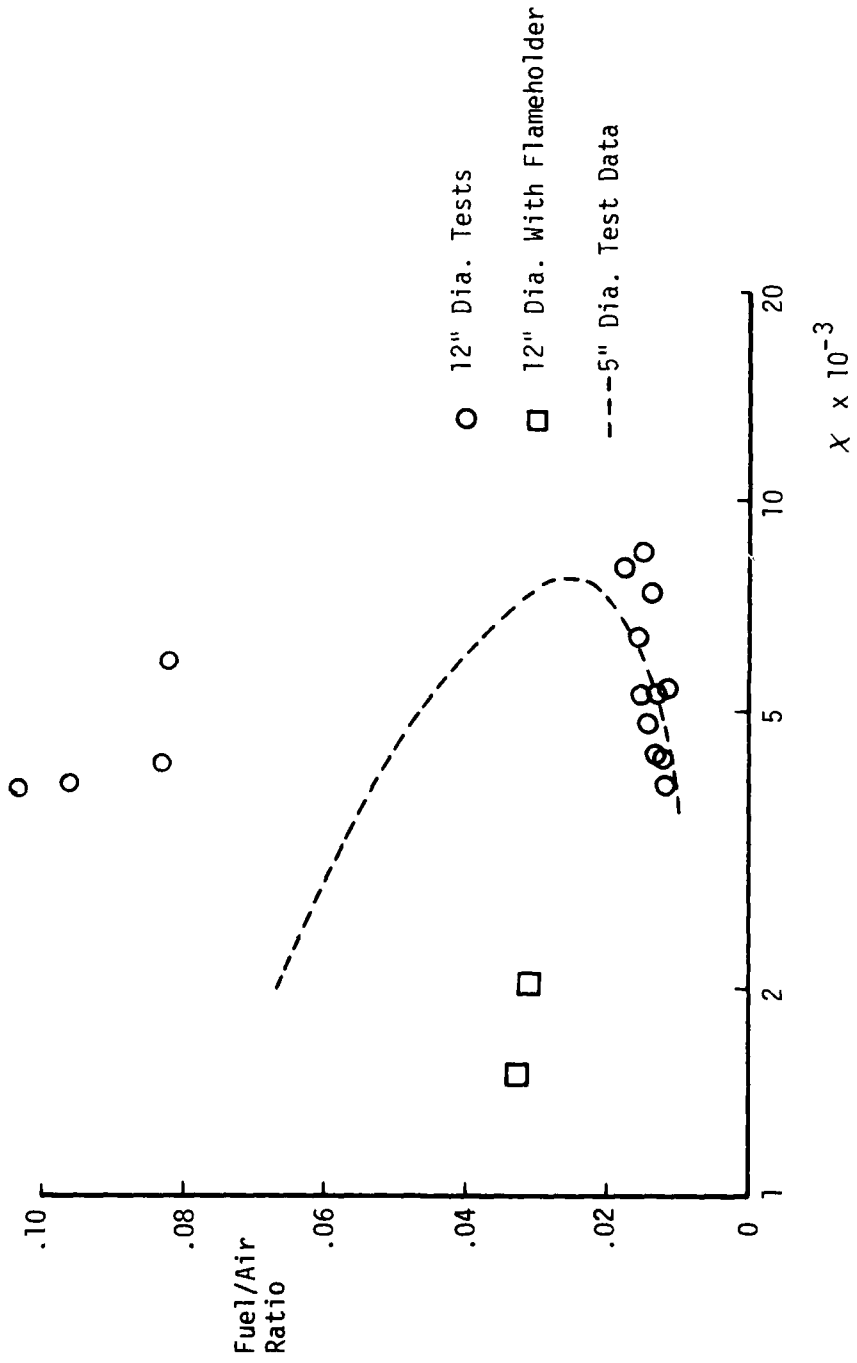


Figure 15. Flame Stability Correlation: 12" Coaxial Dump Combustor

from the dump plane. In this case, the lean extinction limits are similar to those obtained by Stull et al. (Ref 1). However, an interesting observation was that decreasing the step height (h) improved the combustion efficiency, and that the ratio chamber length to step height (L_C/h) was more significant to controlling performance than the length to diameter ratio (L_C/D). Indeed, it was suggested that the optimum step size would be the smallest one capable of sustaining flame over the operating range of the combustor. A further investigation was made by Chambers (Ref 72) of two dump combustors of 4" and 5" internal diameter fed by a 2.5" dia. pipe. In this case, a homogeneous premixed fuel (JP-4/air) mixture was used. Unfortunately, only 30 data points were obtained for various inlet temperatures (660°R to 1248°R) and pressures (16 to 79 psi), and once again it was not possible to study the effect of varying independently the inlet pressure, velocity, and temperature. The reduced data (Ref 72) is displayed in Fig 16. Another investigation of a 10" diameter coaxial dump combustor fed by a 3.35" pipe and using liquid fuel (JP-4) flush-wall injection was reported by Schmotolocha and Economos (Ref 73). This combustor was of relatively low d/D ratio and had an overall length of 35", which was barely long enough to accommodate the recirculation zone generated by the step. Data from this investigation is shown in Fig 15.

Another recent investigation of a 3" diameter coaxial combustor with a 2" diameter inlet has been reported by Choudhury (Ref 74), and the corresponding lean limits are shown in Fig 17. This set of data was apparently obtained at one inlet temperature (590°R) and at approximately atmospheric pressure. An interesting aspect of this investigation was the use of different wall materials which provide an indication of

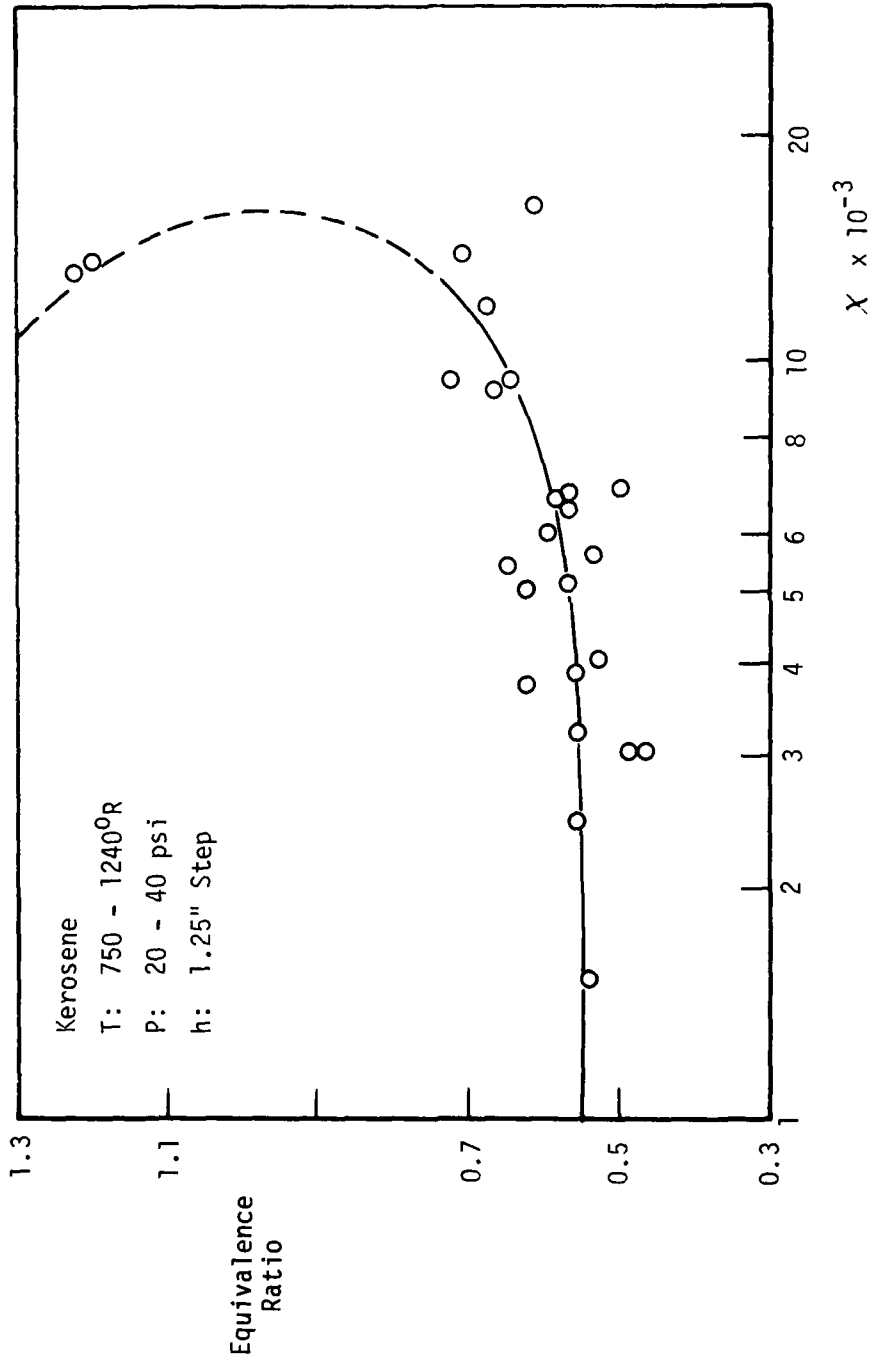


Figure 16. Flame Stability Correlation for Dump Combustors: Pre-Mixed Fuel-Air

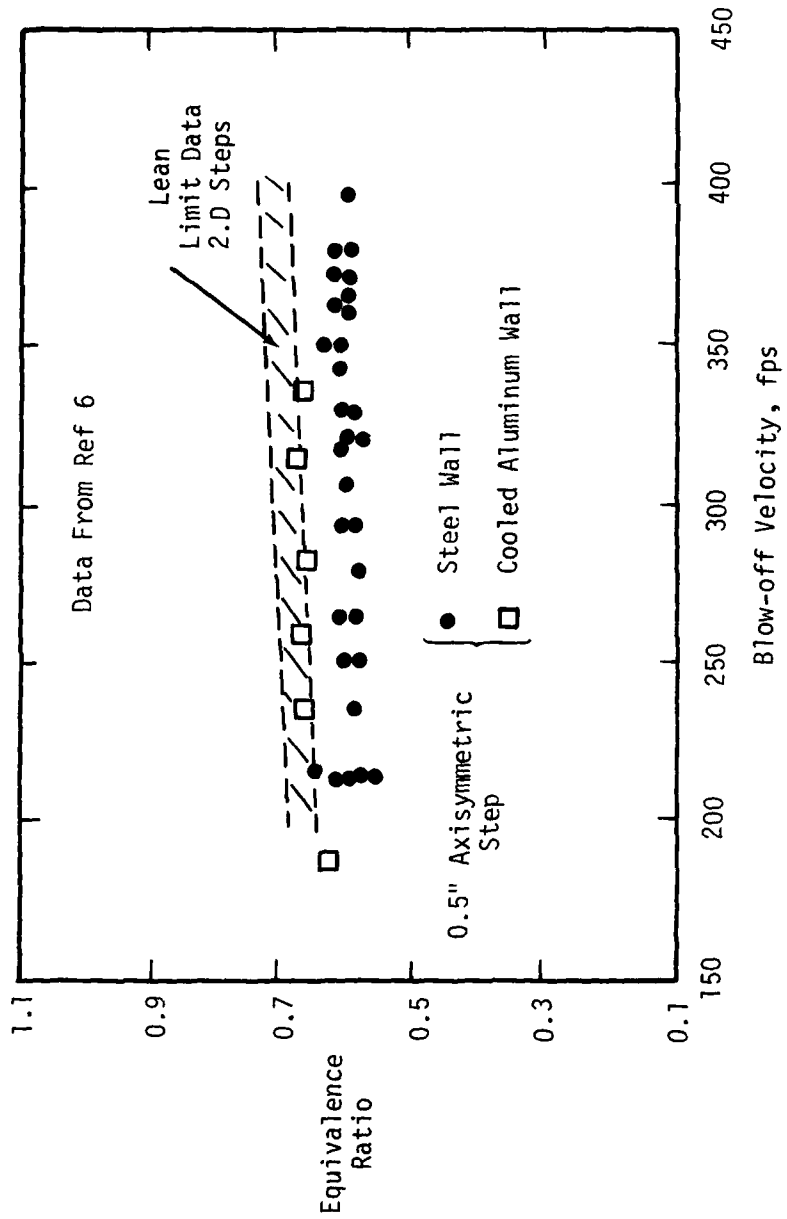


Figure 17. Flame Stability Data for a Coaxial Dump Combustor and for Steps

the effect of wall heat losses on flame stability. In this case, pre-mixed propane was used as a fuel.

All the above investigations were performed in support of ramjet combustor technology. An overall observation concerning the above data is that in no case is the existence of a complete flame stability loop unequivocally confirmed by the data, although some investigators have sketched in the anticipated curves. It is also interesting to note that the data of Choudhury (Ref 74) shows only a slight rise in the lean extinction fuel-air ratio as the velocity increases. Similarly, inspection of Figs 14 to 17 shows a relatively constant lean limit to exist over wide ranges of operation. It will also be noted that the majority of work has been performed with heterogeneous fuel-air mixtures, and little data have been acquired with homogeneous mixtures.

In addition to the above combustor studies, two basic investigations are noteworthy. The first effort by Ross (Ref 75) was a study of the flame stability of a small scale ($D = 1"$, $d = 0.5"$, approximately) coaxial combustor fabricated from Vycor glass tubing. This investigation was conducted to study the effects of oscillatory combustion on the limits of stabilization. A variable length combustor (16"-20") was employed to vary the oscillation frequency. The fuel used was propane, and the data obtained are shown in Fig 18. Although the long test configurations ($L_c = 16"$, $18"$, and $20"$) were not representative of ramjet combustor practice, a number of relevant observations can be made. Because of the transparent combustor, it was possible to observe a distinct annular recirculation zone with attached flame brush. Also, as the lean limit was approached, the flame retreated

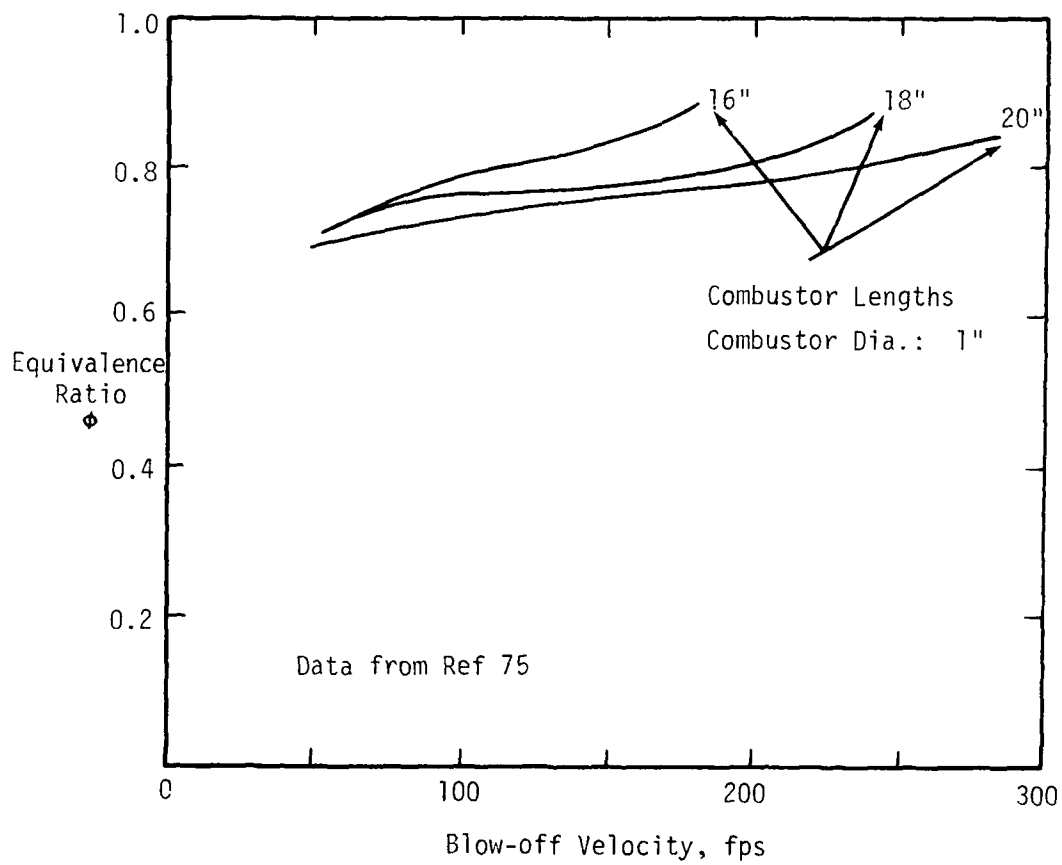


Figure 18. Flame Stability Data for a Small Coaxial Dump Combustor

towards the dump plane, appearing as a faint annular brush just prior to blow-out. For the 16" and 18" chambers, the lean limit equivalence ratio remained relatively constant over a wide range of velocity (90-200 feet/sec), but for the 20" chamber the weak limit value increased progressively with velocity (Fig 13). As noted earlier, a longitudinal resonant oscillation was encountered in this investigation, the occurrence of which completely modified the flame pattern. This was perhaps the first warning of similar oscillatory phenomena which have been manifested in recent dump burner research (Ref 1).

The other basic research effort is that of Baev and Tret'yakov (Ref 58). In this study, a symmetric, two-dimensional dump combustor with transparent side walls was utilized. Two step heights (25 and 17 mm) were studied, and both rich and weak limits were determined as a function of velocity. Although a closed loop was not obtained, reduced step height produced a marked deterioration in both weak and rich limits. The length of the recirculation zones behind the steps was determined from flame photographs. The zone length was not affected by fuel-air ratio, but increased markedly with combustion chamber exit velocity; however, no exhaust nozzle appeared to be used. Unfortunately, the reporting of this important investigation was obscured by its brevity.

For completeness, mention is made of an investigation of a simple coaxial combustor reported by Altenkirch and Mellor (Ref 66). In this case, the flame stabilizing element was formed by a simple orifice in a circular plate spanning the combustor. The combustor geometry is thus similar to that of a coaxial dump combustor. Unfortunately, the stability data reported cannot be readily expressed in terms of

blow-out velocity. So far, attention has been confined to combustion systems of the sudden-expansion type. Several flame-stability investigations have been performed on related geometries such as two-dimension steps and wall recesses. These tests will now be reviewed.

A most recent study is that of Kawamura (Ref 76). In this investigation, propane fuel was ejected as a thin sheet from a slot at the top of backward-facing step. The fuel, mixed with the co-flowing airstream, and the behavior of the resulting ignition front was observed. Although this work is not truly comparable to one with homogeneous fuel-air mixture, two interesting observations can be made. The first is that the lean and rich blow-off limits remained apart, and a closed stability loop was never obtained. Second, the length of the RZ under burning conditions was about half that of the comparable cold flow value (3.5 step heights compared to 7 under cold flow conditions). However, the RZ length exhibited little variation with fuel/air ratio or freestream velocity.

An earlier investigation by Snyder (Ref 77) concerned the flow of pre-mixed propane-air over a step. In this case, the boundary layer thickness at the dump position was systematically varied by using different approach lengths upstream of the step. Unfortunately, the step height (h) was not reported, and it is thus not possible to assess the relative effect of boundary layer thickness. A general observation was that increasing boundary layer thickness improved stability. A complete stability loop was obtained, but the incomplete reporting of test data leaves little room for further comment. However, once again it was noted that the RZ length was found to remain essentially constant above a Reynolds number of 2.5×10^5 .

For completeness, another step-stabilization investigation should be noted. This investigation was performed by DeZubay (Ref 78), with the primary goal of investigating the effect of wall heat transfer with the recirculating zone; some data on rich limits are given, but not introduced here. However, it should be noted that heat loss from the RZ is more likely to occur with dump or step configurations compared to bluff body stabilizers.

Another configuration related to the dump combustor is the flame stabilizer configuration formed by machining a recess in the chamber wall. This "recessed-wall" configuration is attractive for practical combustors (Ref 79 and 80) because it offers flame stabilization with no mechanical blockage of the stream and thus with low pressure loss. However, the floor of the recess is subject to high heat loads due to the recirculating flow in the cavity.

A pioneering investigation of recessed wall flameholders was reported by Huellmantel et al. (Ref 81). In this case, a pre-mixed propane air stream was used, and the test section was a symmetrical rectangular channel with recesses cut on the top and bottom walls of the channel. To determine the effect of recess shape, 12 different recess contours were tested. This study found that recesses of short length provided inadequate RZ volume for stability and were associated with rough burning. The influence of recess depth (i.e., effectively the step height) was also examined; reducing the step height from the maximum of 0.25 in. resulted in reduced stability limits, as would be anticipated.

A further extension of this initial work was made by Povinelli (Ref 82), the main achievement of which was to correlate the data of

Huellmantel et al. on the basis of the Zukoski-Marble criterion. An interesting observation in this case was that the length of the RZ was essentially constant despite variations in flow velocity and equivalence ratio.

A recent and comprehensive investigation of recess wall/step configurations has been carried out by Choudhury (Ref 74). Although the main thrust of this work was the enhancement of stability and combustion efficiency by the use of a system of small air jets injected upstream of the dump plane, much of the experimental work covered basic recessed wall/step geometries. As already shown in Fig 17, the blow-off limits for both two-dimensional steps and an axisymmetric combustor show little change over the range of velocity explored. The effects of varying inlet temperature and pressure were not studied. The effect of step height was, however, examined; basically no effect of step height on stability was found for heights between 0.25 and 0.75 inch. However, reduction in step height below 0.25 in. resulted in degradation of stability. The length of the RZ was found to remain between 6 and 7 step heights for cold flow conditions and "similar behavior" was observed during burning. A major service performed by Choudhury has been to draw increased attention to the pressure fluctuations and noisy operation associated with dump combustors. Even in cold flow the reattachment process associated with the free shear layer gave rise to marked pressure fluctuations and, of course, the related phenomena of "cavity tones" is well known. However, the introduction of combustion into this environment can lead to severe manifestations of rough burning. Choudhury has documented this phenomenon in some detail, and no further discussion of this combustion instability will be given.

The limited results available concerning the flame stabilizing properties of steps/recesses indicate that the overall RZ length (L/h) may change from cold flow to burning conditions. However, no marked variation of L/h occurs with varying flow velocity and fuel-air ratio (Refs 76, 77, and 82). The results concerning the effect of step height variation on stability may be explained by postulating a critical step height of about 0.25 inch. Above this critical height, the step dimension does not appear to affect the stabilizing limits (Ref 74). Below this height, the stability range is narrowed by decreasing step height (Refs 74, 81). However, the results presented earlier (Ref 58) concerning the opposing-step combustor configuration of Baev and Tret'yakov do not harmonize with the above observations concerning the effect of velocity on the RZ length or the existence of a critical step height.

The limited experimental work concerning the flame stability of coaxial dump combustors and related geometries has been reviewed. It is now appropriate to turn to the theoretical analysis of the dump combustor with the object of modelling the flame stabilizing process.

III THEORETICAL ANALYSIS

In Chapter II, it was pointed out that a combustion chamber can be modelled as a network of reactor modules. To preserve this framework of analysis, the lean extinction limits of a coaxial dump combustor will be estimated by assuming the recirculation zone to be a stirred reactor. In order to evaluate the air loading expression, Eq(10), of the stirred reactor, two terms are needed which are determined by the aerodynamics of the combustor. These terms are the recirculation zone volume (V) and the mass flow (\dot{m}_r) entrained into the zone. An extensive review of experimental data concerning flow phenomena in coaxial dump configurations was therefore undertaken and is presented in Appendix A. The results of this review will now be briefly outlined.

Aerodynamics of Coaxial Dump Configurations

The general features of the flow field under non-burning conditions are shown in Fig 19. Separation of the flow occurs at the inlet dump plane and is followed by reattachment to the wall further downstream. The reverse flow velocity in the annular recirculation zone is also depicted. The reattachment process at the wall is a very unsteady phenomenon. Thus, the point of reattachment was observed by DeRossett and Przirembel (Ref 83) to oscillate at a frequency of the order of several hundred Hertz. Thus, reattachment occurs over a region rather than on a line. Furthermore, the width of this region has been found (Ref 83) to broaden with both the step height and the initial thickness of the inlet boundary layer; appreciable pressure fluctuations also accompany the reattachment process. The recirculation zone was also found (Ref 83) to include a sub-zone just downstream

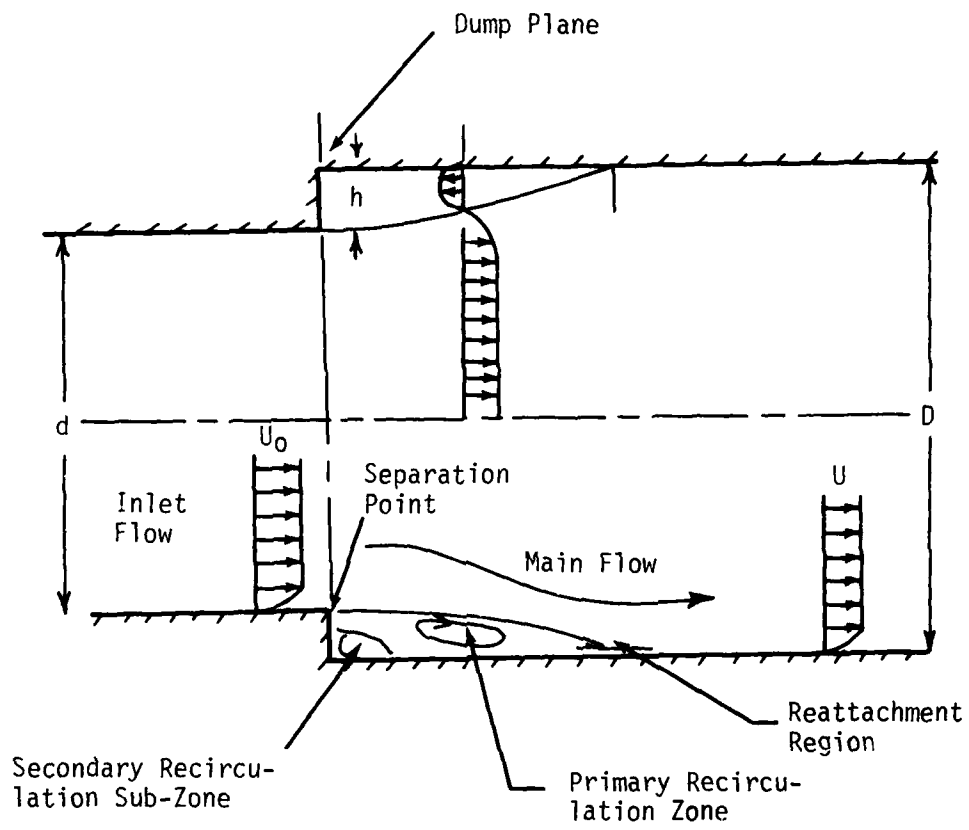


Figure 19. Flow Field of a Coaxial Dump Configuration

of the step, and this is also shown in Fig 19. Also, several investigators (Refs 84, 85, and 86) have shown evidence that a rotary motion about the chamber axis occurs within the recirculation zone. Despite the complexity of the reattachment process, the time-mean length (L) of the recirculation zone may be determined within reasonable limits. In Fig 20, a composite plot of the values of L/h obtained by various investigators is given. It will be noted that at high Reynolds numbers, the ratio L/h appears to become relatively constant and independent of the flow Reynolds number. Typically, the length (L) is found to be between 8 and 9 step heights (Refs 84 and 85). However, both Pennucci (Ref 84) and Drewry (Ref 85), who tested coaxial chambers fitted with terminal convergent nozzles, observed that a reduction in nozzle throat size appeared to reduce the reattachment length (L) slightly. Limited experimental data (Refs 87 and 88) indicate that L/h may also be affected by the diameter ratio (d/D). However, for modelling purposes, one may assume that $k = L/h$ is approximately constant for Reynolds numbers greater than about 3×10^5 .

The boundary of the recirculation zone determined in experimental studies may be approximated by a parabolic curve as shown by the data of Chaturvedi (Ref 89). Thus, with the length and shape of the recirculation zone known, the corresponding volume can be calculated.

In addition to the recirculation zone volume, the mass flow entering into the recirculation process is required in order to calculate the air loading of the reaction zone. Typically, in analyses of bluff body flame stabilizing processes, this entrained mass flow is usually calculated (Ref 21 and 31) by an expression of the form

$$\dot{m}_r \propto \bar{\rho} S U \quad (47)$$

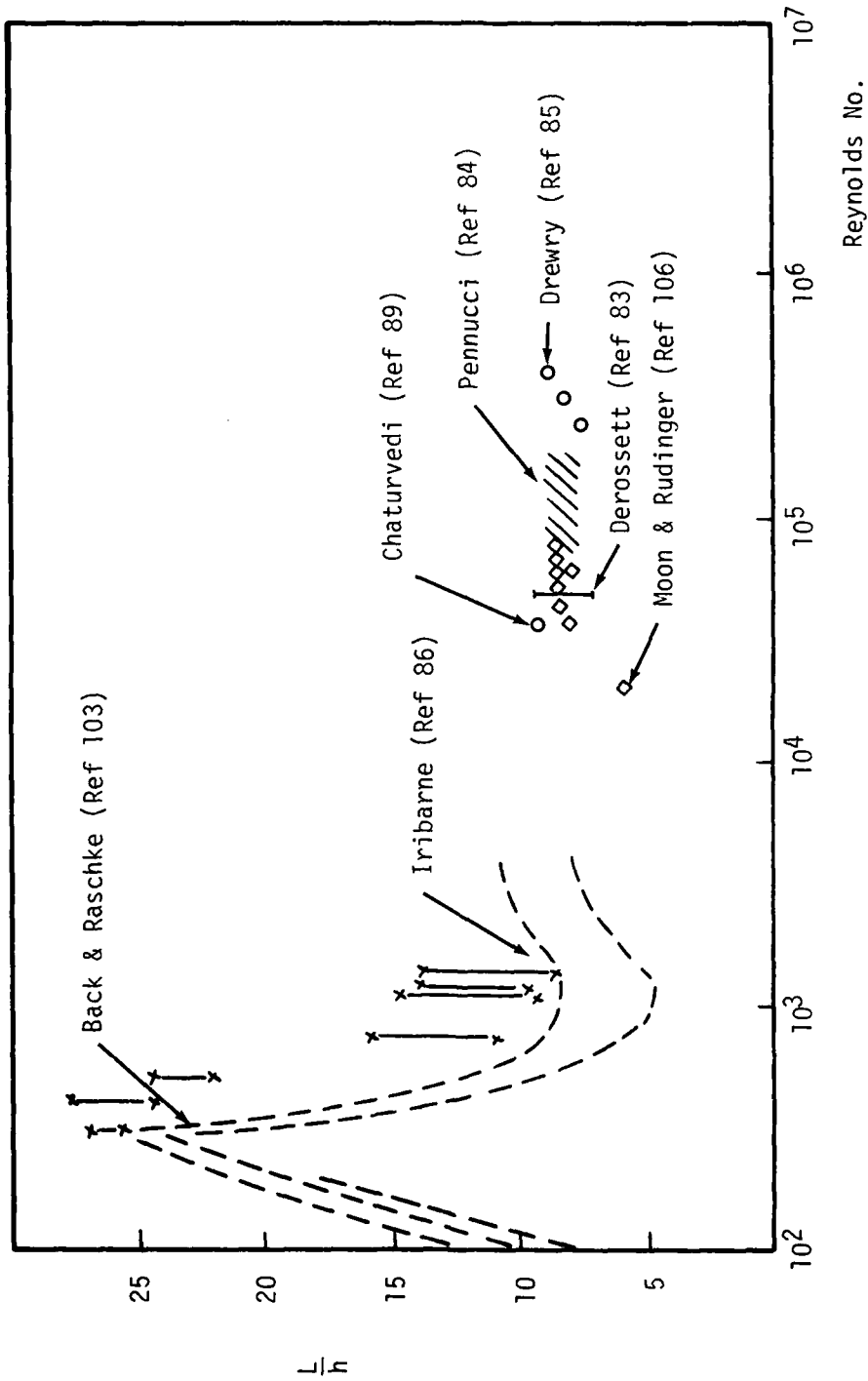


Figure 20. Recirculation Zone Length Ratio as a Function of Reynolds Number

where S is an effective entrainment surface area, U is the local flow velocity at the trailing edge of the bluff body, and $\bar{\rho}$ is an appropriate density.*

Usually S is assumed proportional to D_f^2 , yielding the result that

$$\dot{m}_r \propto \bar{\rho} D_f^2 U \quad (48)$$

However, in the case of the coaxial dump geometries, a number of investigations has been made, in connection with industrial furnace development, to measure the maximum fraction of the inlet mass flow entering into the recirculation process. This extensive literature is also reviewed in Appendix A.

Typically, industrial furnaces are fed by two streams consisting of a primary jet which carries the fuel, surrounded by a secondary flow of air. With zero secondary air flow, the furnace operation corresponds to that of a coaxial dump combustor. This case is documented in the literature (Refs 90, 91, and 92). Unfortunately, the diameter ratio (d/D) of a typical furnace is usually much smaller than that of a ram-jet coaxial combustor. However, some useful data have been obtained from furnace investigations. The results of various furnace studies are given in Fig 21, showing recirculated mass flow fraction (\dot{m}_{rc}/\dot{m}_0) as a function of diameter ratio (d/D). The data are well represented by the following equation due to Wingfield (Ref 91).

$$\frac{\dot{m}_{rc}}{\dot{m}_0} = 0.398 \left\{ \frac{1}{d/D} - 1.059 \right\} \quad (49)$$

where \dot{m}_0 denotes the primary jet mass flow and \dot{m}_{rc} is the measured recirculation mass flow. At this point, one may now proceed to evaluate the air loading parameter of the recirculation zone.

* See discussion in Appendix B.

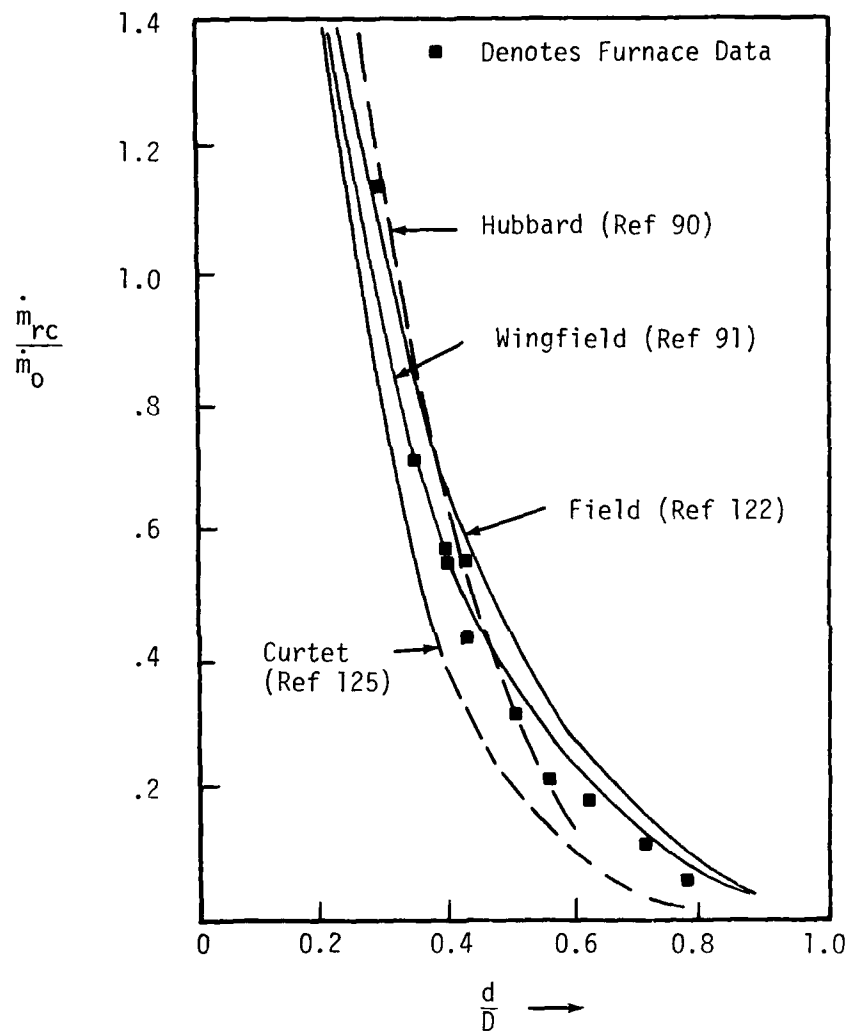


Figure 21. Recirculated Mass Flow Fraction - Diameter Ratio

Loading Parameter of Recirculation Zone

The loading parameter of interest is that given in Eq(10), and for the moment, attention is drawn to the quantity $\left(\frac{\dot{m}_r}{VP_r^n}\right)$. This may be expressed in terms of a mass flow fraction (\dot{m}_r/\dot{m}_0) as follows:

$$\begin{aligned}\frac{\dot{m}_r}{VP_r^n} &= \left(\frac{\dot{m}_r}{\dot{m}_0}\right) \left(\frac{\dot{m}_0}{VP_r^n}\right) \\ &= \left(\frac{\dot{m}_r}{\dot{m}_0}\right) \left(\frac{A_0}{V}\right) \left(\frac{P_0}{P_r^n}\right) \left(\frac{U_0}{RT_0}\right)\end{aligned}\quad (50)$$

For the coaxial dump combustor, one may set P_r equal to P_0 with negligible error to obtain

$$\frac{\dot{m}_r}{VP_r^n} = \left(\frac{\dot{m}_r}{\dot{m}_0}\right) \left(\frac{A_0}{V}\right) \left(\frac{1}{P_0^{n-1}}\right) \left(\frac{U_0}{RT_0}\right)\quad (51)$$

Thus for given inlet conditions, the terms (\dot{m}_r/\dot{m}_0) and (A_0/V) determine reactor loading. Alternatively, the quantity (\dot{m}_r/VP_r^n) may be evaluated using the conventional expression for the entrained mass flow given in Eq(47). In this case

$$\begin{aligned}\frac{\dot{m}_r}{VP_r^n} &\propto \rho_0 S U_0 \left(\frac{1}{VP_r^n}\right) \\ &= k_\epsilon \left(\frac{S}{V}\right) \left(\frac{P_0}{P_r^n}\right) \left(\frac{U_0}{RT_0}\right)\end{aligned}\quad (52)$$

where k_ϵ represents an entrainment factor, and $\bar{\rho}$ has been put equal to ρ_0 .

From Eq(50) and Eq(52) one has the equality

$$\frac{\dot{m}_r}{\dot{m}_0} = k_\epsilon \left(\frac{S}{A_0}\right)\quad (53)$$

In this case, an estimate of the consumed mass fraction (\dot{m}_r/\dot{m}_0) may be derived from Eq(53) if the geometry of the recirculation zone and the effective value of k_ϵ are known. As a crude approximation, one may assume that the zone is bounded by a straight line extending from the point of separation at the dump plane to the point of reattachment at the chamber wall. It is further assumed that the point of reattachment is located at a distance kh from the dump plane. As noted previously, k is approximately equal to 8.5 for cold flows. The surface area of the recirculation zone can be obtained by integration, and is given by

$$S_l = \pi k h (D - h) \left\{ 1 + \frac{1}{k^2} \right\} \quad (54)$$

where S_l denotes the surface area based on a straight line boundary. The corresponding volume is

$$V_l = \frac{\pi k h^2}{6} (3D - 2h) \quad (55)$$

For $k \gg 1$, Eq(54) may be approximated as

$$S_l = \pi k h (D - h) \quad (56)$$

and the corresponding recirculated mass flow fraction becomes

$$\frac{\dot{m}_r}{\dot{m}_0} = k_\epsilon k \left\{ \frac{1}{(d/D)^2} - 1 \right\} \quad (57)$$

which for high diameter ratios (d/D), and with appropriate choice of coefficients, yields results similar in form to those given by Eq(49).

A characteristic dimension may also be derived for this linear RZ geometry by writing

$$\bar{h}_l = \frac{V_l}{S_l} = \frac{D}{6} \left(\frac{2h}{D} \right) \left(\frac{3 - \frac{2h}{D}}{2 - \frac{2h}{D}} \right) \quad (58)$$

Correspondingly, Eq(52) may be expressed as

$$\frac{\dot{m}_r}{V P_r^n} = k \epsilon \frac{1}{\bar{h} l} \left(\frac{P_o}{P_r^n} \right) \left(\frac{U_o}{RT_o} \right) \quad (59)$$

and this form of equation is relatively insensitive to variations in the value of k . Also \bar{h} is effectively proportional to h .

However, as noted earlier, a better approximation to the recirculation zone shape is obtained with a parabolic curve. In this case, the expression for the surface area (S_p) becomes *

$$S_p = \frac{\pi kh}{2} \left[d + h + \frac{k^2 h}{8} \right] \sqrt{1 + \frac{4}{k^2}} - \frac{\pi k^2 h}{4} \left[\frac{k^2 h}{4} - d \right] \text{Ln} \left[\frac{2}{k} + \sqrt{1 + \frac{4}{k^2}} \right] \quad (60)$$

The corresponding volume is given by

$$V_p = \pi kh^2 \left[\frac{2}{3} d + \frac{4}{5} h \right] \quad (61)$$

Once again a characteristic dimension (\bar{h}_p) may be defined expressed as

$$\frac{\bar{h}_p}{D} = \frac{1}{D} \frac{V_p}{S_p} = \left(\frac{V_p}{D^3} \right) \cdot \left(\frac{D^2}{S_p} \right) \quad (62)$$

The ratio \bar{h}_p/D may be calculated from Eq(60) and Eq(61), using the identity $D = d + 2h$. A curve of \bar{h}_p/D versus $2h/D$, for various values of k , is given in Fig 22. For $k = 8.5$, a good representation of this relationship is

$$\frac{\bar{h}_p}{D} \propto \left(\frac{2h}{D} \right)^{1.095} \quad (63)$$

where $0.1 \leq \frac{2h}{D} \leq 0.6$.

* See Appendix A, Eq(A-1) and Eq(A-2).

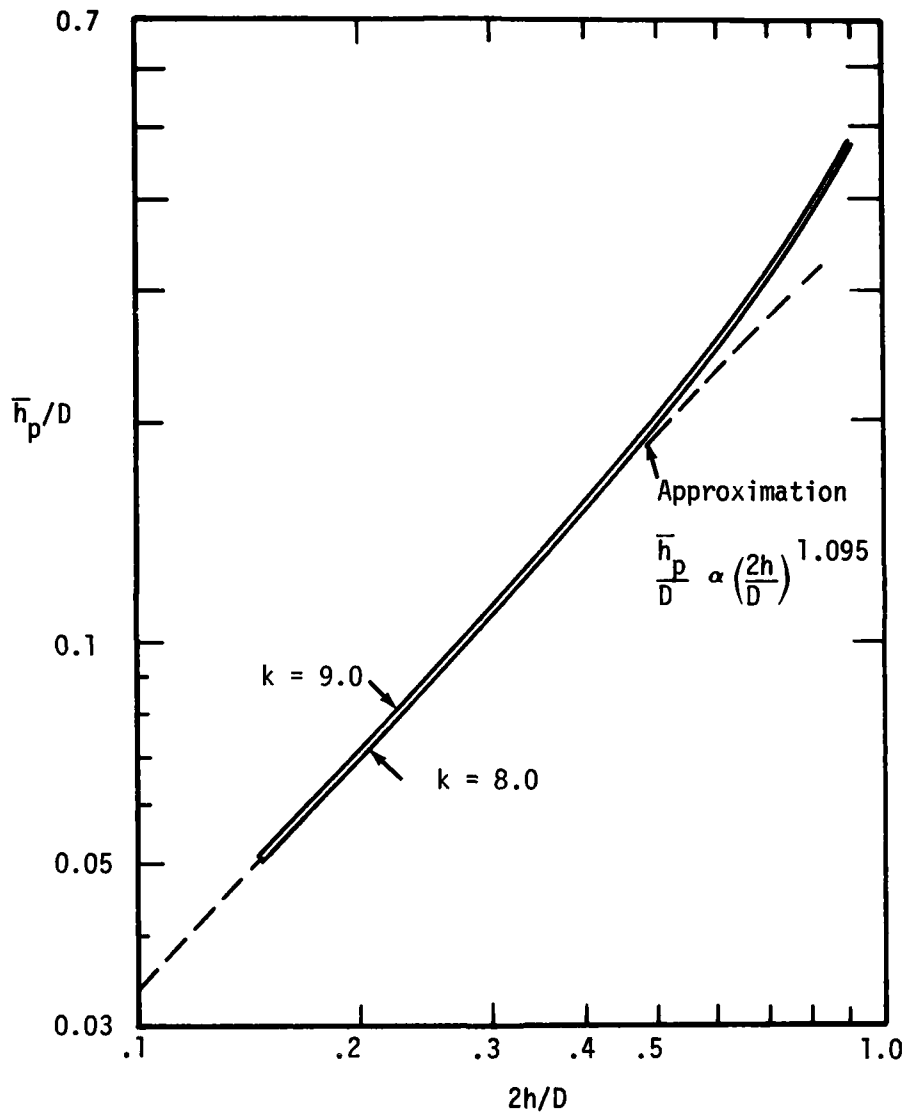


Figure 22. Parabolic Recirculation Zone Shape: Variation of \bar{h}_p/D

If the exponent in Eq(63) were equal to unity, the diameter D could be eliminated and \bar{h}_p would be exactly proportional to h .

In addition to the theoretical estimates and measured values of recirculated mass flow fraction, it is possible in principle to measure the amount of air entrained into the recirculation zone and consumed under actual operating conditions by a technique introduced by Lefebvre et al. (Ref 93). This technique was used to study the air entrainment into the recirculation zone of a bluff body and consists of injecting a small fraction of the total fuel flow directly into the recirculation zone. Both the mainstream fuel flow (\dot{f}_0) and the fuel flow (\dot{f}_r) injected into the recirculation zone are measured at the lean extinction condition. The total fuel flow (\dot{f}_t) entering the recirculation zone is then

$$\dot{f}_t = \dot{f}_r + \left\{ \frac{\dot{f}_0}{\dot{m}_0} \right\} \dot{m}_r \quad (64)$$

where \dot{m}_r is the air mass flow burned in RZ, and \dot{m}_0 denotes the total air mass flow at the dump plane.

The assumption is made that the lean extinction occurs at the same overall fuel-air ratio in the recirculation zone irrespective of whether the fuel enters the zone by direct injection or by entrainment. Thus, for fixed upstream conditions, the total fuel flow (\dot{f}_t) should remain constant irrespective of the division of fuel between the mainstream and the recirculation zone. The following relationship then exists between the various fuel flows

$$\dot{f}_r = \dot{f}_t - \left\{ \frac{\dot{m}_r}{\dot{m}_0} \right\} \dot{f}_0 \quad (65)$$

Consequently, for given upstream conditions, a plot of \dot{f}_r against \dot{f}_0 should give a straight-line relationship, the slope of which yields the desired quantity (\dot{m}_r/\dot{m}_0).

This technique has been successfully applied to a gas turbine combustor configuration by Verduzio and Campanaro (Ref 94).

Chemical Reaction Model

In order to estimate the lean stability limit of the coaxial dump combustor, the annular recirculation zone is modelled as a stirred reactor. For the combustion of a hydrocarbon denoted by $C_x H_y$ with excess air, an expression for the air loading term ϕ was given in Eq(5). This equation was, however, for a reaction of order two. The more general expression for a reaction of order n is derived in Appendix C and is given in the following equation:

$$\phi = \frac{\dot{m}_r}{V P_r^n} = \frac{k_1}{R^n} (m+1) \frac{e^{-E/RT}}{T^{n-0.5}} \frac{1}{\epsilon \phi} \frac{\left\{ (\phi - \epsilon \phi)(1 - \epsilon \phi)(x + y/4) \right\}^{n/2}}{\left\{ (m+1)(x + y/4) + \phi + \epsilon \phi (y/4 - 1) \right\}^n} \quad (66)$$

It is assumed that an effective activation energy (E) and a reaction order (n) can be assigned for the combustion reaction. Then for a given equivalence ratio (ϕ) and initial air temperature (T), the air loading achieves a maximum value (ϕ_{max}) at a certain value of ϵ . This maximum value ϕ_{max} is the highest loading the reaction zone can sustain before extinction. Values of $\frac{1}{k_1} \phi_{max}$ have been calculated for both ethylene and JP-4 fuels burning in air, for inlet temperatures varying from 600-1200^oR, and for equivalence ratios ranging from 0.3 to 1.0. These calculations were made for values of E varying from 30 to 54 KCal/Gm Mole, and for values of n from 1.25 to 2.00.

Ballal and Lefebvre (Ref 31) have shown that the term ϕ_{\max} can be approximately represented as a function of equivalence ratio and initial temperature, of the form

$$\phi_{\max} \propto \left\{ \exp T/b \right\} \phi^t \quad (67)$$

where b and t are constant for an assumed activation energy and reaction order. Alternatively, one may express the variation of ϕ_{\max} as

$$\phi_{\max} \propto T^s \phi^t \quad (68)$$

Calculated values of s and t are shown in Fig 23 for ethylene; similar data for JP-4 is given in Appendix C. For ethylene, an activation energy of about 42 KCal/Gm Mole would be anticipated. If a reaction order of 1.75 is assumed, then the corresponding value of s is 2.86 and the value of t is 5.3.

From Eq(68), the maximum loading may be expressed as

$$\frac{\dot{m}_r}{VP_r^n} = k_3 T^s \phi^t \quad (69)$$

In practice the actual loading at which a combustor blows out is significantly less than the theoretical maximum value ϕ_{\max} , principally because the combustor is not perfectly mixed. This proportionate reduction in actual loading compared to the ideal loading is included in the constant term k_3 .

From Eq(59), with $P_o \approx P_r$, one may write

$$\frac{\dot{m}_r}{VP_r^n} \propto \left\{ \frac{1}{h} \right\} \left\{ \frac{1}{P_o^{(n-1)}} \right\} \frac{U_o}{RT_o}$$

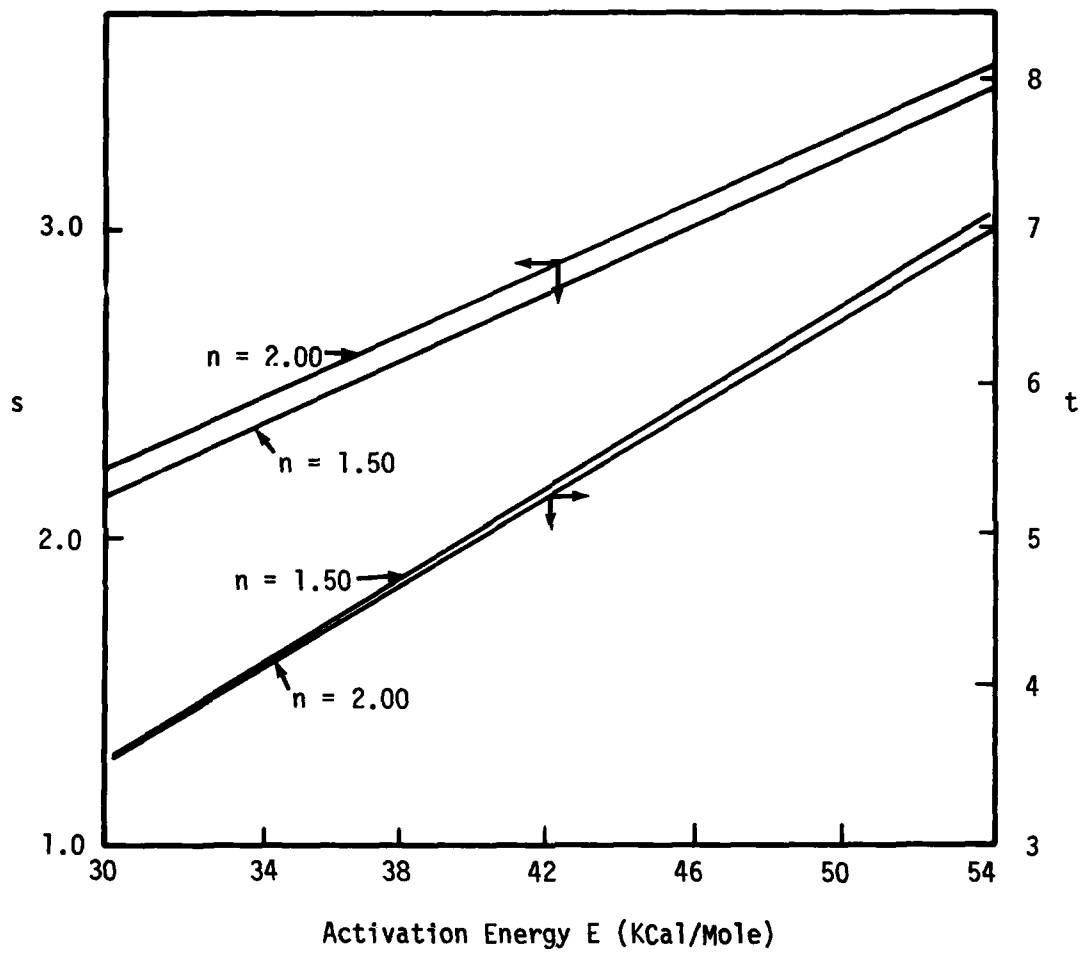


Figure 23. Variation of Exponents s and t as a Function of E and n (Ethylene)

Finally, using Eq(69), and assuming $\bar{h}_l \propto h$, one obtains the following expression for the lean blow-out limit

$$\phi_{LBO} \propto \left\{ \frac{1}{h} \cdot \frac{1}{P_0^{(n-1)}} \cdot \frac{U_0}{T_0^{(s+1)}} \right\}^{\frac{1}{t}} \quad (70)$$

Thus for the previous assumptions made for ethylene ($E = 42$ KCal/Gm Mole, $n = 1.75$) yielding $s = 2.86$, $t = 5.3$, one obtains

$$\phi_{LBO} \propto \left\{ \frac{1}{h^{.19}} \cdot \frac{U_0^{.19}}{P_0^{.14} T_0^{.73}} \right\} \quad (71)$$

Thus a correlating parameter is anticipated of the following form:

$$\phi_{LBO} = k_4 \frac{U_0^\alpha}{P_0^\beta h^\gamma T_0^\delta} \quad (72)$$

In practical applications, the use of the stagnation temperature T_{t_0} is usually preferred rather than T_0 . For modest flow velocities, $T_{t_0} \approx T_0$ and direct substitution of T_{t_0} in Eq(72) is permissible. For those higher inlet velocities where compressibility effects are important, Eq(72) may be expressed in terms of M_0 and T_{t_0} rather than U_0 and T_0 . However, the use of U_0 and T_{t_0} is a preferred form, and the small errors involved in assuming $T_{t_0} \approx T_0$ are usually accepted.

It should be emphasized that the exponents given in Eq(71) are obtained on the basis of a one-step reaction model described by a given activation energy and reaction order. A perfectly stirred adiabatic reaction zone was also assumed. Consequently, the values of these exponents derived from practical combustors which are neither perfectly stirred nor completely adiabatic may deviate substantially

from the theoretical values. Furthermore, the common assumption made in Eq(52) that $\bar{\rho} \approx \rho_0$ will also contribute to such deviations.

It is now appropriate to consider the experimental program planned both to explore the validity of the form of correlation given in Eq(72) and to estimate the value of the recirculated mass flow fraction.

IV EXPERIMENTAL PROGRAM

Aims of the Experimental Program

The first goal of the experimental program is to determine the lean extinction limits of the stabilizer geometry created by the sudden expansion section of a coaxial dump combustor. In particular, the effects of inlet pressure, temperature, velocity, and geometry on the lean extinction limit are sought. Ideally, the effect of combustor scale would also be included in this investigation; however, in order to keep the scope within available resources, this investigation is restricted to a 6" diameter combustor. Geometry variation is accomplished by varying the diameter of the inlet from 2.5" to 5.0" with corresponding step heights varying from 1.75" to 0.5". The second goal of the experimental program is to evaluate the utility of the form of correlating parameter given in Eq(72) over the range of experimental conditions and geometries available.

The third goal is to determine experimentally values of the recirculated mass flow fraction by employing the technique of split-fuel injection introduced by Lefebvre et al. (Ref 93).

Before describing the design of the experimental hardware and execution of the experimental program, it is appropriate to highlight some of the problems peculiar to determining flame stability limits.

Determination of Stability Limits

The experimental determination of accurate blow-off limits for a dump combustor is not a simple task because of the complex flow interactions which occur between the chemical, aerodynamic, and acoustic phenomena associated with combustion. A practical dump combustor

experiences highly turbulent conditions due to the nature of the separation/reattachment process so that perturbations continually exist in local flow conditions. As the lean blow-out limit (LBO) is approached, the combustion process becomes increasingly vulnerable to disturbances, and successive determinations of the blow-off fuel-air ratios will exhibit substantial scatter, even under apparently similar operating conditions.

Detection of the actual point of blow-off is another source of difficulties. A typical experimental procedure to determine a lean blow-off point is to gradually reduce the fuel flow until extinction occurs. Unfortunately, reduction in fuel flow is usually accompanied by a corresponding increase in air flow, and the fuel and air flows at the exact instant of blow-out can be difficult to determine with precision. Additionally, the detection of the point of blow-out can be difficult if the cessation of combustion cannot be visually observed or aurally detected. In many cases, a thermocouple can be placed in the recirculation zone to signal blow-off, but the resulting lags in detection can be appreciable. Additionally, the rate at which the fuel flow is changed as the blow-off limit is approached can significantly affect the result; this is not a trivial matter because in many cases blow-off points have to be determined expeditiously to avoid overheating of the combustor.

In the case of isolated bluff body stabilizers or simple derivatives of such systems, testing can be accomplished under non-constrained (constant pressure) or constrained (constant area) conditions. In non-constrained operation, testing can be carried out in a "free-jet" mode, enabling the velocity and temperature at the

flameholder to be varied independently, while the pressure level remains constant. In constrained operation, the presence of a choked exhaust nozzle constrains the inlet velocity to vary in a manner which is related to the effective heat release in the combustion chamber. Typically, in most experimental tests the combustor may be operated either at chosen inlet pressure and temperature conditions, with the inlet velocity varying with fuel-air ratio, or at constant mass flow and temperature conditions with the inlet pressure and velocity changing with fuel-air ratio. If the flameholder is subjected to identical inlet conditions under both "constrained" or "non-constrained" operation, then the corresponding blow-off fuel-air ratios should be the same. In practice, significant and unpredictable differences can exist due to the dynamic coupling effects which occur under constrained operation. Generally, the unconstrained stable operating range decreases when a choked exhaust nozzle terminates the chamber, and also as the combustion chamber length is increased. These effects could be classified as changes in the downstream boundary conditions which affect the behavior of flow-induced oscillations and thereby the blow-off condition.

An unexpected bonus from the use of a choked exhaust nozzle, however, is that the lean blow-off is usually attained crisply and can be determined with increased precision. Furthermore, the test chamber is effectively decoupled from the vagaries of the facility exhaust system. Another source of dynamic interaction is the inlet piping system upstream of the combustor. Pressure pulses arising from the combustion process can cause significant changes in inlet flow conditions, particularly if the inlet duct is operating near an incipient separation condition.

The above comments are made in the context of determining lean blow-out limits. The determination of rich blow-out limits is even more problematical because of the generally violent, and sometimes near explosive, behavior of combustors as the rich limit is approached. Indeed, the discharge of fuel-rich products into facility exhaust systems can be extremely hazardous, and for this reason such determinations are often prohibited.

From the above discussion, it will be appreciated that the determination of accurate flame stability limits is not entirely straightforward. However, because of the ability to test bluff body stabilizers in an unconstrained environment, several in-depth studies or recirculation zone processes have been made (Refs 49, 56, and 57). Such stabilizers can be examined with comparative ease, using either optical or probe instruments.

In contradistinction to the bluff body case, the coaxial dump combustor presents a much more challenging task. Firstly, the stabilizing element cannot be decoupled from the combustor chamber proper because it is inherently part of the chamber geometry. Secondly, the hot, recirculating gases directly scour the chamber walls, thus making it difficult to use transparent materials and usually restricting operating time due to excessive wall heating. It is also very difficult to optically probe just one segment of the recirculation zone since the line of sight will generally pass through two zones. Thirdly, it is undesirable to use physical probes in this particular environment because the presence of a relatively large, cooled probe leads to significant disturbance of a recirculating flow field. Finally, the basic nature of the separation-reattachment process

yields a highly turbulent quasi-steady flow field which, given the needed instrumentation, would require extensive and time-consuming measurements for detailed characterization.

The foregoing considerations have been taken into account in the design of the experimental combustors and their associated instrumentation. The design of the test hardware will now be discussed.

Combustor Design

The basic combustor chamber was of 6" diameter; a size suited to the test facilities available. A given test combustor was made up of three components, as shown in Fig 24. These components consisted of a 10" long convergent inlet section, the chamber proper, and a convergent exhaust nozzle. The convergent inlet section was selected rather than the usual inlet pipe in order to obtain a more uniform inlet velocity profile and a reduced level of turbulence. The combustor chamber consisted of one master section to which additional sections could be added to vary overall length. The master section was 18" long and instrumented with 15 wall static pressure taps. The chamber was machined internally to provide a truly circular cross-section. For some later tests, 11 external wall thermocouples were added along the length of this master section. For the majority of tests, a 12" uninstrumented chamber was added to the master section, yielding a 30" overall length and a chamber length:diameter ratio of 5. This value was selected because of its relevance to current ramjet engine designs, and also it provided sufficient length to avoid interference with the anticipated recirculation zone sizes. A prime geometric variable is the step height. Thus, six inlet sections were fabricated, yielding dump plane diameters of 2.5, 3.0, 3.5, 4.0, 4.5,

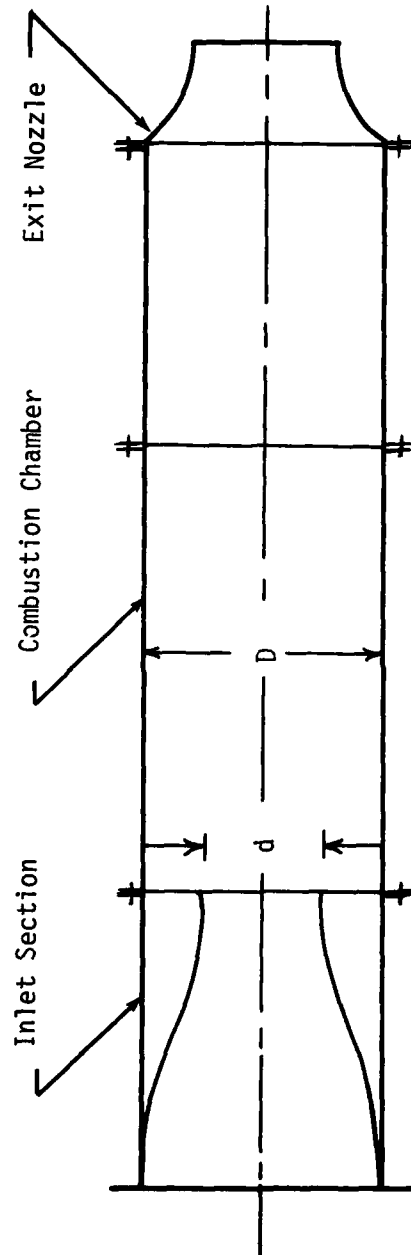


Figure 24. Components of Test Combustor

and 5.0 inches; correspondingly the step height could be varied from 1.75 to 0.5 inches by increments of 0.25 inches.

In order to vary the entry velocity over a meaningful range, three convergent exit nozzles of area ratios A^*/A equal to 0.40, 0.50, and 0.60 were utilized; thus together with straight-pipe operation ($A^*/A = 1.0$) four nozzle sizes were available. Subsequently, operation of the combustor in a straight pipe mode yielded very scattered data, and two more nozzles ($A^*/A = 0.20$ and 0.80) were fabricated to provide a wider range of velocity values.

All components were joined together by flanges. Considerable care was taken during assembly to ensure the concentricity of the inlet and combustor at the dump plane. This was to ensure that a uniform step height was maintained. Previous experience has shown that lack of concentricity could result in partial flame extinction instead of a precise, complete blow-off.

The inlet-to-combustor joint incorporated a specially designed plate to permit fuel injection directly into the annular RZ. A number of tests were run with secondary fuel injection in order to assess the air flow entrained into the recirculation zone. Typical injection plates are shown in Fig 25; six plates were manufactured, one for each dump size.

The available test hardware configurations are summarized in Table I. All components were fabricated from steel.

Test Facility

This investigation was part of a continuing series of combustor studies carried out in-house by the Ramjet Engine Division of the USAF Aero Propulsion Laboratory (AFAPL). Consequently, the AFAPL test



Figure 25. Secondary Injection Plates

facilities were utilized for this investigation. A brief discussion of relevant parts of this facility follows.

The combustor test rig is mounted on a floating thrust stand which is suspended from four flexures; a load cell measures the thrust forces associated with the combustor. The stand is illustrated in Fig 26. The air supply to the test rig is supplied through 12 two-inch diameter flexible hoses. The thrust stand is statically calibrated periodically, using a reference load cell. Additionally, prior to actual testing, the accuracy of the thrust reading is checked under no-flow and flowing conditions.

The air supply and exhaust systems are shown schematically in Fig 27. The air is obtained from a 300 psi laboratory supply and may be heated by an indirectly fired gas furnace or by an in-line combustion heater. The latter heater is a modified J-85 combustion chamber and is operated on ethylene with an oxygen make-up flow added upstream of the heater. However, to avoid the effects of vitiation by combustion products, only the clean air heater was used in this test series. The air mass flow rate to the combustor is measured, using flange-tap square-edge orifice plates, and two orifice installations are available, depending on the mass flow level.

After leaving the combustor, the exhaust gases are cooled by a water-spray and sucked out through a high capacity exhaust system. The exhaust pressure may be reduced down to pressures of 3 psia. The only hydrocarbon fuel readily available in large quantities was commercial grade ethylene, and the bulk of the experimental work was performed using this gas. Subsequently, supplies of this gas were interrupted, and several tests were later run using JP-4.

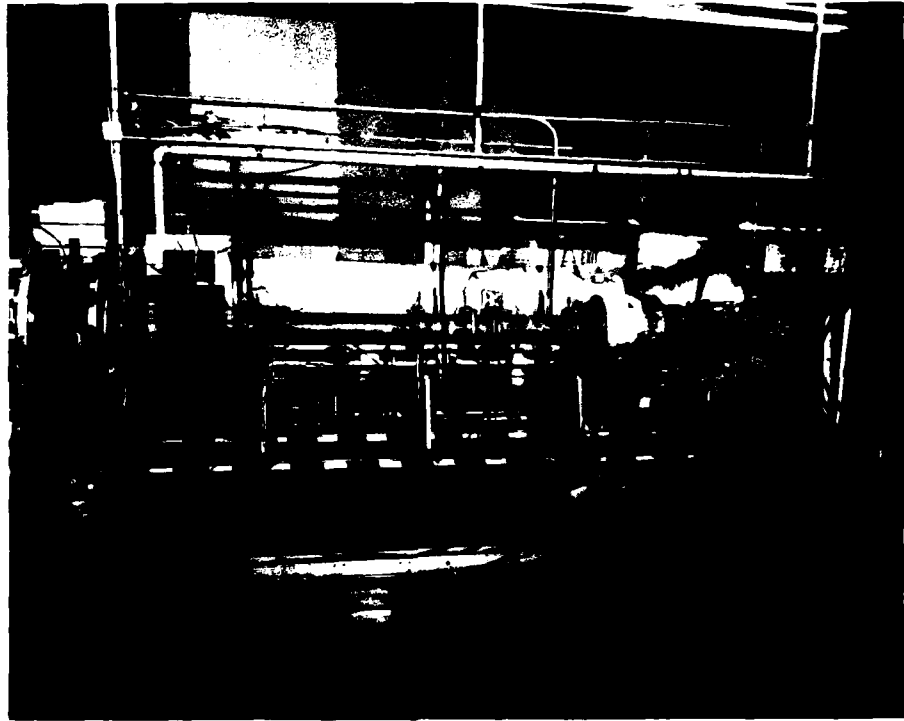


Figure 26. Ramjet Test Stand

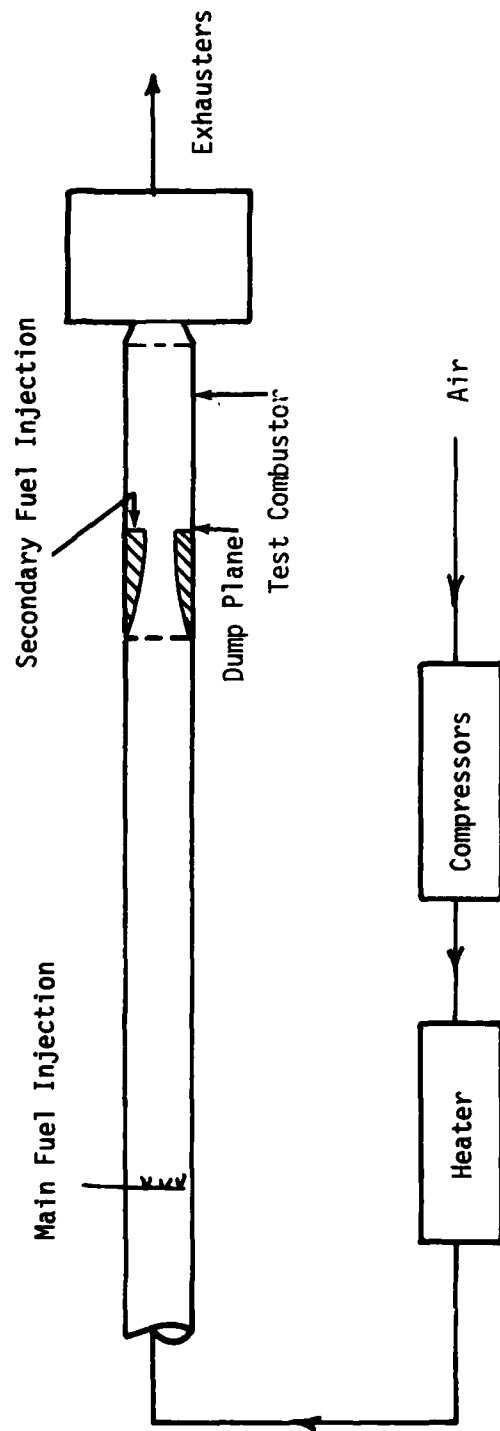


Figure 27. Schematic Arrangement of Test Stand Flow Systems

For some tests with ethylene, both mainstream injection and secondary injection into the RZ were required. Consequently, the bottled gas supply was split into two feed lines and the fuel flow measured by Cox turbine-type flowmeters. Once again calibration of these flowmeters was periodically accomplished, using a reference flowmeter. When JP-4 was used, only one feed line was required; JP-4 was pumped from a main storage tank and the flow rate also measured by a Cox flowmeter.

The data acquisition system is shown schematically in Fig 28. Thus, incoming sensor information can be fed from a patch panel to either a Hewlett-Packard digital data system or a Mod Comp II computer controlled data system. This latter system samples at a rate of about 5000 channels per sec. Each data point is the average of about 45 separate scans of the data system in order to average out electrical noise.

In addition to acquiring, storing, and processing all raw data, the Mod Comp II system displays on a video screen, mounted on the test console, all parameters needed to run the combustor at the required test conditions. Furthermore, at the end of any given test run, selected data is displayed on a Tektronix graphics display terminal; hard copies of this data are readily available, and selected quantities may be cross-plotted to further aid analysis of the data.

The gas flow path through the test rig and some associated instrumentation are shown in Fig 29. Initially, a flow straightening honeycomb and several flow smoothing grids were installed; however, due to occasional occurrences of "flashback," these components received substantial damage and were subsequently removed from the

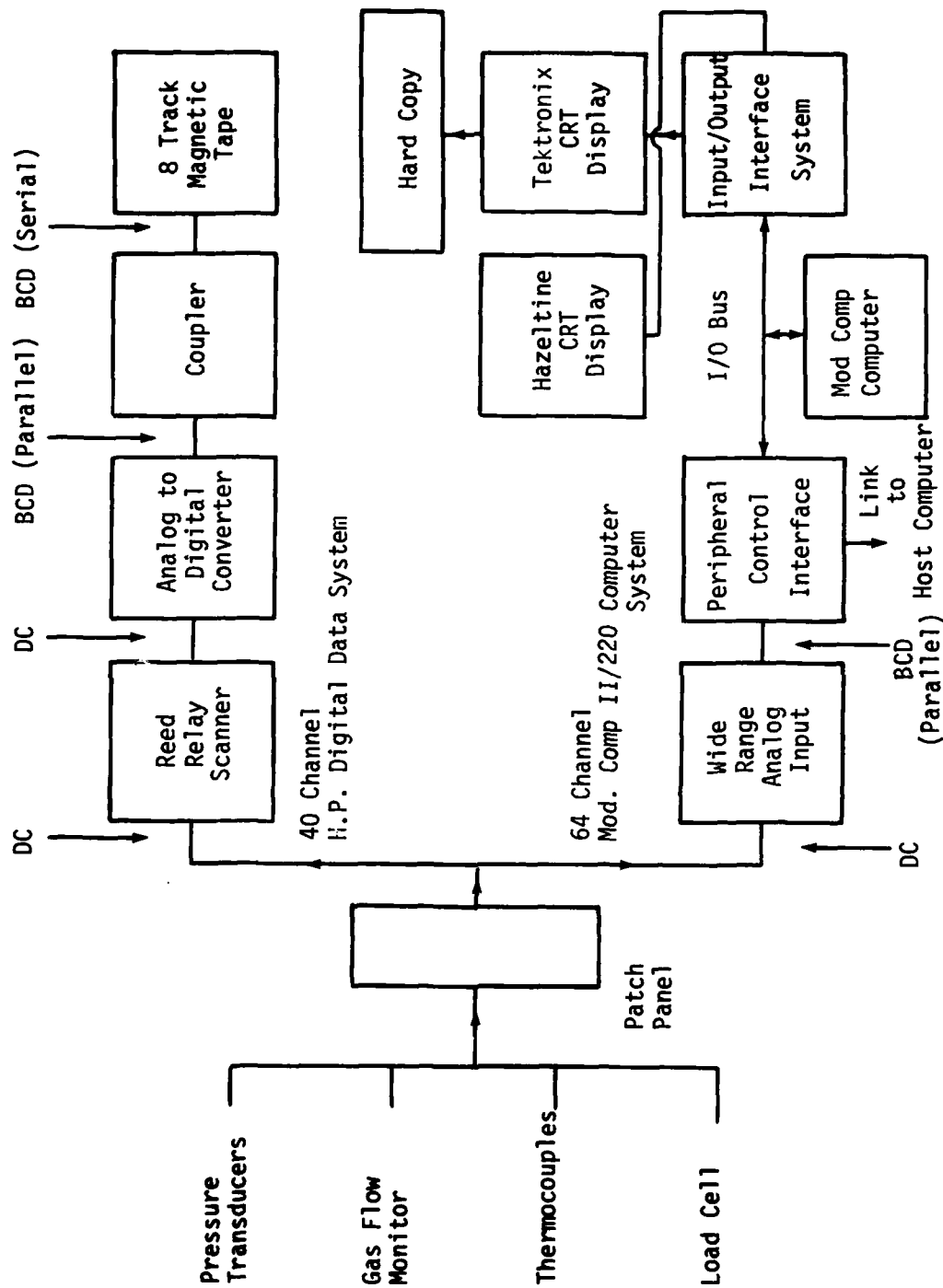


Figure 28. Schematic Arrangement of Data Acquisition System

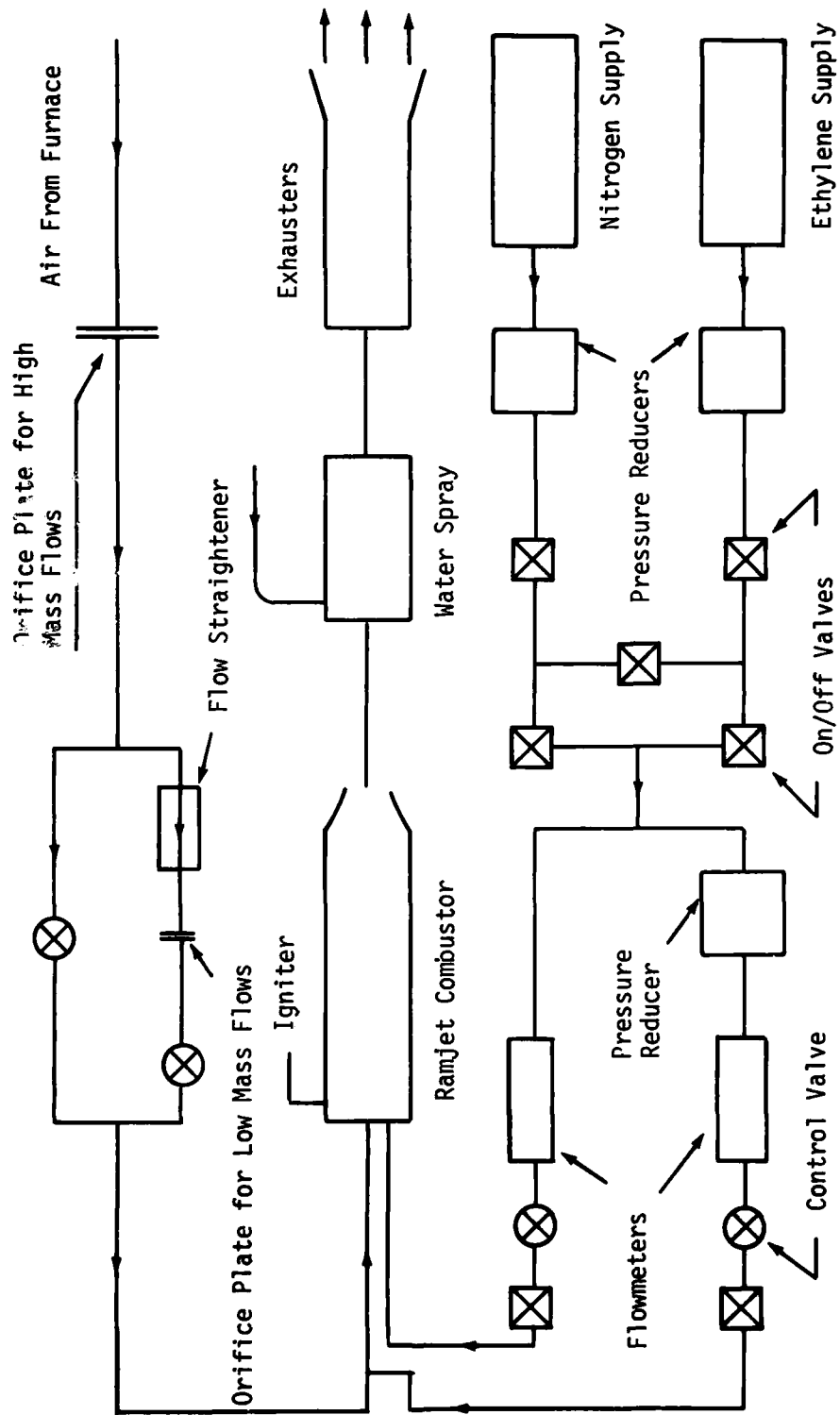


Figure 29. Gas Flow Paths Through Test Rig

rig. Fuel was injected into the stream some seven feet upstream of the dump station through a 32-point injection system to ensure that a uniform fuel-air mixture was obtained. The injector consisted of eight radial spokes, each carrying four holes, with injection perpendicular to the flow direction.

Experimental Investigations

Three distinct test series were performed as follows:

- a. Flame stability of plain dump combustors.
- b. Blow-out limits with additional fuel injection into RZ.
- c. Flame visualization studies with a quartz combustor.

The first and major investigation was the effect of geometric variables on flame stability. The configurations tested are shown in Table I. The baseline inlet configuration was the 3.5" diameter dump size, and the effect of varying this inlet size from 2.5" to 4.5" was of prime interest. A standard procedure that was executed prior to any combustion tests was to check the functioning of the test rig over a wide range of cold mass flows. At each mass flow, a read-out of key data was obtained, thus providing a final check on the integrity of line connections and data acquisition system performance. An incidental benefit was the accumulation of a broad data base on the fluid mechanics of dump combustors.

As noted earlier, the majority of tests was performed using ethylene (95% pure), supplies of which were readily available. Two main problems were encountered with this gas. These were: the violent and explosive combustion conditions encountered in the determination of rich blow-out limits and the occurrence of "flashback" phenomenon. The determination of rich blow-out limits was difficult because of the

increasingly unsteady nature of the combustion process as the rich blow-off limit was approached; this led to poor repeatability of data. Furthermore, the accumulation of fuel-rich gases in the exhaust ducting led to several explosions from which minor mechanical damage resulted. Consequently, rich-limit testing was soon eliminated. The second phenomenon experienced with ethylene was combustion upstream of the main burner. This phenomenon occurred occasionally during ignition transients or when adjusting fuel and air mass flows at low air flow rates, and also with small area exit-nozzles. The mechanism of this phenomenon was not explored nor its brief occurrence documented; when it occurred its effects were very damaging, leading to destruction of turbulence-reducing screens, pitot probes, and even part of the 5" inlet converging section. Plee and Mellor (Ref 95) have recently reviewed this phenomenon.

Opportunity was taken to obtain flame stability limits with pre-mixed JP-4 and air. In this case the flow at the rich blow-off limit was much smoother, and repeatable data were obtained. Also, the occurrence of flashback was much reduced.

For either fuel, the experimental procedure to determine blow-off limits was the same. At a given inlet temperature, the combustor was tested over a range of mass flows. For a given mass flow, the combustor was ignited at a high fuel-air ratio (typically 0.05), and the mass flow readjusted to the desired condition. The lean blow-off limit was determined by incrementally reducing the fuel flow while maintaining the desired air mass flow level until extinction occurred. This process had to be accomplished expeditiously to avoid overheating of the combustor, but slowly enough to ensure that steady flow prevailed after

each incremental change of fuel flow. Several tests were performed at the same flow conditions to ensure that repeatable data were obtained. A Kistler pressure transducer located at the dump plane was used to give a precise indication of blow-off. The visual display of the transducer output clearly indicated the cessation of combustion at blow-off. A thermocouple was also located in the RZ, but the Kistler display was a much superior indicator of blow-off. Rich blow-off limits were determined in a similar fashion. During the test phase, two experimental constraints were generally encountered. Considerable care was required both to maintain a constant inlet temperature as the air mass flow varied and to avoid combustion instability effects. The temperature problem was due to the thermal inertia associated with the extreme length of the air supply pipe from the air heater to the rig (several hundred feet). This problem was overcome by running test points alternately at high and low air mass flows. Combustor "screech" was encountered at high pressure, high mass flow conditions, and was generally avoided by testing at reduced pressures. It was also noted that the "screech" generally disappeared as the lean blow-off limit was approached. However, this phenomenon was of sufficient interest that a separate investigation using the same hardware has subsequently been initiated.

As part of a general upgrading of facility equipment, the clean air heater initially used in this investigation was subsequently replaced by a more energy-efficient unit. During the replacement phase, some of the flame stability tests were repeated, using a vitiated heater with oxygen make-up. A considerable narrowing of the stability range was immediately noted, and no further testing was accomplished with this heater.

The second type of investigation performed was to study the effect of additional fuel injection into the RZ. As noted previously, the motivation for this investigation was that the determination of the lean blow-off limits of a split injection system enables an estimate to be made of the air entrainment rate into the recirculation zone. The procedure for determining the lean blow-off limits in this case was similar to that outlined previously except that the fuel injection rate into the RZ was maintained at a constant value while the main fuel flow was varied to obtain the lean blow-off limit. The fuel injection plates utilized for secondary fuel injection were of the type shown in Fig 25. Secondary fuel is injected axially through concentric rings of holes. A large number of holes was utilized to keep the fuel injection velocity low so as to minimize interference with the main recirculation zone. Furthermore, for each test geometry the effect of secondary fuel injection on the recirculation zone was studied by observing the effect of fuel flow on the wall static pressure distribution. Gaseous nitrogen was substituted for fuel in these tests to conserve fuel. In general, no significant effect of gas flow on the structure of the recirculation zone was observed and, indeed, no effect was anticipated because such fuel flow rates were very small. Two interesting effects were observed with secondary fuel injection. Firstly, two types of blow-off were observed. For relatively low secondary fuel flows a normal lean blow-off was obtained as the main fuel flow was reduced. However, at higher secondary fuel flows, as the lean blow-off was approached, a change in combustion mode was observed, and the combustor would not extinguish until the secondary flow was reduced. This latter mode had to be avoided in order to prevent ambiguity in the desired test data.

Another significant observation was that under certain conditions the injection of small quantities of secondary fuel led to a much quieter-running combustor; thus, secondary injection may suppress some instability mechanisms.

A final test series was performed to observe the blow-off phenomenon. For this series, an annealed quartz combustor was utilized, and the installation is shown in Fig 30. It will be seen that the combustor is secured between the upstream and downstream flanges by four spring-loaded steel rods. Each end of the quartz combustor was sealed with a ring gasket fabricated from "carborundum fiber frax" material to which was applied a silicone rubber coating. After curing of the coating, an effective high temperature gasket was obtained. This method of installing a quartz chamber functioned quite satisfactorily under combustion conditions provided that "screech" was avoided. Flame blow-off was observed with three inlet sizes: 2.5", 3.5", and 4.5". Additionally, some studies were made of flame blow-off phenomena when secondary fuel injection was employed. All flame visualization studies were photographically recorded, usually at a frame speed of 500 frames per second.

The results obtained from the various test series outlined above will now be described.

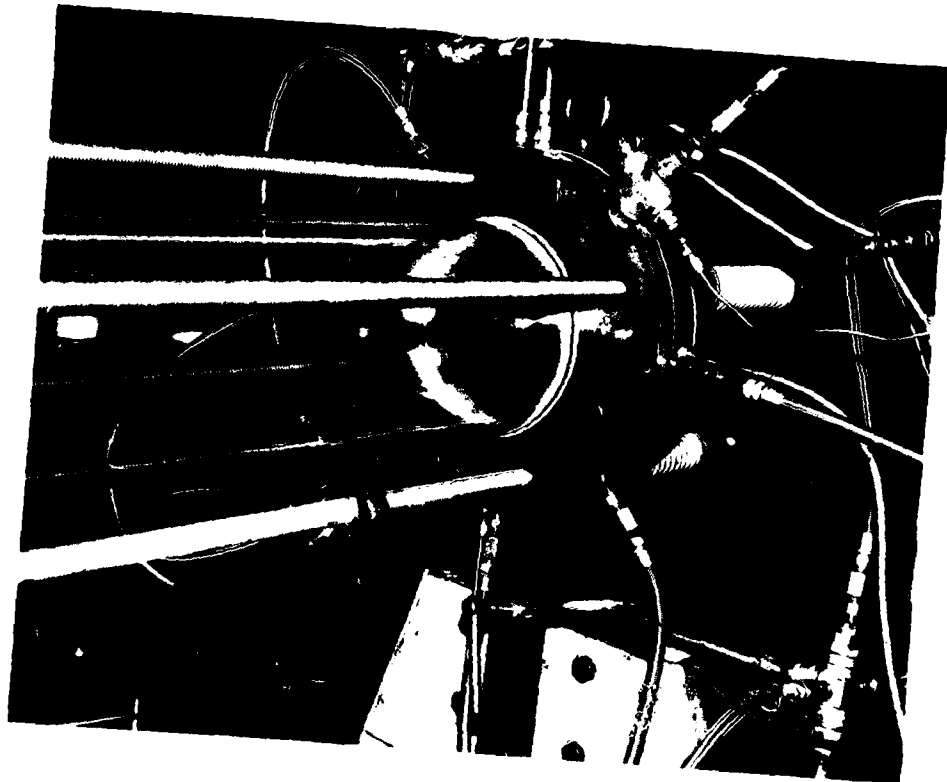


Figure 30. Installation of Quartz
Combustor

V RESULTS AND DISCUSSION

It will be recalled from the preceding Chapter IV that three distinct test series were performed as follows:

- a. Determination of the flame stability limits of plain dump combustors, using both ethylene and JP-4 as fuels.
- b. Determination of lean extinction limits with additional injection into the recirculation zone.
- c. Flame visualization studies using a transparent quartz combustor.

In addition to the three basic test series, a cold-flow test was run to determine the velocity profiles associated with each combustor inlet. These tests were run over a range of inlet Reynolds and Mach numbers. The results are shown in Appendix D, and it will be noted that substantially constant velocity profiles were obtained.

The results of each basic test series will now be presented and discussed.

Flame Stability Tests

In order to investigate the effects of the primary variables of temperature, pressure, step height, and velocity on the stable operating range, it is obviously desirable to vary these quantities independently of one another. The first three variables are easily controlled; however, for a given combustor configuration operating at a given inlet temperature and with a choked exit nozzle, the Mach number at the dump plane is dependent on the effective heat release in the combustor.

At the blow-out condition, the dump plane velocity will typically satisfy Eq(49), i.e., $\phi_{LBO} \propto \frac{U_0^\alpha}{P_0 \beta h^\gamma T_0^\delta}$, and will simultaneously

correspond to a value determined by the effective heat release in the combustor. It will be recalled from Chapter IV that for a given test, the lean blow-out condition was determined by progressively reducing the fuel flow while the inlet temperature and mass flow were maintained constant. For successive tests at a given inlet temperature but with various mass flow levels, it was found that the dump plane Mach number at blow-out remained practically constant over the relatively limited range of variation of fuel-air ratios which occurred in determining the lean extinction points. Thus, for a given inlet temperature the dump plane velocity at lean extinction is approximately constant even though the mass flow (and therefore the pressure) is varied. Obviously, for a given nozzle throat size the dump plane velocity will decrease with increasing dump diameter, and conversely for a given dump diameter this velocity will rise if the throat area is increased. With this introductory note on flow conditions concluded, one may now proceed to consider the data. The results obtained with ethylene will be considered first.

Tests with Ethylene. The test matrix performed with ethylene was presented in Table I. It will be noted that all dump sizes were successfully run, the dump plane diameters varying from 2.5" to 5.0". In the latter case, it was interesting to observe that successful flame stabilization and combustor operation was achieved with only a 1/2" step. Unfortunately, only limited testing was possible as the 5.0" convergent section received severe damage due to "flashback" of the flame upstream of the combustor.

The experimental data acquired for a typical dump plane diameter (3.5") are shown in Figs 31, 32, and 33; each figure corresponds to a given nozzle area ratio. Only lean extinction data are

TABLE I COMBUSTOR GEOMETRIES TESTED

Test Series	A*/A	d"	2.5	3.0	3.5	4.0	4.5	5.0
2	0.20		J	--	J	--	--	--
1	0.40		E,J,R	E	E,J,R	E	E,J,R	--
1	0.50		--	E	E	--	--	--
1	0.60		E,R	--	E,R	E	E,J,R	E
2	0.80		--	--	J	--	J	--
1	1.00		E,J	E	E	E	E,J	E

Legend

E Denotes testing with Ethylene

J Denotes testing with JP-4

R Denotes test with RZ Injection (Ethylene only)

All of the above testing was with clean air.

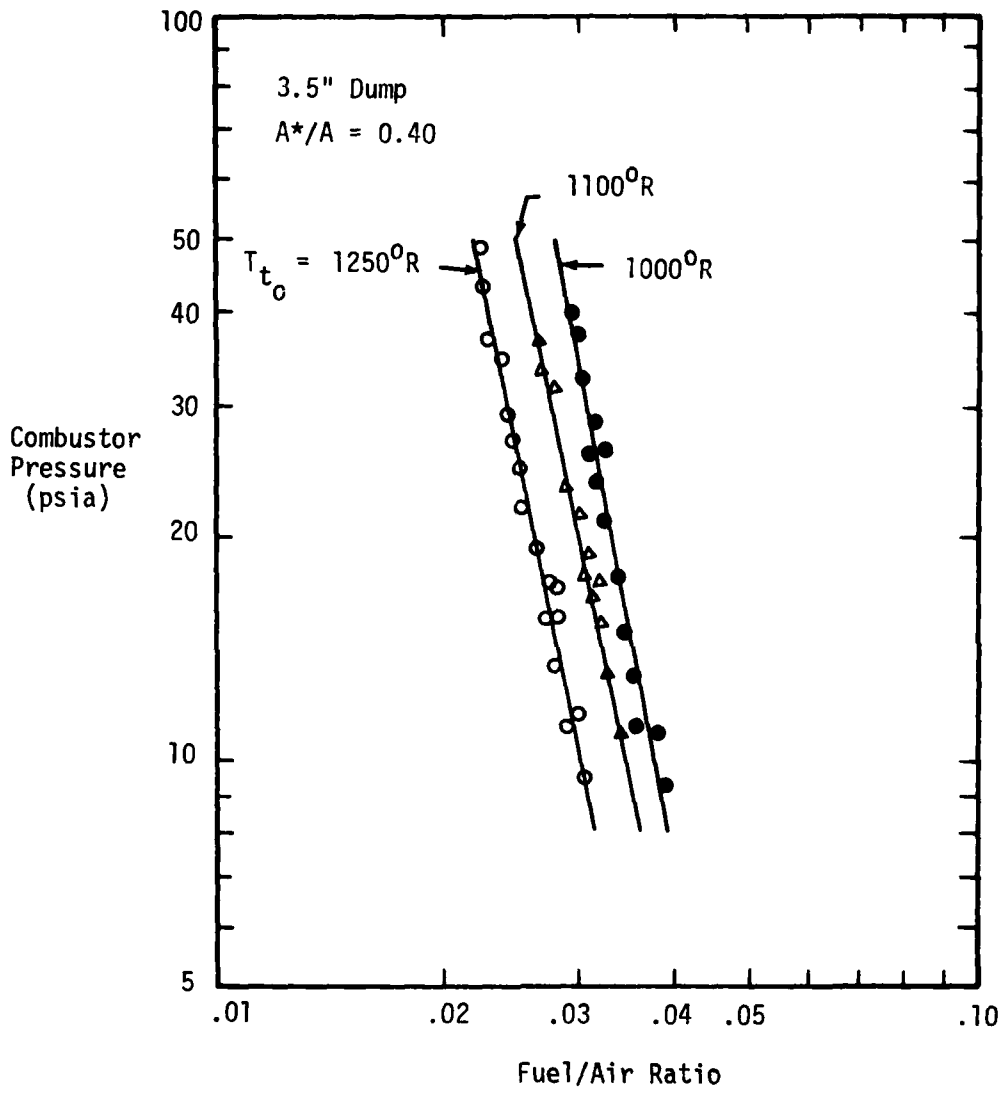


Figure 31. Lean Extinction Limits: 3.5" Dump Dia., 0.40 Nozzle Area Ratio; Ethylene Fuel

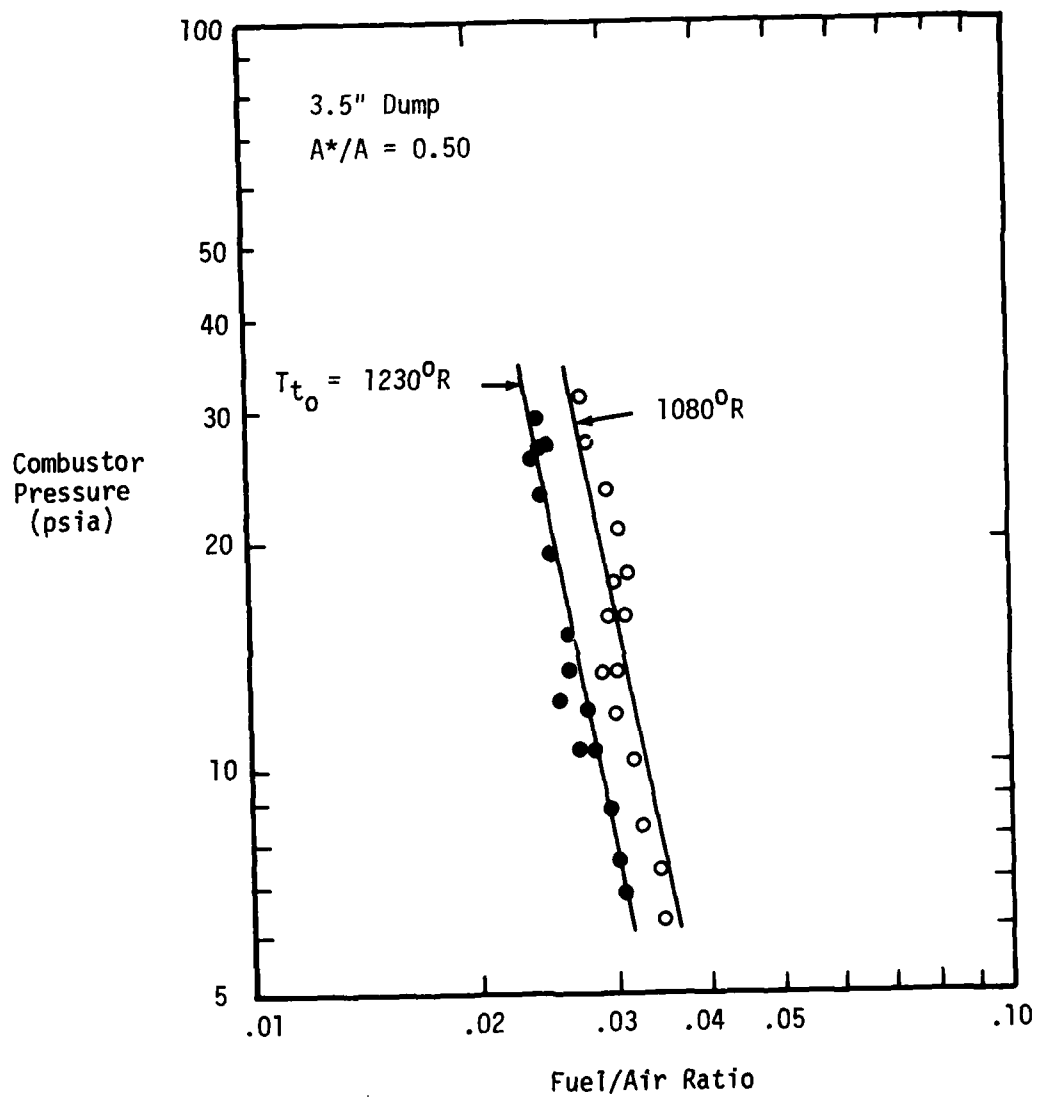


Figure 32. Lean Extinction Limits: 3.5" Dump Dia., 0.50 Nozzle Area Ratio; Ethylene Fuel

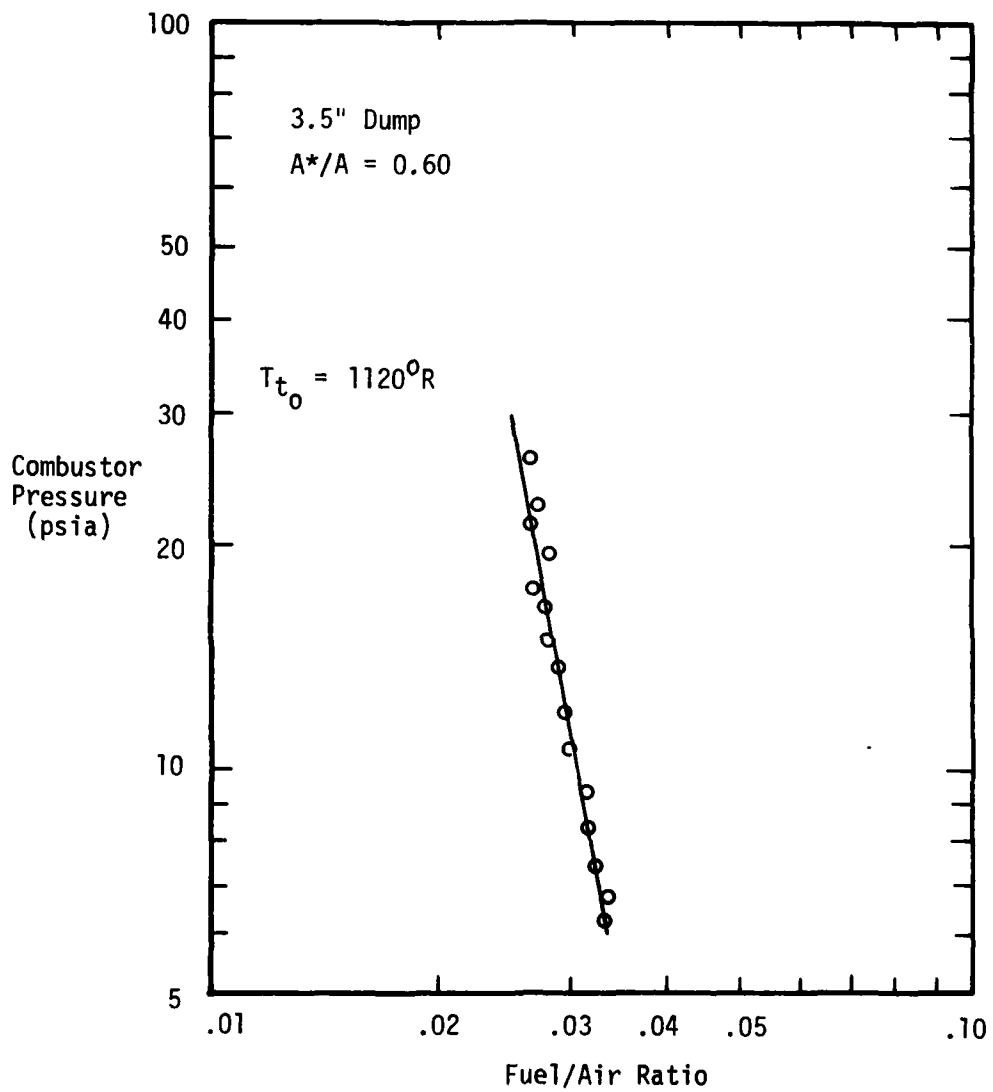


Figure 33. Lean Extinction Limits: 3.5" Dump Dia., 0.60 Nozzle Area Ratio; Ethylene Fuel

shown because of the hazardous nature of the rich limit testing. Considering Fig 32, it will be recalled that a line of constant inlet temperature operation also corresponds effectively to a line of constant velocity. It is immediately apparent that, at a given temperature and velocity, the effect of increasing pressure is to reduce the lean extinction fuel-air ratio. This variation is also in accord with that anticipated from Eq(71).

The effect of velocity on the lean extinction limit was evaluated by two methods. The first was to compare the data from combustors of the same step height, operated at identical inlet pressure and temperature conditions, but with different exit nozzle throat sizes. Such a comparison is shown in Fig 34, and it is apparent that inlet velocity does not exert a strong effect on lean extinction limits. Unfortunately, only one such comparison could be made because of the difficulty of expeditiously setting-up identical temperature conditions at the entrance of each of the desired combustor configurations. This was due to the thermal inertia of the heater-inlet pipe system. A second approach was therefore adopted, and this consisted of operating a given combustor in a straight-pipe (i.e., no exit nozzle) unchoked mode. Under these conditions, the inlet pressure and temperature were maintained approximately constant, and the velocity varied by changing the mass flow. Typical data are shown in Fig 35, using Mach number for convenience; thus the lean limit is relatively insensitive to velocity. A regression analysis of the data showed that a slight increase of lean limit fuel-air ratio with velocity is present.

Returning to Fig 31, it is quite clear that temperature exerts a major effect on the lean limit fuel-air ratio. Thus with

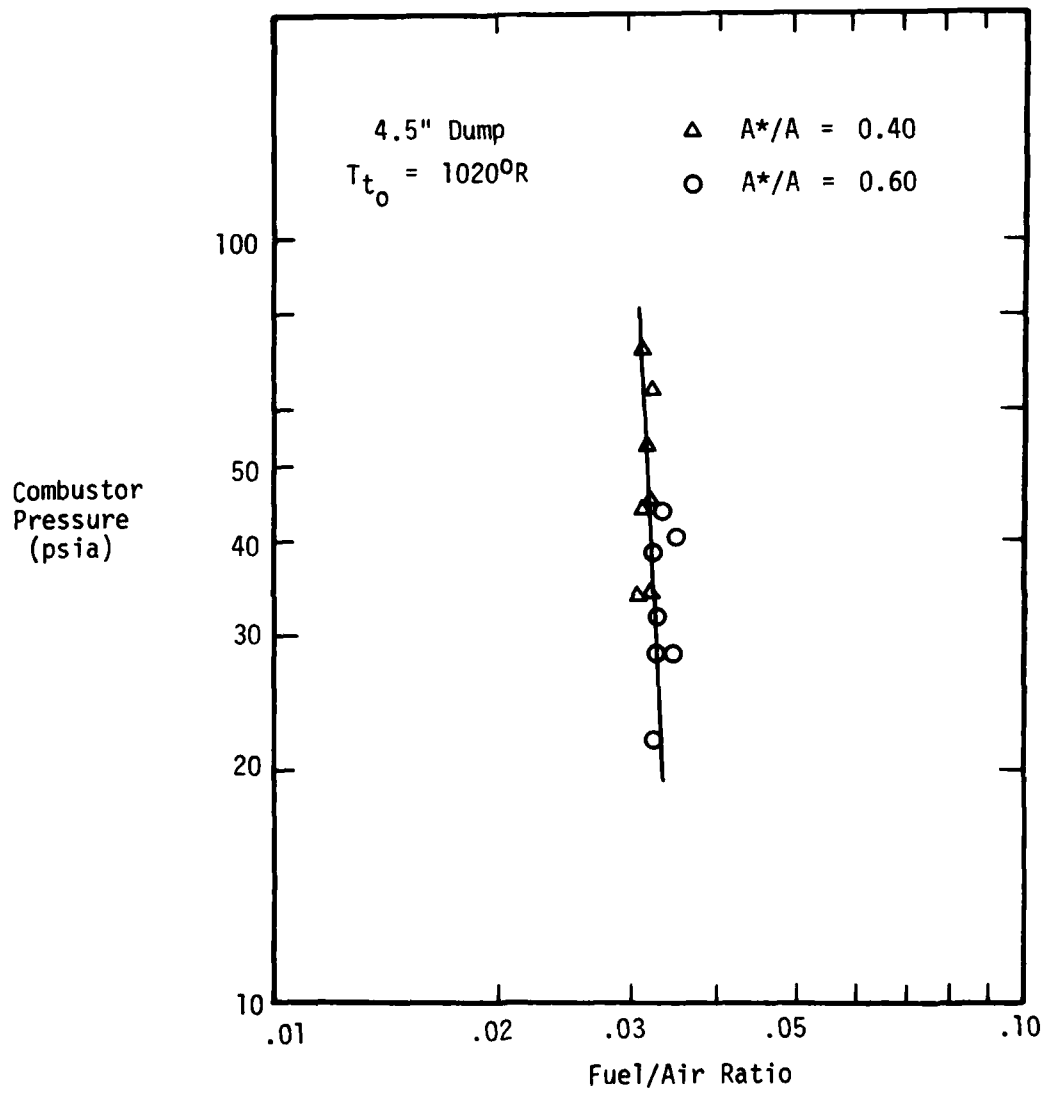


Figure 34. Effect of Nozzle Area Ratio on Lean Extinction Limit; Ethylene Fuel

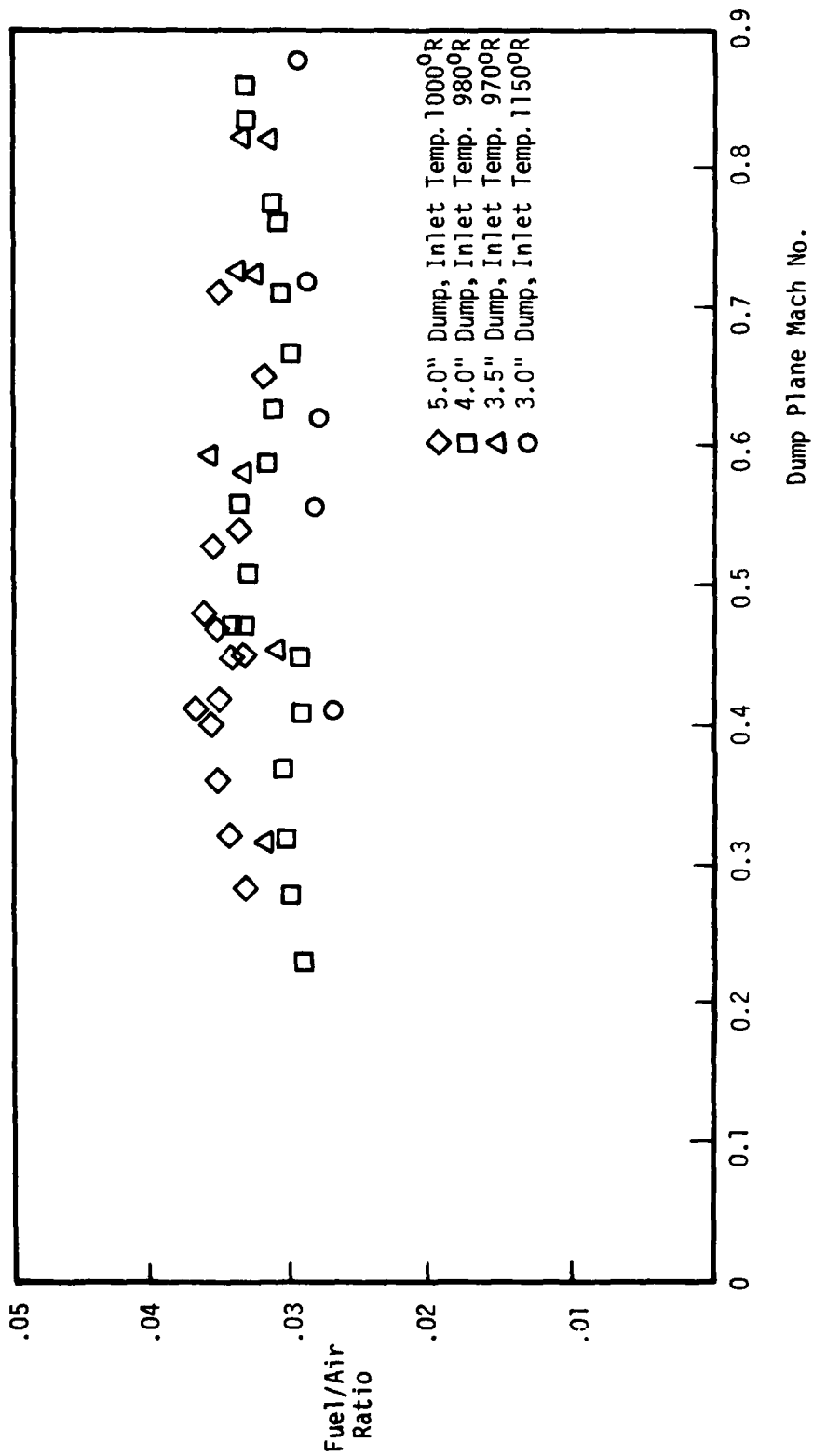


Figure 35. Effect of Inlet Mach Number on Lean Extinction Limit; Ethylene Fuel

increasing temperature, the lean extinction fuel-air ratio decreases markedly. This observation is also in accord with Eq(71). The effect of step height variation on the lean limit is illustrated in Fig 36: in this case the lean extinction limits of two combustors, operated under identical inlet conditions, are compared. The expected beneficial effect of increased step height is clearly seen, and this observation also accords with Eq(71).

Following the conclusion of the tests with ethylene, two sets of tests were run using JP-4 as fuel. These results will now be described.

Tests With JP-4. The first test series performed with JP-4 is presented in Table I. It will be noted that once again three nozzle area ratios were available; namely, 0.40, 0.50, and 0.60. A second set of tests was performed with two additional nozzle area ratios equal to 0.20 and 0.80, respectively. Some difficulty was experienced with the smaller nozzle because of the occurrence of "flashback" at the low dump plane velocities corresponding to this nozzle area ratio, and only limited data were obtained. An additional feature of the tests with JP-4 was that rich blow-out limits were also obtained. In the case of JP-4, the rich limit extinction was relatively quiet and less hazardous than with ethylene. Also, the availability of a larger exhaust nozzle permitted full stability loops to be demonstrated for the first time for dump configurations.

A typical set of data acquired for a given configuration is shown in Fig 37, and both lean and rich extinction limits are shown. The lean limit variation is similar to that obtained previously with ethylene. It will be noted that increasing pressure improves the stable operating range. The effect of velocity on the lean limit

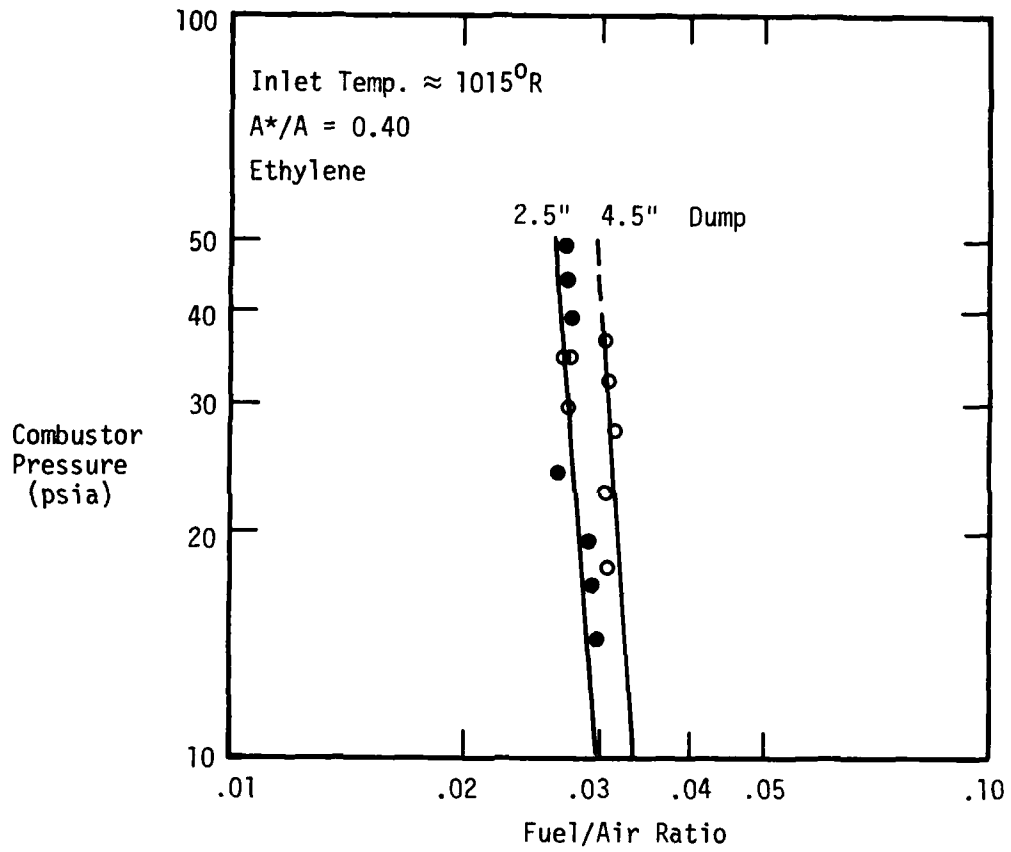


Figure 36. Effect of Step Height on Lean Extinction Limit; Ethylene Fuel

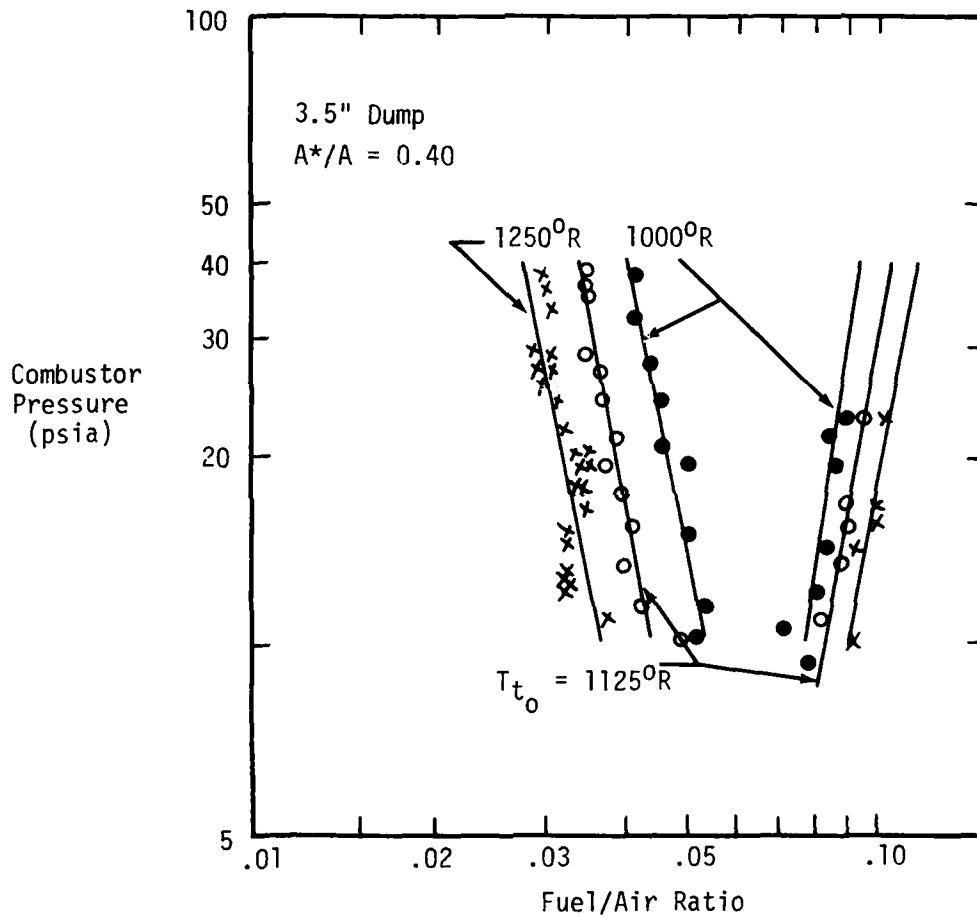


Figure 37. Flame Stability Limits: 3.5" Dump Dia., 0.40 Nozzle Area Ratio; JP-4 Fuel

fuel-air ratio was only studied in this case by operating combustors of the same diameter ratio (d/D) at identical inlet pressure and temperature conditions but with different nozzle throat sizes. A comparison is shown in Fig 38, and once again it is apparent that velocity has only a small effect on the lean extinction limit. Returning to Fig 37, it is clear that increasing temperature exerts a major beneficial effect on the lean extinction limit. The effect of step height variation is shown in Fig 39, and once again increasing step height reduces the lean extinction fuel-air ratio. Thus the effects of pressure, temperature, velocity, and step height are very similar to those observed with ethylene.

One noteworthy effect encountered in the JP-4 test series was the occurrence of combustor "screech" at high inlet temperatures. In one instance this produced considerable scatter in the lean-extinction data as shown in Fig 40. The "screech" condition was eliminated by moving the fuel injectors upstream into the highly turbulent area where air enters the test rig. The multi-hole finger injectors were also replaced with fan-spray injector elements. The improvement of the data that occurred with "screech" elimination is also shown in Fig 40.

Another test excursion was to investigate the effect of combustor length to diameter ratio (L_c/D) on the lean stability limit. It is well known that for conventional stabilizers, an increase in combustor length results in a decreased stable operating range. The reason for this decrease is usually attributed to increased flow perturbations arising from acoustic effects. The significance of this variable was assessed by operating the 2.5" dump combustor with combustor lengths of 18", 30", and 36". The corresponding results are shown in Fig 41; it will be noted that only a minor reduction in stable operating range occurred in this case.

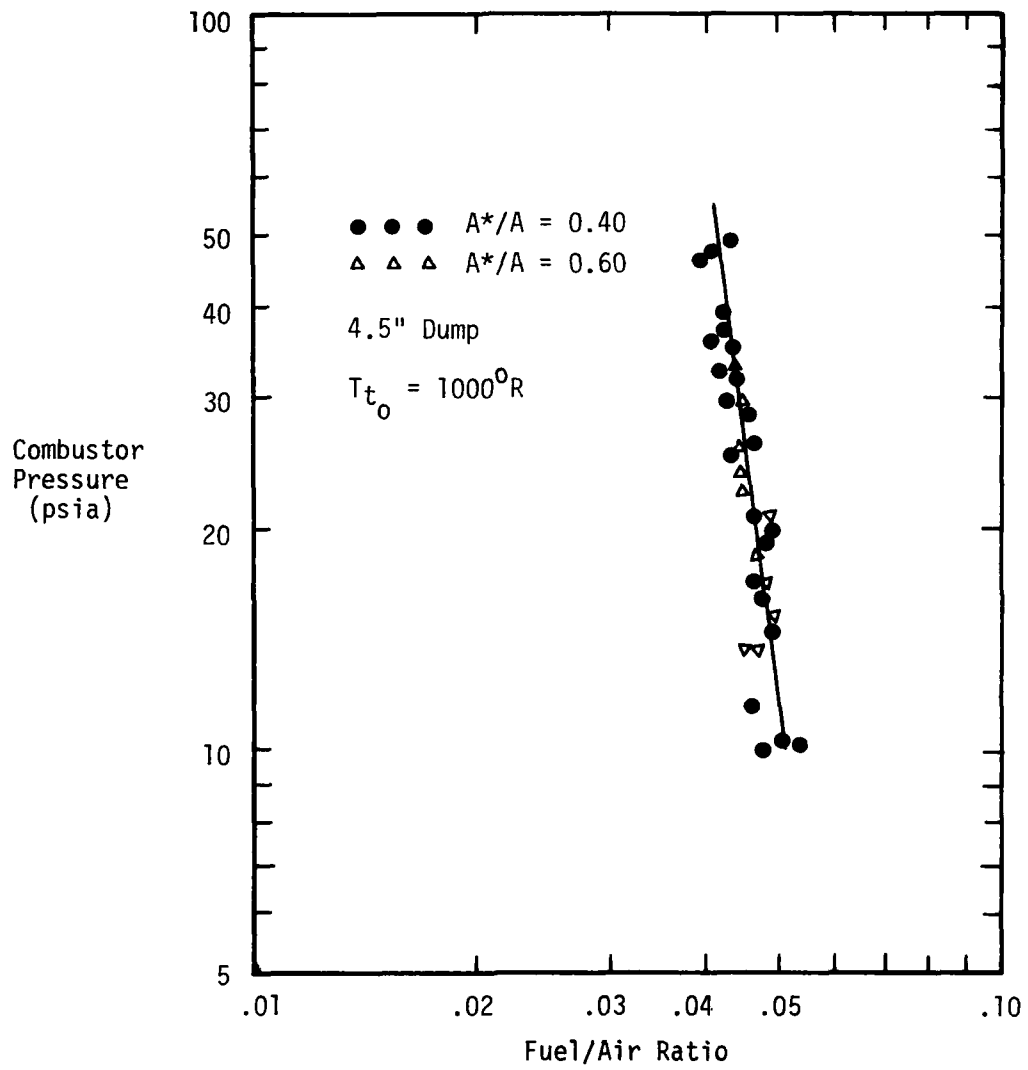


Figure 38. Effect of Nozzle Area Ratio on Lean Extinction Limit; JP-4 Fuel

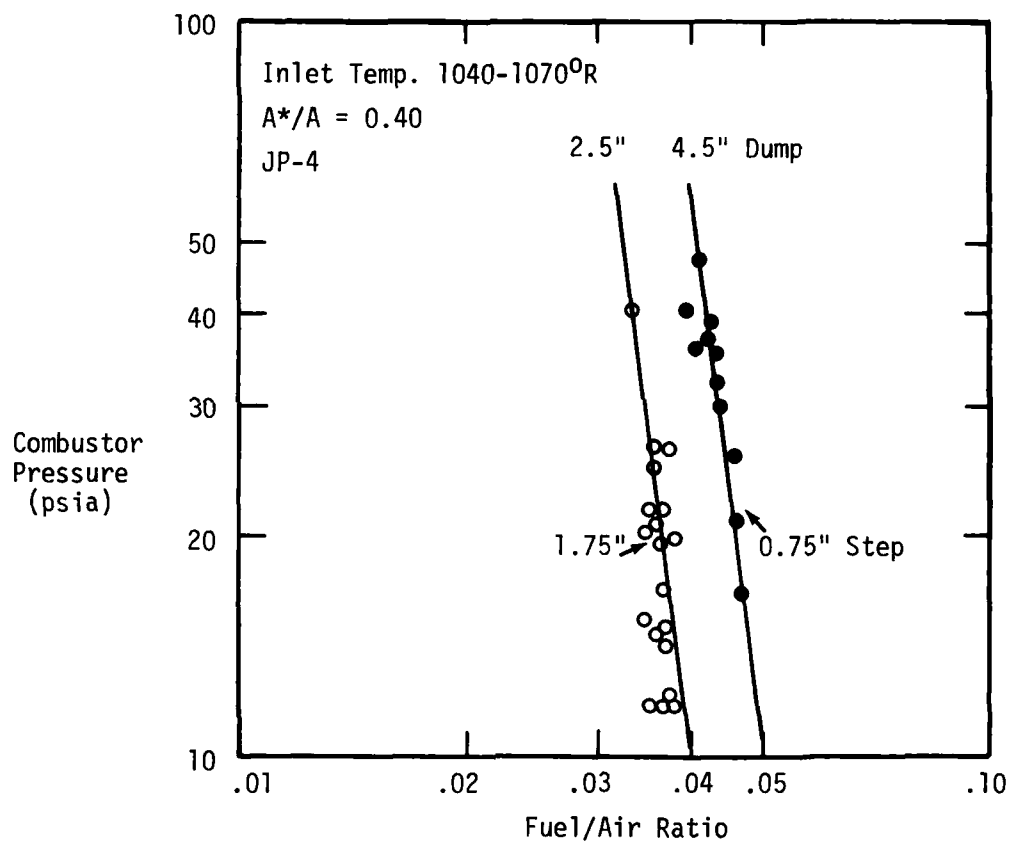


Figure 39. Effect of Step Height on Lean Extinction Limit; JP-4 Fuel

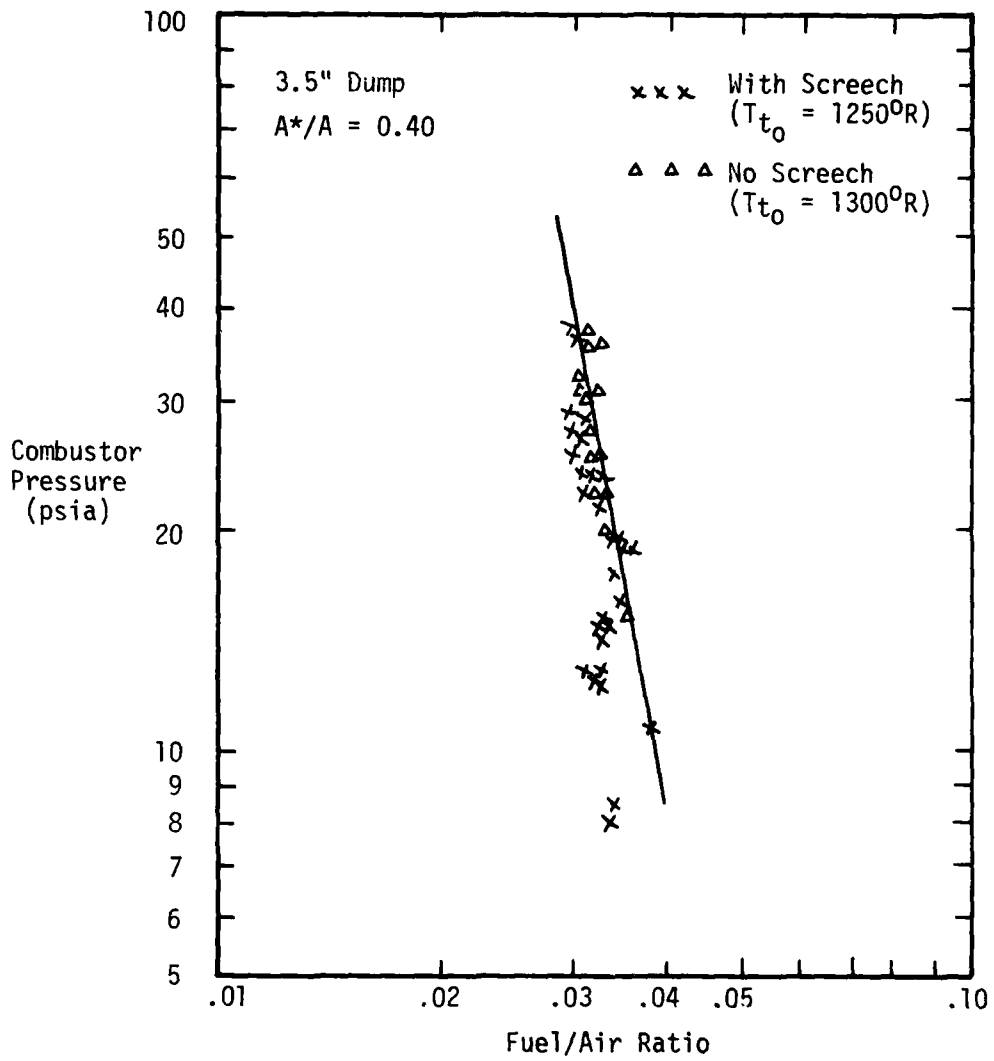


Figure 40. Effect of Screech on Quality of Data; JP-4 Fuel

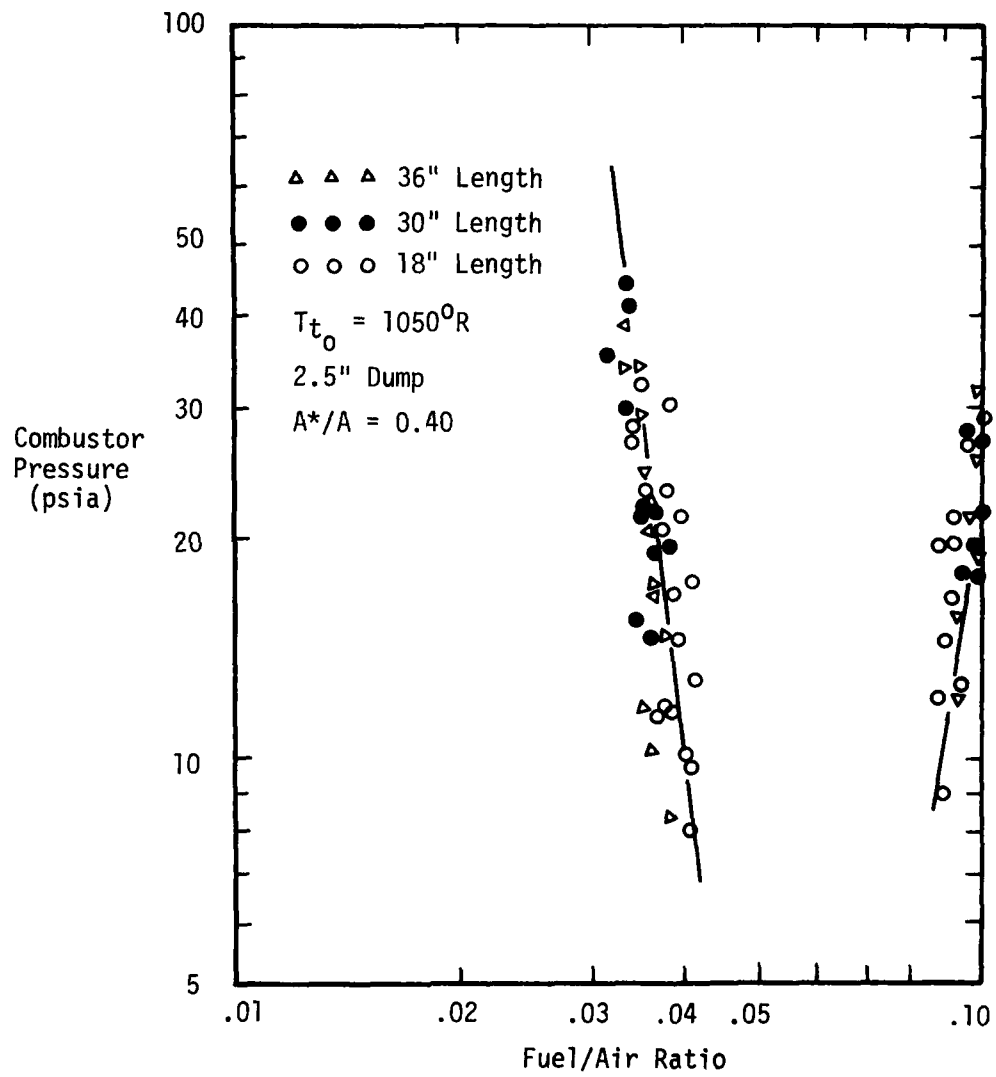


Figure 41. Effect of Combustor Length to Diameter Ratio on Stability Limits; JP-4 Fuel

Another brief test excursion was to investigate the effect of using vitiated air on the stable operating range. In this case an ethylene-fueled combustion heater was used with oxygen make-up. Despite the replenishment of the oxygen, a distinct reduction in stable operating range was experienced as shown in Fig 42. This result was rather surprising considering that the incoming air was only heated from 600 to 1000°R.

As a final test goal, it was decided to determine the complete stability loop for given combustor configurations. This was successfully accomplished by operating these combustors at very low pressures, typically at less than 10 psia. The results obtained are shown in Figs 43 and 44, and they demonstrate conclusively that stability loops do exist for the sudden expansion configuration. This demonstration concluded the flame stability tests of the plain dump combustor. No general discussion has been given of data obtained with the 3", 4", and 5" diameter inlets. This was due firstly to the fact the 5" inlet was destroyed due to "flashback" early in the test program. Secondly, the 3" and 4" inlets were tested only with ethylene, and the limited data obtained simply confirmed the results obtained with the 2.5", 3.5", and 4.5" combustors. The second test series which utilized direct injection into the recirculation zone will now be described.

Lean Extinction Tests With Split Flow Injection

The purpose of these tests was to determine the amount of air entrained and consumed in the recirculation zone. It will be recalled that in order to estimate the fraction of air entrained, it is necessary to use a split fuel injection system. Thus fuel is injected both into the main air flow and directly into the recirculation zone.

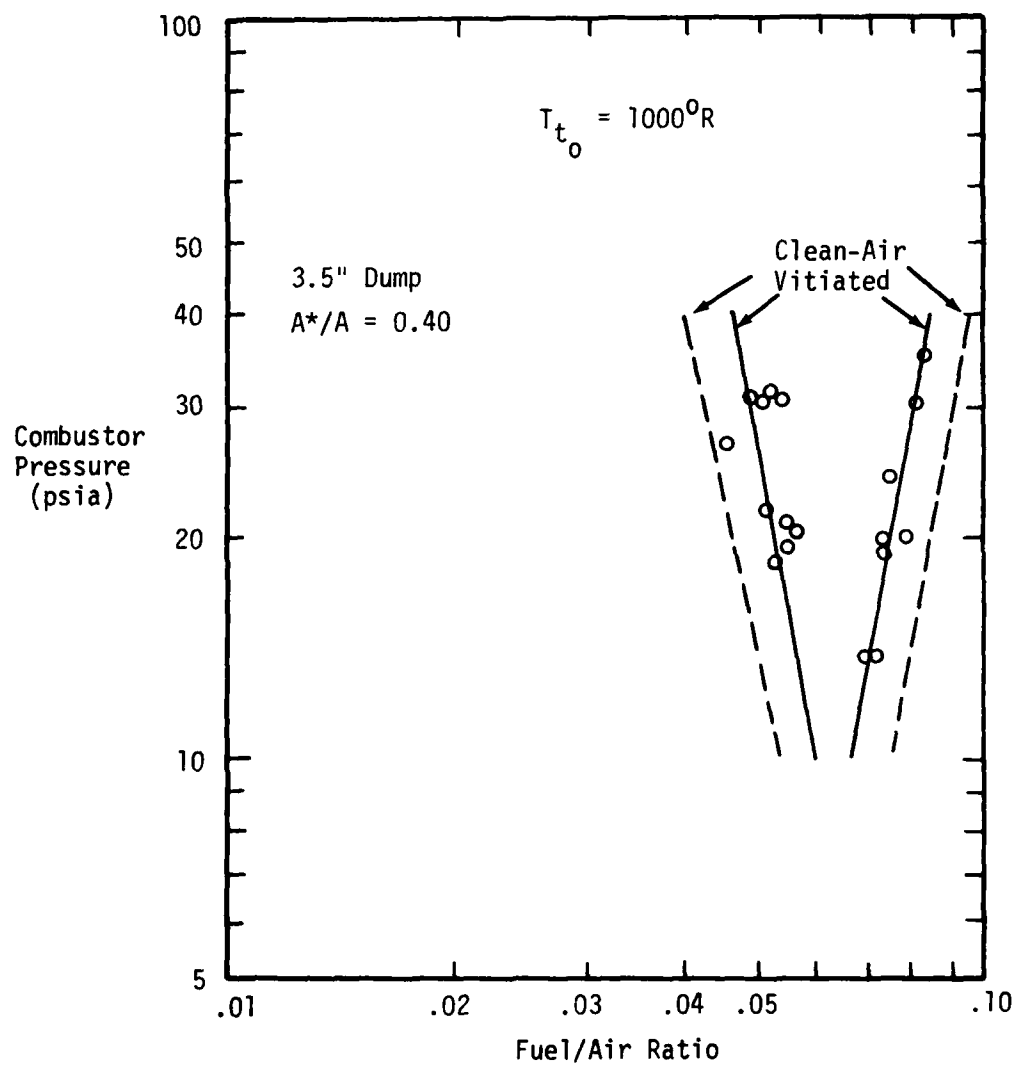


Figure 42. Effect of Vitiation on Stable Range; JP-4 Fuel

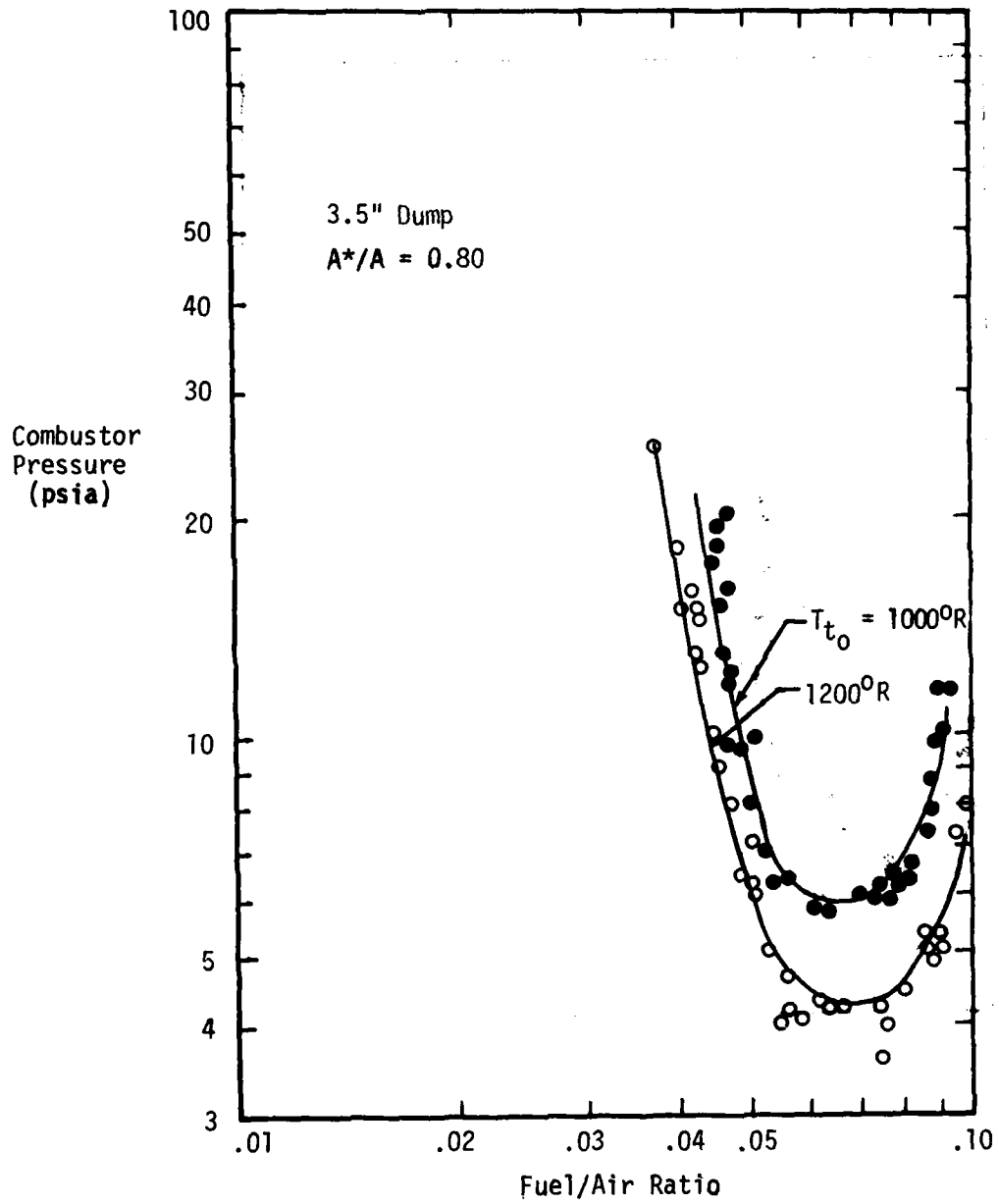


Figure 43. Complete Stability Loop; JP-4 Fuel

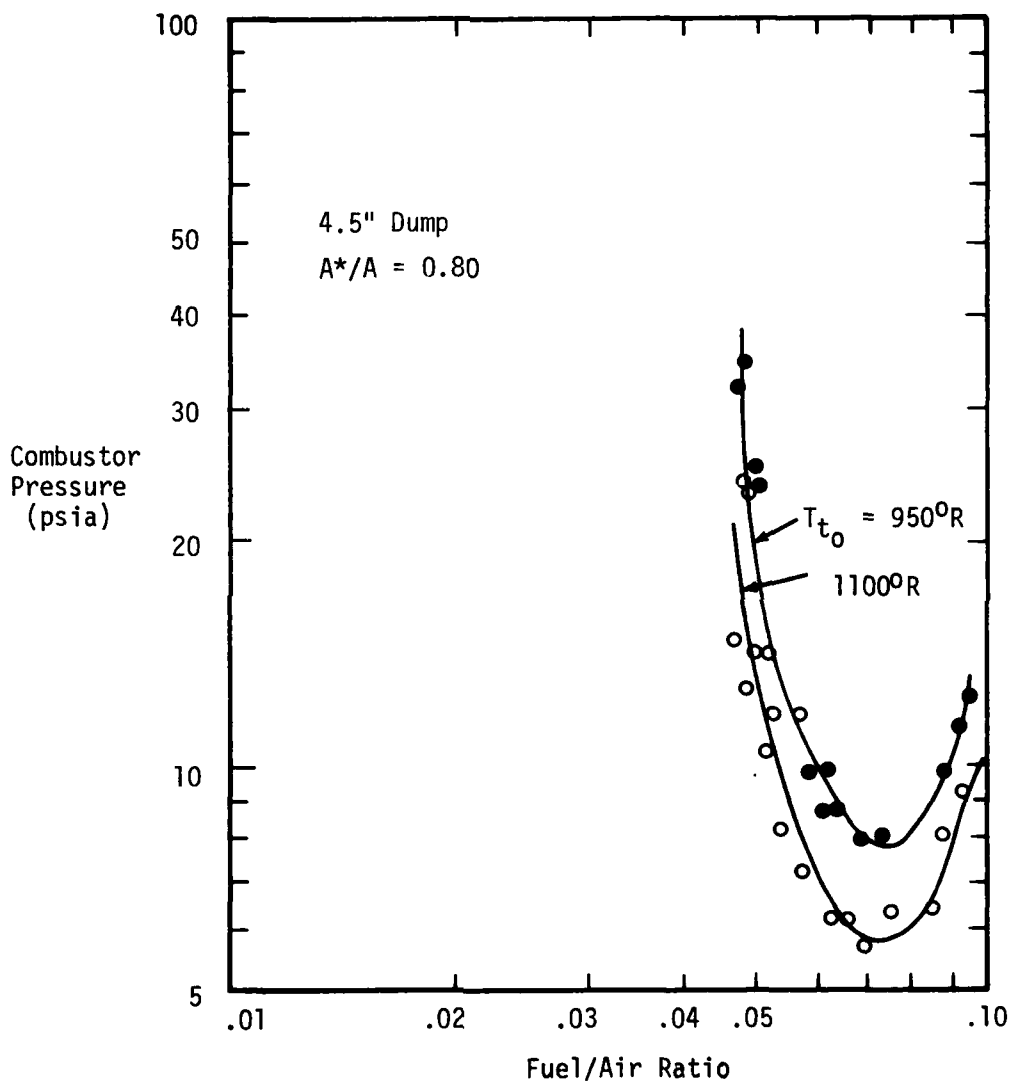


Figure 44. Complete Stability Loop; JP-4 Fuel

The fuel injection plates used for secondary fuel admission are illustrated in Fig 25. Tests were performed with these inlet sizes: 2.5", 3.5", and 4.5". The data for the 2.5" inlet is shown in Fig 45. It will be observed that the tests were performed for various air mass flow and temperature levels. The data scatter increases slightly with the more turbulent conditions experienced at higher mass flows. Attention is also drawn to the very small fuel flow injected into the recirculation zone. This required precise fuel flow metering for accurate results. It will also be seen that all test conditions yielded parallel straight line relationships between the primary and RZ fuel flows at lean extinction, which implies that the recirculated mass flow fraction does not vary with the mass flow rate.

Testing at the smaller step sizes corresponding to the 3.5" and 4.5" inlet diameter had to be accomplished deftly and expeditiously to prevent the combustor wall from overheating. The data for the 4.5" diameter inlets are shown in Fig 46. The data for the 3.5" inlet had to be discarded because of erroneous secondary-fuel flowmeter readings.

The test work was concluded by a brief visual study of the lean extinction process utilizing a quartz combustor.

Quartz Combustor Tests

The installation of the quartz combustor is shown in Fig 30. High speed movies (500 frames per second) were taken of the combustion process with the aim of determining the mechanism of lean extinction. In general, the precise manner of blow-out could not be discerned, primarily because of the rapid occurrence of extinction which could not be captured at the frame speed used. Another difficulty was the oscillatory nature of the combustion process. Under conditions which were

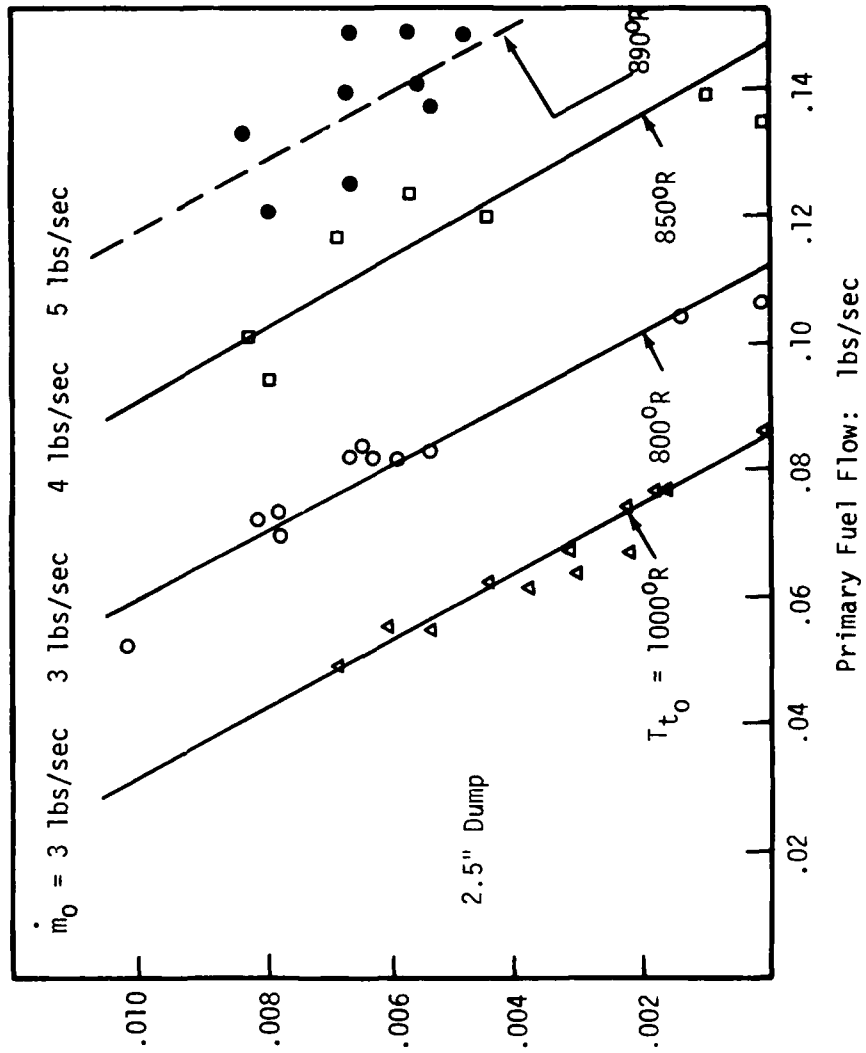


Figure 45. Primary and RZ Fuel Flows at Lean Extinction: 2.5" Dump

RZ
Fuel Flow
-lbs/sec-

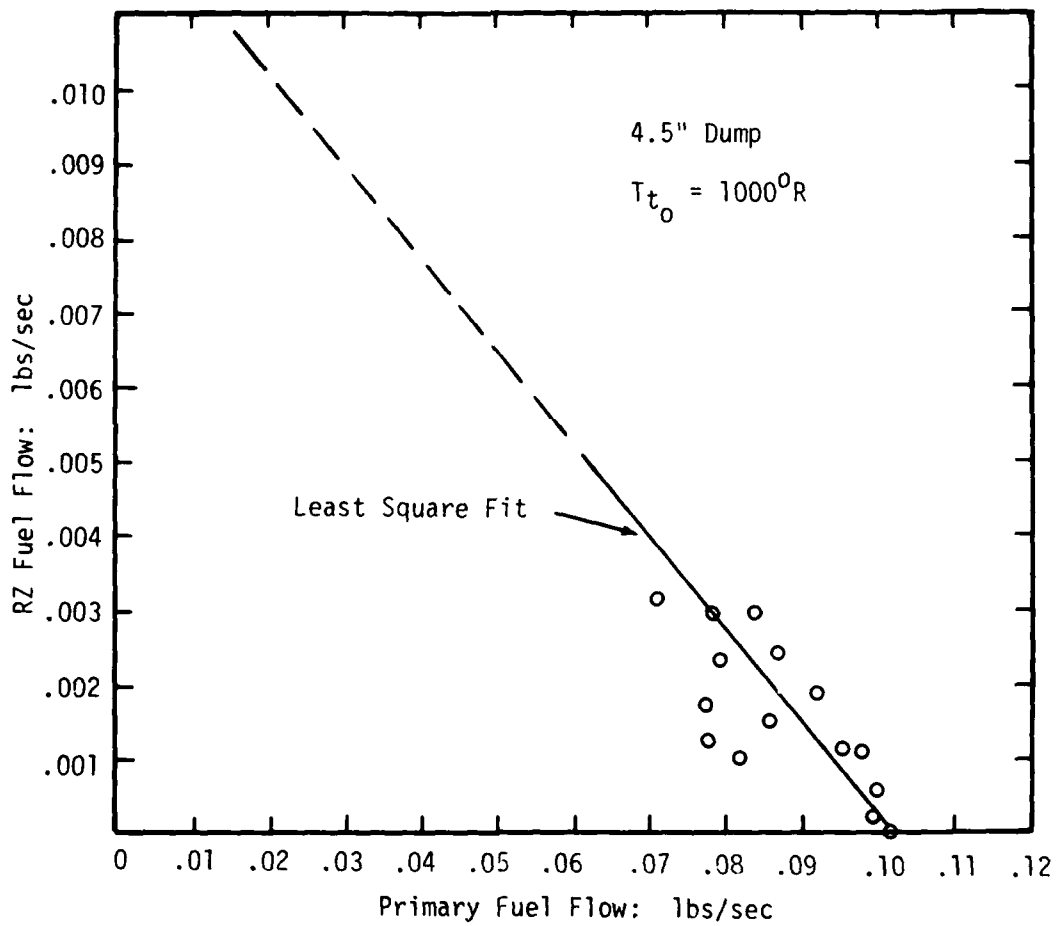


Figure 46. Primary and RZ Fuel Flows at Lean Extinction:
 4.5" Dump

apparently quite steady to the naked eye, a frame-by-frame examination of the film showed that a bright reaction zone oscillated to and fro along the combustor. This phenomenon may have been related to the fluctuating nature of the reattachment process. In any event, the sequence of the extinction process was not clearly discernible, and extinction occurred quite abruptly.

Discussion of Flame Stability Data

It will be recalled from the discussion of dump combustor stability given in Chapter II that a commonly accepted parameter for correlating stability data is the X parameter given in Eq(46). Attempts to correlate both the ethylene and JP-4 data obtained during this investigation are shown in Figs 47 to 50. It is apparent that neither the effects of dump height nor of inlet temperature were successfully correlated. Attention was therefore focused on the expression given in Eq(71) for the equivalence ratio at lean blow-out. For the assumptions made, namely that both the ethylene and JP-4 combustion processes were described by a single-step reaction with an apparent activation energy, $E = 42$ Kcal/mole, and reaction order $n = 1.75$, the expression given in Eq(71) is, with T_o put equal to T_{t_o} ,

$$\phi_{LBO} \propto \left\{ \frac{1}{h^{0.19}} \frac{U_o^{0.19}}{P_o^{0.14} T_{t_o}^{0.73}} \right\} \quad (71)$$

Turning first to the ethylene data, it was found that for the range of inlet conditions tested, the data could be correlated by an expression of the form similar to that of Eq(71) but, as previously anticipated, with modified exponents. Thus, for ethylene, one obtains

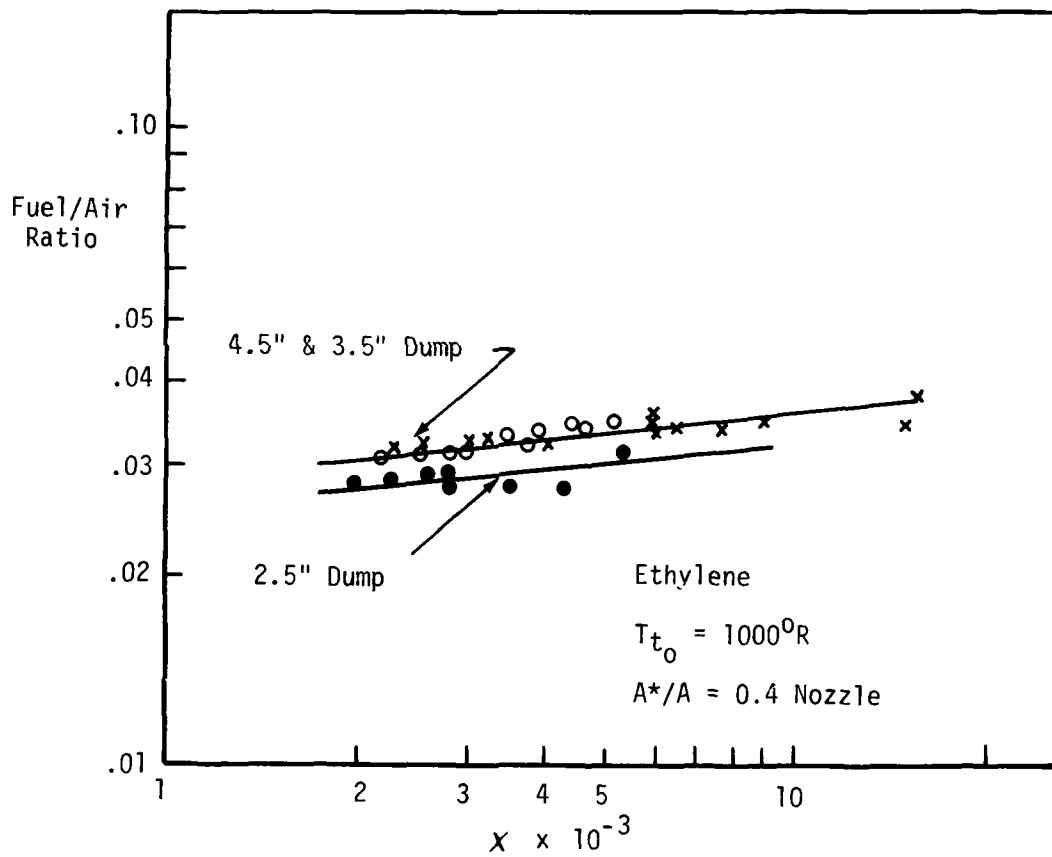


Figure 47. Trial Correlation by X Parameter: Effect of Step Size

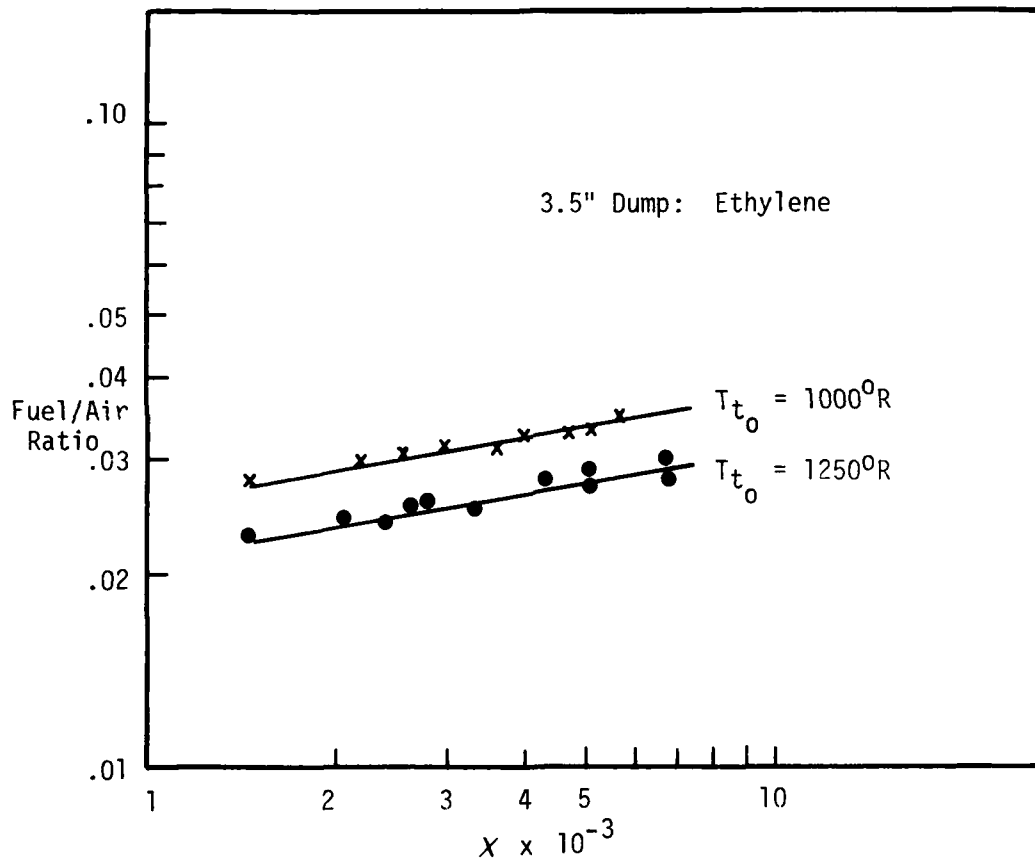


Figure 48. Trial Correlation by X Parameter:
Effect of Inlet Temperature

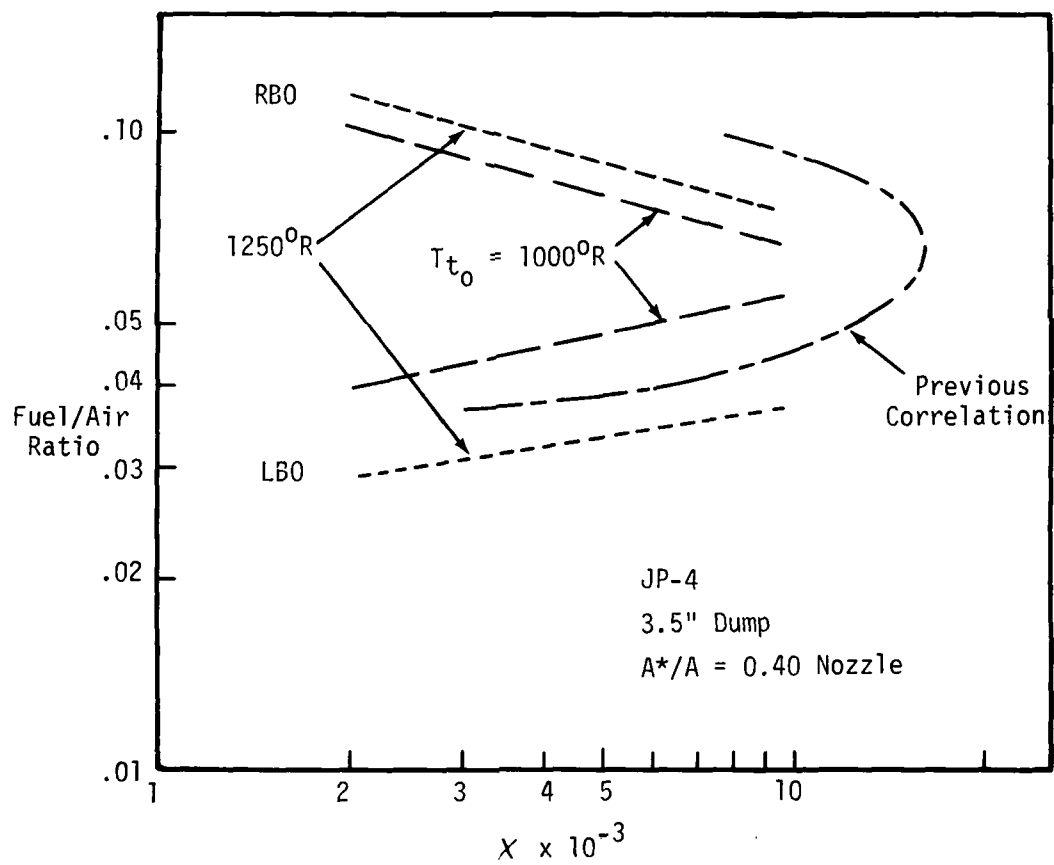


Figure 49. Trial Correlation by X Parameter:
Effect of Inlet Temperature

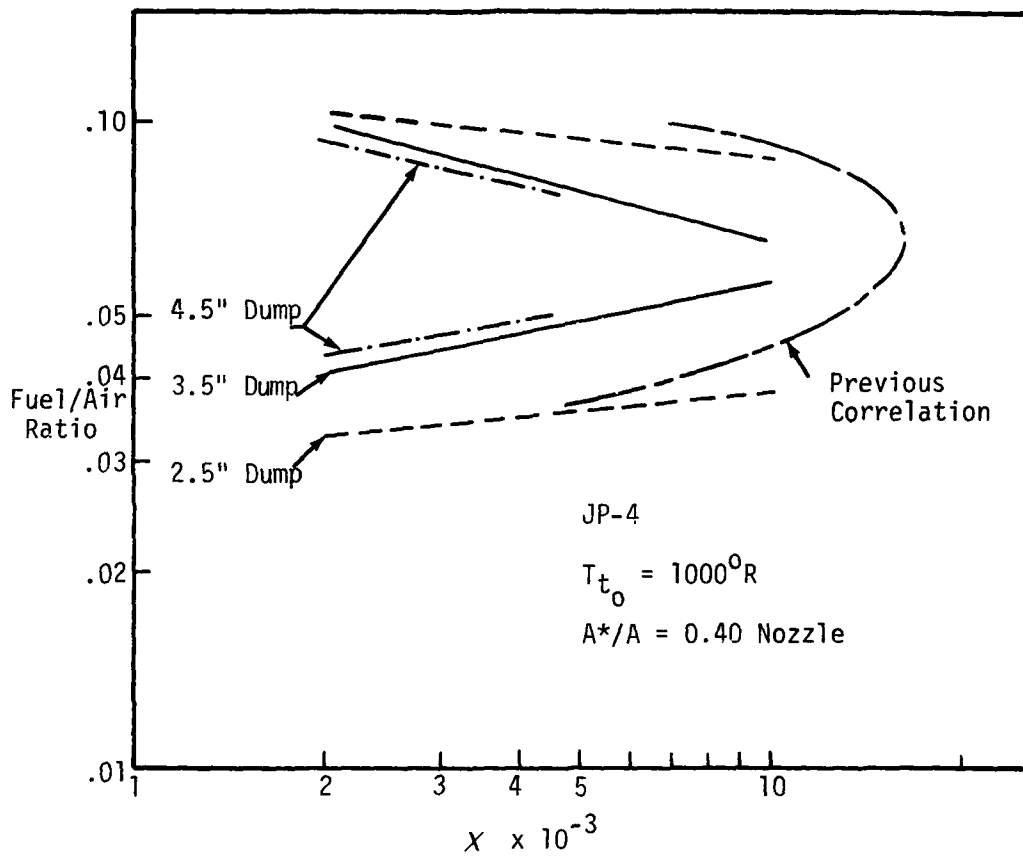


Figure 50. Trial Correlation by X Parameter: Effect of Step Size

$$\phi_{LBO} \propto \frac{1}{h^{0.20}} \frac{U_o^{0.10}}{P_o^{0.16} T_{t_o}^{0.80}} \quad (73)$$

Lean stability limits have been expressed in the "reduced" form of these variables, namely

$$\phi_{LBO} = k_5 \frac{1}{(h/12)^{0.2}} \frac{U_o^{0.10}}{(P_o/14.7)^{0.16}} \frac{1}{(T_{t_o}/1000)^{0.8}} \quad (74)$$

where $k_5 = 0.16$. The ethylene data from the 2.5", 3.5", and 4.5" dump diameter combustors are shown in Figs 51, 52, and 53, respectively. The effect of step size h is included in the overall data correlation shown in Fig 54: this correlation is valid over the range of inlet conditions tested; namely,

$$\begin{aligned} 10 < P_o < 40 \text{ psia} \\ 1000 < T_{t_o} < 1250^\circ\text{R} \\ 0.2 < M_o < 0.9 \end{aligned}$$

A similar approach was taken with the JP-4 test data, and successful correlations of the form given in Eq(71) were developed. In this case, the appropriate exponents were

$$\phi_{LBO} \propto \frac{1}{h^{0.2}} \frac{U_o^{0.10}}{P_o^{0.15} T_{t_o}^{0.8}} \quad (75)$$

and in terms of reduced variables, this becomes

$$\phi_{LBO} = 0.22 \frac{1}{(h/12)^{0.2}} \frac{U_o^{0.10}}{(P_o/14.7)^{0.15}} \frac{1}{(T_{t_o}/1000)^{0.8}} \quad (76)$$

The overall correlation using "reduced variables" is shown in Fig 55, and this is valid for the same range of conditions previously noted for the ethylene test series. Once again, a very satisfactory data correlation is obtained.

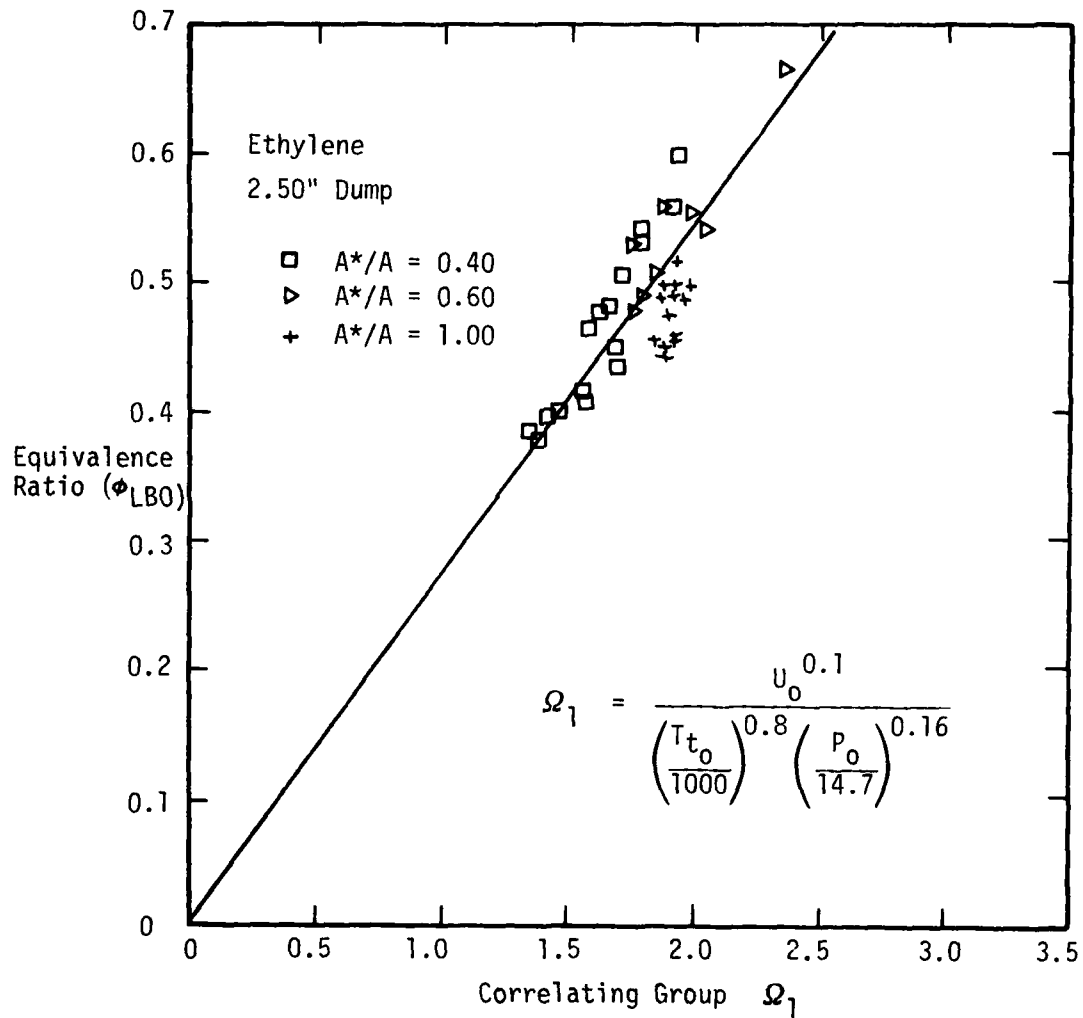


Figure 51. Lean Stability Limit Correlation: 2.5" Dump Diameter; Ethylene Fuel

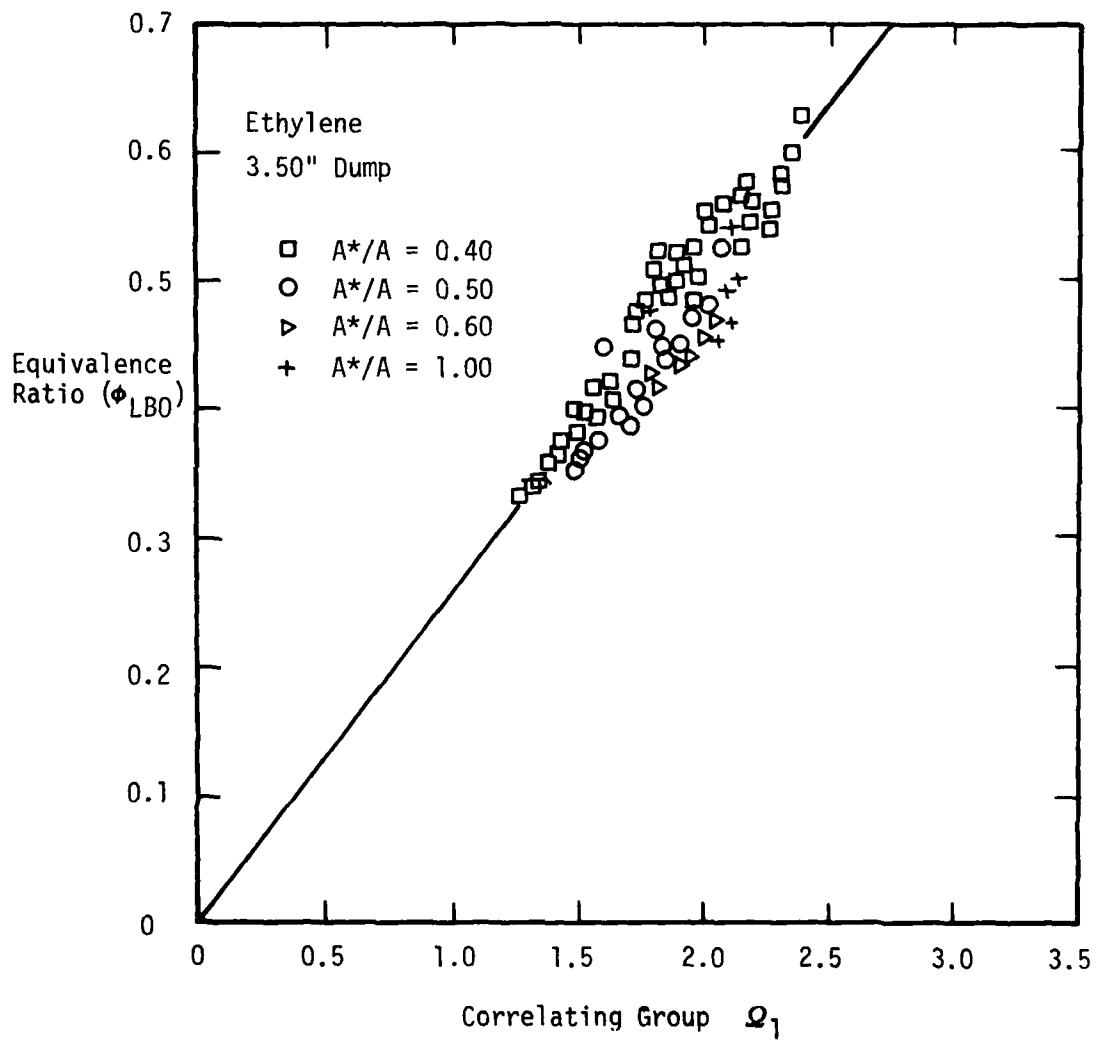


Figure 52. Lean Stability Limit Correlation: 3.5" Dump Diameter; Ethylene Fuel

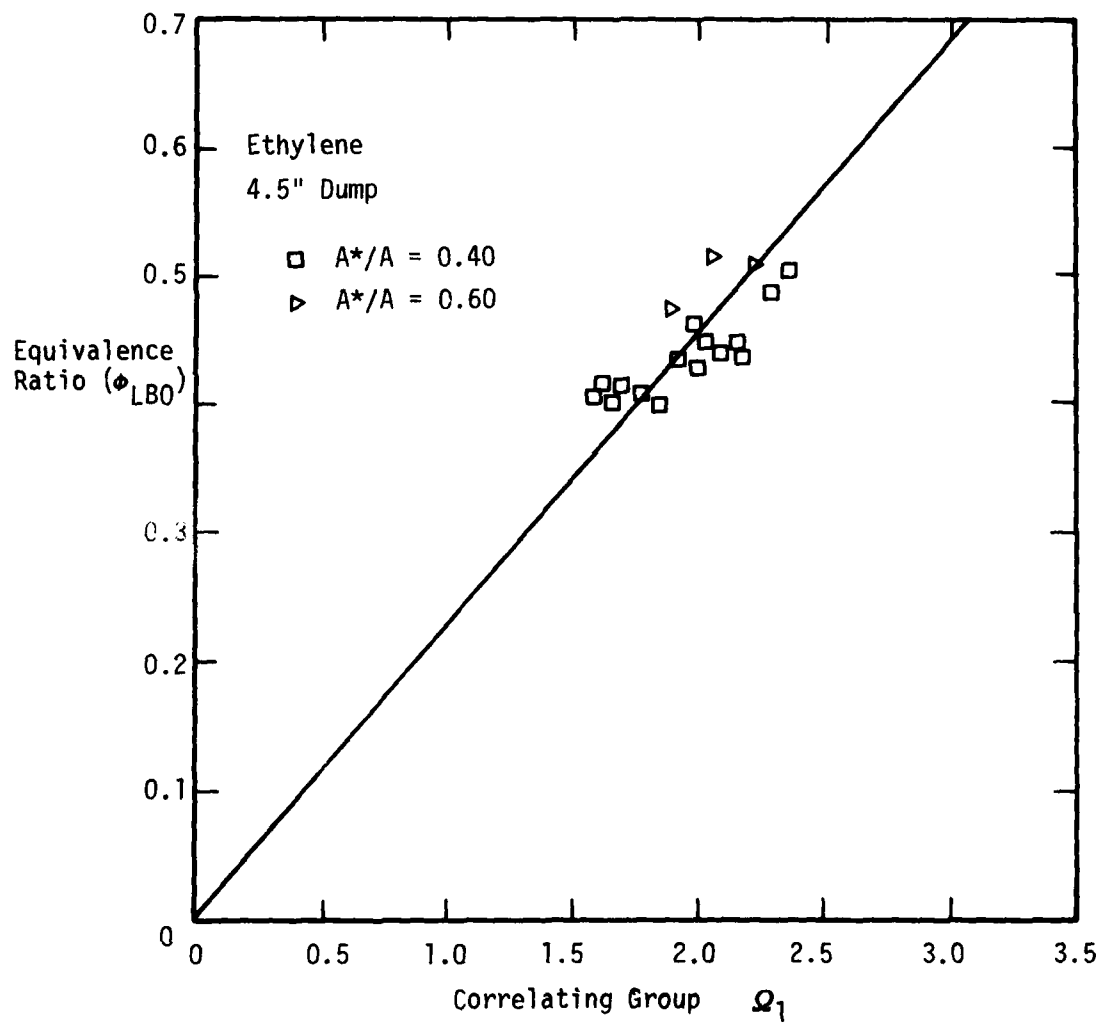


Figure 53. Lean Stability Limit Correlation: 4.5" Dump Diameter; Ethylene Fuel

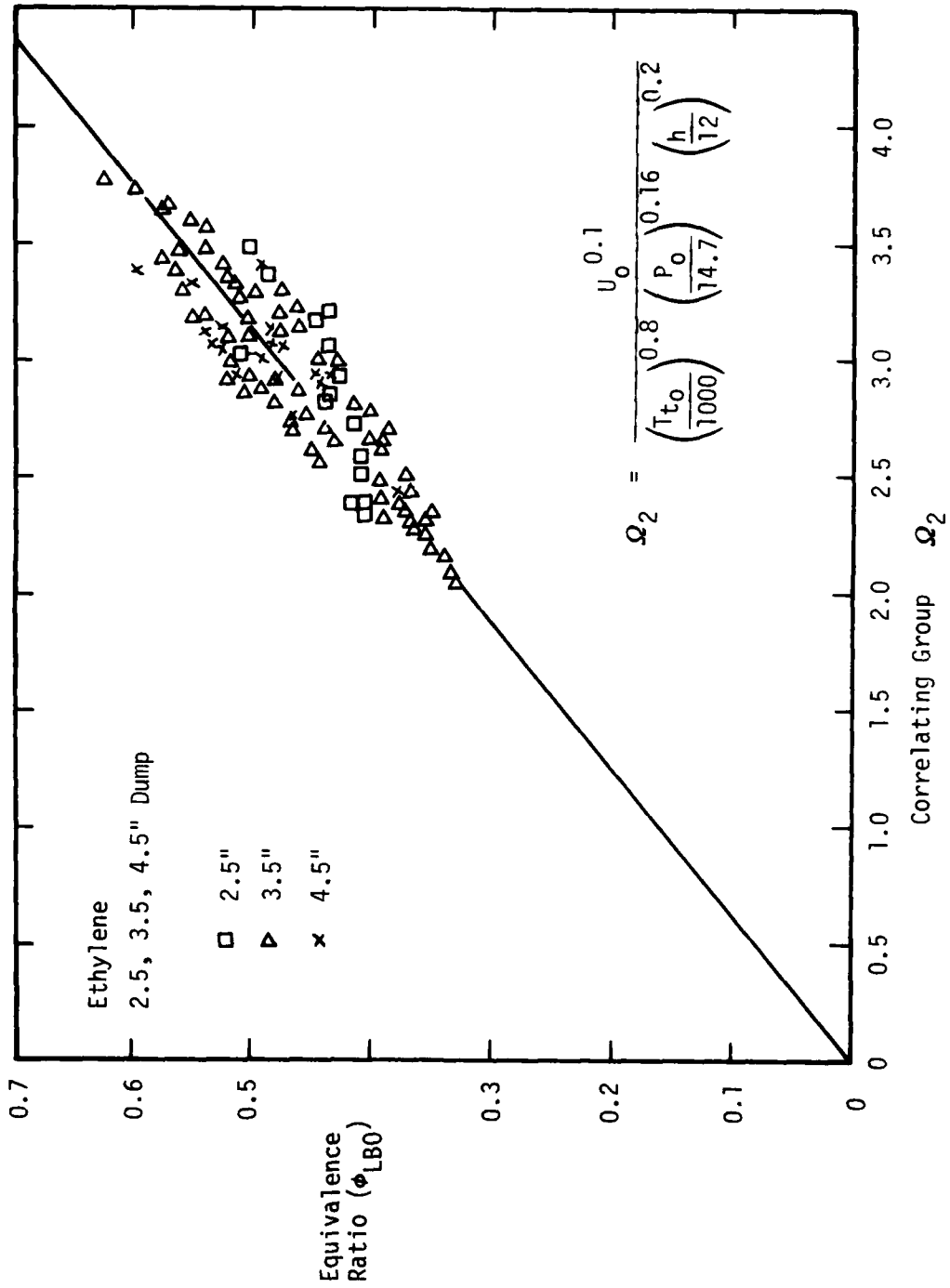


Figure 54. Lean Stability Limit Correlation: All Dump Sizes; Ethylene Fuel

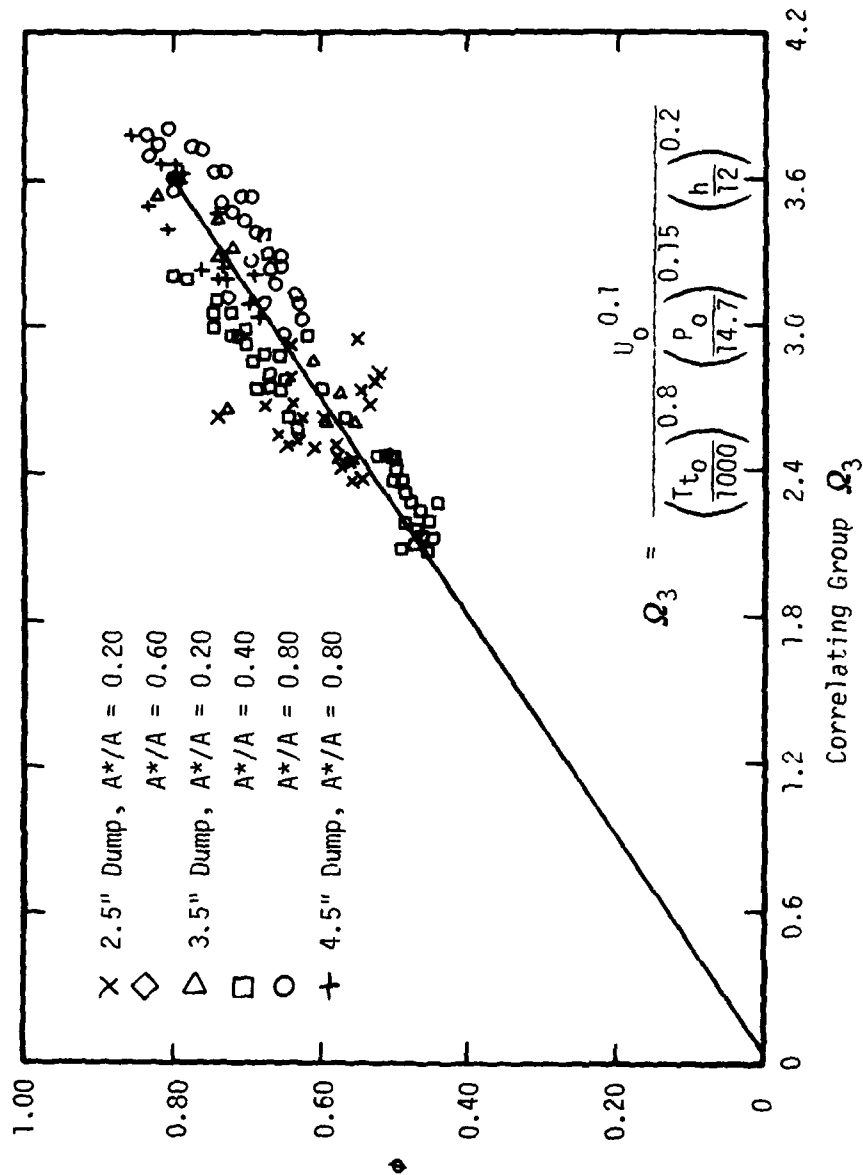


Figure 55. Lean Stability Limit Correlation: All Dump Sizes; JP-4 Fuel

Thus the data correlations obtained are in general agreement with the form anticipated by stirred reactor theory. Indeed the exponents for h , P_0 , and T_{t0} are quite close to the anticipated values. However, an interesting feature of the correlations given in Eq(73) and Eq(75) is the relative insensitivity of the weak limit equivalence ratio to velocity variation. Although this dependence is normally low for bluff bodies (Ref 31), it appears to be even less in the case of coaxial configurations. Moreover, inspection of Figs 17 and 18 confirms this weak dependence for both two-dimensional steps and for coaxial geometries. This phenomenon must therefore be associated with the flow features which are unique to step geometries. The features which are specific to the step compared to a bluff body stabilizer include: the presence of a wall bounding the recirculation zone, the existence of a well-developed boundary layer, and a shear layer which reattaches to the wall. From Fig 17, it is observed that the use of different wall materials which affect the heat loss to the wall did not appear to change the velocity dependence. It is also noted that the velocity enters the analysis by way of the \dot{m}_r term as shown in Eq(47); it is therefore presumed that the specific aerodynamic features of the recirculation zone flow which affect entrainment are responsible for the low velocity dependence. Future investigations are needed to clarify this phenomenon. For a given inlet stagnation temperature, an upper limit is set on the flow velocity at the dump plane by the occurrence of choking at that plane. Thus the term $U_0^{0.1}$ is bounded. In many cases it follows that extinction will occur due primarily to the existence of low temperature (T_{t0}) or low pressure (P_0) conditions rather than due to blow-off due to excessive velocity.

In view of the satisfactory agreement of the data with the prediction of the stirred reactor model, and with regard to the relative insensitivity of the lean extinction limit to velocity, no application of alternate stabilization criteria, i.e., time-ratio models, is made. It is appropriate to note, however, that many flame stability data can be explained equally well by either stirred reactor or time-ratio models. This dual approach would also be anticipated to apply to the flame stability data associated with step geometries. In this case, however, a time-ratio model would have to explain the relative insensitivity of the lean limit to inlet velocity variation. This, in turn, would require a characteristic length scale whose magnitude was approximately proportional to inlet velocity. Thus, further investigations of the shape and structure of the RZ, and the associated shear layer, under actual operating conditions, are of considerable interest. Furthermore, it could be anticipated that the θ_L^{-1} parametric expression given in Eq(24) would not correlate the data due to the demonstrated weak effect of the velocity term; such proved to be the case. Indeed the most useful parameter for collapsing both weak and rich limit data was the correlating group given in Eq(75). Thus all the data obtained from the JP-4 tests are displayed in terms of this correlating group in Fig 56. This correlation is much more satisfactory than that shown in Fig 16.

Discussion of Split-Flow Injection and Quartz Combustor Tests

Useful data were obtained for the 2.5" and 4.5" diameter inlets. The recirculation fraction obtained from the 2.5" inlet is shown in Fig 57. Also plotted are the maximum recirculation fractions predicted by Wingfield's expression given in Eq(49). Also, a correction to allow for the change in density between hot and cold conditions is displayed

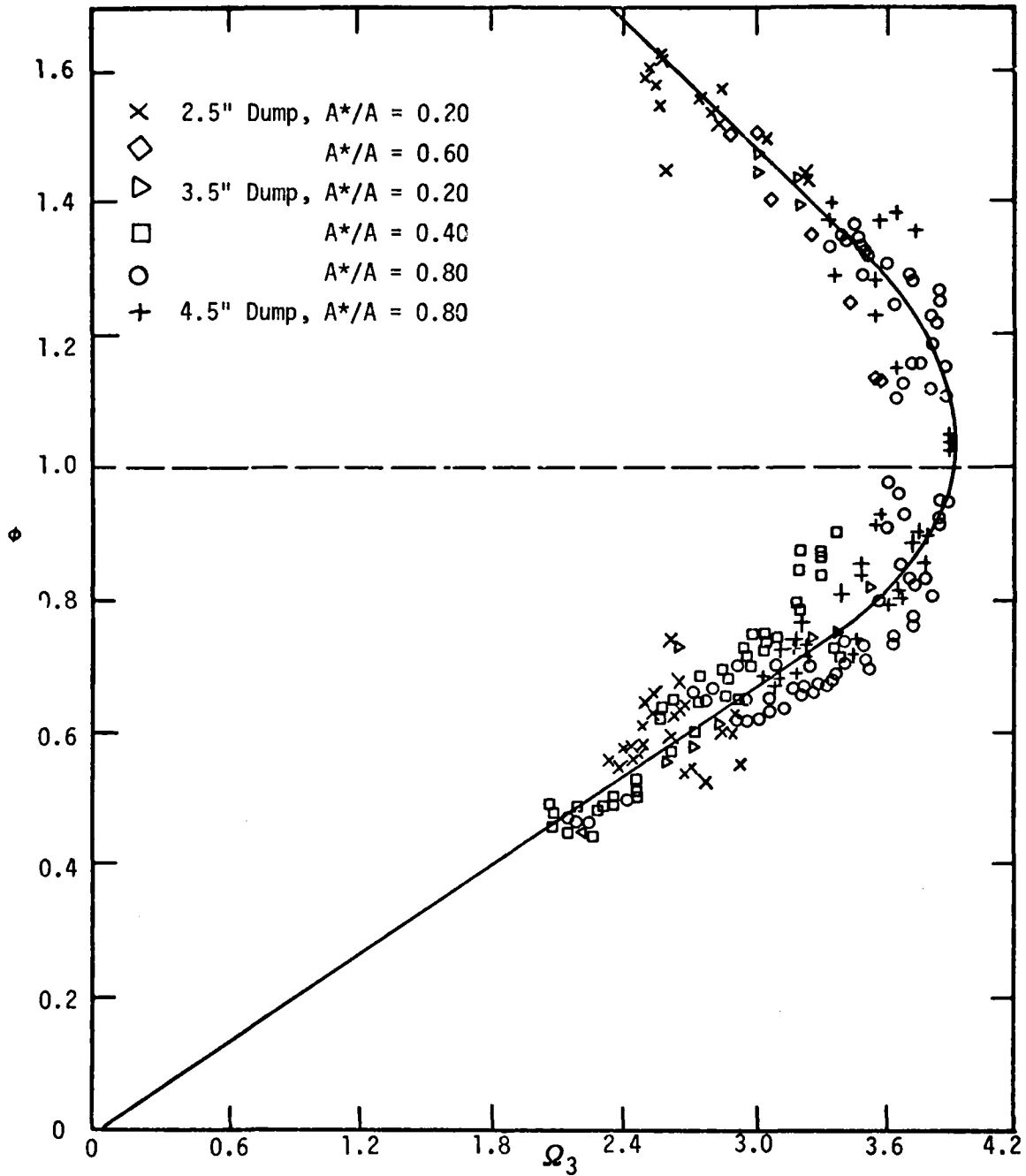


Figure 56. Overall Stability Limit Correlation: All Dump Sizes; JP-4 Fuel

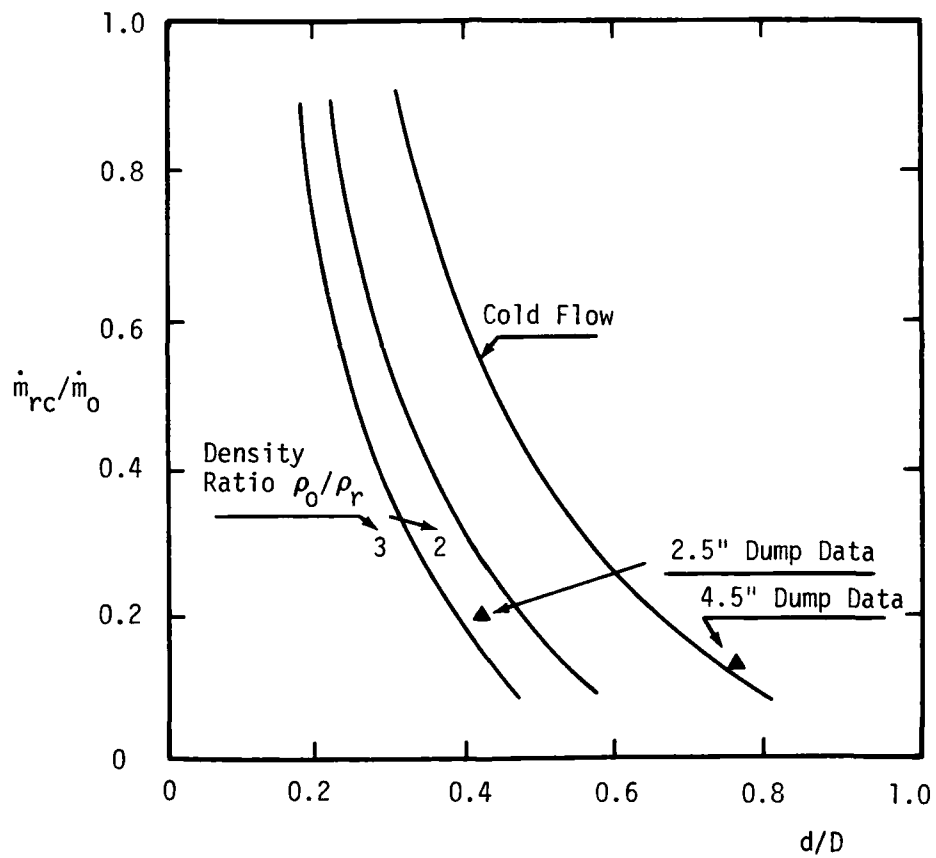


Figure 57. Experimental Values of Recirculated Mass Flow Fraction

in Fig 57. This correction for density ratio is given in Appendix A, Eq(A-30). Curves corresponding to density ratios of 2 and 3 are given in Fig 57. It will be seen that the experimentally determined recirculation fraction is in good agreement with the expression of Wingfield if a density ratio of approximately 2.5 is assumed. A cross check on the density ratio was made based on the reading of the thermocouple installed in the recirculation zone. Although the purpose of this thermocouple was to signal flame extinction, it does provide an approximate indication of the RZ temperature. Examination of the temperature data shows that the temperature ratio at the point of extinction lies generally in the range 2.5-3.0. This agreement between Wingfield's expression and the experimental data is gratifying. Of course, the 2.5" inlet corresponds to the smallest value of diameter ratio (d/D) tested. Thus it is expected to yield recirculation fraction data approaching that predicted by theories devised for industrial furnaces of low diameter ratio. One may then conclude that all the air entering into the recirculation process is in fact taking part in the combustion process. However, it is considered that more data from similar low diameter ratio combustors is required to confirm this interesting result.

The 4.5" diameter inlet data are also shown in Fig 57. In this case the experimental point lies on the cold flow line predicted by Wingfield's expression. In this case the combustor diameter ratio (0.75) is much too high for the similarity theories discussed in Appendix A to apply. Nevertheless, the data are of the right order of magnitude, and it is interesting to speculate whether the agreement is fortuitous, or if indeed the presence of a hot shear layer close to a small step (0.75") invalidates the density correction applicable to

geometries of lower diameter ratio. Once again further data are required to supplement these exploratory investigations.

The experimentally determined values of \dot{m}_{rc}/\dot{m}_0 were not employed, however, in the evaluation of reactor loading expression given in Eq(50). This is due to the fact that Eq(50) includes the term A_0/V . The magnitude of this term is dependent on the length ratio (k) of the hot recirculation zone, and the precise value of k is uncertain. However, the applicability of the split-fuel flow technique to dump combustors has been demonstrated. Also, the recirculated mass flow values derived from these tests will be of distinct value to those engaged in creating reactor-network models of the combustor process.

Turning to the tests of the transparent quartz combustor, the prime value of these tests was twofold. Firstly, they demonstrated that the combustion process in the coaxial combustor can be observed under actual operating conditions. Further work is definitely required with higher frame speeds to study the actual mechanism of flame extinction. Secondly, visual inspection of the movies on a frame-by-frame basis revealed a bright reaction zone which oscillated rapidly up and down the chamber. The recirculation region appeared as an annular, dark zone with flame originating at the circumferential lip of the step. The actual flame surface appeared as a turbulent brush intermittently anchored at the circumference of the dump inlet. Thus the basically unsteady nature of combustion in a dump combustor was clearly visualized.

As a result of these various test series, several conclusions may be drawn. These are itemized in the next chapter.

VI CONCLUSIONS

The research described in this document was conducted to explore the stability of flames located in the sudden expansion region of a coaxial dump combustor. The associated goals of the investigation were: to determine the flame stability characteristics over a range of geometries and inlet conditions; to model the stabilizing process and derive a correlating parameter; and to explore a split fuel injection technique to determine the recirculated mass flow fraction. It was also desired to review the literature concerning the flame stability and aerodynamics of coaxial dump combustors.

An experimental investigation was therefore performed to determine the flame stability associated with a 6" diameter combustor with step heights varying from 0.5" to 1.75". Inlet conditions were varied over the approximate ranges: pressure, 10-40 psia; inlet total temperature, 1000-1250^oR; and Mach number, 0.2-0.9.

From this study the following conclusions were drawn:

1. The mechanism of flame stability in a sudden expansion region is similar to that observed with bluff body stabilizers, and the presence of a wall bounding the recirculation zone does not produce any marked differences in overall behavior. Thus, as in the case of a bluff body, the lean stability limit is enhanced by increased inlet pressure, inlet temperature, and step height, and degraded by increased inlet velocity.

2. Over the range of this investigation, the effect of velocity on the weak extinction limit is very small ($\phi_{LBO} \propto U_0^{0.1}$).

This weak dependence is a common feature of two-dimensional step geometries and coaxial dump systems.

3. The dominant influence in flame stability is the inlet temperature; the subsidiary variables are step height, inlet pressure, and velocity.

4. The recirculation zone associated with a sudden expansion can be successfully modelled as an adiabatic stirred reactor using a one-step chemical reaction. From this model a correlating group for the lean stability limit may be derived in the form

$$\phi_{LBO} \propto \frac{U_o^\alpha}{P_o^\beta h^\gamma T_o^\delta}$$

Specific correlating groups were derived for both ethylene and JP-4 fueled systems and are given by the following equations:

Ethylene

$$\phi_{LBO} = 0.16 \frac{1}{(h/12)^{0.2}} \frac{U_o^{0.10}}{(P_o/14.7)^{0.16}} \frac{1}{(T_{to}/1000)^{0.8}} \quad (74)$$

JP-4

$$\phi_{LBO} = 0.22 \frac{1}{(h/12)^{0.2}} \frac{U_o^{0.10}}{(P_o/14.7)^{0.15}} \frac{1}{(T_{to}/1000)^{0.8}} \quad (76)$$

These expressions apply in the following range of conditions:

- a. Inlet Pressure: $10 < P_o < 40$ psia
- b. Inlet Temperature: $1000 < T_{to} < 1250^{\circ}R$
- c. Mach Number: $0.2 < M_o < 0.9$

5. For JP-4 fuel, the existence of complete stability loops for a coaxial step was demonstrated for the first time by operating at very low combustor pressures. Rich extinctions were not studied with ethylene due to the hazardous nature of operating at these conditions. Both the

lean and rich limit data for JP-4 fuel were collapsed, using a correlating group of the form

$$\phi_{LBO} = f \left\{ \frac{U_o^{.10}}{h^{0.2} p_o^{0.15}} \frac{1}{T_{to}^{0.8}} \right\}$$

6. Neither the ethylene nor JP-4 data were collapsed by the correlating parameter (X) previously employed in dump combustor studies.

7. The effect of vitiation is to reduce the stable operating range of a given combustor.

8. A variation in combustor length to diameter ratio from 3 to 6 produced little variation in flame stability characteristics.

9. The split fuel-flow technique to determine the air mass flow fraction consumed in the recirculation zone can be successfully applied to coaxial dump combustors. For small diameter ratios (d/D), the result obtained was compatible with estimates drawn from industrial furnace theory.

10. For the conditions investigated in this study, it was observed that direct injection of fuel into the recirculation zone resulted in a reduction in combustor noise and much smoother operation.

11. It was demonstrated that a transparent quartz combustor can be successfully employed to observe the combustion process under realistic operating conditions. It was shown that combustion is, in fact, an oscillatory process with the reaction zone moving to and fro along the combustor; such combustion appeared quite steady to the naked eye.

12. A comprehensive review of the literature concerning the flame stability and aerodynamics of coaxial dump combustors has been presented.

VII RECOMMENDATIONS FOR FUTURE WORK

The experimental investigation of flame stability, together with the state-of-the-art reviews undertaken in this study, have uncovered many important research areas relevant to the development of both coaxial and multi-inlet dump burners. These research areas are dealt with in this section under the following headings: flame stability, combustion, and aerodynamics.

Flame Stability of Coaxial Dump Burners

The current investigation was limited to one size of combustion chamber ($D = 6$ "). However, the correlating group for lean extinction limits would be expected to depend on combustor size as shown by Eq(63). Thus it is important that the effect of varying the combustor diameter (D) be explored. This is an essential extension of the present test series, both to demonstrate and expand the application of the correlating groups given in Eq(74) and Eq(76). Another recommended investigation would be to utilize a fluid-cooled combustor which would enable the effect of wall temperature on flame stability to be systematically explored. It should also be noted that the use of ablative liners on practical combustors will create a hot wall condition. If wall temperatures are maintained at high levels, then significant modification of the flame stabilizing mechanism will ensue. Thus both hot and cold wall effects need to be studied. The basic stirred reactor analysis may readily be extended to non-adiabatic boundary conditions.

More basic research investigations of the flame stabilizing process associated with both sudden expansion and step configurations are needed. No data are apparently available on the structure of the recirculation

zone or of the associated shear layer. A first task is to undertake detailed flow visualization of a flame stabilized on a two-dimensional step so as to observe the mechanism of extinction. The current investigation has also shown that a transparent quartz combustor may be successfully utilized under "smooth" burning conditions. Investigation of such a combustor with non-intrusive instrumentation would yield data on the flow field, including the geometry of the recirculation zone, and on the flame stabilizing mechanism of the sudden expansion configuration.

Combustion in Coaxial Dump Combustors

Two effects which were observed in this current investigation are important to combustor development. The first is the basically unsteady nature of a combustion process associated with the fluctuating reattachment of the flow to a solid surface. This effect was observed in the movies made of the combustor under burning conditions. This basically unsteady flow appears to couple with various acoustic and instability mechanisms producing sudden excursions of efficiency, heat transfer, and noise level. It is therefore important in all tests of dump combustors that appropriate quick response instrumentation be employed to characterize the unsteady modes of operation, and thereby relate the changes in performance to the driving phenomena. A second observation concerns the noticeable reduction in combustion noise level which occurred when using direct injection into the recirculation zone. This injection technique is not generally employed in current dump combustors. However, it offers the immediate advantage of direct control of the local fuel-air ratio in the recirculation zone together, apparently, with the possibility of suppressing unsteady modes of operation.

Aerodynamics of Coaxial Dump Burners

As will be noted in Appendix A, much activity has been focused on the one-dimensional analysis of sudden-expansion flows. However, little has been done to explore the structure of the recirculation zone. Thus there are little data even on the basic size and shape of the recirculation zone as a function of Reynolds number, Mach number, and the geometric variables such as the ratios L_c/D , d/D , and d^*/D (where d^* is the exit nozzle throat diameter). In particular, existing flow studies do not appear to embrace the range of Reynolds number from 10^3 to 10^5 . Again, few investigations have examined the unsteady aspects of these flows; most data refer to time-mean quantities. Also, the effects of initial boundary layer thickness, inlet flow profile, and initial turbulence characteristics on the flow structure downstream of the dump plane require investigation. Finally, the effect of combustion on the aerodynamics of the flow is an area which appears to have received little attention; in this case the detailed study of the aerodynamics of reacting flows associated with a two-dimensional step would be a good starting point. The associated heat and mass transfer phenomenon are, of course, of considerable relevance to combustor design. Finally, the use of residence-time distribution (RTD) techniques to observe the gross mixing characteristics of dump combustors should be explored. A few investigations of the coaxial configuration have been made and are referenced in this document. However, much work is needed to characterize the coaxial geometries relevant to ramjet combustors. Such techniques should be explored to permit a relatively simple approach to the modelling of the complex flow structures observed in multi-inlet combustors.

Summary

It is clear from the above discussion that the coaxial combustor offers many opportunities for research relevant to integral-rocket-ramjet combustors. Such problems may conveniently be addressed with relatively simple test geometries but will require sophisticated instrumentation. This area of endeavor should prove a fertile field of work. However, such work needs to be regarded as a stepping stone to the understanding and modelling of the complex combustion processes associated with multi-inlet combustor systems which are currently under development.

Bibliography

1. Stull, F. D., R. R. Craig, and J. T. Hojnacki, "Dump Combustor Parametric Investigation," AFAPL TR-74-90, Wright-Patterson AFB, Ohio: Air Force Aero Propulsion Laboratory, 1974.
2. Avery, W. H., and R. W. Hart, "Combustor Performance with Instantaneous Mixing," Industrial and Engineering Chemistry, 45; 1634-1637 (August 1953).
3. Longwell, John P., Edward E. Frost, and Malcolm A. Weiss, "Flame Stability in Bluff Body Recirculation Zones," Industrial and Engineering Chemistry, 45; 1629-1633 (August 1953).
4. Bragg, S. L., and J. B. Holliday, "The Influence of Altitude Operating Conditions on Combustion Chamber Design," Selected Combustion Problems--II: 270-295, 364, 365, edited by M. W. Thring et al, London: Butterworths Scientific Publications (1956).
5. Way, S., "Combustion in the Turbojet Engine," Selected Combustion Problems--II: 296-327, edited by M. W. Thring et al, London, England, Butterworths Scientific Publications (1956).
6. Greenhough, V. W. and Lefebvre, A. H., "Some Applications of Combustion Theory to Gas Turbine Development," Sixth Symposium (International) on Combustion, 858-868, New York, Reinhold Publishing Corporation, 1957.
7. Spalding, D. B., "Performance Criteria of Gas Turbine Combustion Chambers," Aircraft Engineering, 28: 104-110 (April 1956); 168-172 (May 1956).
8. Childs, J. Howard, "Preliminary Correlation of Efficiency of Aircraft Gas Turbine Combustors for Different Operating Conditions," NACA RM E50F15, September 1950.
9. Harsha, P. T., and R. B. Edelman, "Application of Modular Modelling to Ramjet Performance Prediction," AIAA Paper No. 78-944, Presented at the AIAA/SAE 14th Joint Propulsion Conference, Las Vegas, Nevada, July 25-27, 1978.
10. Craig, R. R., J. E. Drewry, and F. D. Stull, "Coaxial Dump Combustor Investigation," AIAA Paper No. 78-1107, Presented at the AIAA/SAE 14th Joint Propulsion Conference, Las Vegas, Nevada, July 25-27, 1978.
11. Bragg, S. L., "Application of Reaction Rate Theory to Combustion Chamber Analysis," Unpublished Rolls Royce Reports, 1953. (See also British ARC Paper No. 16170.)

12. Beer, J. M., and K. B. Lee, "The Effect of Residence Time Distribution on the Performance and Efficiency of Combustors," Tenth Symposium (International) on Combustion, 1187-1202, Pittsburgh, The Combustion Institute, 1965.
13. Vulis, L. A., Thermal Regimes of Combustion, New York: McGraw-Hill Book Company, 1961.
14. Wen, C. Y., and L. T. Fan, "Models for Flow Systems and Chemical Reactors," New York: Marcel Dekker, Inc., 1975.
15. Essenhigh, Robert H., "An Introduction to Stirred Reactor Theory Applied to Design of Combustion Chambers," Chap. XIV, Combustion Technology: Some Modern Developments, edited by Howard D. Palmer and J. M. Beer, New York, Academic Press, 1974.
16. Essenhigh, Robert H., et al., "Current Status of Fluid Mechanics in Practical Heterogeneous Combustors," Paper Presented at the Spring Meeting, Central States Section, The Combustion Institute, NASA Lewis Research Center, March 28-30, 1977.
17. Essenhigh, Robert H., "A New Application of Perfectly Stirred Reactor (P.S.R.) Theory to Design of Combustion Chambers," Office of Naval Research Technical Report FS67-1(U), March 1967.
18. Swithenbank, J., "Combustion Fundamentals," Sheffield University Report H.I.C. 155, 1970.
19. Swithenbank, J., "Flame Stabilization in High Velocity Flow," Chap. IV, Combustion Technology: Some Modern Developments, edited by Howard B. Palmer and J. M. Beer, New York, Academic Press (1974).
20. Aris, R., Elementary Chemical Reactor Analysis, New Jersey: Prentice-Hall Inc., 1969.
21. Herbert, M. V., "A Theoretical Analysis of Reaction Rate Controlled Systems--Part I," Combustion Researches and Reviews--1957: 76-111, London, Butterworths Scientific Publications (1957).
22. Herbert, M. V., "A Theoretical Analysis of Reaction Rate Controlled Systems--Part II," Eighth Symposium (International) on Combustion, 970-982, Baltimore, The Williams and Wilkins Company, 1962.
23. Longwell, J. P., and M. A. Weiss, "High Temperature Reaction Rates in Hydrocarbon Combustion," Industrial and Engineering Chemistry, 47, 8, 1634-1643 (1955).
24. Hottel, H. C., G. C. Williams, and M. L. Baker, "Combustion Studies in a Stirred Reactor," Sixth Symposium (International) on Combustion: 398-411, New York, Reinhold Publishing Corporation, 1957.
25. Hottel, H. C., G. C. Williams, and A. H. Bonnell, "Application of Well-Stirred Reactor Theory to the Prediction of Combustor Performance," Combustion and Flame, 2: 13-34, 1958.

26. Clarke, A. E., J. Odgers, and P. Ryan, "Further Studies of Combustion Phenomena in a Spherical Combustor," Eighth Symposium (International) on Combustion, 982-994, Baltimore, The Williams and Wilkins Company, 1962.
27. Clarke, A. E., J. Odgers, F. W. Stringer, and A. J. Harrison, "Combustion Processes in a Spherical Combustor," Tenth Symposium (International) on Combustion, 1151-1166, Pittsburgh, The Combustion Institute, 1965.
28. Kretschmer, D., and J. Odgers, "Modelling of Gas Turbine Combustors-- A Convenient Reaction Rate Equation," Journal of Engineering for Power 94: 173-180 (1972).
29. Odgers, J., and C. Carrier, "Modelling of Gas Turbine Combustors; Considerations of Combustion Efficiency and Stability," Journal of Engineering for Power, 95: 105-113 (1973).
30. Levy, A., and F. J. Weinberg, "Optical Flame Structure Studies: Examination of Reaction Rate Laws in Lean Ethylene-Air Flames," Combustion and Flame, 3: 2, 259 (June 1959).
31. Ballal, D. R., and A. H. Lefebvre, "Weak Extinction Limits of Turbulent Flowing Mixtures," ASME Paper No. 78-6T-144, Presented at the Gas Turbine Conference, London, England, April 9-13, 1978.
32. DeZubay, E. A., "Characteristics of Disc-Controlled Flame," Aero Digest, 54: 54-56 (January 1950).
33. Barrère, M., and A. Mestre, "Stabilization des Flammes Par Des Obstacles," Selected Combustion Problems: 426-446, London, England, Butterworths Scientific Publications (1954).
34. Herbert, M. V., "Aerodynamic Influences on Flame Stability," Progress in Combustion Science and Technology, Volume 1: 61-109, Edited by J. Ducarme, M. Gerstein, A. H. Lefebvre; Pergamon Press (1960).
35. Humphries, W., and Vincent, J. H., "Near Wake Properties of Axisymmetric Bluff Body Flows," Applied Scientific Research, 32: 649-669 (December 1976).
36. Wright, F. H., "Bluff Body Flame Stabilization: Blockage Effects," Combustion and Flame, 3(3): 319-337 (September 1959).
37. Lefebvre, A. H., "A Method of Predicting the Aerodynamic Blockage of Bluff Bodies in a Ducted Airstream," College of Aeronautics Report Aero No. 188, 1965.
38. Plee, S. L., and A. M. Mellor, "Flame Stabilization in a Simplified Prevaporizing, Partially Vaporizing, and Conventional Gas Turbine Combustor", AIAA Paper No. 78-1038, Presented at the AIAA/SAE 14th Joint Propulsion Conference, Las Vegas, Nevada, July 25-27, 1978.

39. Lefebvre, A. H., "Theoretical Aspects of Gas Turbine Combustion Performance," College of Aeronautics, CoA Note Aero No. 163, August 1966.
40. Lefebvre, A. H., and G. A. Halls, "Some Experiences in Combustion Scaling," Advanced Aero Engine Testing: 177-204, edited by A. W. Morley and J. Fabri, Pergamon Press (1959).
41. Damköhler, G., "The Effect of Turbulence on the Flame Velocity in Gas Mixtures," NACA Technical Memorandum No. 1112, April 1947.
42. Putnam, A. A., and R. A. Jensen, "Application of Dimensionless Numbers to Flash-Back and Other Combustion Phenomena," Third Symposium on Combustion and Flame and Explosion Phenomena: 89-98, Baltimore, The Williams and Wilkins Company, 1949.
43. Spalding, D. B., and B. S. Tall, "Flame Stabilization in High Velocity Gas Streams and the Effect of Heat Losses at Low Pressure," The Aeronautical Quarterly, 5: 195-215 (1954).
44. Spalding, D. B., Some Fundamentals of Combustion, New York, Academic Press Inc., 1955.
45. Shchetinkov, Ye. S., "The Physics of the Combustion of Gases," FTD-HT-23-498-68, Vol. I, Wright Patterson AFB, Ohio, Foreign Technology Division, 1968.
46. Karlovitz, B. et al., "Studies on Turbulent Flames," Fourth Symposium (International) on Combustion, Baltimore: The Williams and Wilkins Company, 1953.
47. Lewis, B., and G. von Elbe, Combustion, Flames, and Explosion of Gases, New York: Academic Press, Inc., 1961.
48. Melvin, A., and J. B. Moss, "Evidence for the Failure of the Flame Stretch Concept for Premixed Flames," Combustion Science and Technology, 7: 189-196 (1973).
49. Bovina, T. A., "Studies of Exchange Between Recirculation Zone Behind the Flame-Holder and Outer Flow," Seventh Symposium (International) on Combustion: 692-696, London, England, Butterworths Scientific Publications, 1959.
50. Zukoski, E. E., and F. E. Marble, "Experiments Concerning the Mechanism of Flame Blow-Off from Bluff Bodies," Proceedings of the Gas Dynamics Symposium on Aerochemistry, Northwestern University, Evanston, Illinois, 1956.
51. Broman, G. E., and E. E. Zukoski, "Experimental Investigation of Flame Stabilization in a Deflected Jet," Eighth Symposium (International) on Combustion: 944-956, Baltimore, The Williams and Wilkins Company, 1962.

52. Damköhler, G., "Einflüsse der Strömung, Diffusion und des Wärmeüberganges auf die Leistung von Reaktionsöfen," Z. Elektrochemie, 42: 846-861, 1936.
53. Mironenko, V. A., "The Use of Thermal Ignition Theory to Determine General Conditions for Flame Stabilization by Means of a Bluff Body," Soviet Aeronautics, 9, 1: 76-78 (1966).
54. Mironenko, V. A., "Calculation of Flameout Conditions in the Wake of a Bluff Body from the Ignition Time Delay," Soviet Aeronautics, 9, 2: 42-45 (1966).
55. Solokhin, E. L., and V. A. Mironenko, "Stable Combustion Limits in GTE Reheat Combustion Chambers," Soviet Aeronautics, 15(1): 114-120 (1972).
56. Winterfeld, G., "On Processes of Turbulent Exchange Behind Flameholders," Tenth Symposium (International) on Combustion: 1265-1275, Pittsburgh, The Combustion Institute, 1965.
57. Winterfeld, G., "Investigations on Mass Exchange Between Recirculation Areas Behind Axially Symmetrical Flameholders and Surrounding Flow," DFVLR Report DVL 803, July 1968.
58. Baev, V. K., and P. K. Tret'yakov, "Criteria Description of Combustion Stability in a Turbulent Homogeneous Fuel-Oxidizer Flow," Combustion, Explosion and Shock Waves, 8: 37-44 (1972).
59. Baev, V. K., and P. K. Tret'yakov, "Characteristic Burning Times of Fuel-Air Mixtures," Combustion, Explosion and Shock Waves, 4(3): 208-214 (1969).
60. Baev, V. K., and P. K. Tret'yakov, "Investigation of Turbulent Flames," Heat and Mass Transfer in Boundary Layers, Vol. 1: 476-488, Edited by N. Afgan, Z. Zaric, and P. Anastasijevic, Pergamon Press (1972).
61. Winterfeld, G., "Investigations on the Stabilization of Hydrogen Diffusion Flames by Means of Flame Retention Baffles in Supersonic Flow," DFVLR Report DLR-FB 76-35, June 1976.
62. Mellor, A. M., "Gas Turbine Engine Pollution," Progress in Energy and Combustion Science, Vol. 1: 111-133, Edited by N. A. Chigier, Pergamon Press, 1976.
63. Plee, S. L., and A. M. Mellor, "Characteristic Time Correlation for Lean Blowoff of Bluff Body Stabilized Flames." WSCI Paper 78-44, Presented at the Western States Section of the Combustion Institute 1978 Fall Meeting, Laguna Beach, California, October 16-17, 1978.
64. Spalding, D. B., "A General Theory of Turbulent Combustion, the Lagrangean Aspects," AIAA Paper No. 77-141, Presented at the AIAA

15th Aerospace Sciences Meeting, Los Angeles, California,
January 24-26, 1977.

65. Shchetnikov, Ye. S., "The Physical Model of Flameholding on Blunt Bodies," FTD-HT-23-247-69, Wright-Patterson AFB, Ohio, Foreign Technology Division, 1969.
66. Altenkirch, R. A., and A. M. Mellor, "Emissions and Performance of Continuous Flow Combustors," Fifteenth Symposium (International) on Combustion: 1181-1189, Pittsburgh, The Combustion Institute, 1975.
67. Meshcheryakov, E. A., and O. V. Makesheva, "Calculation of the Conditions for the Breakaway of Combustion Following a Step or a Depression with a Supersonic Flow of a Hydrogen-Air Combustible Mixture," Combustion, Explosion and Shock Waves, 12(6): 768-774 (July 1977), Original: (Nov/Dec 1976).
68. Baev, V. K., et al., "Diffusional Combustion of Hydrogen in a Flat Channel with Sudden Expansion," Combustion, Explosion and Shock Waves, 12(3): 340-341 (March 1977), Original: (May/June 1976).
69. Orth, R. C., and J. M. Cameron, "Flow Immediately Behind a Step in a Supersonic Combustor," AIAA Paper No. 74-1161, Presented at the AIAA/SAE 10th Propulsion Conference, San Diego, California, October 21-23, 1974.
70. Barclay, L. P., "Flame Stability for a Coaxial Dump Combustor," Unpublished Work at AFAPL, Wright-Patterson AFB, Ohio, 1972.
71. Craig, R. R., P. L. Buckley, and F. D. Stull, "Large Scale, Low Pressure Dump Combustor Performance," AFAPL TR-76-53, Wright-Patterson AFB, Ohio, Air Force Aero Propulsion Laboratory, 1966.
72. Chambers, H. E., "Dump Combustor Stability Limit Test," Internal Memo, Wright-Patterson AFB, Ohio, Air Force Aero Propulsion Laboratory, 1974.
73. Schmotolocha, Stephen N., and Constantino Economos, "An Experimental Combustion and Flame Stabilization Study of Dump Burners," AFOSR-TR-75-1446, September 1975.
74. Choudhury, P. Roy, "Interaction of Turbulent Air Jets with an Impinging Reacting Stream--An Application to an Advanced Air Breathing Propulsion System," AFOSR-TR-77-1234, 1977.
75. Ross, Peter A., "Some Observations of Flame Stabilization in Sudden Expansions," Jet Propulsion, 28: 123-125 (February 1958).
76. Kawamura, Takeshi, "The Ignition Front of a Fuel Jet Stabilized by a Step," Combustion and Flame, 22: 283-288 (1974).
77. Snyder, William T., "Influence of Approach Boundary Layer Thickness on Premixed Propane-Air Flames Stabilized in a Sudden Expansion," Jet Propulsion, 28: 822-825 (December 1958).

78. DeZubay, E. A., "Influence of Hot Surfaces on the Flame Stabilization of a Bluff Body," Proceedings of Midwestern Conference on Fluid Mechanics: 458-468, Columbus, The Ohio State University Press, 1952.
79. Yankovskii, V. M., and A. V. Talantov, "Influence of System Size on Basic Characteristics of the Combustion Process in a Turbulent Homogeneous Mixture Stream," Soviet Aeronautics, 12(3): 78-83 (1969).
80. Majumdar, A. K., and D. Bhanduri, "Mathematical Modelling of Flows in Recessed Wall Flameholder," Applied Math. Modelling, Vol. 1: 125-130 (December 1976).
81. Huellmantel, L. W., R. W. Ziemer, and Ali Bulent Cambel, "Stabilization of Premixed Propane-Air Flames in Recessed Ducts," Jet Propulsion, 27: 31-34, 43 (January 1957).
82. Povinelli, L. A., "Ignition Delay Concept for Recessed Flameholders," Combustion and Flame, 4, 355-356 (1960).
83. DeRossett, T. A., and C. E. G. Przirembel, "Time-Dependent Behaviour of Separated Flow Regions," Proceedings of the 20th International Instrumentation Symposium: 273-280, Albuquerque, N. Mexico, May 1974.
84. Pennucci, M. A., "Parametric Evaluation of Total Pressure and Recirculation Zone Length in a Sudden Expansion Combustor," AFIT Thesis, Wright-Patterson AFB, Ohio, Air Force Institute of Technology, 1974.
85. Drewry, J. E., "Characterization of Sudden-Expansion Dump Combustor Flowfields," AFAPL-TR-76-52, Wright-Patterson AFB, Ohio, Air Force Aero Propulsion Laboratory, 1976.
86. Iribarne, A., et al., "An Experimental Study of Instabilities and Other Flow Properties of a Laminar Pipe Jet," AIChE Journal, 18(4): 689-698 (1972).
87. Teysandier, R. G., and M. P. Wilson, "An Analysis of Flow Through Sudden Enlargements in Pipes," J. Fluid Mech, 64(1): 85-95 (1974).
88. Gol'dshtik, M. A., and B. A. Silant'ev, "Effect of Channel Blockage on Motion in the Separation Zone Behind Bluff Bodies," Journal of Applied Mechanics and Technical Physics, 8(1): 65-66 (1967).
89. Chaturvedi, M. C., "Flow Characteristics of Axisymmetric Expansions," Journal of the Hydraulics Division, Proc Am Soc Civil Engs, 89(HY3): 61-92 (1963).
90. Hubbard, E. H., "Recirculation in Cold Models of Furnaces: A Review of Work Carried Out at SOGREAH," Journal of the Institute of Fuel, 35: 160-173 (1962).

91. Wingfield, G. J., "Mixing and Recirculation Patterns from Double Concentric Jet Burners Using an Isothermal Model," Journal of the Institute of Fuel, 40: 456-464 (1967).
92. Barchilon, M., and R. Curtet, "Some Details of an Axisymmetric Confined Jet with Backflow," Journal of Basic Engineering, 86: 777-787 (1964).
93. Lefebvre, A. H., A. R. A. F. Ibrahim, and N. C. Benson, "Factors Affecting Fresh Mixture Entrainment in Bluff-Body Stabilized Flames," Combustion and Flame, 10(3): 231-239 (1966).
94. Verduzio, L., and D. Campanaro, "The Air Recirculation Ratio in Can-Type Gas Turbine Combustion Chambers," Combustion and Heat Transfer in Gas Turbine Systems: 145-163, Edited by E. R. Norster, Pergamon Press, 1971.
95. Plee, S. L., and A. M. Mellor, "Review of Flashback Reported in Prevaporizing/Premixing Combustors," Combustion and Flame, 32: 193-203 (1978).
96. Benedict, R. P., et al., "Generalized Flow Across an Abrupt Enlargement," Journal of Engineering for Power, 88: 327-334 (July 1976).
97. Hall, W. B., and E. M. Orme, "Flow of a Compressible Fluid Through a Sudden Enlargement in a Pipe," Proceedings of the Institution of Mechanical Engineer, 169: 49, 1007-1020 (1955).
98. Van Driest, E. R., "Steady Turbulent-Flow Equations of Continuity, Momentum and Energy for Finite Systems," Journal of Applied Mechanics, 13: A231-238 (September 1946).
99. Tyler, R. A., and Williamson, R. G., "Sudden Area Enlargement Pressure Recovery with Inflow Distortion," Journal of the Royal Aeronautical Society, 72: 243-244 (March 1968).
100. Truckenbrodt, E., "Naherungslosungen der Stromungsmechanik (Approximate Solutions in Fluid Mechanics and Their Physical Interpretation)," Zeitschrift Für Flugwissenschaften, 24: 177-187 (1976).
101. Kalinske, A. A., "Conversion of Kinetic to Potential Energy In Flow Expansions," Journal of the ASCE, 70: 1545-1565 (December 1944).
102. Vasiliev, O. P., and N. F. Budunov, "Calculation of Turbulent Flow with the Sudden Expansion of Channel," FTD HT/ST-76-161, 325-334, Wright-Patterson AFB, Ohio, Foreign Technology Division, 1976.
101. Back, L. H., and E. J. Roschke, "Shear-Layer Flow Regimes and Wave Instabilities and Reattachment Lengths Downstream of an Abrupt Circular Channel Expansion," Journal of Applied Mechanics, 39: 677-680 (September 1972).

104. Narayanan, M. A., et al., "Similarities in Pressure Distribution in Separated Flow Behind Backward-Facing Steps," The Aeronautical Quarterly, 25(4): 304-312 (November 1974).
105. Roshko, A., and Lau, J. C., "Some Observations on Transition and Reattachment of a Free Shear Layer in Incompressible Flow," Proceedings of the 1965 Heat Transfer and Fluid Mechanics Institute: 157-167, Stanford University Press, 1965.
106. Moon, L. F., and G. Rudinger, "Velocity Distribution in an Abruptly Expanding Circular Duct," Journal of Fluids Engineering, 99: 226-230 (March 1977).
107. Lipstein, N. J., "Low Velocity Sudden Expansion Pipe Flow," ASHRAE Journal, 4: 43-47 (July 1962).
108. Abbott, D. E., and S. J. Kline, "Experimental Investigation of Subsonic Turbulent Flow Over Single and Double Backward Facing Steps," Journal of Basic Engineering, 84: 317-325 (September 1962).
109. DeRossett, T. A., "An Experimental Investigation of Subsonic Steady and Oscillating Flow Over an Axisymmetric Backstep," Ph.D. Dissertation, Dept. of Mechanical, Industrial, and Aerospace Engineering, Rutgers University, May 1973.
110. Rouse, H., and Jezdinsky, V., "Fluctuation of Pressure in Conduit Expansions," Journal of the Hydraulics Division, Proc ASCE, 92: 1-12 (May 1966).
111. Narayanan, R., and A. J. Reynolds, "Pressure Fluctuations in Reattaching Flow," Journal of the Hydraulics Division, Proc ASCE, 94: 1383-1398 (November 1968).
112. Tani, I., "Experimental Investigation of Flow Separation Over a Step," Proceedings of Symposium on Boundary Layer Research: 377-387, Freiburg, Germany, August 26-29, 1957.
113. Matthews, L., and D. Whitelaw, "Plane Jet Flow Over a Backward-Facing Step," Proceedings of the Institution of Mechanical Engineers, 187: 447-454, 1973.
114. Smyth, R., "Experimental Study of Turbulence in Plane Separated Flows," Proceedings of the Fourth Biennial Symposium on Turbulence in Liquids--University of Missouri (Rolla--September 1975), Princeton, Science Press, 1977.
115. Mueller, T. J., H. H. Korst, and W. L. Chow, "On the Separation, Reattachment, and Redevelopment of Incompressible Turbulent Shear Flow," Journal of Basic Engineering, 86: 221-226 (June 1964).
116. Mueller, T. J., and J. M. Robertson, "A Study of the Mean Motion and Turbulence Downstream of a Roughness Element," Proceedings of the First Southeastern Conference on Theoretical and Applied Mechanics: 326-340, Gatlinburg, Tennessee, May 3-4, 1962.

117. Hsu, H. C., "Characteristics of Mean Flow and Turbulence at an Abrupt Two-Dimensional Expansion," Ph.D. Dissertation, State University of Iowa, 1950.
118. Thring, M. W., and M. P. Newby, "Combustion Length of Enclosed Turbulent Jet Flames," Fourth Symposium (International) on Combustion: 789-796, Baltimore, The Williams and Wilkins Company, 1962.
119. Craya, A., and R. Curtet, "On the Spreading of a Confined Jet," (in French), Comptes Rendus Academie des Sciences, Vol. 241, Paris, 621-622, 1955.
120. Guruz, A. G., H. K. Guruz, S. Osuwan, and F. R. Steward, "Aerodynamics of a Confined Burning Jet," Combustion Science and Technology, 9: 103-110 (1974).
121. Steward, F. R., and A. G. Guruz, "Aerodynamics of a Confined Jet with Variable Density," Combustion Science and Technology, 16: 29-45 (1977).
122. Field, M. A., D. W. Gill, B. B. Morgan, and P. G. W. Hawksley, "Combustion of Pulverized Coal," The British Coal Utilization Research Association, Leatherhead, 1967.
123. Ricou, F. P., and D. B. Spalding, "Measurements of Entrainment by Axisymmetrical Turbulent Jets," Journal of Fluid Mechanics, 11: 21-32 (1961).
124. Hill, B. J., "Measurements of Local Entrainment Rate in the Initial Region of Axisymmetric Turbulent Air Jets," Journal of Fluid Mechanics, 51, Part 4: 773-779 (1972).
125. Curtet, R., "Confined Jets and Recirculation Phenomena with Cold Air," Combustion and Flame, 2, No. 4: 383-411 (1958).
126. Becker, H. A., H. C. Hottel, and G. C. Williams, "Mixing and Flow in Ducted Turbulent Jets," Ninth Symposium (International) on Combustion: 7-20, Academic Press, London, 1963.
127. Magnussen, B. F., "Prediction of Characteristics of Enclosed Turbulent Jet Flames," Fourteenth Symposium (International) on Combustion: 553-566, Pittsburgh, The Combustion Institute, 1977.
128. Baev, V. K., et al., "Mixing of Cocurrent Flows in a Channel of Constant Cross-Section in the Presence of a Recirculation Zone," Combustion, Explosion, and Shock Waves, 8(1): 70-76 (1972), Original (Jan-Mar 1972).
129. Beér, J. M., N. A. Chigier, and K. B. Lee, "Modelling of Double Concentric Burning Jets," Ninth Symposium (International) on Combustion: 892-900, Academic Press, 1963.

130. Dealy, J. M., "The Confined Circular Jet with Turbulent Source," ASME Symposium on Fully Separated Flows: 84-91, 1964.
131. Saeyns, L. J., M. Zumer, and J. M. Dealy, "Criteria for Recirculation in Confined Jet Flames," Combustion and Flame, 17: 367-377 (1971).
132. Veeraraghavan, S., and Silveston, P. L., "Residence Time Distributions in Short Tubular Vessels," Canadian Journal of Chemical Engineering, 49: 346-353 (June 1971).
133. Wood, T., "Mixing Characteristics of a Bounded Turbulent Jet," Chemical Engineering Science, 23: 783-789 (1968).
134. Moeller, W. G., and J. M. Dealy, "Backmixing in a Confined Jet," Canadian Journal of Chemical Engineering, 48: 356-361, 1970.
135. Adler, R. J., and R. B. Hovorka, "A Finite Stage Model for Highly Asymmetric Residence Time Distributions," AICHE Preprint No. 3, Second Joint Automatic Control Conference, June 1961.
136. Wood, T., and Hop, N. H., "Mixing Induced by Confined Turbulent Jets: A Residence-Time Model for Flow in Cylindrical Vessels," Proceedings of the Fifth Australian Conference on Hydraulics and Fluid Mechanics, University of Canterbury, N.Z., 1974.
137. Pratt, D. T., "The Distribution of Residence Times in a Confined Round Jet," Paper No. WSCI-70-7, Western States Section, The Combustion Institute, 1970.
138. Crowe, C. T., and D. T. Pratt, "Gross Characterization of Mixing in Combustion Chambers Based on a Fluid Dynamical Model," Paper No. 6, Session 1, Eastern States Section, The Combustion Institute 1970 Fall Technical Meeting, November 1970.
139. Ernst, R. C., "Flameholder Combustion Instability Study," AFAPL TR-78-24, Wright-Patterson AFB, Ohio, Air Force Aero Propulsion Laboratory, May 1978.
140. Richardson, P. D., "Heat and Mass Transfer in Turbulent Separated Flows," Chemical Engineering Science, 18: 149-155 (1963).
141. Quick, A. W., "Ein Verfahren zur Untersuchung des Austauschvorganges in verwirbelten Strömungen hinter Körpern mit abgelöster Strömung," DVL-Bericht Nr. 12 (1956).
142. Winterfeld, G., "Versuche über Rezirkulationsströmungen in Flammen", Z. Flugwiss., 10: 168-178 (1962).
143. Cohen, L. S., and Director, M. N., "Transport Processes in the Two-Dimensional Near-wake," AIAA Paper No. 74-758, Presented at the AIAA 7th Fluid and Plasma Dynamics Conference, Palo Alto, California, June 17-19, 1974.

144. Silent'ev, B. A., "Experimental Investigation of Turbulent Heat Transfer at the Boundary of a Separation Zone," Journal of Applied Mechanics and Technical Physics, 7(5): 90-92 (Russian Original 125-129) (1966).
145. Humphries, W., and J. H. Vincent, "An Experimental Investigation of the Detention of Airborne Smoke in the Wake Bubble Behind a Disk," J. Fluid Mechanics, 73(3): 453-464 (1976).
146. Humphries, W., and J. H. Vincent, "Experiments to Investigate Transport Processes in the Near Wakes of Disks in Turbulent Air Flow," J. Fluid Mechanics, 75(4): 737-749 (1976).
147. Humphries, W., and J. H. Vincent, "The Transport of Airborne Dusts in the Near Wakes of Bluff Bodies," Chemical Engineering Science, 33: 1141-1146 (1978).
148. Humphries, W., and J. H. Vincent, "The Collection of Airborne Dusts by Bluff Bodies," Chemical Engineering Science, 33: 1147-1155 (1978).
149. Zakkay, V., Ram Sinha, and Hector Meduki, "Residence Time Within a Wake Recirculation Region in an Axisymmetric Supersonic Flow," Astronautics Acta, 16: 201-216, 1971.
150. Pavlov, S. M., "Investigation of Mass Transfer Between the Circulation Zone Behind a Bluff Body and the Mainstream and of Conditions of Mixing In It," Teploenergetika, 10 (1958) (given as Ref 3 in Silent'ev (Ref 144)).
151. Burdette, G. W., H. R. Lander, and J. R. McCoy, "High Energy Fuels for Cruise Missiles," AIAA Paper No. 78-267, Presented at the AIAA 16th Aerospace Sciences Meeting, Huntsville, Alabama, January 16-18, 1978.

APPENDIX A
AERODYNAMICS OF THE COAXIAL DUMP COMBUSTOR

It will be apparent from the discussion given in Chapter II that in estimating flame stability limits, both the chemical and aerodynamic aspects of the flameholder flow field must be modelled. It is therefore appropriate to review the aerodynamic phenomena associated with the dump combustor.

A number of studies deal with the one-dimensional analysis of the overall stagnation pressure losses incurred by sudden-expansion systems (Refs 96 and 97). Such analyses are based on the equations of conservation of mass and momentum. A key assumption is that for subsonic flow conditions, the pressure at the plane of the dump face is uniform and equal to the corresponding pressure of the dump plane inlet flow. Good agreement with cold flow experimental pressure losses is obtained, providing that the effects of inlet velocity profile and turbulence are included (Refs 98, 99, and 100). However, for the purposes of this investigation, the specific details of the flow field are of importance rather than the overall description provided by a one-dimensional analysis.

The axisymmetric sudden-expansion configuration is a ubiquitous component of various flow systems. Analyses of the flow characteristics of this device appear in the literature of fluid mechanics, heat transfer, industrial furnace practice, chemical engineering, fluidics, and even biological engineering. However, much of this literature deals with laminar flow conditions and with geometries of low diameter ratio, i.e., d/D less than about 0.1. Unfortunately, for ramjet systems,

data are required for highly turbulent flows and for high diameter ratios, i.e., d/D usually greater than 0.5.

The key feature of the sudden expansion system is the existence of the recirculation zone generated in conjunction with the separation-reattachment process. As shown in Fig A-1, the entering flow separates from the wall and entrains material from the surroundings, thereby increasing the size of the jet flow and progressively reducing jet velocity. The jet flow rate ultimately reaches a maximum value. After this point, a region of fluid loss from the jet to the recirculation region occurs so that subsequently the flow rate of the reattached flow becomes equal once again to the initial flow rate. The variation of the recirculated mass flow fraction $(\dot{m}_{rc}^*/\dot{m}_0)$ with distance is shown schematically in Fig A-2. The process of entrainment and fluid loss (de-entrainment) will be considered in more detail later in this Appendix.

The flow field in a coaxial dump combustor may be sub-divided into three regions: the recirculation zone, the central non-recirculating flow field, and the shear layer which separates the first two regions. Obviously, the volume of the recirculation zone and the mass flow entrained into it are of interest if this zone is modelled as a stirred reactor. The details of the shear layer would also be of interest if a characteristic-time model of the flame stabilizing process were used. The central flow region in which flame is propagated is of interest in the estimation of overall combustion efficiency. The structure of the recirculation zone will now be discussed in more detail.

* \dot{m}_{rc} is used to denote the measured recirculated mass flow.

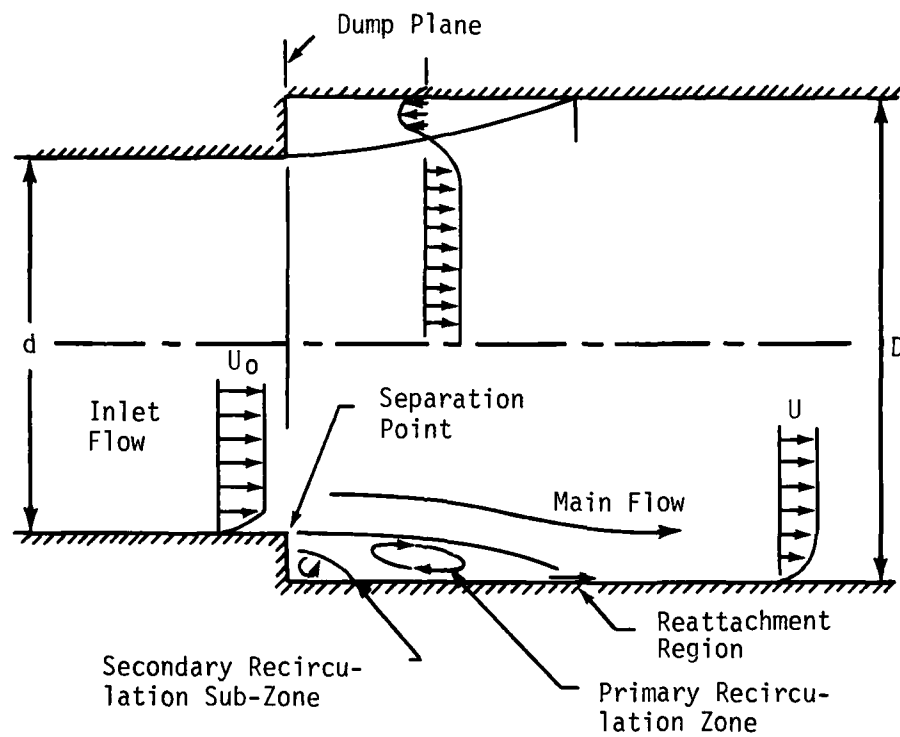


Figure A-1. Flow in a Sudden Expansion

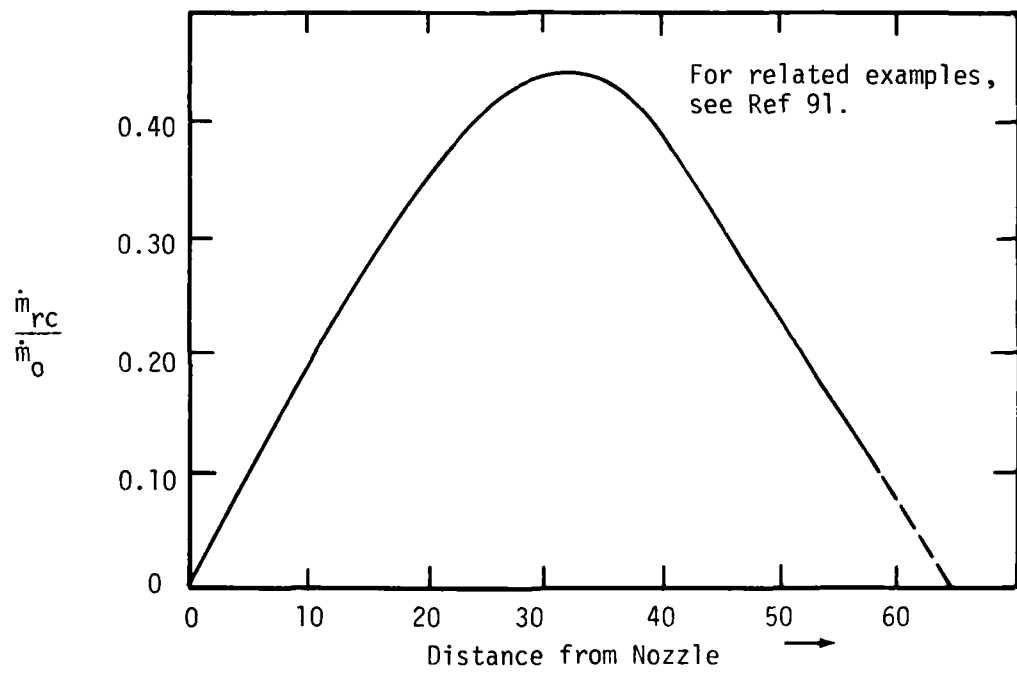


Figure A-2. Typical Variation of Measured Recirculation Flow Fraction with Distance

Characteristics of the Recirculation Zone

Turning first to the area of fluid mechanics, the literature on axisymmetric sudden expansion flows is large. A number of significant theoretical and experimental investigations is listed in Table A-I. Attention is drawn first to the pioneering work of Kalinske (Ref 101), who studied the mean and fluctuating water velocities in a series of divergent pipes including a sudden expansion configuration. This investigation utilized a streak line photographic approach, and thus the reduction of data was a laborious undertaking. An investigation of similar pipe geometries to those of Kalinske was carried out by Chaturvedi (Ref 89), using air as a working fluid. In addition to the mean flow velocity profile, the turbulence quantities u' , v' , and w' were measured, using hot-wire instrumentation. Chaturvedi's data are limited to only one diameter ratio ($d/D = 0.5$), but still represent the most comprehensive data set available, and indeed have served as a standard against which theoretical analyses (Refs 87 and 102) can be assessed. Some descriptive features of the flow field (Ref 89) are shown in Fig A-3. The reverse flow velocity in the recirculation zone is clearly seen. The variation of the axial turbulence intensity with distance is also of considerable interest in that the turbulence is observed to diffuse relatively slowly, and the high intensity level remains closely confined to the shear layer for several diameters downstream.

As noted earlier, a quantity of some importance for combustor modelling is the length from the plane of the dump to the point where the flow attaches to the wall. From a study of water flow in a sudden expansion, Back and Roschke (Ref 103) demonstrated that the reattachment

TABLE A-I INVESTIGATIONS OF AXISYMMETRIC SUDDEN EXPANSIONS

Ref	Investigator	Type of Work	Medium	Area Ratio (D/d)	Wall Pressure Profile	Velocity Profiles	RZ Length
83	DeRossett, Przirembel	Experimental	Air	1.28, 1.60	---	---	*
84	Pennucci	Experimental	Air	2.6, 3.2, 4.0	*	---	*
85	Drewry	Experimental	Air	2.36	*	*	*
86	Iribarne, et al	Experimental	Alcohol/Kerosene	4.0	---	*	*
87	Teyssandier	Analysis	Air	---	---	---	---
89	Chaturvedi	Analysis	Air/Water	4.0	*	*	*
101	Kalinske	Experimental	Water	3.0	*	*	*
102	Vasiliev, Budunov	Analysis	---	---	---	---	---
103	Back, Roschke	Experimental	Water	6.76	---	---	*
166	Moon, Rudinger	Analysis/Exp.	Air	2.0	---	*	*
107	Lipstein	Experimental	Air	1.3-2.5	*	*	*
110	Rouse, Jezdinsky	Experimental	Water	2.25, 4.0, 9.0	---	---	---
130	Dealy	Analysis/Exp.	Water	4.0, 16.0	---	*	---

Data From Ref 89

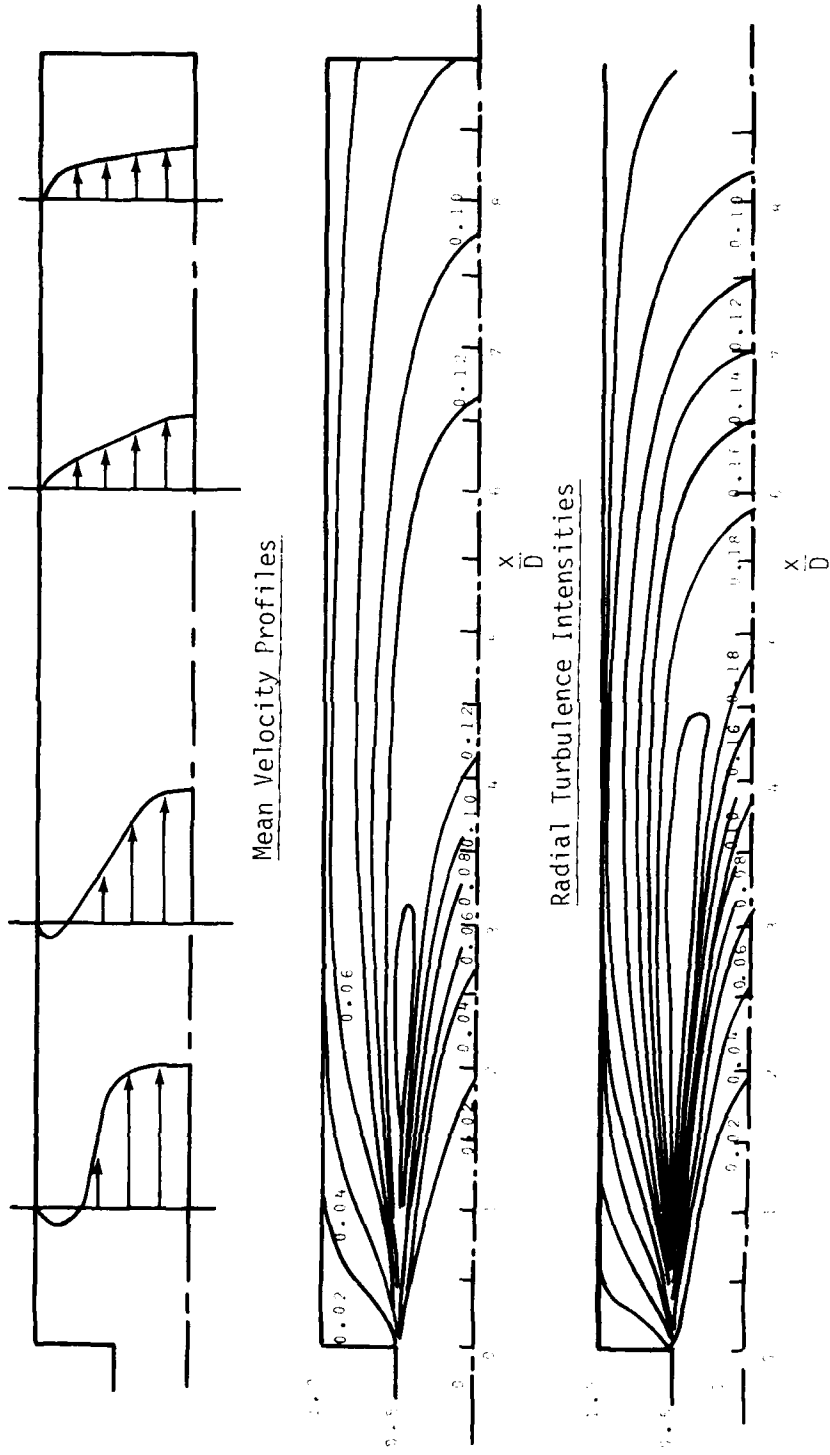


Figure A-3. Flow Phenomena in a Sudden Expansion

distance L , expressed in terms of step height h , varied strongly with the upstream Reynolds number (R_e) in the range $20 < R_e < 4200$. This variation is illustrated in Fig A-4. Many other investigators (Refs 83-86 and 89) have determined this reattachment length, and their data are also shown in Fig A-4. It will be observed that in the laminar flow regime, the reattachment length L increases with R_e . However, a regime is reached where L/h attains a maximum; further increases in R_e result in a decrease in L/h to a minimum followed by a final rise to an approximately constant value at a higher Reynolds number ($R_e > 3 \cdot 10^5$). This constant value of L/h is denoted by k , so that k is approximately equal to 8.5. Two recent investigations of sudden expansion burners are reported by Pennucci (Ref 84) and Drewry (Ref 85), respectively. Both investigators used surface flow visualization to locate the reattachment point; of course, the reattachment process really occurs over a zone, and the choice of a distinct line of reattachment cannot be precise.

In a recent application of the laser-Doppler velocimeter, Moon and Rudinger (Ref 106) measured the value of k , using a coaxial lucite configuration for Reynolds numbers in the region of 10^5 to 10^6 . Their results are also shown in Fig A-4 and are generally consistent with those of other investigators.

It may be inferred from Fig A-4 that, for high values of Reynolds number ($R_e > 3 \cdot 10^5$), the value of k lies between 8 and 9 for cold flow and is independent of R_e . However, there are indications in the literature that two geometric variables, namely the inlet diameter ratio d/D and the exit diameter ratio d^*/D , may influence k . Regarding the latter ratio (d^*/D), both Pennucci and Drewry used geometries which

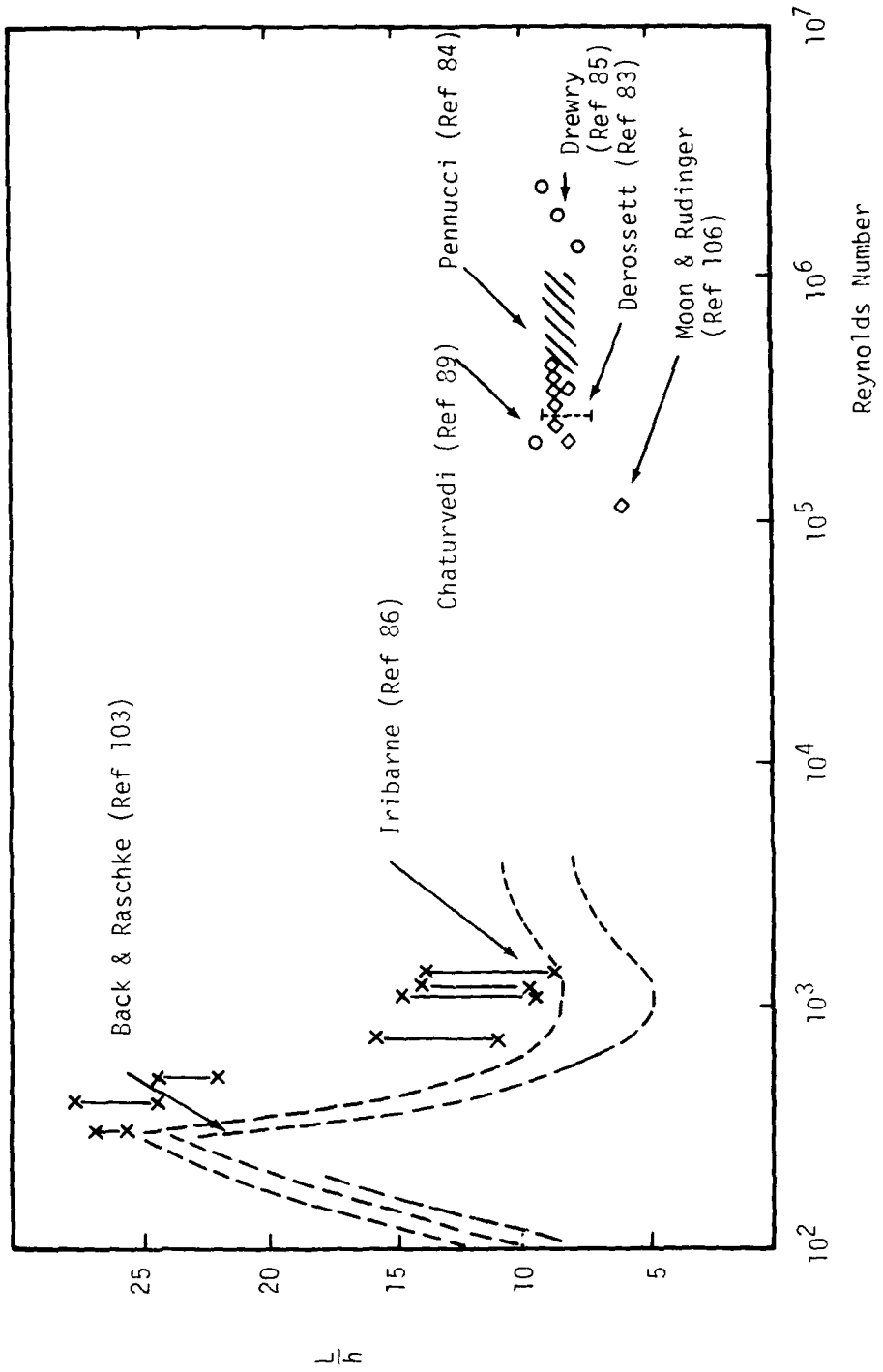


Figure A-4. Recirculation Zone Length-Ratio as a Function of Reynolds Number

incorporated a terminal convergent nozzle, thus imposing a downstream boundary condition. Pennucci observed that for one diameter ratio ($d/D = 0.5$), decreasing d^*/D from 0.63 to 0.45 led to a small decrease in the reattachment distance corresponding to a reduction in k from 9 to 8. A similar effect was noted by Drewry. This result may imply that k exhibits a Mach number dependency. Another intriguing investigation is that of Goldshtik and Silent'ev (Ref 88), who studied the effect of blockage in a two-dimensional opposed-step configuration. Blockage is defined as the ratio of flow area before the step to flow area after the step. In this two-dimensional case, the corresponding value of k varied from 6 at a blockage of 0.4 to a maximum of 7 at a blockage of 0.68, and finally fell to a minimum value of about 3 as the blockage approached unity. Although this investigation was performed on a two-dimensional configuration, similar results may apply to axisymmetric systems. Indeed, Lipstein (Ref 107) indicates such an effect. Thus the assumption that k lies between 8 and 9 step heights (Fig A-4) must be treated with caution pending further investigation of geometric variables.

Both Pennucci and Drewry also recorded wall static pressure variation in the chamber and measured the total pressure losses associated with sudden expansion flows. The typical variation of wall pressure is shown in Fig A-5; it will be noted that pressure continues to rise for some distance after the reattachment zone. Neither Pennucci nor Drewry was able to correlate the location of the flow reattachment point with any characteristic feature of the pressure rise curve. However, a re-examination of their data shows that the reattachment point corresponds closely to the point where the static pressure

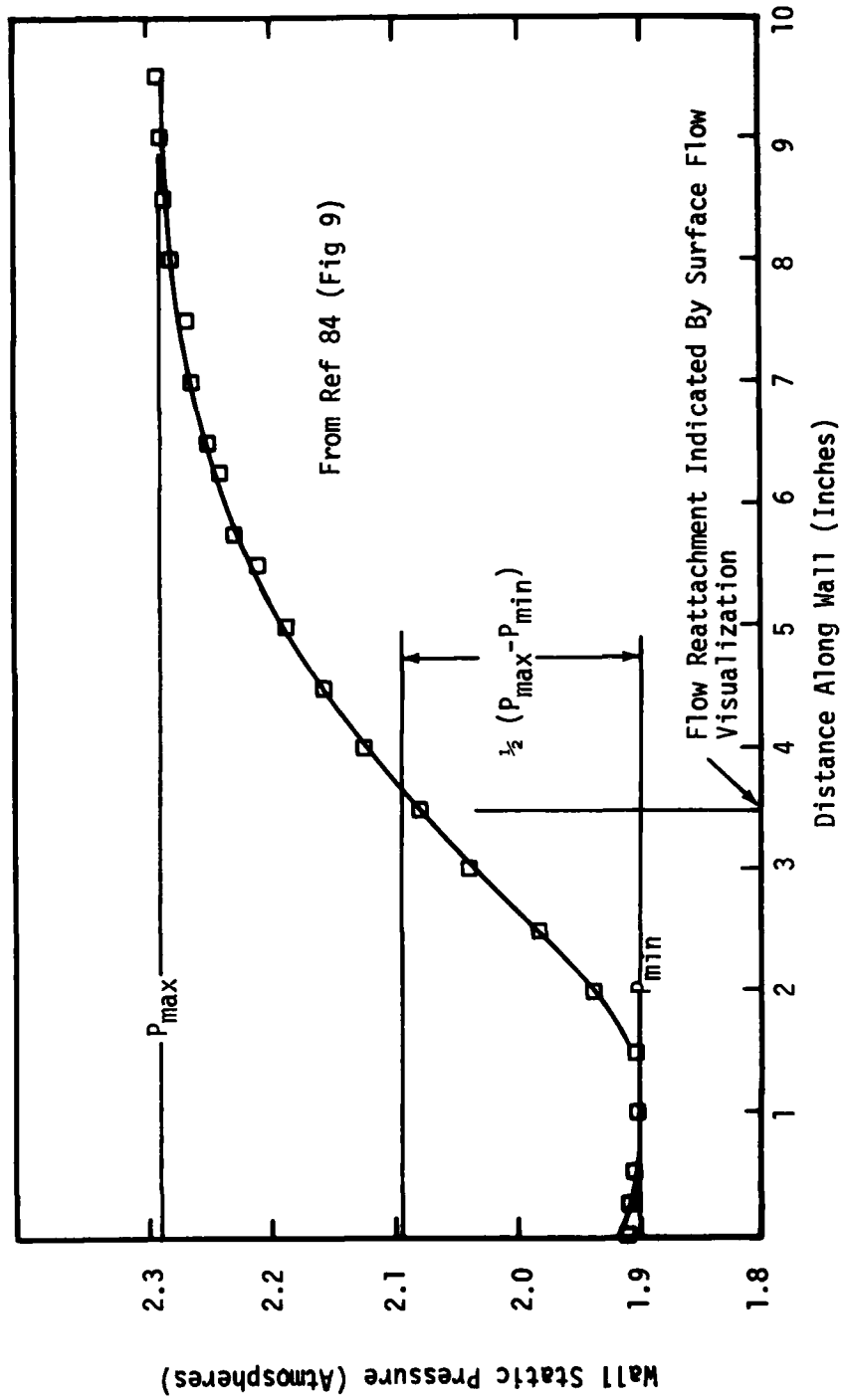


Figure A-5. Wall Static Pressure Distribution for a Coaxial Dump Configuration (Ref 84)

rise reaches half its maximum value; i.e., $1/2 (P_{\max} - P_{\min})$. This is entirely an empirical observation. It is not intended to explore this observation any further in this discussion; the reader is referred to other investigations (Refs 104 and 105) which discuss correlations already obtained in related geometries. Another interesting observation noted by both Pennucci and Drewry was the existence of a rotating flow in the RZ region; looking upstream, this flow rotated in a counterclockwise direction. This phenomenon was also reported by Iribarne et al. (Ref 86).

In connection with the reattachment process, it is important to stress that this reattachment point fluctuates rapidly about the location indicated by flow visualization techniques. An interesting investigation was conducted by DeRossett and Przirembel (Ref 83), who studied the unsteady nature of the reattachment process behind an axisymmetric step. They utilized a dual-element hot film probe to measure the flow velocity close to the wall and demonstrated that in the reattachment region, flow oscillations existed at a frequency of the order of several hundred Hertz. Thus reattachment occurred over a region rather than on a line; furthermore, the width of this region was found to increase with both step height and the thickness of the approaching boundary layer.

Two other facets of this investigation are worth noting. First, in order to describe the reattachment process, a "forward flow probability (FFP)" was defined. At a given location, this was described as the percentage of time that the flow was directed upstream; this was observed over a sufficiently long period to obtain a valid statistic. A typical variation of this FFP with distance from the step is shown

in Fig A-6, and the length of the reattachment zone may be defined in terms of the level of FFP (typically at the zero or 100% level). Second, the shape of the curve confirms the existence of a small vortex-type flow in the corner of the step in addition to the main recirculating flow. The existence of this type of vortex was detected in nominally two-dimensional flows both by Abbott and Kline (Ref 108) and other researchers. In the basic dissertation by DeRossett (Ref 109), information is also given on the fluctuating pressure levels which accompany the reattachment process. The maximum RMS values of the fluctuation associated with various flow velocities appear to be located just upstream of the point of complete reattachment.

This latter result confirms earlier work by Rouse and Jezdinsky (Ref 110) and that of Narayanan and Reynolds (Ref 111) concerning two-dimensional flows. Attention is drawn to the fluctuating nature of the reattachment process because high speed movies of combustion in a coaxial dump combustor, made during this current investigation, clearly revealed the very unsteady nature of the process. Furthermore, this unsteadiness is of considerable technological interest in relation to practical combustors where severe heat transfer and coupled combustion instability effects may result from this basic fluid dynamic phenomenon.

The above discussion has yielded some insight into the nature of the reattachment process and has highlighted the relatively constant value of k (8-9) for highly turbulent flow under non-burning conditions. Currently, no detailed information can be found on the flow structure of the simple axisymmetric sudden expansion under combustion conditions, although it is anticipated that a number of studies will eventually be made with non-interference instrumentation. An investigation was made

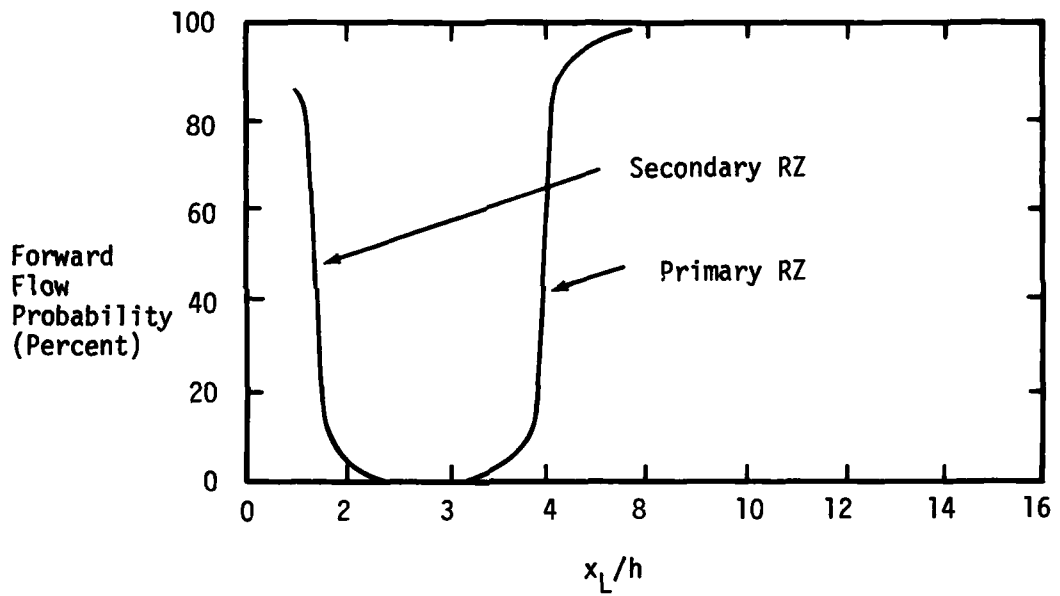


Figure A-6. Illustration of Forward Flow Probability (Ref 83)

by Baev and Tret'yakov (Ref 58), under combustion conditions, of a two-dimensional opposed-step combustor. In this case, the length of the recirculation zone was not affected by fuel-air ratio changes, but increased substantially with the exit velocity from the combustion chamber. No exit nozzle appeared to be used in this combustor.

A similar discussion applies to subsonic flow over two-dimensional steps. Here again a substantial literature exists concerning plane flows (Refs 111-117) on the mean flow structure, the turbulence levels, and on the unsteadiness of the reattachment process. However, only limited observations exist on the flow structure associated with actual combustion. Thus, Kawamura (Ref 76) found that the length of the recirculation zone was about half that of the corresponding cold flow (3.5 step heights compared to 7) and exhibited little variation with either fuel/air ratio or velocity.

In closing this discussion of the length of the recirculation zone, it may be concluded that there are many factors which influence this length, and much research needs to be done, particularly under actual combustion conditions. Nevertheless, as illustrated in Fig A-4, a reasonable assumption is that $k \approx 8.5$ for high Reynolds number flows.

This conclusion is also supported by studies of the heat and mass transfer in sudden-expansion systems. However, such secondary evidence will not be introduced in this discussion.

The volume and surface area of the recirculation zone are also of interest. A typical recirculation zone shape is shown in Fig A-7. This shape may be approximated, as shown, by an equation of the form

$$y_L = \frac{x_L^2}{k^2 h}$$

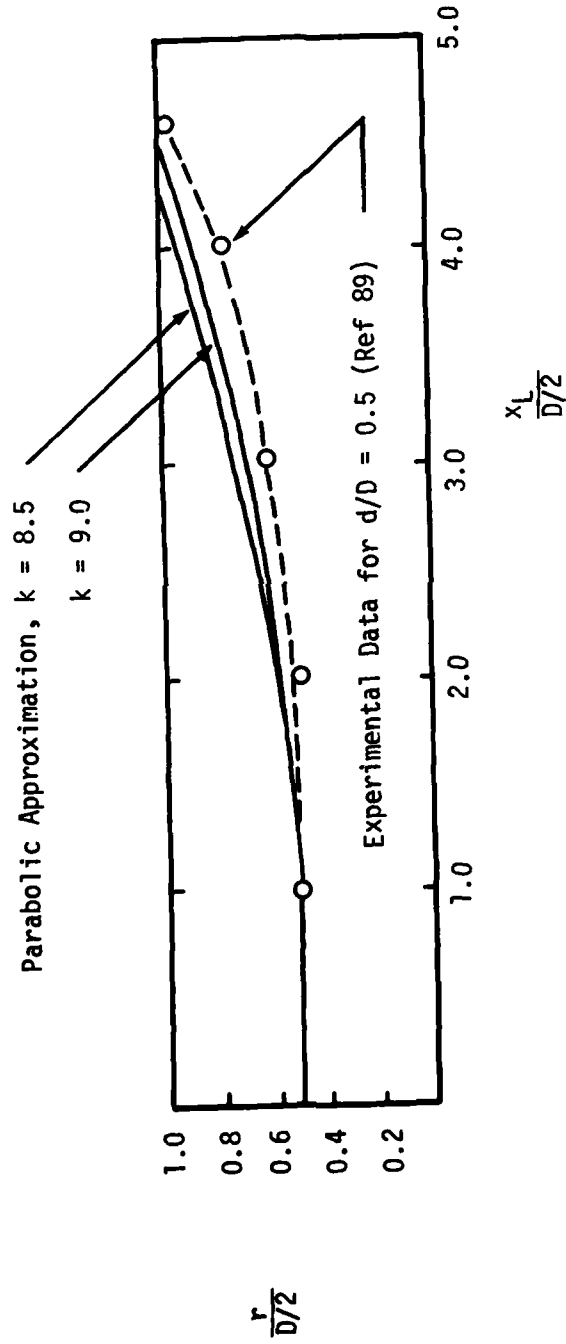


Figure A-7. Shape of Recirculation Zone

The surface area (S_p) corresponding to this parabolic approximation is:

$$\begin{aligned}
 S_p &= 2\pi \int_0^h \left(y_L + \frac{d}{2}\right) \sqrt{1 + \left(\frac{dx_L}{dy_L}\right)^2} \cdot dy_L \\
 &= \frac{\pi kh}{2} \left[d + h + \frac{k^2 h}{8}\right] \sqrt{1 + \frac{4}{k^2}} \\
 &\quad - \frac{\pi}{4} k^2 h \left[\frac{k^2 h}{8} - d\right] \ln \left[\frac{2}{k} + \sqrt{1 + \frac{4}{k^2}}\right] \quad (A-1)
 \end{aligned}$$

The corresponding volume is given by

$$\begin{aligned}
 V_p &= \frac{\pi}{4} khD^2 - \pi \int_0^{kh} \left(y_L + \frac{d}{2}\right)^2 \cdot dx_L \\
 &= \pi kh \left[\frac{2}{3} \cdot hd + \frac{4}{5} h^2\right] \quad (A-2)
 \end{aligned}$$

A characteristic dimension (\bar{h}_p) of the recirculation zone may be defined by writing

$$\frac{\bar{h}_p}{D} = \frac{1}{D} \frac{V_p}{S_p} = \frac{V_p}{D^3} \cdot \frac{D^2}{S_p} \quad (A-3)$$

A curve of \bar{h}_p/D as a function of $\frac{2h}{D}$ for various values of k is given in Fig A-8. For $k = 8.5$, a good representation of this relationship is

$$\frac{\bar{h}_p}{D} \propto \left(\frac{2h}{D}\right)^{1.095}$$

or approximately

$$\frac{\bar{h}_p}{D} \propto \left(\frac{2h}{D}\right)^{1.1} \quad (A-4)$$

where $0.1 \leq \frac{2h}{D} \leq 0.6$.

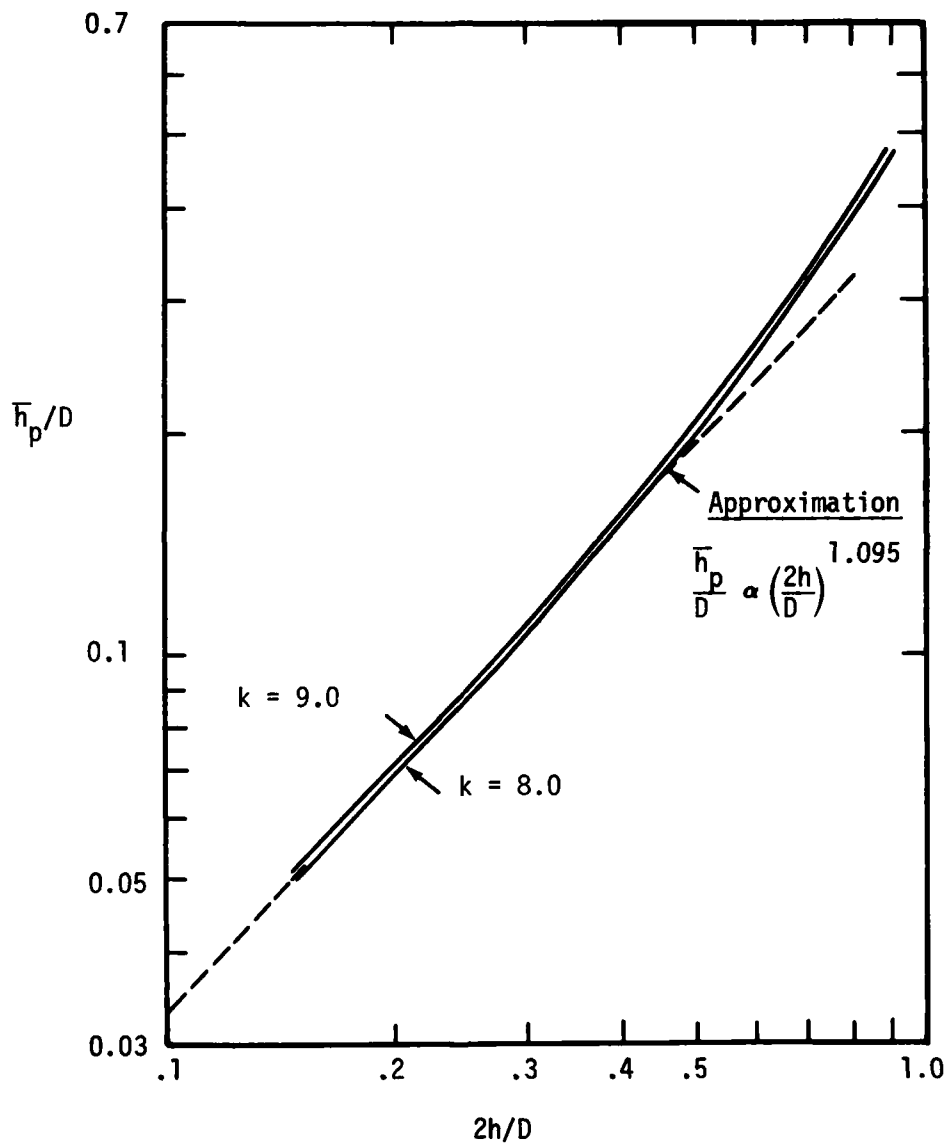


Figure A-8. Parabolic Recirculation Zone: Geometric Parameters

In addition to the reattachment distance (L), another important quantity is the mass flow entrained into the recirculation zone. With few exceptions, information on this quantity is largely found in the literature concerning industrial furnaces and burner systems. Relevant aspects of this literature will now be reviewed.

Entrainment in Confined Jet Systems

A typical arrangement of an industrial furnace is shown schematically in Fig A-9. Unlike the dump combustor, such furnaces are generally fed by two streams. The central or primary jet is typically a high velocity fuel, or fuel-laden, jet. The secondary flow which surrounds the primary provides air for combustion. Two situations can arise: if the secondary air flow is large, then entrainment of air by the primary jet proceeds steadily until restricted by the duct wall. However, if the secondary air flow is below that which the jet can entrain, some downstream fluid will be recirculated upstream and a recirculating flow will be established. Two quantities are then of prime interest; namely, the axial location of the recirculation zone and the maximum quantity of fluid being recirculated. Two theories have been widely used to correlate these quantities: the early work of Thring-Newby (Ref 118) and the more rigorous analysis of Craya-Curtet (Ref 119). These two theories have each yielded a similarity criterion describing confined jet flows commonly denoted by the symbols θ (Thring-Newby criterion) and C_t (Craya-Curtet criterion). An appreciable volume of literature (e.g., Refs 120 and 121) refining and extending these theories has been published in recent years.

The relevance of the above work to the present investigation lies in the fact that the sudden expansion combustor corresponds to an

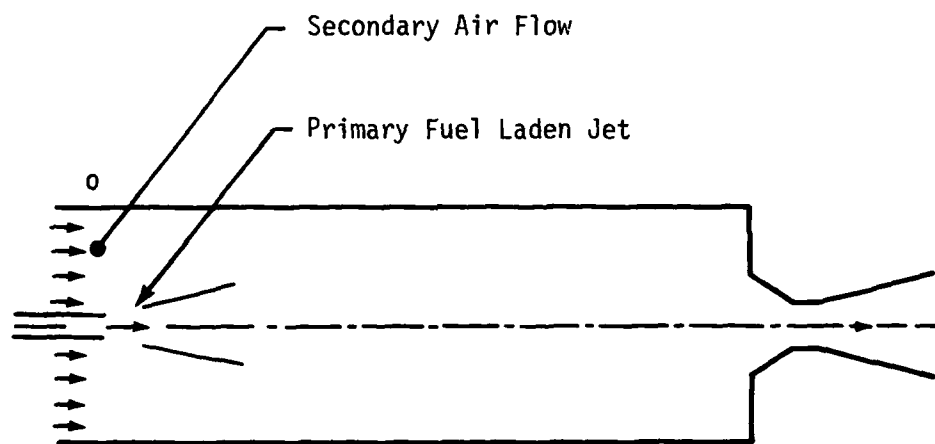


Figure A-9. Schematic Arrangement of an Industrial Furnace

industrial furnace with zero secondary air flow; this special case is documented in the literature. Unfortunately, the area ratios $(d/D)^2$ of industrial furnaces are much lower than those corresponding to ramjet combustors. This fact limits the direct application of available furnace data to ramjets.

Thring and Newby (Ref 118) analyzed the flow within the furnace on the assumption that the primary jet entrained flow in a manner similar to a turbulent free-jet. Field et al. (Ref 122) modified the analysis utilizing the classical expression for free-jet entrainment derived by Ricou and Spalding (Ref 123) from direct flow measurements. This expression is:

$$\frac{\dot{m}_x}{\dot{m}_0} = 0.32 \left(\frac{\rho_a}{\rho_0} \right)^{1/2} \frac{x_L}{d} \quad (\text{A-5})$$

where \dot{m}_x = mass flow rate at distance x_L downstream
 \dot{m}_0 = initial mass flow rate of jet
 ρ_a = ambient density
 ρ_0 = jet fluid density
 d = jet diameter

Eq(A-5) is valid for values of x_L/d greater than about 13. For shorter distances, Hill (Ref 124) has shown that lower rates of entrainment exist.

The corresponding entrained mass flow \dot{m}_e will be given by:

$$\frac{\dot{m}_e}{\dot{m}_0} = \frac{\dot{m}_x}{\dot{m}_0} - 1 = 0.32 \left(\frac{\rho_a}{\rho_0} \right)^{1/2} \frac{x_L}{d} - 1 \quad (\text{A-6})$$

The basis of Field's theory is that emerging jet is assumed to entrain as a free-jet up to a given point Q where entrainment stops

(Fig A-10); disentrainment then takes place until the jet strikes the wall at point R. A jet spreading angle of 9.7 degrees is assumed by Field (which incidentally appears to be twice as high as Field initially intended), leading to

$$x_R = 2.925D$$

where D is the combustor diameter.

A point P is defined as the place where $\frac{\dot{m}_e}{\dot{m}_o}$ defined by Eq(A-6) falls to zero, i.e.,

$$x_P = \frac{d}{.32} \left(\frac{\rho_o}{\rho_a} \right)^{1/2} \quad (A-7)$$

Finally, it is assumed that point Q is located midway between points P and R; thus:

$$\begin{aligned} x_Q &= \frac{1}{2} (x_P + x_R) \\ &= \frac{D}{2} \left(2.925 + \frac{d}{0.32} \cdot \frac{1}{D} \left(\frac{\rho_o}{\rho_a} \right)^{1/2} \right) \\ &= \frac{D}{2} \left(2.925 + \frac{\theta}{0.32} \right) \end{aligned} \quad (A-8)$$

where

$$\theta = \frac{d}{D} \left(\frac{\rho_o}{\rho_a} \right)^{1/2} \quad (A-9)$$

Finally, from Eq(A-6) and Eq(A-8), and equating \dot{m}_{rc} to \dot{m}_e

$$\frac{\dot{m}_{rc}}{\dot{m}_o} = \frac{0.47}{\theta} - 0.50 \quad (A-10)$$

where θ is termed the Thring-Newby parameter.

In some cases all the secondary flow (\dot{m}_a) will be entrained before recirculation starts. A modified parameter is then used, defined as:

$$\theta^1 = \frac{d}{D} \left(\frac{\rho_o}{\rho_a} \right)^{1/2} \frac{\dot{m}_a + \dot{m}_o}{\dot{m}_o} \quad (A-11)$$

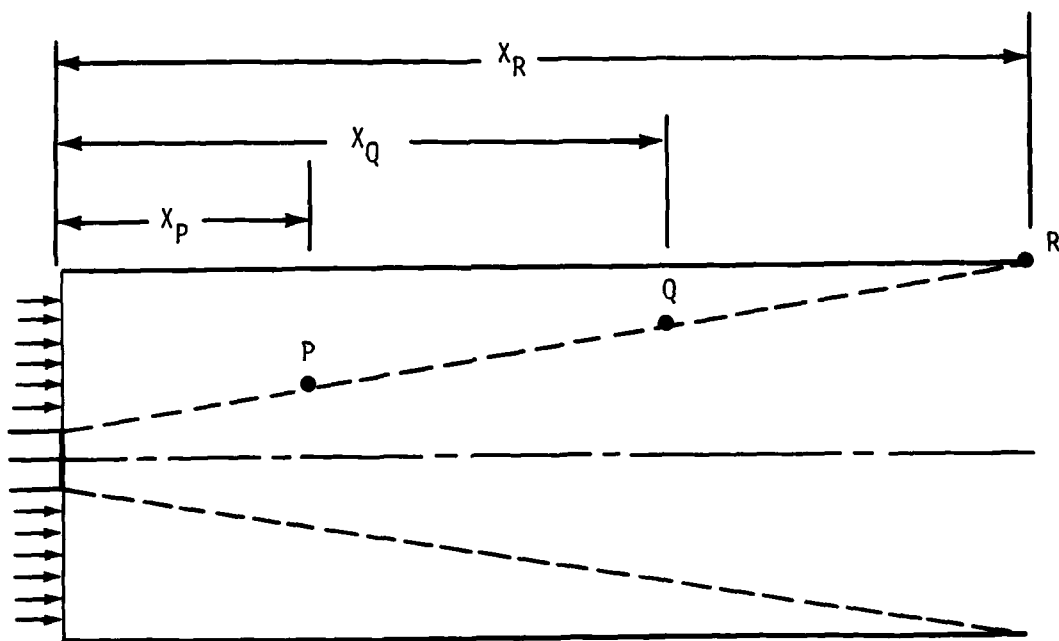


Figure A-10. Geometry of Entrainment Region

The corresponding recirculating flow equation is

$$\frac{\dot{m}_{rc}}{\dot{m}_o + \dot{m}_a} = \frac{0.47}{\theta^1} - 0.50 \quad (A-12)$$

Unfortunately, the above theory is only strictly valid for values of $\frac{d}{D} < 0.05$ whereas in the present investigation, d/D lies in the approximate range 0.40 to 0.80. Nevertheless, it is necessary to discuss the θ parameter so that relevant experimental data may be presented. More exact analyses of furnace-type flows have led to improved similarity parameters.

The first rigorous analysis of confined jet flow was reported initially by Craya and Curtet (Ref 119), and subsequently by Curtet (Ref 125). This work considered the equations of motions for isothermal, incompressible flow and led to a similarity parameter denoted by m_s , which can be expressed as:

$$m_s = \frac{U_{dyn}^2 - \frac{1}{2} U_k^2}{U_k^2} \quad (A-13)$$

where U_k is termed the "kinematic mean velocity" and is expressed as:

$$U_k = \frac{U_d d^2 + U_D (D^2 - d^2)}{D^2} \quad (A-14)$$

where U_d denotes primary jet velocity and U_D corresponds to secondary flow velocity.

The term U_{dyn} is called the dynamic mean velocity and is defined as:

$$U_{dyn}^2 = \frac{U_d^2 d^2 + U_D^2 (D^2 - d^2)}{D^2} - \frac{1}{2} U_D^2 \quad (A-15)$$

In yet another analysis of the general problem of confined jet systems, Becker et al. (Ref 126) defined a parameter which they termed the Craya-Curtet number C_t ; this is related to the m_s parameter given in Eq(A-13) by the expression:

$$C_t = \frac{1}{m_s^{1/2}} \quad (A-16)$$

Corresponding comprehensive experimental studies have shown C_t is in general an appropriate parameter to characterize the mixing of isothermal confined jets. For large duct to jet area ratios, it may be shown that $C_t \approx \theta$. Another similarity parameter is derived by Magnussen (Ref 127), whose theory for recirculation was based on the pressure increase which occurs downstream of the jet region. His similarity parameter is denoted by B , where B is defined as:

$$B = \frac{U^+ (\rho A)_c}{\dot{m}} \quad (A-17)$$

where U^+ is a characteristic entrance velocity and the subscript c denotes conditions at the plane of maximum recirculation.

For a constant area duct with constant density flow, it can be shown that B is related to the Craya-Curtet parameter by:

$$C_t = \frac{1}{\sqrt{B - 0.5}} \quad (A-18)$$

Also for a sudden dump configuration, the following relation between the Thring-Newby parameter (θ) and B exists (Ref 127).

$$\theta = \frac{1}{\sqrt{B}} \quad (A-19)$$

There are thus four similarity parameters in use to describe coaxial confined jet mixing; θ , C_t , m_s , and B . Unfortunately, their use has been predicated on the assumptions of isothermal, incompressible flow, and on large duct-to-jet areas. As noted earlier, investigations have been made to extend the analysis of jet mixing; in particular, to include the case of non-uniform density, and a non-isothermal Craya-Curtet number has been defined (Refs 120 and 121).

Also, another method of analyzing cocurrent flows using flow non-uniformity coefficients has been reported (Ref 128).

The above similarity parameters have been briefly introduced because some data from furnace practice are relevant to ramjet combustors despite the significant differences in duct area ratios. Furthermore, the analysis of the more complicated multi-inlet ramjet combustors (Fig 2) will require an appeal to similarity parameters in order to establish a rational approach to combustor analysis. The similarity parameters for the coaxial dump combustor will now be described.

For the sudden expansion combustor, there is no secondary air flow so that Eq(A-14) yields

$$U_K = U_d \left(\frac{d}{D}\right)^2$$

and

$$U_{dyn} = U_d \left(\frac{d}{D}\right)$$

From Eq(A-13)

$$m_s = \left(\frac{D}{d}\right)^2 - 0.5 \quad (A-20)$$

and from Eq(A-16)

$$C_t = \frac{1}{\left(\left(\frac{D}{d}\right)^2 - 0.5\right)^{1/2}} \quad (A-21)$$

Also, from Eq(A-9)

$$\theta = \frac{d}{D} \quad (A-22)$$

and finally from Eq(A-19)

$$B = \left(\frac{D}{d}\right)^2 \quad (A-23)$$

The values of M , C_t , θ , and B for the combustor geometries utilized in the present investigation are listed in Table A-II. The relevant data from furnace practice will now be reviewed.

A number of investigations have been performed to measure the recirculating mass flow fractions in both cold and combusting flows. A most useful source of data is the work of Hubbard (Ref 90) because several tests were performed with zero secondary air mass flow. Thus Hubbard gives data on axial velocity decay, recirculation zone velocities, and recirculated mass flow fraction. In Fig A-11, it is shown that the recirculated mass flow fraction, corresponding to zero secondary flow, falls on the curve which relates that fraction to the θ parameter. This suggests that data obtained for two stream systems can be utilized for sudden dump combustors. Specifically, it suggests that for constant density mixing, the quantity

$$\theta^1 = \left(\frac{\dot{m}_a + \dot{m}_o}{\dot{m}_o} \right) \frac{d}{D} \quad (A-24)$$

can be regarded as the equivalent diameter ratio for a sudden expansion system. In physical terms, this requires that the dump plane correspond to the point where all the secondary flow is entrained prior to the commencement of recirculation. Another unique feature of Hubbard's data is that they include relatively large values of d/D ; his data is plotted in Fig A-12, together with the recirculation fractions recommended by other sources. The following expressions, suitably modified to apply to the coaxial dump combustor, are recommended by the various sources:

TABLE A-II SIMILARITY PARAMETERS OF EXPERIMENTAL HARDWARE

\underline{d}	\underline{D}	$\frac{(D/d)^2}{m_s}$	$\underline{C_T}$	$\underline{\theta}$	\underline{B}
2.5	6.0	5.760	.4360	.4167	5.759
3.0	6.0	4.000	.5345	.5000	4.000
3.5	6.0	2.939	.6403	.5833	2.939
4.0	6.0	2.250	.7559	.6667	2.2500
4.5	6.0	1.778	.8846	.7500	1.7778
5.0	6.0	1.440	1.0314	.8333	1.4400

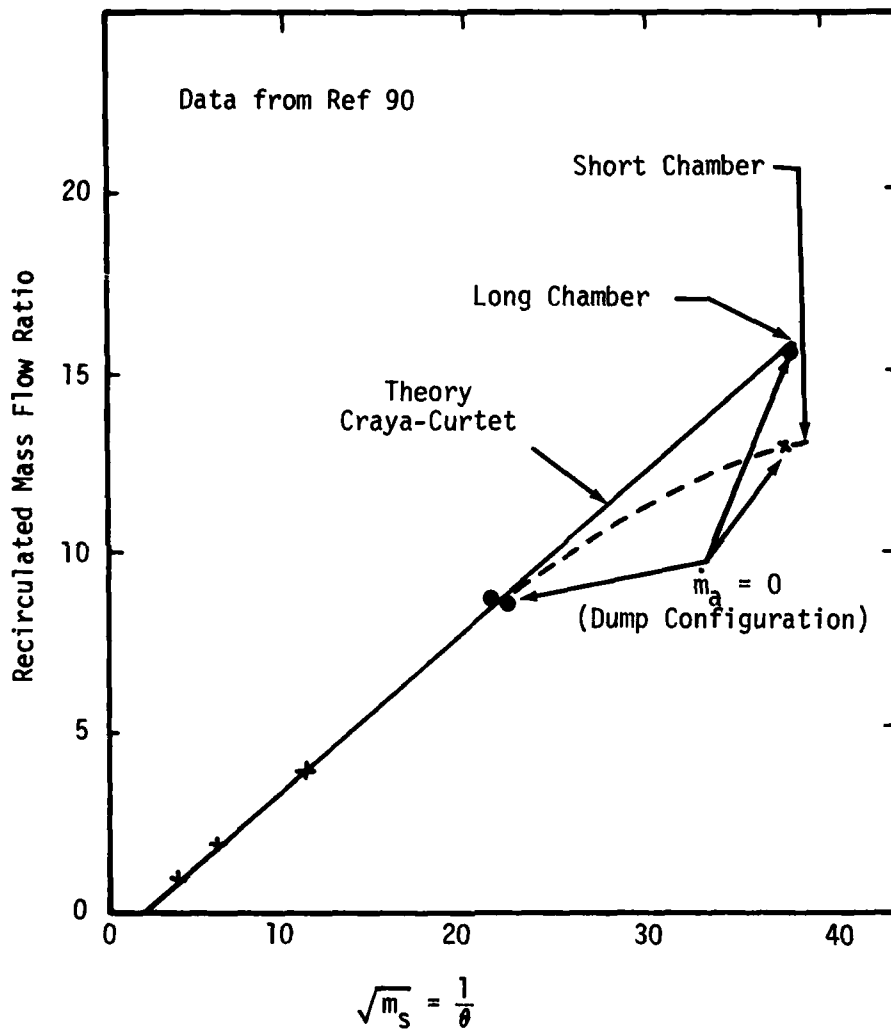


Figure A-11. Variation of Recirculation Mass Flow Fraction with $\sqrt{m_s}$

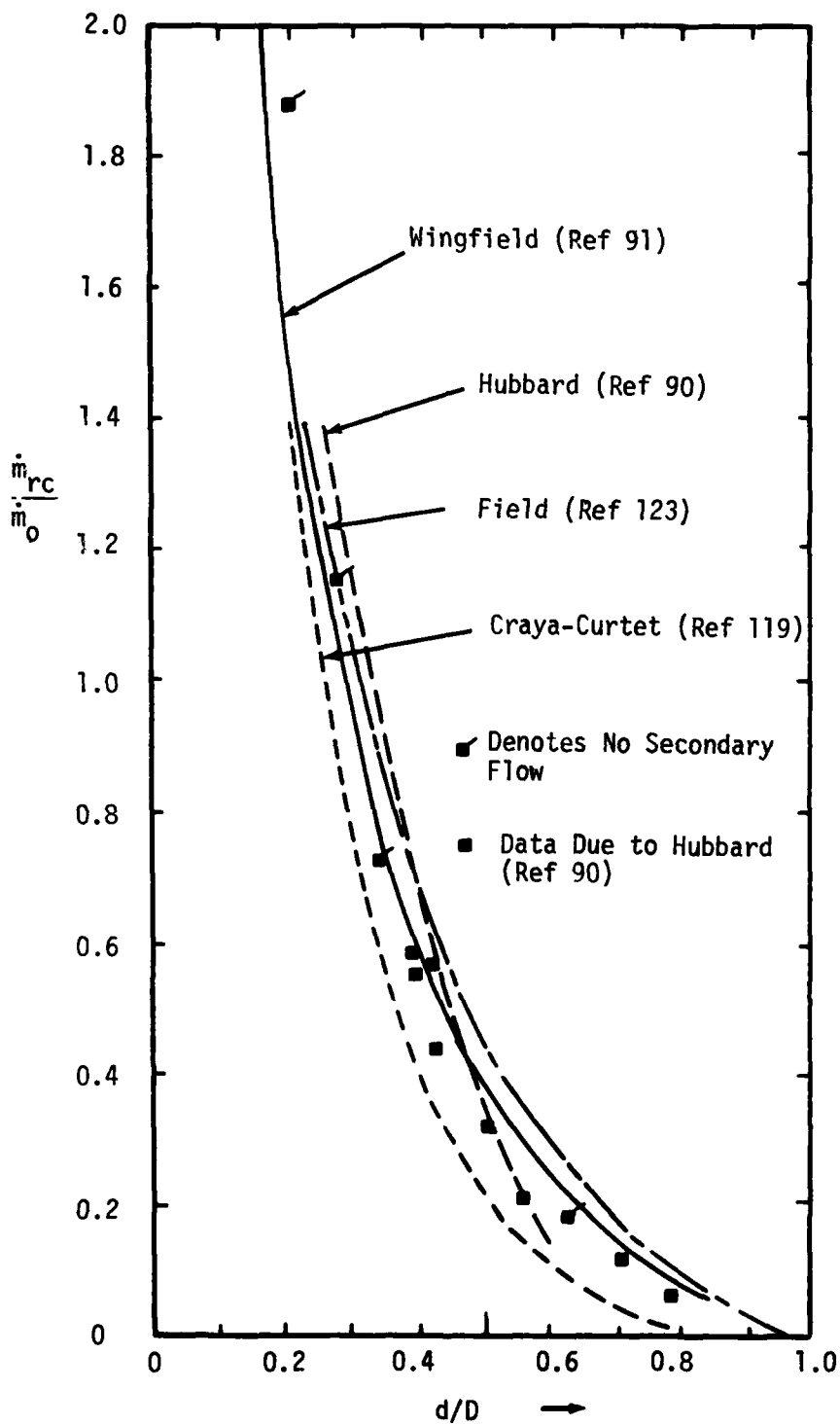


Figure A-12. Estimates of Recirculation Mass Flow Fraction from Various Sources

$$\text{Field (Ref 123): } \frac{\dot{m}_{rc}}{\dot{m}_o} = .47 \left(\frac{1}{d/D} \right) - 0.5 \quad (\text{A-25})$$

$$\text{Hubbard (Ref 90): } \frac{\dot{m}_{rc}}{\dot{m}_o} = .62 \left(\frac{1}{d/D} \right) - 0.9 \quad (\text{A-26})$$

$$\text{Wingfield (Ref 91): } \frac{\dot{m}_{rc}}{\dot{m}_o} = .398 \left\{ \frac{1}{d/D} - 1.059 \right\} \quad (\text{A-27})$$

$$\text{Craya-Curtet (Ref 119): } \frac{\dot{m}_{rc}}{\dot{m}_o} = .44 \left(\frac{1}{d/D} \right) - 0.88 \quad (\text{A-28})$$

Further inspection of Hubbard's data reveals that several of the larger d/D points correspond to sudden dump operation. These points have been flagged in Fig A-12. On inspection, it appears that the limited sudden expansion data arising from furnace studies are reasonably well correlated by Wingfield's expression:

$$\frac{\dot{m}_{rc}}{\dot{m}_o} = 0.398 \left(\frac{1}{d/D} - 1.059 \right) \quad (\text{A-29})$$

It should be recalled that the above discussion related to cold flow models and that appropriate allowance for change of density must be made before applying Eq(A-29) to hot flow situations. In this regard, Beer et al. (Ref 129) have demonstrated similarity of hot and cold mixing patterns using a modified Thring-Newby parameter. The correction for hot flow conditions is simply to use an equivalent primary nozzle diameter (d_h) through which passes the same mass flow and momentum flux as the actual nozzle, but with a density ρ_h instead of ρ_o . Thus

$$\frac{d_h}{d} = \sqrt{\frac{\rho_o}{\rho_h}} \quad (\text{A-30})$$

A rigorous derivation of this correction term is given by Guruz et al. (Ref 121). The effect of density ratio on the recirculated mass flow fraction given by Eq(A-29) is shown in Fig A-13.

In this review of furnace data, it has been stressed repeatedly that the results apply to combustors of lower diameter ratio (d/D) than ramjet systems. In these low diameter ratio systems, the rate of entrainment may be derived from the free-jet expression of Ricou and Spalding (Ref 123) given in Eq(A-5). However, during the course of this review, it was noted that Hill (Ref 124) had obtained entrainment data for the initial region of a free-jet. This data is more appropriate to coaxial combustors of high diameter ratio where the primary jet is not fully developed. In this regard, Dealy (Refs 130 and 131) has shown that similar velocity profiles are developed at $\frac{d}{D} = 0.25$, but not for $\frac{d}{D} = 0.50$. Therefore, the results of Hill were reviewed and an analytical expression derived for his data.

Entrainment in the Initial Region of a Turbulent Jet

The experimental investigation of Hill (Ref 124) utilized the same technique as Ricou and Spalding, but obtained data for entrainment at x_L/d ratios in the region $1 < x_L/d < 21$. Hill's data is reproduced in Fig A-14. This shows the variation of the entrainment coefficient C_2 with x_L/d . Note that the entrainment rate is

$$\frac{dm_e}{dx_L} = C_2 \frac{\dot{m}_0}{d} \left(\frac{\rho_s}{\rho_0} \right)^{1/2} = C_2 \sqrt{\rho_{rel}} \frac{\dot{m}_0}{d} \quad (A-31)$$

where ρ_{rel} is the ratio of secondary stream to primary stream density and by comparison with Eq(A-5), it is seen that $C_2 = 0.32$ in Ricou and Spalding's work.

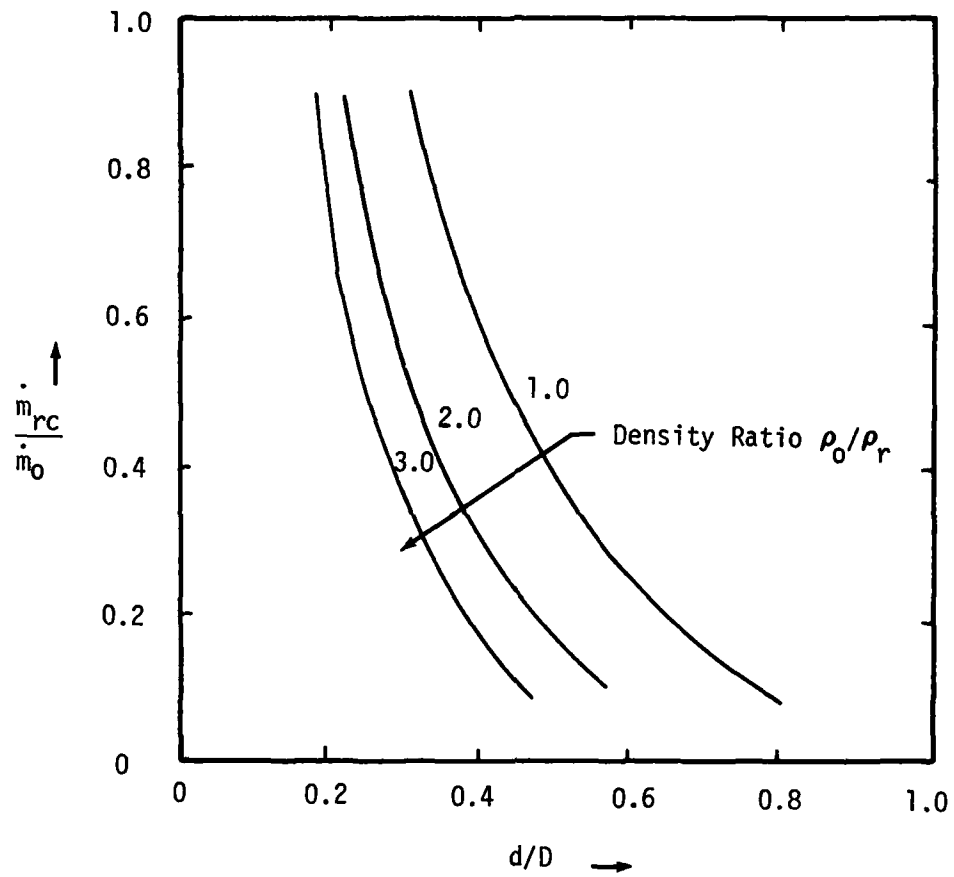


Figure A-13. Effect of Density Ratio on Recirculation Mass Flow Fraction

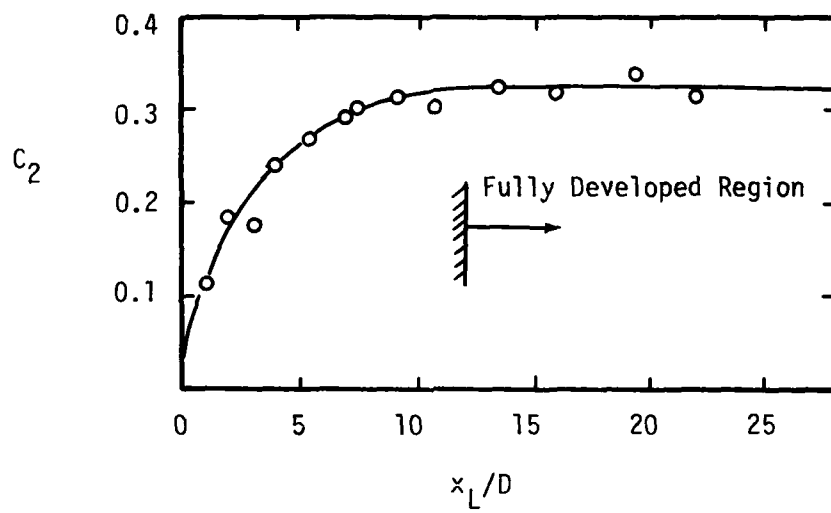


Figure A-14. Entrainment in the Initial Region of a Turbulent Jet

The data given in Fig A-14 may be approximated by the expression:

$$C_2 = \frac{1}{a_1} \left(b_1 + \ln \frac{x_L}{d} \right) \quad 0 < x_L/d < 12$$

yielding

$$\frac{\dot{m}_e(x_L)}{\dot{m}_o} = \frac{\sqrt{\rho_{rel}}}{d} \int_0^{x_L} C_2 dx_L = \sqrt{\rho_{rel}} \int_0^{x_L/d} C_2 d \left(\frac{x_L}{d} \right) \quad (A-32)$$

and Eq(A-32) finally yields

$$\frac{\dot{m}_e}{\dot{m}_o} = \sqrt{\rho_{rel}} \left\{ \frac{x_L}{d} \left[0.033 + 0.083 \ln \frac{x_L}{d} \right] \right\} \quad (A-33)$$

for entrainment fraction, where the range of applicability is

$$0 < \frac{x_L}{d} < 12$$

For $x_L/d > 12$, Ricou and Spalding's (Ref 123) expression applies:

$$\frac{\dot{m}_e}{\dot{m}_o} = \sqrt{\rho_{rel}} \left(0.32 \frac{x_L}{d} - 1 \right) \quad (A-34)$$

A comparison of the entrainment fractions given by Eqs(A-33) and (A-36) is given in Fig A-15.

Residence Time Distribution Diagnostics

As noted in Chapter II, the residence time distribution (RTD) of a combustor will yield information about the type of flow pattern and thus has potential for use as a diagnostic tool. Two types of RTD are of interest; namely, the RTD for the recirculation zone itself, and the RTD for the whole combustor. The RTD for the recirculation zone itself can yield information on the mean residence time (\bar{t}) of fluid in the zone and, given an effective volume (V), the associated mass flow rate can be deduced. Thus the mass flow is given by

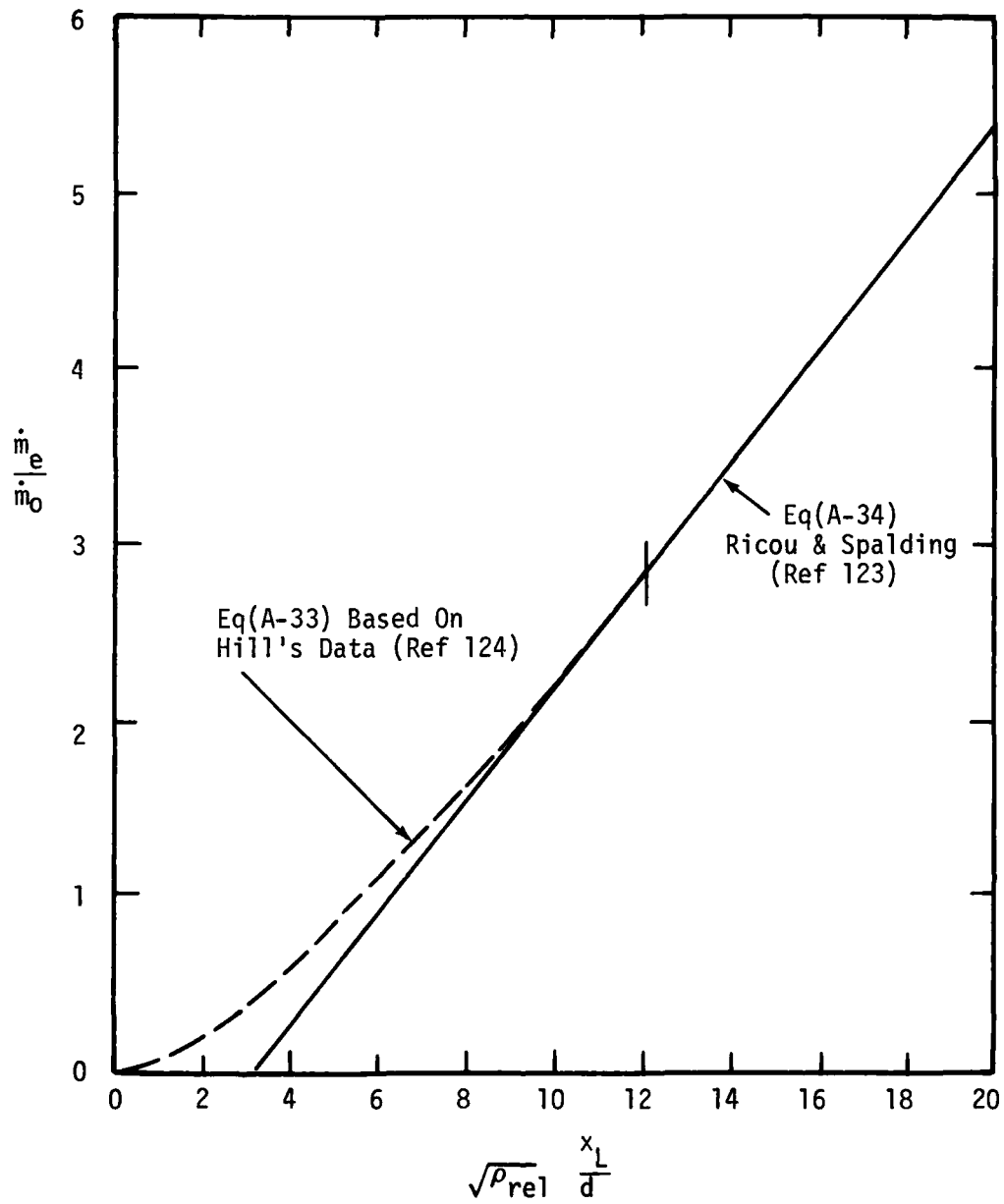


Figure A-15. Comparison of Entrainment Fractions Given by Two Theories

$$\dot{m}_r = \frac{V \rho_r}{\bar{t}} \quad (\text{A-35})$$

Many studies have been made of the RTDs of the recirculation zone behind bluff bodies such as discs (Ref 35). However, the RTD of a simple sudden expansion RZ does not appear to have received attention.

The overall RTD of the combustor may be used to estimate the associated combustion efficiency as demonstrated by Beer and Lee (Ref 129).

A few investigations of the RTDs associated with coaxial dump combustors have been reported in the literature (Refs 131-138). Once again, these have been generally concerned with combustors of low diameter ratio (d/D), and little data of immediate application have been generated. However, the work of Moeller and Dealy (Ref 134) did yield an interesting correlation between mixing effects and the Craya-Curtet parameter (C_t). Thus the RTD approach has considerable potential and may prove to be of distinct value in determining the significant overall characteristics of the complex flow fields found in multi-inlet combustors.

Summary

The purpose of this appendix was to review aerodynamic phenomena associated with the coaxial dump combustor with particular regard to obtaining data on the recirculated mass flow fraction. In accomplishing this review, it is apparent that much further work remains to be done to determine adequate similarity parameters for combustors of high diameter-ratio (d/D) and for multi-inlet combustors.

APPENDIX B

MASS TRANSFER IN RECIRCULATION ZONES

In order to evaluate the air loading of a homogeneous reaction zone, it is necessary to evaluate the term \dot{m}_r/V , where \dot{m}_r is the air mass flow participating in the reaction and V is the associated reactor volume. The evaluation of these terms is not straightforward. For bluff bodies installed in ducts, a number of cold flow studies have been made to establish both the volume of the RZ and the associated mass transfer phenomena (Refs 35, 49, and 56). However, under actual combustor conditions, significant changes in both the V and \dot{m}_r terms occur, and few experimental investigations other than the work of Winterfeld (Ref 56), Bovina (Ref 49), and Lefebvre et al. (Ref 93) have been made. Also, it should be noted that diagnostic explorations of combusting recirculatory flows are usually carried out at conditions well removed from blow-off in order to provide quasi-steady conditions. Thus, the fluid dynamics of the actual unsteady blow-off process are not documented. Thus, even in the case of bluff body stabilizers, there is little experimental data: the sudden-expansion configuration appears to have received no attention.

For engineering purposes, it is desirable to express \dot{m}_r in terms of the upstream flow condition. Thus for a bluff body stabilizer one may write

$$\dot{m}_r = \rho_o U_o A_f C_m = \dot{m}_{of} C_m$$

or

$$C_m = \frac{\dot{m}_r}{\dot{m}_{of}} \quad (B-1)$$

where \dot{m}_{of} is the hypothetical mass flow which would pass through an area equal to the flameholder area A_f . Winterfeld (Ref 56) has called C_m the exchange coefficient, and Ernst (Ref 139) terms C_m the recirculation efficiency. In general, there have been two approaches to the determination of \dot{m}_r . The first is to apply a mass transfer analysis (Ref 140). Typically, such investigations (Refs 21 and 32) led to the result that C_m was approximately constant, and thus the fraction of the approach flow which entered into the recirculation process was constant. With this result one may write

$$\dot{m}_r \propto \rho_0 U_0 A_f \quad (B-2)$$

The second approach to estimating the mass transfer is by the use of residence time measurements. This approach has been pioneered by Quick (Ref 141), Winterfeld (Ref 56), and Bovina (Ref 49).

For a recirculation zone, the transported mass flow \dot{m}_r may be expressed as

$$\dot{m}_r = \frac{\rho_r V}{\bar{t}} \quad (B-3)$$

where ρ_r is the mean density of the recirculation zone and \bar{t} is the mean residence time of a particle in the zone. Winterfeld has shown that for a number of bluff body shapes, and for a given blockage, under burning conditions

$$\bar{t} \propto \frac{1}{U_0} \quad (B-4)$$

And from Eq(B-3) one obtains

$$\dot{m}_r \propto \rho_r U_0 V \quad (B-5)$$

Winterfeld also defined an exchange velocity (E_V) to characterize the turbulent exchange process across the boundary of the recirculation zone. Thus

$$\dot{m}_r = \rho_r S E_V \quad (B-6)$$

The exchange velocity was found to vary directly with the freestream velocity so that

$$\dot{m}_r \propto \rho_r U_0 S \quad (B-7)$$

For a given shape of bluff body flameholder installed in a fixed diameter pipe, the ratio V/S will not vary significantly during operation. Thus Eq(B-5) and Eq(B-7) are quite consistent.

Shchetnikov (Ref 45) has observed from some earlier data of Winterfeld (Ref 142) that the dimensionless volumetric flow rate through the RZ is independent of the presence of combustion and varies little with blockage. Thus

$$\frac{\dot{m}_r}{U_0 D_f^2 \rho_r} = \text{constant}$$

or

$$\dot{m}_r \propto \rho_r U_0 S \quad (B-8)$$

which is a similar relation to that given in Eq(B-7).

In the case of two-dimensional bodies, the phenomenon of vortex shedding occurs and introduces another variable, i.e., the Strouhal number, affecting residence time measurements (Ref 143). With this cautionary remark, attention is drawn to the work of Silant'yev (Ref 144), who investigated transfer phenomena at the boundary of a

recirculation zone generated by the flow over two-dimensional steps. In this investigation the mean residence time was found to vary as follows:

$$\bar{t} \propto \frac{h}{U_0} \quad (\text{B-9})$$

where h = step height.

The final result quoted is

$$\bar{t} = \frac{20 h}{U_0} \quad (\text{B-10})$$

The definition of the free stream velocity (U_0) is a little ambiguous in this investigation (Ref 144), but Eq(B-10) is considered the correct interpretation. No comment appears in the work of Silant'yev on the possible impact of vortex shedding on the mean residence time.

Returning to the discussion of flow around axisymmetric bluff bodies, a significant series of cold-flow studies has recently been reported by Humphries and Vincent (Refs 35, 145-148). They have shown that the dimensionless group $H \equiv U\bar{t}/D_f$ may be expressed as:

$$H = f_1 \left\{ Re, \frac{l_f}{D_f}, \frac{k_f}{U_0^2} \cdot \frac{D_B}{\nu}, St \right\} \quad (\text{B-11})$$

where l_f = integral length scale of free stream turbulence

k_f = energy of free stream turbulence

D_B = molecular diffusion coefficient

ν = molecular kinematic viscosity

St = Strouhal number

If molecular diffusion and vortex shedding are neglected, then

$$H = f_2 \left\{ Re, \frac{l_f}{D_f}, \frac{k_f}{U_0^2} \right\} \quad (\text{B-12})$$

Under "smooth" free stream conditions, H is found to be constant irrespective of R_e . Under turbulent free stream conditions, the corresponding expression for H becomes

$$H = f_3(\Lambda) \quad (\text{B-13})$$

where $\Lambda = \frac{l_f k_f^{1/2}}{D_f U_0}$ is a free stream turbulence parameter.

An interesting experimental result for discs is that H decreases from a value of about 7.5 at $\Lambda = 0$ to $H = 6$ at $\Lambda = .04$: a corresponding reduction in the L/D of the recirculation zone from 2.25 to about 1.5 was noted. The work of Humphries and Vincent has placed the study of cold flow residence times on an improved theoretical basis and has laid a firm foundation for similar studies for reacting flows.

Although residence times have been measured on other geometries, e.g., blunt vehicle bases (Ref 149), no studies of the sudden expansion recirculation zone appear to have been made. Indeed, the only investigation related to the coaxial combustor is that performed by Silant'yev (Ref 144) concerning flow over a step: his results are given by Eq(B-10).

For a coaxial combustor with reacting flow, it may be postulated that the entrainment process is similar to that of a free jet. As noted in Appendix A, this is a reasonable assumption for combustor geometries of low d/D ratio. In this case, mass entrainment from the recirculation zone will take place in the initial region downstream of the dump plane up to a point say x_L' . Subsequently, downstream of x_L' mass will be de-entrained from the jet to supply the recirculation zone. The corresponding entrained mass flow can then be expressed as

$$\frac{\dot{m}_e}{\dot{m}_0} \propto \sqrt{\frac{\rho_r}{\rho_0}} f\left(\frac{x_L}{d}\right)$$

or

$$\dot{m}_e \propto \sqrt{\frac{\rho_r}{\rho_0}} \cdot \rho_0 A_0 U_0 f\left(\frac{x_L}{d}\right) \quad (\text{B-14})$$

and a mean density term appears in this equation.

To recapitulate at this point, it will be recalled that the aim of this Appendix was to evaluate \dot{m}_r in terms of upstream flow conditions. As a result of this review, three methods of expressing \dot{m}_r are seen to be available. Firstly, one may express \dot{m}_r from Eq(B-1) as follows:

$$\dot{m}_r = \rho_0 U_0 A_f C_m$$

where C_m is an exchange coefficient which is frequently assumed to be a constant, yielding

$$\dot{m}_r \propto \rho_0 U_0 A_f \quad (\text{B-15})$$

This assumption has given excellent results in various investigations (Refs 21 and 31). Pavlov (Ref 150) investigated combustion in the wake of a cylinder and obtained experimental confirmation of Eq(B-15) for Reynolds numbers greater than 3.5×10^4 . A second approach is possible based on an observation by Shchetinkov (Ref 45), which resulted in Eq(B-8), namely

$$\dot{m}_r \propto \rho_r U_0 S$$

or

$$\dot{m}_r \propto \left(\frac{\rho_r}{\rho_0}\right) \rho_0 U_0 S \quad (\text{B-16})$$

Similarly, for a two-dimensional step, Silant'yev (Ref 144) obtained

$$\bar{t} \propto \frac{h}{U_0} \quad (\text{B-9})$$

Now

$$\dot{m}_r \propto \frac{\rho_r V}{\bar{t}}$$

so that

$$\dot{m}_r \propto \rho_r U_0 \frac{V}{h}$$

or

$$\dot{m}_r \propto \left(\frac{\rho_r}{\rho_0}\right) \rho_0 U_0 \frac{V}{h} \quad (\text{B-17})$$

Thirdly, if free-jet entrainment theory is applied to a coaxial dump combustor, the following relationship results from Eq(B-14)

$$\dot{m}_r \propto \sqrt{\rho_r \rho_0} U_0 A_0 f\left(\frac{x_L}{d}\right) \quad (\text{B-18})$$

Thus with the exception of the mass flow expression given in Eq(B-15), the density of the recirculation zone appears in all equations.

Typically

$$\rho_r \propto \frac{P_r}{T_r} \approx \frac{P_0}{T_r} \approx \rho_0 \left\{ \frac{T_0}{T_r} \right\} \quad (\text{B-19})$$

Despite their clear difference, the assumption is usually made that $\rho_r = \rho_0$, and the resulting error is absorbed in the empirical evaluation of the right-hand side of the basic stirred reactor equation.

$$\frac{\dot{m}_r}{V \rho_r^2} = \phi_{\max}(\phi, T_0) \quad (\text{B-20})$$

Of course, if the entrainment relation given in Eq(B-14) is truly descriptive of the coaxial combustor, then the error in assuming $\rho_r = \rho_0$ is relatively smaller since the square root of the temperature ratio $\sqrt{\frac{T_0}{T_r}}$ is involved rather than the actual temperature ratio.

APPENDIX C
CHEMICAL REACTION MODEL

In order to model the recirculation zone of the coaxial dump combustor as a stirred reactor, two tasks must be completed. The first is to perform the necessary calculations to determine the maximum reactor loading ϕ_{\max} as a function of equivalence ratio and inlet temperature. However, ϕ_{\max} is a complex function of ϕ and T , and thus the second task is to express ϕ_{\max} in a simplified form suitable for engineering use. Typically, in this study ϕ_{\max} is expressed over a limited range of ϕ and T in the form

$$\phi_{\max} \propto T^s \phi^t \quad (C-1)$$

Thus this Appendix outlines the numerical calculations performed to determine the exponents in expressions of the form given in Eq(C-1). These calculations were performed for both ethylene and JP-4 fuels over a wide range of assumed activation energies (E) and reaction orders (n).

It was shown in Chapter II, Eq(2), that the loading of a stirred reactor may be expressed, for an overall reaction order of two, as

$$\frac{\dot{m}_r}{VP_r^2} = \frac{(1+m)}{R^2} \left\{ \frac{k_1 e^{-E/RT_r}}{T_r^{3/2}} \right\} \frac{1}{\epsilon\phi} X_o X_f \quad (C-2)$$

For a reaction of order n the corresponding expression becomes

$$\frac{\dot{m}_r}{VP_r^n} = \frac{(1+m)}{R^n} \left\{ \frac{k_1 e^{-E/RT_r}}{T_r^{(n-0.5)}} \right\} \frac{1}{\epsilon\phi} X_o^{n/2} X_f^{n/2} \quad (C-3)$$

assuming that X_o and X_f share equal reaction orders. Substituting for X_o and X_f from Eq(4a) and Eq(4b), one obtains

$$\phi = \frac{\dot{m}_r}{VP_r^n} = \frac{k_1}{R^n} (m+1) \frac{e^{-E/RT_r} \left\{ (\phi - \epsilon\phi)(1 - \epsilon\phi)(x + y/4) \right\}^{n/2}}{T_r^{n-0.5} \epsilon\phi \left\{ (m+1)(x + y/4) + \phi + \epsilon\phi (y/4 - 1) \right\}^n} \quad (C-4)$$

If attention is confined to a given hydrocarbon fuel, then x and y are determined. An activation energy E , a reaction order n , and a reaction rate constant k_1 may also be assigned for the reaction.

The reaction temperature is calculated using the expression

$$T_r = T + \eta_c \Delta T$$

where ΔT is the adiabatic temperature rise corresponding to the given values of ϕ and T , η_c is the temperature rise combustion efficiency, and it is assumed that $\eta_c = \epsilon$. As previously illustrated in Fig 6, for a given equivalence ratio and initial temperature, ϕ attains a local peak value, ϕ_{\max} , at a given value of ϵ denoted by ϵ_{opt} . As pointed out previously, the value ϕ_{\max} is of significance in that it determines the maximum mass flow the reactor can sustain before extinction.

For the purposes of this investigation, it was initially desired to express ϕ_{\max} in the following forms:

$$\phi_{\max} \propto e^{T/b} \phi^t \quad (C-5)$$

and

$$\phi_{\max} \propto T^s \phi^t \quad (C-6)$$

The expression given in Eq(C-5) has previously been used successfully by Ballal and Lefebvre (Ref 31). However, Eq(C-6) yields a stability correlating group conveniently expressed in exponent form.

Absolute values of Φ_{\max} are not required for the evaluation of the exponents occurring in either Eq(C-5) or Eq(C-6), so values of $\Phi'_{\max} = \frac{1}{k_1} \Phi_{\max}$ were adequate. Thus values of Φ'_{\max} were calculated both for ethylene (C_2H_4) and JP-4 fuels burning with air, over a range of inlet temperatures varying from 600-1200^oR and for equivalence ratios ranging from 0.3 to 1.0. These calculations were made for ethylene for values of E ranging from 30 to 54 KCal/Mole and for values of n from 1.25 to 2.00. A reduced number of calculations were made for JP-4 using the formula $C_{9.5}H_{18.9}$ given in Ref 151. In Fig C-1, a typical variation of Φ_{\max} with ϕ and T is shown for ethylene with $E = 42$ KCal/Mole and $n = 2$. This latter figure is of particular interest in that it shows that Eq(C-5), expressed in logarithmic form, is a suitable form for approximating the variation of Φ_{\max} with T and ϕ . As noted previously in Eq(9), the term b is, rigorously, a function of the equivalence ratio. Now, for each combination of E and n , a data set of the form shown in Fig C-1 was obtained. For each set of data, expressions of the form given in Eq(C-5) and Eq(C-6) were used to approximate Φ'_{\max} over the range of ϕ and T corresponding to lean extinction conditions. The ranges used were ϕ ; 0.4 to 0.7, and T ; 800-1200^oR. The goodness of fit generally obtained is illustrated in Fig C-2 and Fig C-3. A multiple linear regression program was used to approximate Φ_{\max} and values of the exponents b , s , and t were obtained. In Fig C-4, the variation of the exponents s and t with the assumed activation energy and reaction rate is shown for ethylene; similar results are obtained for JP-4 as shown in Fig C-5.

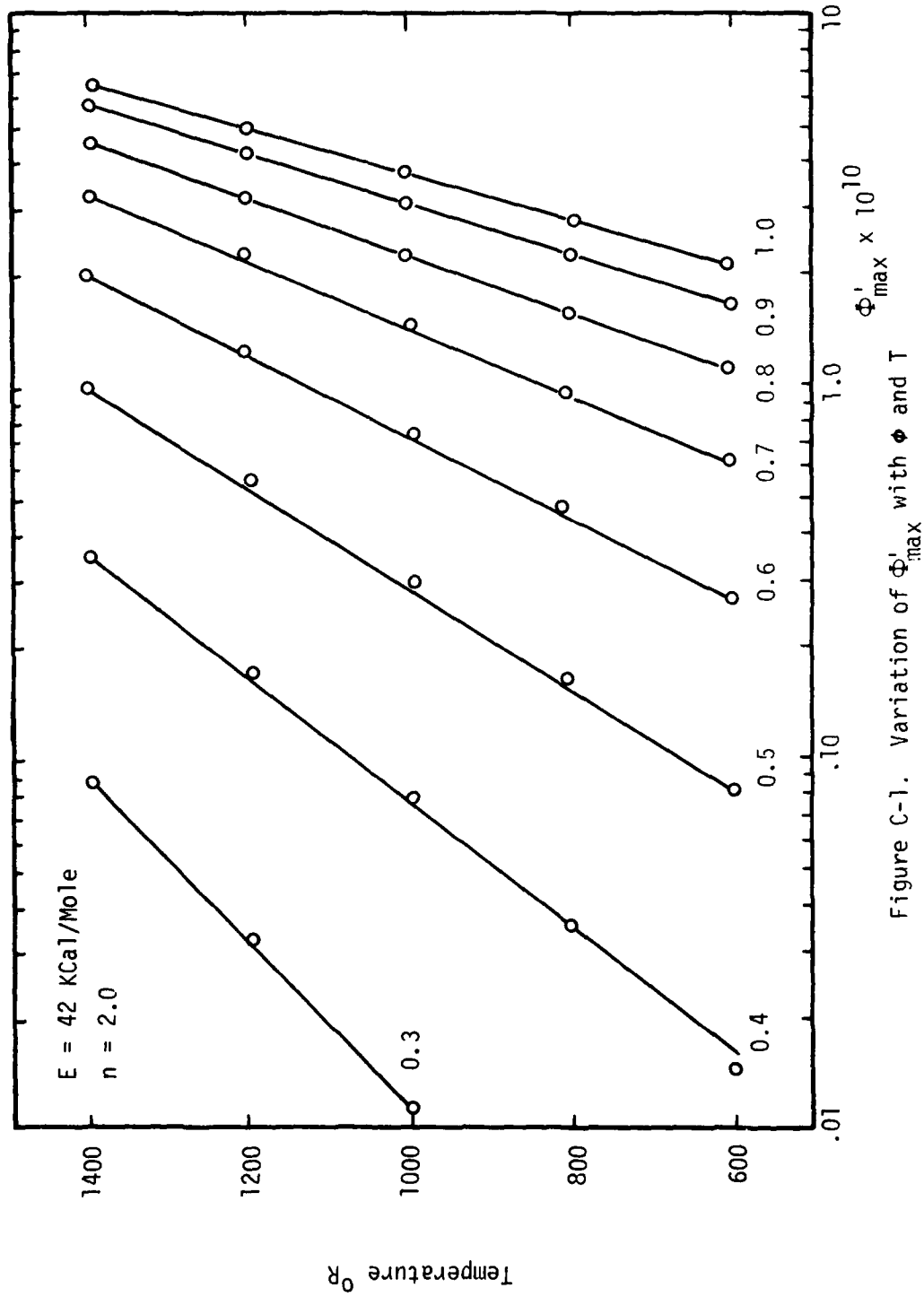


Figure C-1. Variation of Φ'_{\max} with ϕ and T

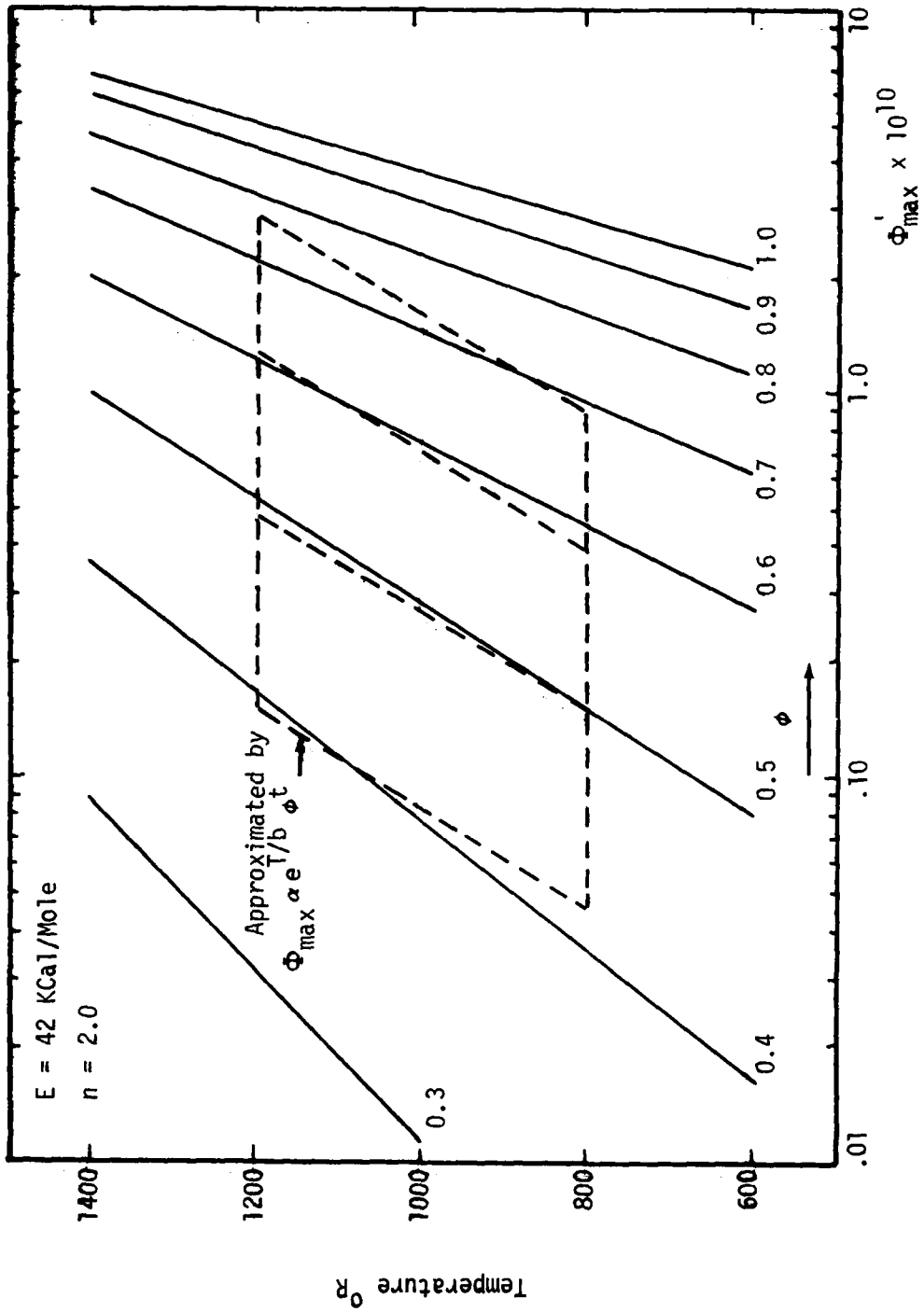


Figure C-2. Approximation to Φ_{max}' Function

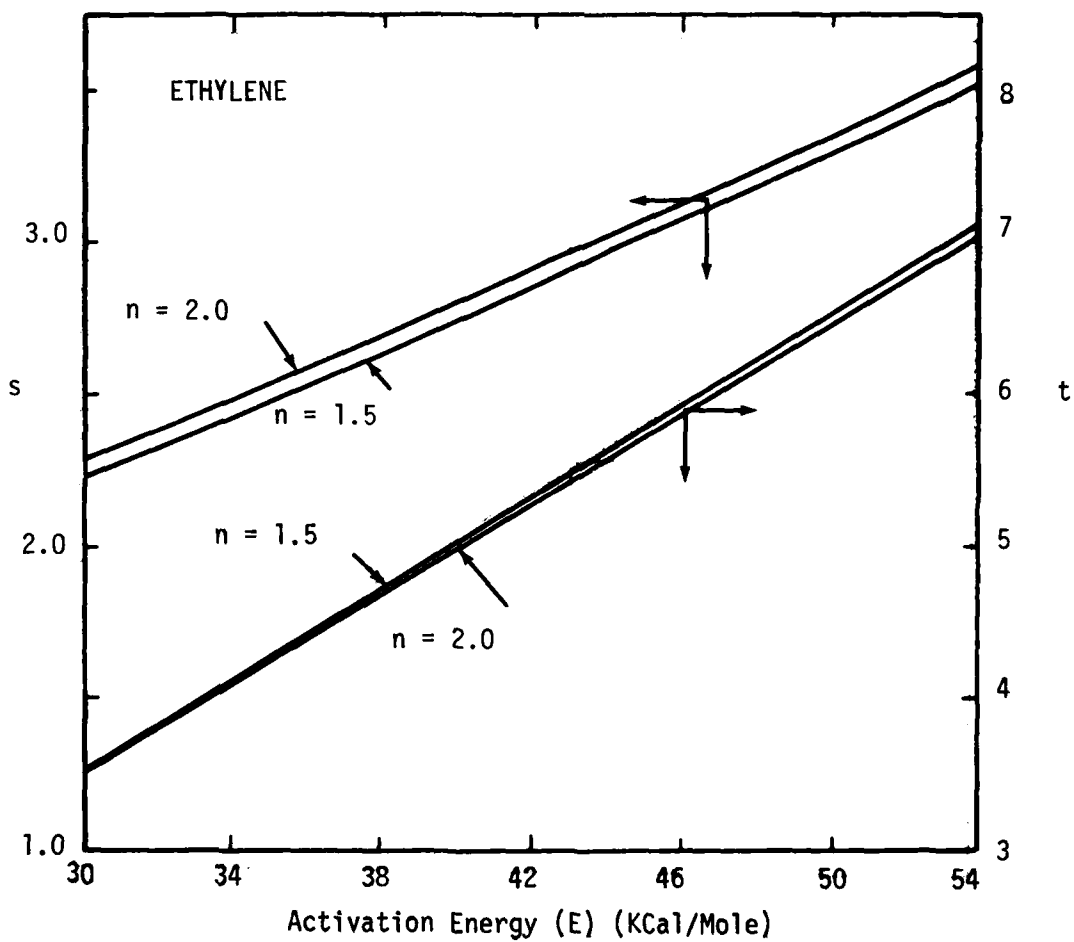


Figure C-4. Variation of s and t: Ethylene

The exponents s and t appear in Eq(70) of Chapter III. These exponents, together with the reaction order n , are used to obtain the quantities $\alpha, \beta, \gamma, \delta$ of Eq(71), which are, of course, exponents of velocity, pressure, step height, and temperature, respectively. A typical variation of these latter exponents with E and n is shown in Fig C-6.

A few values of the exponents α, β, γ , and δ were also calculated for a reactor loading expression based on the hypothesis that the mass flow \dot{m}_r was given by Eq(B-17). In this case the air loading term was given by

$$\Phi_{\max} = \frac{\dot{m}_r}{V P_r^n} = \frac{\rho_r U_0 V}{V \cdot h \cdot P_r^n} \propto \frac{U_0}{h P_r^{n-1}} \cdot \left(\frac{1}{T_r} \right)$$

$$\propto \frac{U_0}{h} \cdot \frac{1}{P_r^{n-1}} \frac{1}{T} \frac{T}{T_r} \quad (C-7)$$

A chemical reaction model based on Eq(C-1) was utilized for Φ_{\max} and the corresponding temperature ratio (T/T_r) appearing on the right-hand side of Eq(C-7) was also evaluated. The values obtained for α, β, γ and δ did not correlate the experimental data and this line of inquiry was not further pursued.

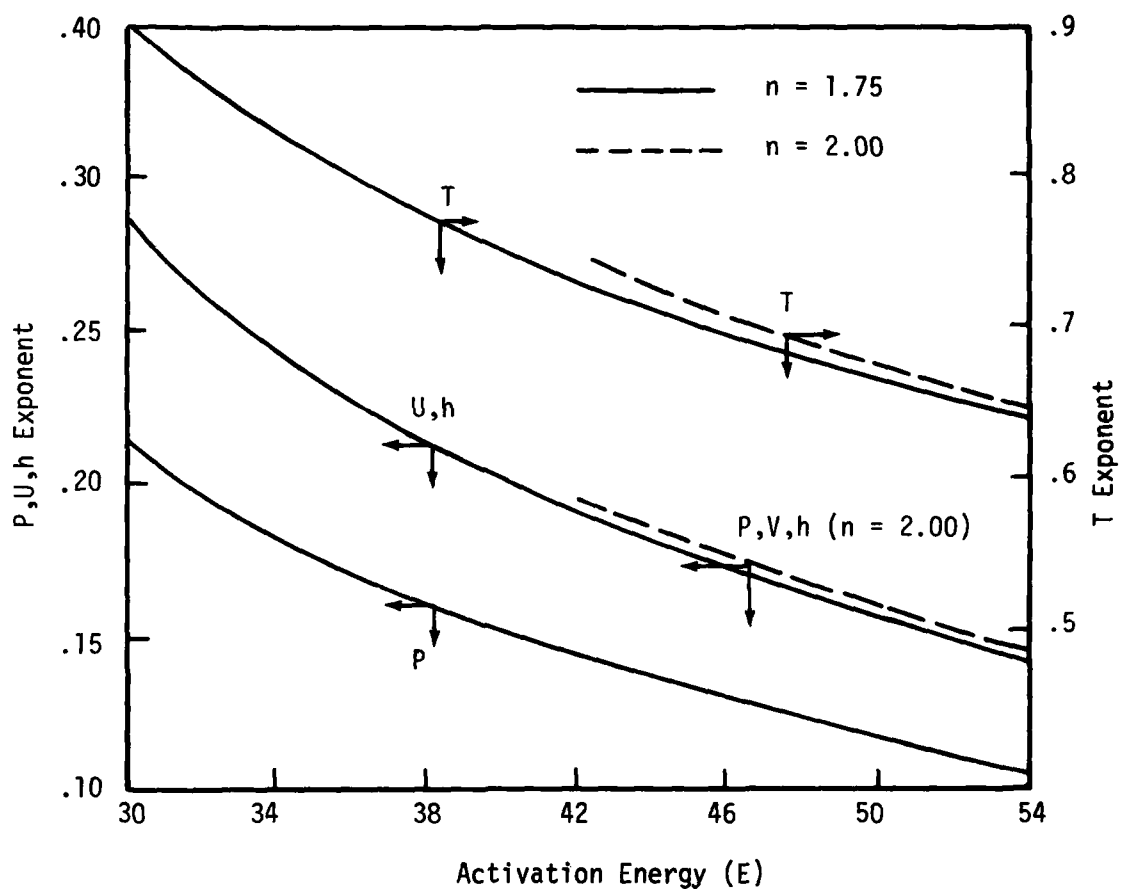


Figure C-6. Variation of Exponents with E and n (Ethylene)

APPENDIX D
INLET FLOW DATA

As pointed out in Chapter IV, one of the experimental goals was to obtain an approximately constant velocity profile at the dump inlet plane. Previous investigators had used straight pipe entries, and little information on the associated velocity profiles was available. For this investigation, a series of convergent inlet sections of cubic wall profile were designed and fabricated. Cold flow calibrations of three dump sizes, namely 2.5", 3.5", and 4.5", were undertaken. For these tests, the convergent section was directly coupled to the combustor, and various exit nozzles were used to vary the Mach number at the dump plane. These inlets were calibrated over a range of dump plane Mach numbers and mass flow levels which bracketed the anticipated operating conditions. All calibrations were carried out at a total temperature of about 530°R. At each condition, the dump plane Mach number profile was measured, utilizing a traversing pitot static tube. The inlet Reynolds number based on dump plane diameter was calculated from the expression

$$R_e = \frac{4\dot{m}}{\mu\pi d} \quad (D-1)$$

The experimental Mach number profiles typically obtained are shown in Figs D-1, D-2, and D-3. It will be observed that profiles of substantially constant Mach number were obtained. The cold flow Reynolds numbers ranged from 4×10^5 to 1.5×10^6 . For hot flow experimental conditions, the corresponding Reynolds number was always in excess of 1×10^5 .

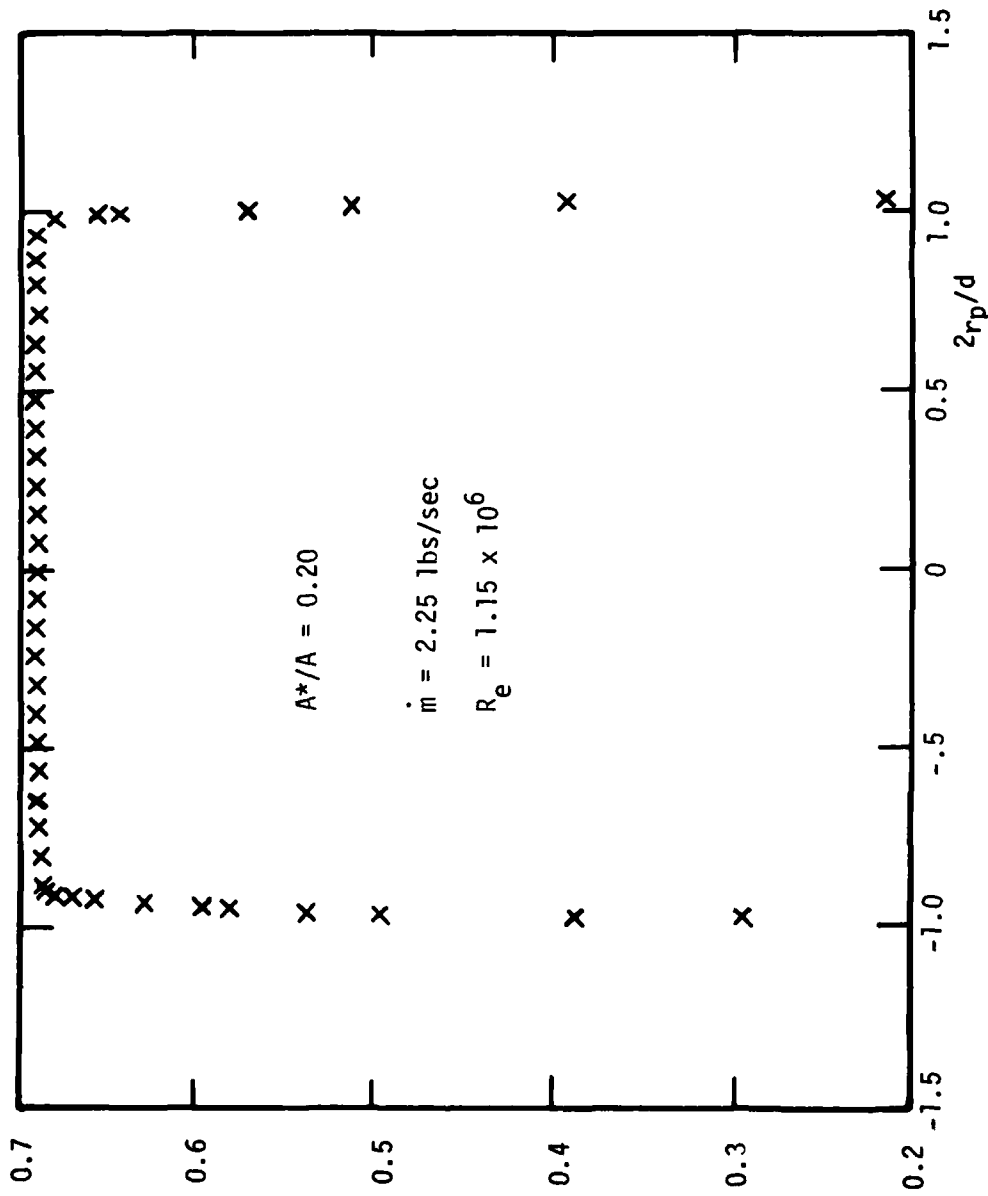


Figure D-1. Flow Profile for 2.5" Inlet

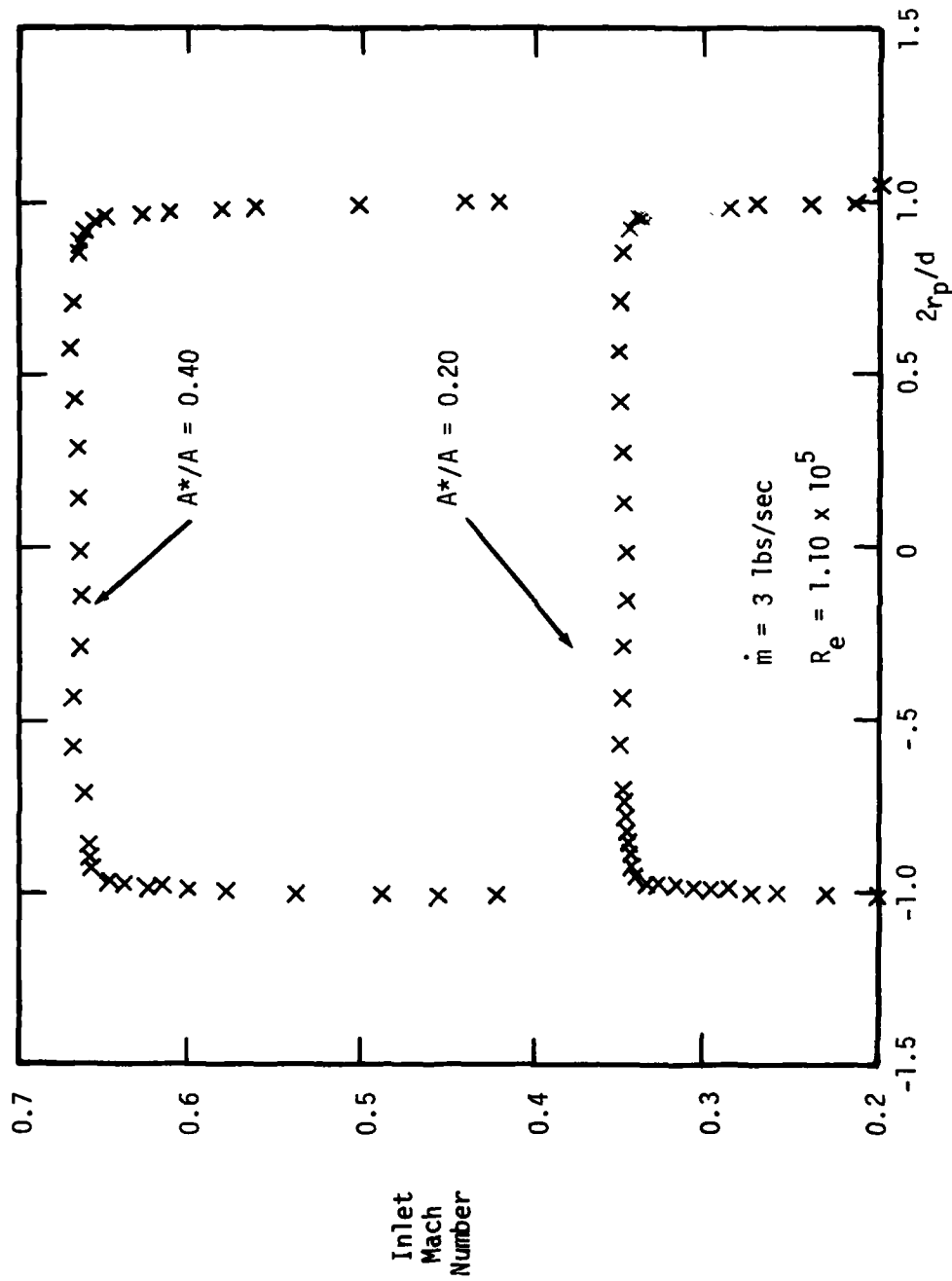


Figure D-2. Flow Profile for 3.5" Inlet

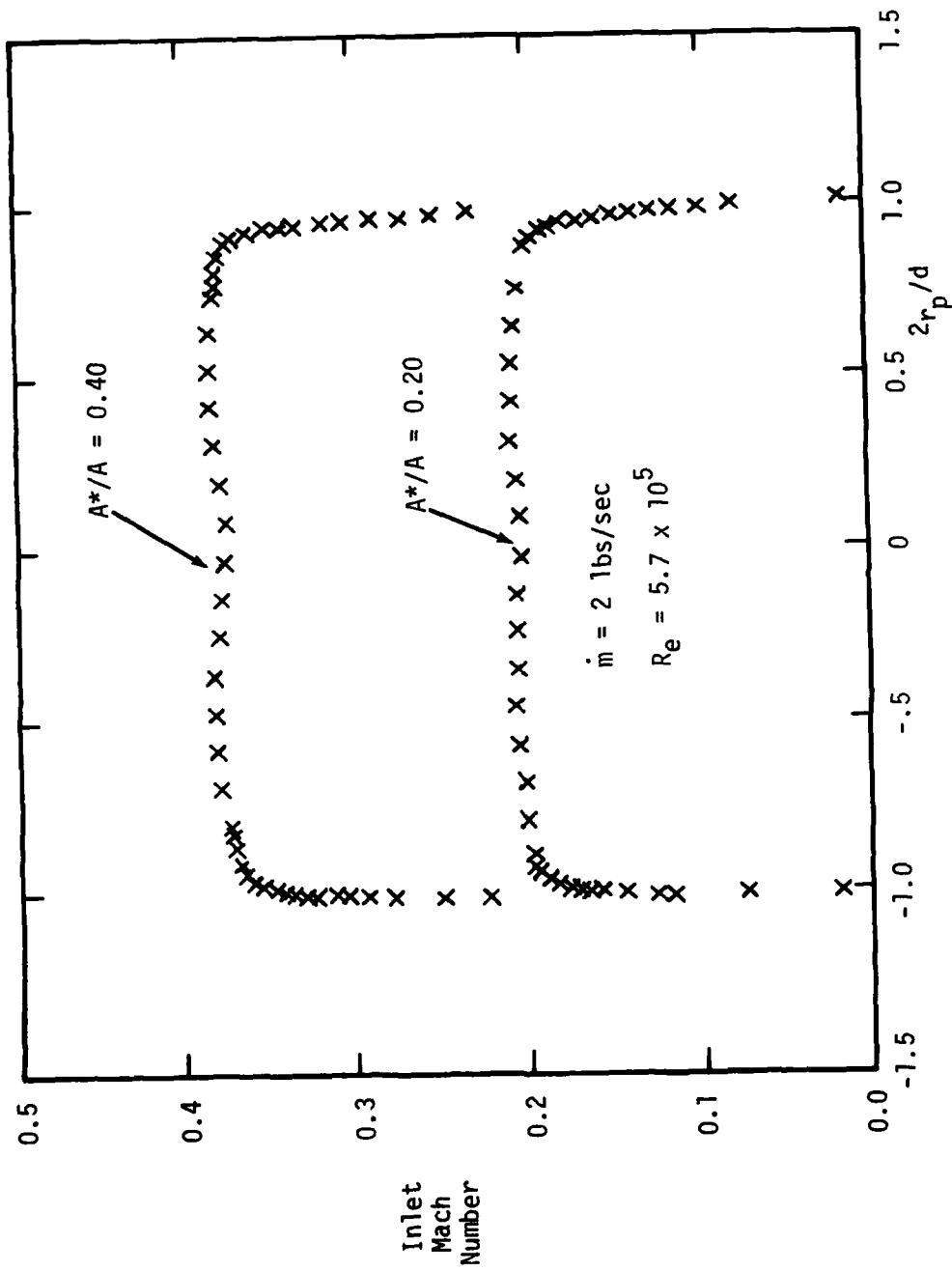


Figure D-3. Flow Profile for 4.5" Inlet

VITA

Edward T. Curran was born on [REDACTED] in [REDACTED]. In June 1948, he received an honors Bachelor of Science (Engineering) degree from the University of London. He entered the Royal Air Force in 1948 and was commissioned as a Pilot Officer in February 1949. In 1952, following tours of duty in operational research, aircraft engineering, and aircraft maintenance, he was assigned to the College of Aeronautics, Cranfield, for graduate studies in Aircraft Propulsion and Electronics. He subsequently received an MSc degree, but stayed at the college for a further year of research on ducted rockets. He was then assigned to the National Gas Turbine Establishment, serving initially on Ramjet Flight trials and subsequently as an Advanced Projects Engineer. He was subsequently appointed officer-in-charge of propulsion training at the RAF Technical College. In 1960, he was assigned to Wright-Patterson AFB as an exchange officer: he served both in the AF Flight Dynamics and AF Aero Propulsion Laboratories. In 1968, he retired from the Royal Air Force and took up permanent residence in the United States, becoming a U.S. Citizen in 1975. Since 1969, he has been employed in the Ramjet Engine Division of the AF Aero Propulsion Laboratory, initially as Chief of the Ramjet Technology Branch and subsequently as Deputy Director. He entered the Doctor of Philosophy program at the Air Force Institute of Technology in October 1973 and completed the academic program in December 1974.

Permanent address: [REDACTED]
[REDACTED]

This dissertation was typed by Ms. Cynthia J. Lines